

**The Genetic Architecture of  
Flight and Climbing Performance in *Drosophila melanogaster***

Adam N. Spierer

A dissertation submitted to the Graduate School of Brown University  
in fulfillment of the requirements for degree of  
Doctor of Philosophy in the Department of Ecology and Evolutionary Biology

Providence, RI

May 2020

© Copyright 2020 by Adam N. Spierer

This dissertation by Adam N. Spierer is accepted in its present form by the  
Department of Ecology and Evolutionary Biology  
as satisfying the dissertation requirements for the degree of Doctor of philosophy.

Date \_\_\_\_\_

\_\_\_\_\_  
David M. Rand, Advisor

Recommended to the Graduate Council

Date \_\_\_\_\_

\_\_\_\_\_  
David M. Rand, Advisor

Date \_\_\_\_\_

\_\_\_\_\_  
Sohini Ramachandran, Reader

Date \_\_\_\_\_

\_\_\_\_\_  
Thomas J. Roberts, Reader

Date \_\_\_\_\_

\_\_\_\_\_  
Marc Tatar, Reader

Approved by the Graduate Council

Date \_\_\_\_\_

\_\_\_\_\_  
Andrew G. Campbell, Dean of the Graduate School

## CURRICULUM VITAE

### ADAM N. SPIERER

Rand Lab at Brown University  
80 Waterman St  
Providence, Rhode Island 02912

### EDUCATION

---

**BROWN UNIVERSITY**, PROVIDENCE, RI Doctor of Philosophy, May 2020  
DEPARTMENT: Ecology and Evolutionary Biology Masters of Science, May 2018

**COLBY COLLEGE**, Waterville, ME Bachelor of Arts, May 2013  
MAJOR: Biology: Cellular and Molecular Biology/Biochemistry (Honors)  
MINOR: Chemistry

### PUBLICATIONS

---

Sujkowski AL, **Spieler AN**, Rajagopalan T, Safdar M, Imsirovic D, Arking R, Rand DM, Wessells RJ.  
(2019) Mito-nuclear interactions modify *Drosophila* exercise performance. *Mitochondrion*. 47:188-205. doi: 10.1016/j.mito.2018.11.005

**Spieler AN**, Mossman JA, Smith SA, Crawford L, Ramachandran S, Rand DM. Natural Variation in the Regulation of Neurodevelopmental Genes Modifies Flight Performance in *Drosophila*. (*in prep*)

**Spieler AN**, Yoon D, Zhuo L, Rand, DM. FreeClimber: Automated High Throughput Quantification of Climbing Performance in *Drosophila*, with Examples from Mitonuclear Genotypes. (*in prep*)

**Spieler AN**, Mossman JA, Rand DM. The Genetic Architecture for Robustness of Flight Performance in *Drosophila*. (*in prep*)

### PRESENTATIONS

---

**Spieler AN**, Mossman J, Rand DM. "Dissecting the genetic modifiers of flight performance using the *Drosophila* Genetic Reference Panel," Society for Integrative and Comparative Biology Annual Meeting. January 2020, Austin, TX.

**Spieler AN**, Mossman J, Rand DM. "Using a mitochondrially-targeted endonuclease to screen modifiers of mtDNA defects influencing flight performance in *Drosophila*," Evolution Meeting. June 2019, Providence, RI.

**Spieler AN**, Mossman J, Rand DM. "Using a mitochondrially-targeted endonuclease to screen modifiers of mtDNA defects influencing flight performance in *Drosophila*," Genetic Society of America's 60<sup>th</sup> Annual *Drosophila* Research Conference. April 2019, Dallas, TX.

Russo K, **Spieler AN**, Held A, Wharton KA. "Comparative analysis of two dSOD1 knock-in ALS models," Genetic Society of America's 60<sup>th</sup> Annual *Drosophila* Research Conference. April 2019, Dallas, TX.

Russo K, Held A, **Spieler AN**, Wharton K. "Characterization of dSOD1 knock-in mutations associated with ALS," Brown-NIH Neuroscience Retreat. October 2018, Woods Hole, MA.

**Spieler AN**, Mossman J, Lemieux F, Brett-Turner E, Rand DM. "Identifying genetic modifiers of flight performance using the *Drosophila* Genetic Reference Panel," Genetic Society of America's 59<sup>th</sup> Annual *Drosophila* Research Conference. April 2018, Philadelphia, PA.

**Spieler AN**, Yoon D, Rand DM, "Manipulation of targeted mitochondrial DNA double strand breaks in a *Drosophila* model," Genetic Society of America's 58<sup>th</sup> Annual *Drosophila* Research Conference. March 2017, San Diego, California.

Yoon D, **Spierer AN**, Rand DM, “Manipulating mitochondrial decay and regeneration in a *Drosophila* model of neurodegeneration,” Society for Neuroscience. November 2016, San Diego, California.

Yoon D, **Spierer AN**, Rand DM, “Mitochondria unplugged: targeted restriction of mtDNA and chemotaxic response in *Drosophila*,” Summer Research Symposium at Brown University. August 2015, Providence, RI.

Rand, DM, Zhu CT, Mossman J, Santiago J, **Spierer AN**, Biancani L, Devlin T, Dewey J, Franklin B, McAteer M, Pataki Z, Hale-Phillips C, Yoon D, “Mitonuclear AxGxE: Genetic and dietary interactions are as important as single factors in explaining *Drosophila* lifespan and healthspan.” Genetic Society of America’s 56th Annual *Drosophila* Research Conference. March 2015, Chicago, IL.

**Spierer AN**, Pascal A, Mabeza R, Rand DM, “Mitochondrial knockdown using tissue specific expression of mitochondrially-targeted restriction enzymes against mtDNA as a model for the decline in organismal performance,” Genetic Society of America’s 56<sup>th</sup> Annual *Drosophila* Research Conference. March 2015, Chicago, IL.

**Spierer, AN**, and Millard, JT, “Relationship of cross-linking potential to mechanism of cell death,” Honors thesis presentation at Colby Undergraduate Research Symposium. May 2013, Waterville, ME.

**Spierer, AN**, and Millard, JT, “Mechanisms of cytotoxicity of bifunctional epoxide cross-linking agents,” American Society for Biochemistry and Molecular Biology Annual Conference. April 2013, Boston, MA.

**Spierer, AN**, and Millard, JT, “Cross-Linking Efficiencies of Bifunctional Alkylating Agents in HL-60 Human Leukemia Cells,” Colby Undergraduate Summer Research Retreat Symposium. July 2012, The Forks, ME.

## TEACHING AND PROFESSIONAL EXPERIENCE

---

Group Fitness Instructor with Graduate Student Council*	April 2020 – Present
Group Fitness Instructor with Brown Recreation*	Jan. 2018 – April 2020
Sheridan Center for Teaching and Learning Discussion Facilitator for Certificate I: Reflective Teaching*	Sept. 2015 – May 2018
NSF-Sponsored Science Outreach Instructor for Second Grade Class at Vartan Gregorian Elementary School in Providence, RI*	Sept. 2015 – June 2016
HHMI Summer Research Program Mentor*	Summer 2014
Fundamentals of Ecology Lead Teaching Assistant*	Spring 2014
Evolutionary Biology Teaching Assistant*	Fall 2013
Exercise Physiology Teaching Assistant at Colby College	Jan 2013
Chemistry Help Center Tutor at Colby College	Sept. 2012 – Jan. 2013
Writing Tutor at Farnham Writers’ Center at Colby College	Sept. 2010 – May 2012

\* Brown University

## LEADERSHIP AND SERVICE

---

Member of Campus Life at Brown Subcommittee on Athletics and Physical Education*	Sept. 2019 – Present
Graduate and Medical Student Free Group Fitness Initiative*	Jan. 2019 – Present
Founder of Astronaut Training Club*	March 2018 – Present
Selected representative on Student Health and Wellness Advisory Council*	Feb. 2018 – Present
Brown Initiative to Maximize Student Development Senior Scholar: Wellness for Success*	June 2019
Graduate Community Fellow for Health and Wellness*	Oct. 2018 – May 2019
BioMed Dean’s Advisory Committee for Events and Professional Development*	Feb. 2014 – Sept. 2019
Community Advisor at Colby College	Sept. 2010 – May 2013
Varsity Men’s Swimming and Diving Team at Colby College	Sept. 2009 – May 2013

Leader for Counselor-In-Training Program at Camp Tel Noar  
Residential Camp Counselor at Camp Tel Noar

Summer 2011  
Summers 2008 – 2011

\* Brown University

## AWARDS AND CURRENT CERTIFICATIONS

Athletics and Fitness Association of America Group Fitness Instructor	Jan. 2018 – Present
American Heart Association Adult CPR/AED	June 2019
Graduate Community Fellowship: Health and Wellness*	Oct. 2018 – Aug. 2018
The Sheridan Center for Teaching and Learning*	
Teaching Certificate IV: Teaching Consultation*	Sept. 2015 – May 2018
Teaching Certificate I: Reflective Teaching*	Sept. 2014 – May 2015
National Science Foundation Integrative Graduate Research Traineeship (IGERT) Fellow*	Sept. 2013 – May 2016
NIH and NIGMS workshop on Metabolomics at University of Alabama Birmingham travel award*	June 2014
Sigma Xi Grants-in-Aid-of-Research to construct a <i>Drosophila</i> “treadmill”*	Dec. 2013
Bechtel Scholarship for Undergraduate Summer Research at Colby College	Summer 2012
Varsity Men’s Swimming and Diving Team at Colby College	
Richard Scholz Award/Coach’s Award	2013
NESCAC Winter All-Academic Team	2011 – 2013
NESCAC Winter All-Sportsmanship Team	2011 & 2012
Un-Sung Hero Award	2011
Rookie of the Year Award	2010
Community Advisor at Colby College	
“Returner of the Semester” Award	Fall 2011

\* Brown University

## PREFACE

One of the central questions driving the field of genetics asks how genotype contributes to phenotype. A simple, single gene trait can be explained as dominant, where one allele determines a phenotype by masking another allele; recessive, where two alleles are required to observe a phenotype; or additive, where the heterozygote lies between the two parental phenotypes. While simple, single gene traits are straightforward, they are not representative of the majority of traits that are polygenic (many genes).

Identifying the genetic factors that make up these polygenic traits (genetic architecture) is challenging because in addition to alleles having additive and dominance effects on the resulting phenotype, pairwise interactions (epistasis) between alleles and environmental effects also have important contributions (MANOLIO *et al.* 2009). Higher-order effects, like genotype x environment, genotype x genotype, and genotype x genotype x environment interactions (MONTTOOTH *et al.* 2010; ZHU *et al.* 2014; MOSSMAN *et al.* 2016) are also a mainstay of these complex traits and further complicate our ability to assess the impact of genetic factors affecting polygenic (complex) traits.

The challenge of uncovering the genetic architecture of complex traits lies in the context-dependent and highly interconnected networks of alleles that interact with each other and the environment to produce a resulting phenotype. It is not possible to generate and test every combination of alleles to assess their individual effects on a phenotype. Instead we must rely on alternative approaches that can estimate how genotype contributes to phenotype. Genome Wide Association Studies (GWAS) are often used for genotype-phenotype mapping to narrow down a large number of possible

genetic factors affecting a trait for more targeted secondary study. Here, a diverse panel of genotypes is used to identify regions of the genome that associate with phenotypic variation. This method is most commonly used to identify additive effects, though other methods leverage similar inputs or the resulting associations and can parse out other effects' contribution to the genetic architecture of a trait (PURCELL *et al.* 2007; NAKKA *et al.* 2016; CRAWFORD *et al.* 2017; REYNA *et al.* 2018). A separate approach lies in mitochondrial-nuclear (mito-nuclear) introgressions for understanding the contribution of higher-order interactions (genotype x genotype x environment) to phenotypic variation. These introgressions contain mitochondrial and nuclear genomes from genetically divergent species, sub-groups, or lineages. By subjecting these individuals to different environmental conditions, we can better study how higher-order effects contribute to phenotypic variation.

Using these two approaches, we build on the existing literature to understand the genetic architecture of complex traits by studying adult insect locomotion. Insects, namely *Drosophila melanogaster*, serve as a genetically tractable model for surveying the genetic architecture of complex traits. Their short generation time, breadth of genetic and computational resources, and strong molecular crossover to humans make them an appealing model for understanding an array of traits with biological and biomedical implications (BELLEN *et al.* 2010; JIN *et al.* 2016; CHOW AND REITER 2017). In adult insects, locomotion is important for the life history of an individual and can be broken down into two sub-categories: aerial (flight) and terrestrial (climbing). Both are energetically demanding and require well-developed and finely tuned morphological,



neuromuscular, metabolic, and homeostatic systems (MONTTOOTH *et al.* 2000; RHODENIZER *et al.* 2008; JONES AND GROTEWIEL 2011; LEHMANN AND BARTUSSEK 2017). We divide these two locomotor traits into four chapters; the first two survey the genetic modifiers of flight performance ability and variability using a GWAS with the *Drosophila* Genetics Reference Panel (DGRP) lines, while the second two place mito-nuclear introgressions in an exercise conditioning program to assess their ability to benefit from exercise conditioning as measured by an attenuation of an aging-associated decline in climbing performance.

The first chapter, “Natural Variation in the Regulation of Neurodevelopmental Genes Modifies Flight Performance in *Drosophila*” focuses on the genetic modifiers of flight performance. Flight is an important life history trait for a fly, enabling it to forage, disperse, migrate, find mates, and evade predators among other roles (BRODSKY 1994; MARCUS 2001). While several individual genes with larger effects are known to affect flight performance (MONTTOOTH *et al.* 2000; SUAREZ 2000; VIGOREAUX 2001; FRYE AND DICKINSON 2004), no recent study has used the available genetic and computational tools to comprehensively survey its genetic architecture. To address this gap in knowledge, we performed a GWAS for flight performance with 197 DGRP lines, a panel of inbred *Drosophila melanogaster* that represent a snapshot of natural variation in a wild population and are commonly used for genotype-phenotype mapping (MACKAY *et al.* 2012; HUANG *et al.* 2014; MACKAY AND HUANG 2018). Using a flight column (BENZER 1973; BABCOCK AND GANETZKY 2014), we quantified each genotypes’ ability to react and respond to an abrupt drop as a function of the mean landing height. We identified 3015

genes identified from additive, marginal, and epistatic variants; whole genes; and altered sub-networks of genes. Many of the genetic modifiers we identified played important roles in general development and neural development and function. Interestingly, we identified a previously unrealized role for the mechanosensory gene *pickpocket 23 (ppk23)* in mediating flight performance through proprioception and several epistatic interactions with *ppk23* that may point toward important biomedical targets for neurological damage-detecting Acid Sensing Ion Channel (ASIC, human homolog) genes in humans (HUANG *et al.* 2015; ORTEGA-RAMIREZ *et al.* 2017). This study also introduced PEGASUS\_flies to the growing battery of genetic tools available for surveying the genetic architecture of complex traits. PEGASUS\_flies is a version of the human-focused PEGASUS platform adapted for *Drosophila*, capable of identifying significant whole genes (NAKKA *et al.* 2016).

The second chapter, “The Genetic Architecture for Robustness of Flight Performance in *Drosophila*” worked to expand on the first chapter by investigating the genetic modifiers affecting the consistency, or robustness, of flight performance within inbred lines of *Drosophila melanogaster*. Using a similar experimental design as the first chapter, we performed a GWAS on the coefficient of variation (mean-normalized standard deviation), which served as a proxy for phenotypic robustness (micro-environmental or non-genetic variation). We identified additive, marginal, and epistatic variants, as well as whole genes associated with robustness in flight performance. Our results suggest 15-20% of the genes and variants that associated with overall flight performance in the first chapter were also important for affecting the consistency of performance, and that the

majority of genes and variants associated with each study were largely distinct. From this study, we uncovered additional genes involved in neurodevelopmental processes, including cell-cell adhesion molecules that co-opt stochastic developmental processes to pattern more interconnected neural networks (AYROLES *et al.* 2015; HIESINGER AND HASSAN 2018). We also identified a number of pleiotropic (affecting multiple phenotypes) genes uncovered in independent DGRP screens for genetic modifiers of micro-environmental variation (MORGANTE *et al.* 2015), courtship behavior (TURNER *et al.* 2013; GAERTNER *et al.* 2015), and wing morphology (PITCHERS *et al.* 2019) that may speak to interesting connections underlying evolutionary pressures affecting shared structures (wings and hairs).

The third chapter “Mito-Nuclear Interactions Modify *Drosophila* Exercise Performance” focuses on the mito-nuclear genetic interactions that modulate flies’ exercise capacity. The mitochondrion, powerhouse of the cell, is maternally inherited and contains its own genome that encodes ~37 genes involved in aerobic metabolism. It must coordinate with its symbiotic partner, the nuclear genome, to coordinate the genes required to generate enough cellular energy to sustain energetically demanding processes (RAND *et al.* 2004). The genetic interactions underlying their partnership are essential and contribute to reproductive fitness, longevity, and certain diseases (WALLACE 2005; WALLACE 2010). In collaboration with the Wessell’s lab at Wayne State University, we sought to understand how different pairings of distantly related mitochondrial-nuclear genotype combinations (MONTTOOTH *et al.* 2010; MA AND O’FARRELL 2016) impacted an energetically demanding trait: exercise performance (PIAZZA *et al.* 2009; JONES AND

GROTEWIEL 2011; TINKERHESS *et al.* 2012). We found evidence for both beneficial and deleterious effects of different mito-nuclear pairings, and demonstrated a novel example of genotype x genotype x environment interactions.

The fourth chapter “FreeClimber: Automated High Throughput Quantification of Climbing Performance in *Drosophila*, with Examples from Mitonuclear Genotypes” presents a novel, image analysis pipeline that improves on the methods used in the third chapter and expands on the mitochondrial-nuclear genotypes panel used to include two more distantly related mitochondrial haplotypes: *D. mauritiana* and *D. yakuba*. Negative geotaxis (climbing) assays are among the most frequently used tools used in *Drosophila* to assess whole animal health, where they take advantage of flies’ reliable and instinctive response to climb upward when startled. Traditional methods startle flies by knocking them down and record photos or videos of them climbing. These are then processed manually by measuring the average height they climb after a prescribed time limit (2-4 seconds), or the percent that cross an arbitrary line after a time interval (GARGANO *et al.* 2005; PIAZZA *et al.* 2009). These methods are accessible and easy to perform, but are equally tedious and prone to human error. Our platform, FreeClimber, returns reliable and reproducible results that quantify the most linear portion of a mean vertical-position vs. time (velocity) curve using a local linear regression. The platform is also capable of working with inconsistent backgrounds where most background pixels are otherwise static to enable other labs with less sophisticated recording set ups take advantage of the tool. FreeClimber is open-source and written in Python, available with a Tutorial on GitHub:

<https://github.com/adampierer/FreeClimber>. We applied our novel method to a longitudinal study of six mitochondrial haplotypes from across three *Drosophila* subgroups (*D. melanogaster*, *D. simulans*, and *D. yakuba*) and found the most distantly related pairing, a *D. yakuba* mitochondrial genome paired with a *D. melanogaster* nuclear genome had the greatest exercise capacity and slowest age-associated decline in performance. This finding corroborates a past finding that this introgression shows increased vigor, evidenced by its increased longevity over the native pairing (MA AND O'FARRELL 2016).

We expand our understanding of the complex architecture underlying physiologically demanding traits related to locomotor performance by uncovering novel associations between genetic modifiers, establishing causal links between variation in certain genes and variation in performance, and lending support to initial observations throughout the literature. As our knowledge of complex traits continues to grow, so too will our ability to treat complex diseases: it is our hope that in addition to the knowledge this body of work generates, it will continue to assist others in making important discoveries through use of the open source and freely available computational platforms we developed (PEGASUS\_flies and FreeClimber). We look forward to seeing how others build on the knowledge we uncovered and utilize the tools we developed.

## LITERATURE CITED

- Ayroles, J. F., S. M. Buchanan, C. O'Leary, K. Skutt-Kakaria, J. K. Grenier *et al.*, 2015 Behavioral idiosyncrasy reveals genetic control of phenotypic variability. *Proceedings of the National Academy of Sciences of the United States of America* 112: 6706-6711.
- Babcock, D. T., and B. Ganetzky, 2014 An Improved Method for Accurate and Rapid Measurement of Flight Performance in *Drosophila*. *Jove-Journal of Visualized Experiments*.
- Bellen, H. J., C. Tong and H. Tsuda, 2010 TIMELINE 100 years of *Drosophila* research and its impact on vertebrate neuroscience: a history lesson for the future. *Nature Reviews Neuroscience* 11: 514-+.
- Benzer, S., 1973 GENETIC DISSECTION OF BEHAVIOR. *Scientific American* 229: 24-37.
- Brodsky, A. K., 1994 *The evolution of insect flight*. Oxford University Press.
- Chow, C. Y., and L. T. Reiter, 2017 Etiology of Human Genetic Disease on the Fly. *Trends in Genetics*.
- Crawford, L., P. Zeng, S. Mukherjee and X. Zhou, 2017 Detecting epistasis with the marginal epistasis test in genetic mapping studies of quantitative traits. *Plos Genetics* 13.
- Frye, M. A., and M. H. Dickinson, 2004 Closing the loop between neurobiology and flight behavior in *Drosophila*. *Current Opinion in Neurobiology* 14: 729-736.
- Gaertner, B. E., E. A. Ruedi, L. J. McCoy, J. M. Moore, M. F. Wolfner *et al.*, 2015 Heritable Variation in Courtship Patterns in *Drosophila melanogaster*. *G3-Genes Genomes Genetics* 5: 531-539.
- Gargano, J. W., I. Martin, P. Bhandari and M. S. Grotewiel, 2005 Rapid iterative negative geotaxis (RING): a new method for assessing age-related locomotor decline in *Drosophila*. *Experimental gerontology* 40: 386-395.
- Hiesinger, P. R., and B. A. Hassan, 2018 The Evolution of Variability and Robustness in Neural Development. *Trends in Neurosciences* 41: 577-586.
- Huang, W., A. Massouras, Y. Inoue, J. Peiffer, M. Ramia *et al.*, 2014 Natural variation in genome architecture among 205 *Drosophila melanogaster* Genetic Reference Panel lines. *Genome Research* 24: 1193-1208.
- Huang, Y., N. Jiang, J. Li, Y. H. Ji, Z. G. Xiong *et al.*, 2015 Two aspects of ASIC function: Synaptic plasticity and neuronal injury. *Neuropharmacology* 94: 42-48.
- Jin, M., S. Aibar, Z. Q. Ge, R. Chen, S. Aerts *et al.*, 2016 Identification of novel direct targets of *Drosophila* *Sine oculis* and *Eyes absent* by integration of genome-wide data sets. *Developmental Biology* 415: 157-167.
- Jones, M. A., and M. Grotewiel, 2011 *Drosophila* as a model for age-related impairment in locomotor and other behaviors. *Experimental Gerontology* 46: 320-325.
- Lehmann, F. O., and J. Bartussek, 2017 Neural control and precision of flight muscle activation in *Drosophila*. *Journal of Comparative Physiology a-Neuroethology Sensory Neural and Behavioral Physiology* 203: 1-14.
- Ma, H. S., and P. H. O'Farrell, 2016 Selfish drive can trump function when animal mitochondrial genomes compete. *Nature Genetics* 48: 798-+.

- Mackay, T. F., and W. Huang, 2018 Charting the genotype–phenotype map: lessons from the *Drosophila melanogaster* Genetic Reference Panel. Wiley Interdisciplinary Reviews: Developmental Biology 7.
- Mackay, T. F. C., S. Richards, E. A. Stone, A. Barbadilla, J. F. Ayroles *et al.*, 2012 The *Drosophila melanogaster* Genetic Reference Panel. Nature 482: 173-178.
- Manolio, T. A., F. S. Collins, N. J. Cox, D. B. Goldstein, L. A. Hindorff *et al.*, 2009 Finding the missing heritability of complex diseases. Nature 461: 747-753.
- Marcus, J. M., 2001 The development and evolution of crossveins in insect wings. Journal of Anatomy 199: 211-216.
- Montooth, K. L., A. G. Clark and J. H. Marden, 2000 Physiological genetics of flight performance in *Drosophila melanogaster*. American Zoologist 40: 1135-1136.
- Montooth, K. L., C. D. Meiklejohn, D. N. Abt and D. M. Rand, 2010 Mitochondrial–nuclear epistasis affects fitness within species but does not contribute to fixed incompatibilities between species of *Drosophila*. Evolution: International Journal of Organic Evolution 64: 3364-3379.
- Morgante, F., P. Sorensen, D. A. Sorensen, C. Maltecca and T. F. C. Mackay, 2015 Genetic Architecture of Micro-Environmental Plasticity in *Drosophila melanogaster*. Scientific Reports 5.
- Mossman, J. A., L. M. Biancani, C. T. Zhu and D. M. Rand, 2016 Mitonuclear Epistasis for Development Time and Its Modification by Diet in *Drosophila*. Genetics 203: 463-+.
- Nakka, P., B. J. Raphael and S. Ramachandran, 2016 Gene and Network Analysis of Common Variants Reveals Novel Associations in Multiple Complex Diseases. Genetics 204: 783-+.
- Ortega-Ramirez, A., R. Vega and E. Soto, 2017 Acid-Sensing Ion Channels as Potential Therapeutic Targets in Neurodegeneration and Neuroinflammation. Mediators of Inflammation.
- Piazza, N., B. Gosangi, S. Devilla, R. Arking and R. Wessells, 2009 Exercise-Training in Young *Drosophila melanogaster* Reduces Age-Related Decline in Mobility and Cardiac Performance. Plos One 4.
- Pitchers, W., J. Nye, E. J. Marquez, A. Kowalski, I. Dworkin *et al.*, 2019 A Multivariate Genome-Wide Association Study of Wing Shape in *Drosophila melanogaster*. Genetics 211: 1429-1447.
- Purcell, S., B. Neale, K. Todd-Brown, L. Thomas, M. A. R. Ferreira *et al.*, 2007 PLINK: A tool set for whole-genome association and population-based linkage analyses. American Journal of Human Genetics 81: 559-575.
- Rand, D. M., R. A. Haney and A. J. Fry, 2004 Cytonuclear coevolution: the genomics of cooperation. Trends Ecol Evol 19: 645-653.
- Reyna, M. A., M. D. M. Leiserson and B. J. Raphael, 2018 Hierarchical HotNet: identifying hierarchies of altered subnetworks. Bioinformatics 34: 972-980.
- Rhodenizer, D., I. Martin, P. Bhandari, S. D. Pletcher and M. Grotewiel, 2008 Genetic and environmental factors impact age-related impairment of negative geotaxis in *Drosophila* by altering age-dependent climbing speed. Experimental Gerontology 43: 739-748.
- Suarez, R. K., 2000 Energy metabolism during insect flight: biochemical design and physiological performance. Physiological and Biochemical Zoology 73: 765-771.

- Tinkerhess, M. J., S. Ginzberg, N. Piazza and R. J. Wessells, 2012 Endurance Training Protocol and Longitudinal Performance Assays for *Drosophila melanogaster*. Jove-Journal of Visualized Experiments.
- Turner, T. L., P. M. Miller and V. A. Cochrane, 2013 Combining Genome-Wide Methods to Investigate the Genetic Complexity of Courtship Song Variation in *Drosophila melanogaster*. *Molecular Biology and Evolution* 30: 2113-2120.
- Vigoreaux, J. O., 2001 Genetics of the *Drosophila* flight muscle myofibril: a window into the biology of complex systems. *Bioessays* 23: 1047-1063.
- Wallace, D. C., 2005 A mitochondrial paradigm of metabolic and degenerative diseases, aging, and cancer: A dawn for evolutionary medicine, pp. 359-407 in *Annual Review of Genetics*.
- Wallace, D. C., 2010 Bioenergetics, the origins of complexity, and the ascent of man. *Proceedings of the National Academy of Sciences of the United States of America* 107: 8947-8953.
- Zhu, C. T., P. Ingelmo and D. M. Rand, 2014 GxGxE for Lifespan in *Drosophila*: Mitochondrial, Nuclear, and Dietary Interactions that Modify Longevity. *Plos Genetics* 10.



## **ACKNOWLEDGEMENTS**

This work was made possible by the personal and academic support I received throughout this process. This support meant the most when my family, friends, advisor and lab mates, committee members, Brown Ecology and Evolutionary Biology (EEB) community, doctors and therapists, and many others rallied around me after I was hit head on by a car while cycling. I sustained a severe concussion and extensive physical injuries that made me a charismatic vegetable with limited mobility for most of a year. Thanks to everyone's help, understanding, and accommodations over the years as I worked back to where I was before the accident. Because of this, I can present the work I've done since then instead of surrendering to a highly unfortunate situation.

An immeasurable thank you to my family for their sacrifices, contributions, and encouragement. Thank you to my late grandparents, Mary and Harry Spierer & Sylvia and David Goldfarb, for living out the American dream and instilling a high value in education in our family that found its way to me. Thank you to my parents, Shelley and Joe Spierer, for fostering a lifelong sense of curiosity, encouraging a love of the natural world and physical activity, and creating a loving and supportive environment that allowed me to flourish. Thank you to my siblings, Hannah and Eric Spierer, for their thoughtfulness, positivity, and friendship and to my sister-in-law, Jessica Spierer, for her warmth and enthusiasm with every interaction. A shout out to Rhody, my fluffy partner in crime who was all too willing to provide a welcome distraction, and to Squishy, my 16 year old leopard gecko who kept me company when I was awake later than I wanted.

Also a shout out to my nephew (David Spierer; Eric x Jess) for being a cute and wiggly human that also provided a welcome distraction in the final throes of this work.

Thank you to countless friends whose support and companionship have kept me sane throughout the process. Thank you to many friends from Colby College (especially Charlie Wulff, Jamie Suzuki, and Sarah Nalven) who were among the most influential in my academic, athletic, and social lives. Thank you to my cohort mates (David Boerma, Robbie Lamb, Cat Munro, Priya Nakka, Kim Neil, Brooke Osborne, Kara Pellowe, and David Sleboda) and honorary cohort mates (KC Cushman and Emily Hollenbeck) for making my transition and time at Brown enjoyable and productive. And thank you to the many waves of friends I have made from my department (including Nikole Bonacorsi, John Capano, Elska Kaczmarek, and Morgan Turner), Brown, and Providence (including Jessica Boerma, Greg Martin, and Johana Montalvo Lamb) as a whole!

Thank you to Julie Millard for taking me into her research lab and serving as one of my advisors while I was at Colby College. Her guidance was instrumental in helping me get to where I am today and her friendship is one I treasure. Thank you to Judy Stone, Josh Kavalier, Kevin Rice, Ethan Kohn, and all the other professors I had at Colby for working with me as I came into my own.

Thank you to my lab mates (Jim Mossman, Shawn Williams, Kim Neil, Denise Yoon, Marissa Holmbeck, Leann Biancani, and Faye Lemieux), research floor (including Aleksandra Norton, Rochele Yamamoto, and Stephanie Post), and the Brown Fly

(including Leila Reider, Brian Jones, and Kathryn Russo) community who made life more enjoyable and my research more fruitful. And especially big shout out to Jim Mossman for being a great officemate, collaborator, mentor, and friend and for being there for me as I rode my various intellectual and emotional rollercoasters. Thank you to my many collaborators (RJ Wessells and Aly Sujkowski, Sam Smith, Lorin Crawford, Sohini Ramachandran, Kathryn Russo, and my IGERT team(s)) for accepting/extending invitations to enhance the scope of our respective research programs. Thank you to the administrative staff in EEB (Shannon Silva, Alexandria Collins, Lianne Mendonca, Kim Abbott, Danielle Leona-Camara, Irena Nedeljkovic, and Jesse Marsh) and the BioMed Office for Graduate and Postdoctoral Studies (OGPS; Tracey Cronin, Brenda Slaney, Cheryl Whiteside) for setting up infrastructure that allowed me succeed as a student and for saving me from myself more times than I care to admit. And thank you to the Deans (Andrew Campbell, Beth Harrington, and Vanessa Ryan) who helped guide and enable me during my time at Brown.

Thank you to my past teammates (from Executive Swim Club, Colby Swim and Dive Team), coaches, workout/swim partners, and the Brown Recreation fitness community for providing me a physical, social, and stress-reducing outlet that I've carried with me over the years. Thank you to my Astronaut Training club members, past and present, who helped me start/continue the social workout group, encouraged me to become a certified instructor, and continued to support me in my classes. An especially big thank you to Becca Thorsness for being there from the club's infancy, helping me navigate my

free group fitness initiative from start to finish, and most of all for being a great friend, listener, enabler, and cycling partner/COVID-19 social distancing walking buddy.

A huge thank you to my committee members, Sohini Ramachandran, Tom Roberts, and Marc Tatar. Each helped me develop and refine an important facet of the scientist and person that I have become since beginning at Brown. Sohini introduced me to command line-based programming and helped humanize my time in Graduate School. Tom gave me the confidence to pursue micro-computer and circuit tinkering, which was an academic and intellectual curiosity of mine that ultimately reduced experimental time and stress. Marc challenged me to think much differently about what constitutes “good” and “interesting” science and provided the encouragement and guidance about all things cycling (road riding, racing, and recovering from a bad crash). Most of all, I am most grateful for their patience (as a group and individuals) at various times in my journey—especially mid and post-concussion.

Finally, an all caps THANK YOU to David Rand. There is a lot I am grateful for and this acknowledgement page would go on indefinitely if I listed it all, but I am most appreciative of his kindness and compassion when I was at my most vulnerable. I am thankful that he stood by me when my future was uncertain and again as I recalibrated my research direction and focus going into my fourth year. His patience and guidance when I was lost and assistance in channeling my enthusiasm when I was not, will always be remembered. Looking back on this body of work, I am very proud of what

we've accomplished and am glad to have him as a mentor, partner, and friend throughout.

To everyone who has accompanied me on this journey, thank you! These last seven years have been quite the trip and I am fortunate to have had such an extensive support system to help me through it all.

PS. An anti-acknowledgement to SARS-CoV-2 (COVID-19) for creating a pandemic that has sowed social discord, turmoil, and economic uncertainty—especially as I graduate.

## TABLE OF CONTENTS

PREFACE AND ACKNOWLEDGEMENTS.....	vii
LIST OF TABLES.....	xxiii
LIST OF ILLUSTRATIONS.....	xxiv
<b>CHAPTER 1.</b> Natural variation in the regulation of neurodevelopmental genes modifies flight performance in <i>Drosophila</i> .....	1
<b>CHAPTER 2.</b> The Genetic Architecture of Robustness for Flight Performance in <i>Drosophila</i> .....	74
<b>CHAPTER 3.</b> Mito-Nuclear Interactions Modify <i>Drosophila</i> Exercise Performance.....	132
<b>CHAPTER 4.</b> FreeClimber: Automated High Throughput Quantification of Climbing Performance in <i>Drosophila</i> , with Examples from Mitonuclear Genotypes.....	150

**LIST OF TABLES**

CHAPTER 1

**Table 1.** Six additive variants surpassed the Bonferroni significance threshold ..... 58

**Table 2.** Aggregated gene and variant counts by sex-based phenotype for each analysis.....59

**Supplemental Tables 1-18 and Supplemental Files 1-3**.....60

CHAPTER 2

**Table 1.** Different approaches uncover different types of genetic modifiers affecting the focal phenotype..... 112

**Table 2.** Eight additive variants passed the Bonferroni threshold..... 113

**Table 3.** Each analysis and sex-based phenotype identified varying enrichment for genetic modifiers.....114

**Table 4.** Significant variants are non-uniformly distributed across site classes....115

**Table 5.** Summary of top marginal variants, representing these variants more likely to interact with other variants, significant for robustness for flight performance....116

**Supplemental Tables 1-10**.....118

CHAPTER 3

**Table 1.** Repeated measures analysis of climbing speed by genotype, training and age..... 136

**Table 2.** ANOVAs of Endurance by Genotype and Training..... 139

**Table 3.** Post-training assessment..... 145

CHAPTER 4

**Table S1.** Experimental variables available for modification in FreeClimber.....171

**Table S2.** Mitochondrial haplotype significantly impacted climbing performance..172

## LIST OF ILLUSTRATIONS

### CHAPTER 1

<b>Figure 1.</b> DGRP lines show differences in flight performance across lines.....	61
<b>Figure 2.</b> Variation in flight performance associated with several additive variants, some of which were functionally validated.....	62
<b>Figure 3.</b> PEGASUS_flies identifies different genetic modifiers than the additive screen.....	63
<b>Figure 4.</b> Flight performance is a larger complex trait comprised of several smaller traits.....	64
<b>Figure S1.</b> DGRP lines' mean flight performance is highly repeatable across generations.....	65
<b>Figure S2.</b> Sex-average and sex-difference phenotypic distributions are amenable to an association study.....	66
<b>Figure S3.</b> QQ-plots show enrichment for some additive variants across each of the sex-based phenotypes.....	67
<b>Figure S4.</b> Top additive associations are spaced throughout the genome.....	68
<b>Figure S5.</b> Additional sex-based phenotype Manhattan plots for additive analysis.....	69
<b>Figure S6.</b> Genetic crosses performed for deriving experimental and control stocks used to validate candidate genes.....	70
<b>Figure S7.</b> Significant whole genes are distributed throughout the genome and sex-based phenotypes.....	71
<b>Figure S8.</b> Significant marginal variants are unevenly distributed across sex-based phenotypes.....	72
<b>Figure S9.</b> Trait-relationship correlation matrix shows no correlation between measured phenotypes and young adult transcriptome.....	73

### CHAPTER 2

<b>Figure 1.</b> The <i>Drosophila</i> Genetic Reference Panel lines demonstrate variation for robustness in flight performance across genotypes and sexes.....	119
<b>Figure 2.</b> Several genes validated for robustness of flight performance.....	120



<b>Figure 3.</b> Several genetic variants positively associate with flight performance across different types of analyses.....	121
<b>Figure 4.</b> Robustness of flight performance is comprised of an interconnected genetic architecture.....	122
<b>Figure S1.</b> Coefficient of variation is near-normally distributed across sexes.....	123
<b>Figure S2.</b> Phenotypic distributions for sex-average and sex-difference phenotypes.....	124
<b>Figure S3.</b> Significant variants in additive analysis by sex-based phenotype.....	125
<b>Figure S4.</b> Quantile-quantile (QQ) plots suggest several additive variants associate with robustness in flight performance.....	126
<b>Figure S5.</b> Significant additive variants are broadly distributed across the genome.....	127
<b>Figure S6.</b> Non-synonymous variant (3R_4379159_SNP) in <i>Odorant receptor 85d</i> lies in a strongly conserved region across several insect species.....	128
<b>Figure S7.</b> <i>Drosophila</i> crossing scheme used to generate control and experimental lines for candidate gene validation.....	129
<b>Figure S8.</b> Several whole genes were identified across each sex-based phenotype using PEGASUS_flies.....	130
<b>Figure S9.</b> Significant marginal variants were identified across each sex-based phenotype.....	131

## CHAPTER 3

<b>Figure 1.</b> Mito-nuclear interactions differentially modulate climbing speed during endurance exercise.....	138
<b>Figure 2.</b> Acute climbing speed is affected by both nuclear and mitochondrial genotype in <i>Drosophila</i> .....	141
<b>Figure 3.</b> Exercise training increases endurance in <i>Drosophila</i> with matched nuclear and mitochondrial genotypes.....	142
<b>Figure 4.</b> Exercise increases endurance independent of mito-nuclear	

mismatch.....	143
<b>Figure 5.</b> Mito-nuclear incompatibility negatively impacts cardiac health.....	144
<b>Figure 6.</b> Enhancements in flight performance are weakly affected by mito-nuclear interactions.....	147
<b>Figure 7.</b> Mito-nuclear interactions strongly affect lysosomal activity in <i>Drosophila</i> fat body after endurance exercise.....	148
<b>Figure 8.</b> Citrate Synthase Specific Activity parallels climbing speed and endurance in closely-related <i>Ra</i> and <i>La</i> lines.....	149

#### CHAPTER 4

<b>Figure 1.</b> Overview of FreeClimber platform.....	174
<b>Figure 2.</b> Method comparison demonstrates a local linear regression is more biologically relevant than quantifying height after 2 seconds of climbing.....	175
<b>Figure 3.</b> Mitochondrial haplotypes show a differential response to endurance exercise training and resistance to endurance fatigue.....	176
<b>Figure S1.</b> Experimental set ups for exercise conditioning <i>Drosophila</i> and assaying climbing performance.....	177
<b>Figure S2.</b> Individual mitotype performance vs. time curves.....	178

## **Chapter 1**

*Natural variation in the regulation of neurodevelopmental genes  
modifies flight performance in Drosophila*

Adam N. Spierer, Jim A. Mossman, Samuel A. Smith, Lorin Crawford,  
Sohini Ramachandran, David M. Rand

Modified from submission to *PLoS Genetics* (in prep)

## Abstract

The winged insects of the order *Diptera* are colloquially named for their most recognizable phenotype: flight. These insects rely on flight for a number of important life history traits, like dispersal, foraging, and courtship. Despite the importance of flight, relatively little is known about the genetic architecture of variation for flight performance. Accordingly, we sought to uncover the genetic modifiers of flight using a measure of flies' reaction and response to an abrupt drop in a vertical flight column. We conducted an association study using 197 of the *Drosophila* Genetic Reference Panel (DGRP) lines, and identified a combination of additive and marginal variants, epistatic interactions, whole genes, and enrichment across interaction networks. We functionally validated 13 of these candidate genes' (*Adgf-A/Adgf-A2/CG32181*, *bru1*, *CadN*, *CG11073*, *CG15236*, *CG9766*, *CREG*, *Dscam4*, *form3*, *fry*, *Lasp/CG9692*, *Pde6*, *Snoo*) contribution to flight, two of which (*fry* and *Snoo*) also validate a whole gene analysis we introduce for the DGRP: PEGASUS\_flies. Overall, our results suggest modifiers of muscle and wing morphology, and peripheral and central nervous system assembly and function are all important for flight performance. Additionally, we identified *ppk23*, an Acid Sensing Ion Channel (ASIC) homolog, as an important hub for epistatic interactions. These results represent a snapshot of the genetic modifiers affecting drop-response flight performance in *Drosophila*, with implications for other insects. It also draws connections between genetic modifiers of performance and BMP signaling and ASICs as targets for treating neurodegeneration and neurodysfunction.

## Introduction

Flight is one of the most distinguishing features of winged insects, especially the taxonomic order *Diptera*. Colloquially named “flies,” these insects rely on their namesake for many facets of their life history: dispersal, foraging, evasion, migration, and mate finding (BRODSKY 1994). Because flight is central to flies’ life history, many of the most critical genes for flight are strongly conserved (EDWARDS 1997; UGUR *et al.* 2016).

These “flight-critical” genes are necessary for flight, even as the structures and neural circuits they form are co-opted for other phenotypes, like courtship song and display (PAVLOU AND GOODWIN 2013; WEITKUNAT AND SCHNORRER 2014). For example, *Wingless* is an important developmental patterning gene necessary for wing formation (QUIJANO *et al.* 2010) and *Act88F* is one of the main actin isoforms in the indirect flight muscles (NONGTHOMBA *et al.* 2001). We will designate these types of genes that play outsized roles in enabling flight “flight critical” genes, since altering their sequence or expression profile is more likely to result in large flight performance deficits. On the other hand, we will designate “flight-important” genes as those with more modest effects on flight, since they are important but not critical. In an evolutionary context, purifying selection would act on flight-critical genes more strongly than flight-important genes, meaning flight-important genes can harbor natural variants that might otherwise vary the flight phenotype. These genes are found across systems, including metabolism (MONTTOOTH *et al.* 2003), muscle function (KAO *et al.* 2019), neuronal function (FRYE AND DICKINSON 2004a; LEHMANN AND BARTUSSEK 2017), and anatomical development (MARCUS 2001;

OKADA *et al.* 2016). Genes filling multiple roles across systems are pleiotropic, and those with sufficient natural variation are likely to contribute to complex traits and disease (LOBELL *et al.* 2017; WATANABE *et al.* 2019). These traits and diseases' independent, yet interconnected, genetic architecture make them inherently challenging to study because they are comprised of several modifiers of small to moderate effect size (McCARTHY *et al.* 2008; MANOLIO *et al.* 2009; McCLELLAN AND KING 2010).

We can leverage natural variants in flight-important genes to uncover novel associations between genotype and phenotype that otherwise modify flight-critical genes' function, via Genome Wide Association Study (GWAS). The *Drosophila* Genetics Reference Panel (MACKAY *et al.* 2012; HUANG *et al.* 2014) (DGRP) is a common resource for performing this type of analysis. The DGRP is a panel of 205 genetically distinct *D. melanogaster* lines represents a snapshot of natural variation. Previous studies on complex and highly polygenic, quantitative traits identify several candidate loci contributing to insect- and *Drosophila*-specific traits (CHOW *et al.* 2013; ARYA *et al.* 2015; BATTLEAY *et al.* 2018), as well as traits affecting human health and disease (MONTGOMERY *et al.* 2014; CARBONE *et al.* 2016; CHOW *et al.* 2016; ZHOU *et al.* 2016).

Accordingly, this study was designed to identify the genetic modifiers of flight performance and map the underlying genetic architecture. We screened males and females from 197 of the 205 DGRP lines and analyzed both sexes, as well as the average and difference between sexes. Traditional association studies focus on the contribution of additive and dominant variants, however, these fail to identify different

types of modifiers with different effect sizes. Accordingly, we took several approaches to identify modifiers at the individual variant, whole gene, and network levels. Accordingly, we identified 180 additive variants, 70 marginal variants, 12161 unique epistatic interactions, and nine interaction sub-networks containing 539 genes contributing to flight performance. We also identified 72 whole genes using PEGASUS\_flies, a novel modification of the human-based PEGASUS program (NAKKA *et al.* 2016) that we modified to work with *Drosophila* and DGRP studies <[https://github.com/ramachandran-lab/PEGASUS\\_flies](https://github.com/ramachandran-lab/PEGASUS_flies)> (File S4).

Taken together, our results strongly suggest variation in flight performance across natural populations is affected by cis- and trans-regulatory elements' role in modifying 1) development of wing morphology, indirect flight musculature, and sensory organs; and 2) the connectivity between the peripheral and central nervous systems. These results are further supported by functional validations of 13 candidate genes, many with known roles in altering neurogenesis and development. Overall, our results suggest important roles for modifiers of BMP signaling in neurodevelopment and pickpocket 23 (ppk23)—a degenerin/epithelial sodium channels (DEG/ENaC) homologous in humans with Acid Sensing Ion Channels (ASIC)—in altering affecting flight performance. These findings address an underexplored body of literature (XIONG AND XU 2012; PINTO *et al.* 2013; HUANG *et al.* 2015b; DESHPANDE *et al.* 2016) calling for genetic and pharmacological targets of BMP signaling genes and ASIC for treating neuroinjury and neurodegenerative diseases in humans.

## Methods

### *Drosophila Stocks and Husbandry*

All stocks were obtained from Bloomington *Drosophila* Stock Center (<https://bdsc.indiana.edu/>), including 197 *Drosophila* Genetic Reference Panel (DGRP) lines (HUANG *et al.* 2014), 23 *Drosophila* Gene Disruption Project lines using the Mi{ET1} construct (METAXAKIS *et al.* 2005a; BELLEN *et al.* 2011a), and two genetic background lines ( $w^{1118}$  and  $y^1w^{67c23}$ ; Table S1).

Flies were reared at 25° under a 12-h light-dark cycle. Stocks were density controlled and grown on a standard cornmeal media (ELGIN AND MILLER 1978). Two to three days post-eclosion, flies were sorted by sex under light CO<sub>2</sub> anesthesia and given five days to recover before phenotyping.

### *Flight performance assay*

Flight performance was measured following the protocol refined by Babcock and Ganetzky (BABCOCK AND GANETZKY 2014). Briefly, each sex-genotype combination consisted of 100 flies, divided into groups of 20 flies across five glass vials. These vials were gently tapped to draw flies down, and unplugged before a rapid inversion down a 25 cm chute. Vials stopped at the bottom, ejecting the flies into a 100 cm long x 13.5 cm diameter cylinder lined with a removable acrylic sheet coated in TangleTrap adhesive. Free falling flies instinctively right themselves before finding a place to land, which ended up immobilizing them at their respective landing height.



After all vials in a run were released, the acrylic sheet was removed and pinned to a white poster board. A digital image was recorded on a fixed Raspberry PiCamera (V2) and the x,y coordinates of all flies were located with the ImageJ/FIJI Find Maxima function with a noise tolerance of 30 (SCHINDELIN *et al.* 2012). For each sex-genotype combination, the mean landing height was calculated for only the flies that landed on the acrylic sheet.

#### High-speed video capture of flight column

High-speed videos of flies leaving the flight column were recorded at 1540 frames per second using a Phantom Miro m340 camera recording at a resolution of 1920 x 1080 with an exposure of 150  $\mu$ s (Data available in File S1). The camera was equipped with a Nikon Micro NIKKOR (105 mm, 1:2.8D) lens and Veritas Constellation 120 light source.

#### Estimating heritability

Individual fly landing heights were adjusted for covariate status by adding the difference between the DGRP webserver's adjusted and raw line means for each sex, and added them back to the individual landing height of the respective sex and genotype. Using these adjusted landing heights by sex, we performed a random effects analysis of variance using the R (v.3.5.2) package lme4 (v.1.1.23):  $Y \sim \mu + L + \varepsilon$ . Here,  $Y$  is the adjusted flight score,  $\mu$  is the combined mean,  $L$  is the line mean, and  $\varepsilon$  is the residual. From this, sex-specific broad sense heritability ( $H^2$ ) estimates were calculated from the among line ( $\sigma_L^2$ ) and error ( $\sigma_E^2$ ) variance components:  $H^2 = \sigma_L^2 / (\sigma_L^2 + \sigma_E^2)$ .

### Genome wide association mapping

Flight performance scores for males and females were submitted to the DGRP2 GWAS pipeline (<http://dgrp2.gnets.ncsu.edu/>) (MACKAY *et al.* 2012; HUANG *et al.* 2014) and results for each sex, and the average (sex-average) and difference (sex-difference) between them were all considered (Table S3). In total, 1,901,174 variants with a minor allele frequency (MAF)  $\geq 0.05$  were analyzed (Data available in File S2). All reported additive variant *P*-values result from a linear mixed model analysis, including *Wolbachia* infection and presence of five major inversions as covariates. Variants were filtered for significance using the conventional  $P \leq 1E-5$  threshold (MACKAY AND HUANG 2018). Effect size estimates were calculated as one-half the difference between the mean landing heights for lines homozygous for the major vs. minor allele. The contribution of individual variants to the overall effects was estimated as the absolute value of an individual variant's effect size divided by the sum of the absolute values for all conventionally significant ( $P < 1e-5$ ) variants' effect sizes.

### Candidate gene disruption screen

Candidate genes were validated using insertional mutant stocks generated from Gene Disruption Project (BELLEN *et al.* 2011b). These stocks contain a *Minos* enhancer trap construct Mi{ET1}(METAXAKIS *et al.* 2005b) and were built on either  $w^{1118}$  or  $y^1 w^{67c23}$  backgrounds (BDSC\_6326 and BDSC\_6599, respectively).

Control and experiment line genetic backgrounds were isogenized with five successive rounds of backcrossing the insertional mutant line to its respective control. Validation of

flight phenotypes was done using offspring of single-pair (1M x 1F) crosses between the control and insert lines. Heterozygous flies from these crosses were mated in pairs and the homozygous offspring lacking the insertion were collected as the control. Candidate heterozygous/homozygous positive lines were mated as pairs once more and lines producing only homozygous positive offspring were used as experimental lines (Figure S1). Experimental lines were checked for a GFP reporter three generations later to confirm their genotype. The finalized recombinant backcrossed control and experimental lines for each sex-genotype combination were assayed for flight performance, and tested for significance, via Mann-Whitney U-tests.

#### Calculating gene-score significance

Gene-scores were calculated using Precise, Efficient Gene Association Score Using SNPs (PEGASUS) (NAKKA *et al.* 2016). Originally implemented with human datasets, we modified the program to work with *Drosophila* datasets, which we call PEGASUS\_flies. It also contains default values adjusted for *Drosophila*, a linkage disequilibrium file, and gene annotations drawn from the FB5.57 annotation file, available on the DGRP webserver. PEGASUS\_flies is available at: [https://github.com/ramachandran-lab/PEGASUS\\_flies](https://github.com/ramachandran-lab/PEGASUS_flies), and as File S4.

#### Identifying altered sub-networks of gene-gene and protein-protein interaction networks

Returned gene-scores were filtered for genes of high confidence using the Twilight package (v.1.60.0) in R (Scheid and Spang 2005). Here, we estimated the local False Discovery Rate (lFDR) of all previously output gene scores using the *twilight* function.

Taking the inflection point of the  $(1 - \text{IFDR})$  curve, our high-confidence gene scores ranged from 0.65 – 0.73 for the four, sex-based phenotypes (Table S8). High confidence genes were  $-\log_{10}$  transformed, while the remaining were set to 0.

Hierarchical HotNet was used to identify altered sub-networks of interacting genes or proteins (REYNA *et al.* 2018) based on network topology generated from several gene-gene or protein-protein interaction networks. The four adjusted, sex-based gene-score vectors were mapped in the program to fifteen interaction networks obtained from High-quality INTeractomes (HINT)(DAS AND YU 2012), the *Drosophila* Interactions Database (Droidb)(YU *et al.* 2008; MURALI *et al.* 2011), and the *Drosophila* RNAi Screening Center (DRSC) Integrative Ortholog Prediction Tool (DIOPT)(Hu *et al.* 2011a). Consensus networks were calculated from 100 permutations of all four gene-score vectors on each of the fifteen interaction networks and filtered to include at least three members. The largest sub-network and the remaining eight sub-networks were passed to Gene Ontology enRIchment anaLysis and visualIzAtion tool (GORilla) to identify enrichment for gene ontology (GO) categories (EDEN *et al.* 2007; EDEN *et al.* 2009).

### Screening for epistatic interactions

Epistatic hub genes were identified using MArginal ePIstasis Test (MAPIT), a linear mixed modeling approach that tests the significance of each SNP's marginal effect on a chosen phenotype. MAPIT requires a complete genotype matrix, without missing data. SNPs were imputed using BEAGLE 4 . 1 (BROWNING AND BROWNING 2007; BROWNING AND

BROWNING 2016) and then filtered for  $MAF \geq 0.05$  using `VCFtools` (v.0.1.16) (DANECEK *et al.* 2011). `MAPIT` was run using the Davies method on the imputed genome (File S2), DGRP2 webserver-adjusted phenotype scores for each sex-based phenotype (Table S2), DGRP2 relatedness matrix, and covariate file containing *Wolbachia* infection and the presence of five major inversions.

Resulting marginal effect  $P$ -values (data available File S3) were filtered to a Bonferroni threshold ( $P \leq 2.56e-8$ ) and tested for pairwise epistatic interactions in a set-by-all framework against the initial 1,901,174 SNPs (unimputed;  $MAF \geq 0.05$ ) using the `PLINK` `-epistasis` flag (v.1.90)(PURCELL *et al.* 2007). Results were filtered for all  $P$ -values that exceeded a Bonferroni threshold, calculated as  $0.05 / (\text{the number of Bonferroni marginal effect } P\text{-values} \times 1,901,174 \text{ SNPs})$ .

#### Annotating FBgn and orthologs

Flybase gene (FBgn) identifiers were converted to their respective *D. melanogaster* (Dmel) or *H. sapiens* (Hsap) gene symbols using the *Drosophila* RNAi Stock Center (DRSC) Integrative Ortholog Prediction Tool (DIOPT)(Hu *et al.* 2011b). FBgn were filtered for all high to moderate confidence genes, or low confidence genes if they contained the best forward and reverse score.

#### Calculating an empirically simulated significance threshold

We sought to simulate an empirically derived significance threshold that was unique to our data set and separate from the traditional DGRP and Bonferroni thresholds used in

other studies. Using the genotype-phenotype matrix, two separate datasets were simulated ( $n = 1000$ ) for each sex-based phenotype. The first randomized the genotype-phenotype matrix using all available line means, while the second randomized subsets of 150 genotype-phenotype pairs.

Simulated associations were run with PLINK (PURCELL *et al.* 2007)(v.1.90) on each dataset type for each sex-based phenotype. The 5<sup>th</sup> percentile most-significant  $P$ -value across all permutations in a simulation type was deemed the “empirically simulated significance threshold.”

#### GO term analysis

GOWINDA (KOFILER AND SCHLÖTTERER 2012) was implemented to perform a Gene Ontology (GO) analysis that corrects for gene size in GWA studies. We conducted this analysis for male ( $n=418$ ), female ( $n=473$ ), sex-average ( $n=527$ ), and sex-difference ( $n=214$ ) candidate SNPs exceeding a relaxed  $P < 1E-4$  significance threshold, against the 1,901,174 SNPs with  $MAF \geq 0.05$ . We ran 100,000 simulations of GOWINDA using the gene mode and including all SNPs within 2000 bp.

Gene Ontology enRiChment anaLysis and visualizAtion tool (GORilla)(EDEN *et al.* 2007; EDEN *et al.* 2009) was run on PEGASUS\_flies gene-scores and Hierarchical Hotnet sub-networks using the default commands and a gene list compiled from all genes available in the FB5.57 annotation file.

### Weighted Gene Co-expression Network Analysis

To test whether ambient adult transcriptomes could explain the observed phenotypic variation, we turned to the publically available DGRP2 microarray data, downloaded from the DGRP2 webserver (HUANG *et al.* 2014). These data represent the transcriptomes for untreated young adult flies of each sex. We performed Weighted Gene Co-expression Network Analysis (WGCNA) analyses using the available R package (LANGFELDER AND HORVATH 2008) to cluster and correlate the expression profiles of genes from 177 shared, DGRP lines. This analysis was run using the following parameters: power = 16 (from soft threshold analysis  $\geq 0.9$ ), merging threshold = 0.0, signed network type, maximum blocksize = 1000, minimum module size = 30.

### Data availability

All data required to rerun the outlined analyses either publically available through FlyBase (<http://flybase.org/>) (GRUMBLING *et al.* 2006; CHINTAPALLI *et al.* 2007b; DOS SANTOS *et al.* 2015), the DGRP2 webserver (<http://dgrp2.gnets.ncsu.edu/>), or available as a Supplemental File.

## Results

### Variation in flight performance across the DGRP

Cohorts of approximately 100 flies from 197 lines of the DGRP (Table S1) were tested for flight performance using a flight column (BABCOCK AND GANETZKY 2014) (Figure 1A).

We confirmed the repeatability of our assay by retesting 12 lines of varied ability reared 10 generations apart. We observed very strong agreement between generations ( $r = 0.95$ ; Figure S1), affirming a role for genetic, rather than environmental or experimental, variation in driving phenotypic variation. We recorded high-speed videos for a weak, intermediate, and strong genotype entering the flight column (Figure 1B-D; File S1) and concluded this assay is best for studying the reaction and response to an abrupt drop.

There was strong agreement between sex-pairs' mean landing height for each genotype ( $r = 0.75$ ; Figure 1E), suggesting the genetic architecture is mostly shared between the sexes. As expected, there was a modest degree of sexual dimorphism in performance, with males outperforming females (male:  $0.80\text{m} \pm 0.06$  SD; female:  $0.73\text{m} \pm 0.07$  SD; Figure 1F; Table S2), though the broad sense heritability ( $H^2$ ) for each sex was nearly the same ( $H^2_{Male} = 13.5\%$ ;  $H^2_{Female} = 14.4\%$ ). In addition to males and females, we also investigated the phenotypic variation in the average (sex-average) and difference (sex-difference) between sexes (Figure S2).

Before running the association analysis, we tested whether flight performance was a unique phenotype. We compared our phenotype scores for males and female against publically available phenotypes on the DGRP2 webserver. We found no significant regression between flight performance and any of the phenotypes in either sex after



correcting for multiple testing ( $P \leq 1.85E-3$ ; Table S3). This negative result suggests our measure of flight performance is a unique phenotype among those reported.

### Association of additive SNPs with flight performance

We conducted a Genome Wide Association Study (GWAS) to identify genetic markers associated with flight performance. We performed an analysis with 1,901,174 common variants ( $MAF \geq 0.05$ ) on the additive genetic effects of four sex-based phenotypes: males, females, sex-average, and sex-difference. Some phenotypes covaried with the presence of major inversions (Table S4), so we analyzed association results using a mixed model (Figure 2A) to account for *Wolbachia* infection status, presence of inversions, and polygenic relatedness (Figures S3-4). Annotations and unreferenced descriptors of genes' functions, expression profiles, and orthologs were gathered from autogenerated summaries on FlyBase (GRUMBLING *et al.* 2006; DOS SANTOS *et al.* 2015). These summaries and descriptors were compiled from data supplied by the Gene Ontology Consortium (ASHBURNER *et al.* 2000; CARBON *et al.* 2019), the Berkeley *Drosophila* Genome Project (FRISE *et al.* 2010), FlyAtlas (CHINTAPALLI *et al.* 2007b), The Alliance of Genome Resources Consortium (CONSORTIUM 2020), modENCODE (DOS SANTOS *et al.* 2015), PAINT (GAUDET *et al.* 2011), the DRSC Integrative Ortholog Prediction Tool (DIOPT) (HU *et al.* 2011b), and several transcriptomics and proteomic datasets (CHINTAPALLI *et al.* 2007b; KARR 2007; MUMMERY-WIDMER *et al.* 2009; BROWN *et al.* 2014; OKADA *et al.* 2016; CASAS-VILA *et al.* 2017; KAO *et al.* 2019).

We filtered additive variants with a strict Bonferroni threshold ( $P \leq 2.63E-8$ ). Taking a MinSNP approach, which identifies significant genes if their lowest (most significant) variant  $P$ -value crosses a threshold (NAKKA *et al.* 2016), we identified six unique variants, five of which mapped to six genes (*CG15236*, *CG34215*, *Dscam4*, *Egfr*, *fd96Ca*, *Or85d*) (Table 1). Variants mapping to *Egfr* and *fd96Ca* also contained known embryonic cis-regulatory elements (transcription factor binding sites (TFBS) and a silencer) (NEGRE *et al.* 2011). Of note, *Dscam4* was deemed “damaged” in 38 of the lines tested (MACKAY *et al.* 2012); however, the difference between mean landing heights of the damaged vs. undamaged lines was less than 1 cm ( $P = 0.32$ , Welch’s T-test).

Using the traditional DGRP significance threshold ( $P \leq 1E-5$ ) (MACKAY AND HUANG 2018), we identified 180 variants across all four sex-based phenotypes (Figures 2B and S5, Table S5). The individual additive variant with the largest effect size contributed 0.045 meters (or 0.97% of the sum of all significant variants) for males and 0.064 meters (1.1% of the sum of all significant variants) for females. For reference, the variant with the smallest significant effect size was  $1.7E-4$  meters (or 0.0036% of the sum of all significant variants) for males and  $5.7E-3$  meters (or 0.095% of the sum of all significant variants) for females. All but 19 variants mapped to intergenic or non-coding regions, which are generally indicative of cis-regulatory regions. Of the non-coding variants, 149 mapped to 136 unique genes across the sex-based analyses (Table 2). These included development and function of the nervous system (*aru*, *CadN*, *ChAT*, *chinmo*, *chn*, *CNMaR*, *CSN6*, *DIP-delta*, *Dscam4*, *Egfr*, *fd96Ca*, *form3*, *fry*, *hll*, *htk*, *jeb*,

*kek2, klg, klu, Mbs, Mmp2, nompC, Or46a, Or85d, Pdp1, Ptp10D, pyd, Rbp6, rut, Sdc, SK, SKIP, Spn, Snoo, Tmc*), neuromuscular junction (*fend, Gad1, Gao/Galphao, jeb, Sdc, Syt1*), muscle (*bru1, bves, CG17839, jeb, Lasp, Pdp1, rhea*), cuticle and wing morphogenesis (*CG15236, CG34220, CG43218, Egfr, frtz, fry, Tg*), endoplasmic reticulum (*CG33110, CG43783, tbc, Vti1b*) and Golgi body functions (*Gmap, Rab30, Vti1b*), and regulation of translation (*mip40, mxt, Rbm13, Wdr37*). Approximately half of all variants were present in two or three sex-based analyses, though the remainder were unique to one (Figure 2B). Several variants mapped to transcription factors (*Asciz, Camta, CG18011, chinmo, chn, Eip78C, fd96Ca, Pdp1, run*) broadly affecting development and neurogenesis (GRUMBLING *et al.* 2006; DOS SANTOS *et al.* 2015). Despite the enrichment for several annotations, we failed to identify any significant gene ontology (GO) categories using GOwinda (KOFLER AND SCHLÖTTERER 2012), a GWAS-specific gene set enrichment analysis.

### General development and neurodevelopmental genes validated to affect flight performance

We performed functional validations on a subset of the genes mapped from variants identified in the Bonferroni and sex-average analysis. We identified 21 unique candidate genes for which a *Minos* enhancer trap *Mi{ET1}* insertional mutation line (METAXAKIS *et al.* 2005b) was publically available (BELLEN *et al.* 2011b) (Table S1; *Adgf-A/Adgf-A2/CG32181, bru1, CadN, CG11073, CG15236, CG9766, CREG, Dscam4, form3, fry, Lasp/CG9692, Pde6, Snoo*). Three additional stocks for *CadN, Dscam4*, and *CG11073* were also tested for their strength of association. Finally, an insertion line for *CREG* was

also included as a negative control, since it was not significant in the additive or subsequent analyses.

Candidate genes were functionally validated by comparing the distribution in mean landing heights of stocks homozygous for the insertion and their paired control counterpart (Figure S6) using a Mann-Whitney-U test (Figures 2C; Table S6). Several were involved in neurodevelopment (*CadN*, *CG9766*, *CG11073*, *CG15236*, *Dscam4*, *form3*, *fry*, and *Snoo*), muscle development (*bru1* and *Lasp*), and transcriptional regulation of gene expression (*Pde6* and *CREG*). Both *CG9766* and *CG11073* are unnamed candidate genes. In validating roles for both these genes, we are naming them *tumbler* (*tumbl*) and *flapper* (*flap*), respectively, based on the tumbling and flapping motions of weaker flies struggling to right themselves in the flight performance assay.

#### Association of gene-level significance and interaction networks with flight performance

The minSNP approach on the additive variants prioritizes the identification of genes containing variants with larger effects (NAKKA *et al.* 2016). However, this approach ignores linkage blocks and gene length, which can bias results. It is important to account for gene length because many neurodevelopmental genes can be lengthy and exceed 100kb (*CadN*, 131kb). One alternative approach is Precise, Efficient Gene Association Score Using SNPs (PEGASUS), which assesses whole gene significance scores based on the distribution of a gene's variant *P*-value distributions with respect to a null chi-squared distribution (NAKKA *et al.* 2016). This approach enriches for whole

genes of moderate effect and enables the identification of genes that might go undetected in a minSNP approach.

While PEGASUS is configured for human populations, we developed PEGASUS\_flies, a modified version for *Drosophila* <[https://github.com/ramachandran-lab/PEGASUS\\_flies](https://github.com/ramachandran-lab/PEGASUS_flies)>. This platform is configured to work with DGRP data sets, and can be customized to accept other *Drosophila*-based or model screening panels. From our additive variants, PEGASUS\_flies identified 72 unique genes across the all sex-based phenotypes, whose gene scores passed a Bonferroni threshold ( $P \leq 3.03E-6$ ; Table S7). These genes were present on five of the six chromosome arms tested (Figure 3A). They were generally different from those identified in the additive approach's minSNP analyses (Figure 3B and S7), though 15 overlapped (*CG17839*, *CG32506*, *CG33110*, *Gmap*, *Mbs*, *Pdp1*, *Rab30*, *VAcHT*, *aru*, *bves*, *fry*, *mip40*, *mxt*, *oys*, *sdk*). The relatively low overlap between these two gene sets is to be expected, since they prioritize variants of large effect vs. whole genes of moderate effect. Overall, genes annotations were enriched for neural development and function (*aru*, *bchs*, *CG13506*, *ChAT*, *Ccn*, *daw*, *dsf*, *Dip-δ*, *dpr6*, *fry*, *fz2*, *Mbs*, *Pdp1*, *sdk*), wing and development (*CycE*, *daw*, *dsx*, *egr*, *fry*, *fz2*, *Gart*, *HnRNP-K*, *Mbs*, *sno*), Rab GTPase activity (*ca*, *CG32506*, *Gmap*, *plx*, *Rab30*), and regulators of transcription (*dsf*, *fry*, *HBS1*, *luna*, *MED23*, *mip40*, *Pdp1*, *Rab30*, *SAP130*, *Tgi*). Different sex-based phenotypes varied in how unique certain whole genes were to a given phenotype (Figure 3C). Genes identified in the sex-average analysis were generally shared with the male and female phenotypes, while genes in the sex-difference analysis were generally unique. Interestingly, *Ccn* was

present in both the male and sex-difference, and *dsf* and *sdk* were both present in the sex-average and sex-difference.

Taking advantage of the gene-level significance scores, we leveraged publicly available gene-gene and protein-protein interaction networks to identify altered sub-networks of genes that connect to the flight performance phenotype. A local False Discovery Rate (lFDR) was calculated for each sex-based phenotype (Table S8), for which gene-scores were either  $-\log_{10}$  transformed if they passed or set to 0 if they did not. Transformed scores for each sex-based phenotype were analyzed together in Hierarchical HotNet (REYNA *et al.* 2018), which returned a consensus network consisting of nine sub-networks of genes (Table S9). The largest network identified 512 genes and was significantly enriched for several GO terms, including transcription factor binding, histone and chromatin modification, regulation of nervous system development, and regulation of apoptosis (Table S10). The other eight networks were comprised of 27 genes, which together had several significant GO terms, including regulation of gene expression through alternative splicing, maintenance of the intestinal epithelium, and the Atg1/ULK1 kinase complex (Table S11).

#### Association of epistatic interactions with flight performance

Epistatic interactions account for a substantial fraction of genetic variation in complex traits (HUANG *et al.* 2012) but they are statistically and computationally challenging to identify. To circumvent the barriers associated with performing an exhaustive, pairwise search across all possible combinations ( $n = 1.81E12$ ), we turned to MArginal ePIstasis

Test (MAPIT) to focus the search area. MAPIT is a linear mixed modeling approach that identifies variants more likely to have an effect on other variants. These putative hub variants represent more central and interconnected genes in a larger genetic network proposed by the Omnigenic Inheritance model (BOYLE *et al.* 2017; LIU *et al.* 2019). Accordingly, we identified 70 unique significant marginal variants exceeding a Bonferroni threshold ( $P \leq 2.56E-8$ ) across male, female, and sex-average phenotypes. The sex-difference analysis yielded no significant variants (Figure S8; Table S12). From these, only 14 had significant epistatic interactions with other variants in the genome (Table S13), which we will discuss in order of the male, female, and sex-average results and contextualized with their epistatic interactions.

In males, there were seven significant marginal variants that mapped to five genes (*CG5645*, *CG18507*, *cv-c*, *sog*, *Ten-a*). Of the variants, only one (X\_15527230\_SNP) that mapped to a novel transcription start site in the BMP antagonist of *short gastrulation* (*sog*; human ortholog of *CHRD*) had significant interactions. This marginal SNP interacted with 42 other variants across 28 unique genes (Table S13). Several of these genes are important in neuron development, signaling, and function (*CG13579*, *Dh31*, *nAChRalpha4*, *Sdc simj*, *sqz*, and *trio*), supporting accumulating evidence of a neurodevelopmental basis for variation in flight performance.

In females, there were 14 significant marginal variants that mapped to six genes (*CG6123*, *CG7573*, *CG42741*, *ppk23*, *Src64B*, *twi*). Of these variants, five mapped to two genes (*CG42671* and *ppk23*) with epistatic interactions. One intronic SNP

(3L\_11217593\_SNP) mapped to *CG42671*. Little is known about this gene and there are no human orthologs, but we can gain insights into its function based on the 51 epistatic variants that mapped to 37 genes with annotations for regulation of gene expression (*arx, bi, CG6843, Ches-1-like, dve, HDAC1, Moe, and RpL26, Sdc, Tgi*), and neural development, signaling, and function (*cact, CG13579, HDAC1, ed, ngl3, nrm, numb, Sdc*). The other four variants (*X\_17459818\_SNP, X\_17459830\_SNP, X\_17460743\_DEL, X\_17460820\_SNP*) mapped to a 1002 bp region downstream of *pickpocket 23 (ppk23)*; human homologs in ASIC gene family). *ppk23* is a member of the degenerin (DEG)/epithial Na<sup>+</sup> channel (ENaC) gene family that functions as subunits of non-voltage gated, amiloride-sensitive cation channels. It is involved in chemo- and mechanosensation, typically in the context of foraging, pheromone detection, and courtship behaviors (ADAMS *et al.* 1998; LU *et al.* 2012). These marginal variants significantly interacted with 2162 variants, which mapped to 1042 genes that were also largely found in the sex-average analysis.

The sex-average phenotype had 62 significant marginal variants (11 also found in females) mapping to 21 genes (*Art2, CG10936, CG15630, CG15651, CG18507, CG3921, CG42671, CG42741, CG5645, CG6123, CG9313, CR44176, cv-c, Fad2, natalisin, ppk23, Rbfox1, Rgk1, Src64B, twi*). Of the 62 marginal variants, 18 had significant epistatic interactions: nine were intergenic, seven mapped to *ppk23*, and the remaining four mapped to single genes: *CG42671, CG10936, CG9313, and CG15651* (Table S13). Previously identified in the female analysis, *ppk23* had the greatest number of interactions, placing it close to the center of a highly interconnected genetic



landscape (Figure 4A). The seven marginal variants interacted with 4895 variants across 2010 unique genes, 11 of which mapped to genes that also contained significant marginal variants (*A2bp1*, *cv-c*, *Fad2*, *CG9313*, *CG10936*, *CG42741*, *Rgk1*, *sog*, *Src64B*, *twi*, *Ten-a*). The 2010 unique genes had significant GO term enrichment for neuronal growth, organization and differentiation (Table S14). One of *ppk23*'s interactors was *CG42671*, itself a gene with a significant marginal variant in the sex-average epistasis screen and previously mentioned in the female epistasis screen. For the sex-average epistasis screen, *CG42671* interacted with 1013 variants across 616 genes. These genes were significantly enriched in a gene set enrichment analysis for genes involved in neurodevelopment, particularly neuron growth and movement (Table S15). While this gene is understudied and lacks substantive annotations, but based on its interactors' significant GO categories, it is very likely *CG42671* is involved in growth and neuronal target finding. *CG10936* has few annotations, though it was identified in a screen for nociception (NEELY *et al.* 2010). It paired with 29 genes annotated for neurogenesis and function (*CG42788*, *Dh31*, *fru*, *hiw*, *lilli*, *nAChRalpha4*), as well as regulation of gene expression through chromatin modification (*Etl1* and *lilli*) and alternative splicing (*Srp54* and *U2af38*). One SNP (2R\_16871314\_SNP) was mapped to both the 3' UTR of *CG9313* and 29 bp downstream of *CG15651*. *CG9313* (orthologous to human DNAI1) is an ATP-dependent microtubule motor and is involved in the sensory perception of sound in *Drosophila* and proprioception, as well as sperm development (ZUR LAGE *et al.* 2019). *CG15651* is predicted to localize to the rough endoplasmic reticulum and Golgi body during embryogenesis, early larval, and late pupation stages where it is expressed in the central nervous system. Its human

ortholog, FKR (fukutin related protein), is implicated in intellectual disability and it is a candidate gene therapy target for muscular dystrophy (BROCKINGTON *et al.* 2001; INLOW AND RESTIFO 2004; VANNOY *et al.* 2017). These genes' shared function in nervous system development is reflected in the variants that map to 87 genes with annotations for neuron development, patterning, and function (*5-HT2B, cwo, dally, dx, Dysb, enok, erm, mbl, Ng1, nmo, Sdc, Sema1a, sNPF, tup,*). Several genes were also annotated for endoplasmic reticulum function (*bark, CG5885, CG15651, Fatp3, PAPLA1, Trc8, Uggf*); chromatin remodeling (*CG43902, enok, erm, lncRNA:roX1, tim*); transcription and alternative splicing (*cwo, bru3, CG6841, CG9650, CG15710, enok, luna, mbl, tim, tup*); and gene product regulation (*bru3, cwo, CG5885, CG9650, CG15710, luna, tRNA:Arg-TCT-2-1, tup*). Finally, there was a 669 bp region with six intergenic variants (chr3L:6890373 - 6891042). This region lacked regulatory annotations, yet collectively interacted with 513 variants mapping to 309 genes, many of which were shared with *ppk23, CG42671, and CG10936*. Similarly, these genes had significant GO term enrichment for neurodevelopment and neuron function (Table S16).

There were epistatic interactions between several of the genes identified from marginal variants (Figure 4A). Since marginal variants represent those more likely to interact with other variants, their interaction with one another suggests a highly interconnected genetic architecture underlying flight performance. Additionally, the breadth of epistatic interactions from a small, focused subset of marginal variants supports an important role for epistasis in the genetic architecture of flight performance. There are likely many more variants that interact with one another. But based on strong enrichment for

neurodevelopmental genes from the very limited subset of marginal variants we tested, we hypothesize that flight performance in wildtype *Drosophila* is modulated by neural function and circuitry.

#### *No evidence for adult transcriptome variation affecting flight performance*

Since many variants mapped to cis-regulatory elements and trans-regulatory genes, we sought to test whether regulatory variation was affecting developmental or adult homeostasis. Accordingly, performed a Weighted Gene Co-expression Network Analysis (WGCNA)(LANGFELDER AND HORVATH 2008) using 177 publically available DGRP transcriptomic profiles for young adults of both sexes (HUANG *et al.* 2015a). We clustered genes by similarity in expression profile, then correlated those clusters' eigenvalues with the mean and standard deviation of flight performance, as well as the proportion of flies that fell through the column over the total assayed. No clusters across sex or phenotype had a significant correlation. This result squares well with our previous observation that many of the significant variants map to genes involved in pre-adult development, rather than genes that maintain adult homeostasis (Figure S9).

#### *Flight performance is modulated by an interconnected genetic architecture*

The genetic architecture of flight performance is comprised of many different types of genetic modifiers. Many of the variants map to genes that are found across analytic platforms (Figure 4B). Most variants were unique to a single analysis, suggesting that association studies should consider using multiple different analyses to enhance the power to detect variants and genes in their study. However, many genes and genes

identified from variants were identified in two (148) or three (23) analyses. Those involved in three analyses include: *aru*, *CG2964*, *CG13506*, *CG15651*, *CG17839*, *CG42671*, *CycE*, *daw*, *Diap1*, *Egfr*, *fz2*, *Gart*, *Gmap*, *Mbs*, *MED23*, *mip40*, *mxt*, *Pdp1*, *Rab30*, *rhea*, *sog*, *sona*, *Tgi*) analyses. This suggests that individual genes can contain variants with different types of effects or have differential contributions to the overall genetic architecture. A complete lookup table of all genes and genes identified from variants is available (Table S17).

## Discussion

We tested flight performance of 197 DGRP lines, identifying several additive and marginal variants, epistatic interactions, whole genes, and a consensus network of altered sub-networks that associated with variation our phenotype. We identified many cis-regulatory variants mapped to genes with annotations for wing morphology, indirect flight muscle performance, and neurodevelopment of sensory and neuromuscular junctions.

### Variation in gene regulation drives variation in flight performance

Variation in gene expression is a major contributor to phenotypic variation (OLEKSIAK *et al.* 2002; CHEATLE JARVELA AND HINMAN 2015). Association studies with the DGRP lines often map variants to intergenic and non-coding regions of genes (WITTKOPP *et al.* 2004; CHOW *et al.* 2013; MACKAY AND HUANG 2018). These regulatory elements can be cis-regulators, like transcription factor binding sites (TFBS), enhancers, or silencers; or they can be trans-regulatory, like transcription factors, splicosomes, or chromatin modifiers. In the present study, the vast majority of variants in the additive, marginal, and epistatic analyses mapped to introns or within 1kb of a gene, suggesting a cis-regulatory role.

When cis-regulatory elements lie in important developmental genes, their effects can be magnified as the organism continues through development. The most significant additive variant we identified mapped to an *epidermal growth factor receptor* (*Egfr*, human homolog *EGFR*) intron. Encoding a key transmembrane tyrosine kinase receptor, *Egfr* is a pleiotropic gene affecting developmental and homeostatic processes

throughout the life and anatomy of the fly. It is well known for its role in embryonic patterning and implications in human cancers (SIBILIA *et al.* 2007; CROSSMAN *et al.* 2018). The variant also mapped to several overlapping TFBS for transcription factors known to affect embryonic development in a highly dose-dependent manner (*bcd, da, dl, gt, hb, kni, Med, prd, sna, tll, twi, disco, Trl*). Variation in patterning cells fated to become tissues and organs can be magnified through the adult stage, especially when that receptor is also known to affect other developmental processes (PAUL *et al.* 2013). Other intronic variants were identified in *Egfr* through the epistatic interactions with *ppk23*, illustrating how different types of genetic modifiers can exist within the same gene.

The role of cis- and trans-regulatory elements goes even further when there is variation in cis-regulatory elements of trans-regulatory genes. One of the Bonferroni additive variants mapped to an intronic region of *Forkhead domain 96Ca* (*fd96Ca*; human homologs *FOXB1* and *FOXB2*), a TFBS for *dorsal* (*dl*), and a silencer for *histone deacetylase 1* (*HDAC1*). *fd96Ca* is a fork head box transcription factor expressed in neuroblasts along the longitudinal axis of the embryo and in some sensory neurons in the embryonic head (HACKER *et al.* 1992). Trans-regulators, like *fd96Ca*, are proposed to have a large impact on phenotypic variation under the Omnigenic Inheritance model (BOYLE *et al.* 2017; LIU *et al.* 2019). Similar to *Egfr*, regulatory variation in a gene that helps determine cell fates can have larger effects if not enough cells are allocated for differentiation later in life. This can begin a cascade that amplifies downstream (ALBERT

AND KRUGLYAK 2015) and may hint at why trans-regulators were significant Gene Ontology (GO) terms in the consensus network.

There are likely non-coding regions of the genome that correspond with more cryptic regulatory regions. Six intergenic, marginal variants in a 669bp stretch (chr3L:6890373 - 6891042) had a number of significant epistatic interactions with developmental and neurodevelopmental genes. These variants lacked regulatory annotations in the DGRP2 annotation file, however these annotations were collected during embryogenesis (NEGRE *et al.* 2011) so it is possible these sites are activated by trans-regulators during different times in development. Nonetheless, based on its epistatic interactions, it is likely an important cis-regulatory region that affects general development from an early stage in the fly life cycle.

Our results suggest genetic variation in regulatory (non-coding) regions has a greater affect on variation of flight performance than variation in protein coding regions. While non-synonymous variants can have large effects on flight performance (DRUMMOND *et al.* 1991; MAUGHAN AND VIGOREAUX 1999; HAIGH *et al.* 2010), they were uncommon in our screen compared with variation in non-coding regions. This may be a result of strong purifying selection acting against them in a natural setting. Many of the candidate modifiers of flight are more commonly expressed during development (CHINTAPALLI *et al.* 2007b; BROWN *et al.* 2014; CASAS-VILA *et al.* 2017). This observation is supported by our lack of evidence for adult transcriptomic variation correlating with flight performance. Additionally, the flight phenotype was highly heritable, suggesting our phenotype was

not an artifact of environmental or experimental variation. Finally, the constructs we used to validate candidate genes created genetic variation in intronic regions, rather than post-transcriptionally modifying gene expression with an RNAi construct. Our successful validation of several candidate genes suggests variation in the non-coding regions of the candidate genes is sufficient for observing phenotypic differences. Further, insertion of the constructs into intronic regions both positively and negatively affected performance, even when done at independent sites in the same gene, suggesting a more nuanced impact of genetic variation in cis-regulatory regions. We conclude that modifiers of cis- and trans-regulation in pre-adult stages are more likely to modify flight performance in wild populations than variation in coding sequence.

*Variation in wing and indirect flight muscle development contributes to variance in flight performance*

Flight performance is a complex trait comprised of coordination across several smaller developmental and functional, complex traits (ENNOS 1989; MARCUS 2001; PITCHERS *et al.* 2019). The central role of *Egfr* in development means it can have wide range of functional effects on adult morphology. Natural variants in *Egfr* are known to cause developmental differences in wing morphology that can significantly alter flight performance (PAUL *et al.* 2013; PITCHERS *et al.* 2019), in part through interactions with the Bone Morphogenetic Protein (BMP) signaling pathway (MARCUS 2001; PAUL *et al.* 2013; HEVIA *et al.* 2017). BMP signaling is also an established modifier of wing development, as it forms dose-dependent gradients that pattern the wing size and



shape (YU *et al.* 1996; CRUZ *et al.* 2009), as well as sensory and neuromuscular circuits (BALL *et al.* 2010; QUIJANO *et al.* 2010). We identified several modifiers of BMP signaling (*cmpy*, *Cul2*, *cv-2*, *cv-c*, *dpp*, *dally*, *daw*, *egr*, *gbb*, *hiw*, *kek5*, *Lis-1*, *Lpt*, *lqf*, *ltl*, *Mad*, *nmo*, *scw*, *srw*, *Snoo*, *tkv*, *trio*) across all analyses and functionally validated *Snoo*—discussed below. Among the modifiers of BMP signaling, *short gastrulation* (*sog*; human homolog *Chordin*) stood out as a known source of natural variants that modifies flight performance in natural populations (MARCUS 2001). *sog* affects wing morphology through its role as a *dpp* antagonist in patterning the dorsoventral axis of the wings (YU *et al.* 1996; O'CONNOR *et al.* 2006; WHARTON AND SERPE 2013). *sog* is also noteworthy for its interconnectedness to other genes containing both a significant marginal variant and variants that had epistatic interactions with other significant marginal variants: *ppk23* and *CG42671* (formerly *CG18490* and *CG34240*)—discussed below. Marginal variants represent a class of variants that are statistically more likely to interact with other variants (CRAWFORD *et al.* 2017), via epistasis. Their identification hints at a more interconnected role in the genetic architecture. In this case, identification of *sog* suggests a more interconnected role for this antagonist of BMP signaling in modifying flight performance.

In addition to wing morphology, we identified several modifiers known to affect flight muscle function. The indirect flight muscles (IFM) power flight through the alternating dorsoventral and dorsolongitudinal muscle contraction to deform the cuticle and move the wings (DICKINSON AND TU 1997; LEHMANN AND DICKINSON 1997), while the direct flight muscles control flight through precise adjust of the wing angle (KOZOPAS AND NUSSE

2002). We identified two genes with known roles in flight (FERNANDES AND SCHOCK 2014; SPLETTER *et al.* 2015) from the additive screen that we successfully validated: *Lasp* and *bru1*. *Lasp* (human ortholog *LASP1*), is the only nebulin family gene in *Drosophila*, and shown to modify sarcomere and thin filament length, and myofibril diameter (FERNANDES AND SCHOCK 2014). We also identified *bruno 1* (*bru1* or *aret*; human homolog *CLEF1* and *CLEF2*), a transcription factor that controls alternative splicing of myofibrils in the IFM (SPLETTER *et al.* 2015; KAO *et al.* 2019), among other developmental processes. *bru1* had two intronic variants, one of which mapped to a TFBS for *twi*—one of the genes identified from a significant marginal variant.

Using our newly developed platform PEGASUS\_flies to find significant whole genes, we also identified *tropomodulin* (*tmod*; human homolog *TMOD1*) and *Glycerol-3-phosphate dehydrogenase 1* (*Gpdh1*; human homolog *GPD1*). These two genes were previously validated for their roles in flight performance (MARDAHL-DUMESNIL AND FOWLER 2001; MONTTOOTH *et al.* 2003) and are responsible for muscle function and metabolism within muscles, respectively. The identification and previous validation of *tmod* and *Gpdh1* is noteworthy because neither had a significant variant exceed the additive screen's significance threshold ( $P \leq 1E-5$ ). This finding demonstrates a successful proof-of-principle for PEGASUS\_flies' ability to identify genetic modifiers that would otherwise be overlooked in a traditional minSNP approach in an additive screen. Additionally, we successfully validated *fry*, identified in both the additive and whole gene screens. Taken together, the prior and current validation of these genes

establishes PEGASUS\_flies as a verified platform for identifying modifiers of complex traits.

### Neurodevelopmental genes play an important role in modifying flight performance

Many neurodevelopmental genes with diverse functions were identified across analyses. Because neurodevelopmental genes can play several roles, many of which are unannotated in GO databases, GO term enrichment analyses can be underpowered. This may explain why we failed to identify any GO terms for additive variants in the GOwinda analysis (CHOW *et al.* 2013). However, their identification through other GO analyses on the epistatic and network-based analyses is encouraging.

Several neurodevelopmental genes overlapped between the additive minSNP and PEGASUS\_flies whole gene approach. These genes (*aru*, *ChAT*, *Ccn*, *DIP- $\delta$* , *dsf*, *dsx*, *fry*, *Mbs*, *sdk*, *VACHT*), lend additional support to the likelihood these genes were not false positives. For example, *fry* and *Sidekick* (*sdk*) both coordinate dendritic target finding functions with DSCAM family genes (YAMAGATA AND SANES 2008; FUERST AND BURGESS 2009). This is in agreement with several significant GO terms for axon guidance and neuronal targeting in the consensus network's largest sub-network (Table S11) and for the genes identified from epistatic interactions with *ppk23*, *CG42671*, and an intergenic region (chr3L:6890373 - 6891042)(Tables S14-16). Accordingly neurodevelopmental genes are present throughout our study, and represent a highly interconnected group of genes that likely plays an important role in flight performance.

Underscoring this interconnectedness is the identification of several neurodevelopmental genes that mapped to epistatic interactions with a common, significant marginal variant in *sog*. This variant was significant in males and mapped to a new transcription start site. In addition to affecting wing morphology, *sog* also plays a role in neurodevelopment (*CG13579*, *dib*, *Hk*, *lncRNA:rox1*, *nAChRa4*, *Sdc*, *simj*, *sqz*, *Toll-4*, *trio*) (ASHBURNER *et al.* 2000; BALL *et al.* 2010; WHARTON AND SERPE 2013; CARBON *et al.* 2019). Several of these genes were involved in neuromuscular growth and function (*CG13579*, *Hyperkinetic (Hk)*, *nicotinic acetylcholine receptor  $\alpha$  4 (nAChRa4)*, *Syndecan (Sdc)*, *squeeze (sqz)*, *trio*) (FONTAINE *et al.* 1988; HEWES AND TAGHERT 2001; ALLAN *et al.* 2003; UEDA AND WU 2009; BALL *et al.* 2010; NGUYEN *et al.* 2016), suggesting an important connection between neurodevelopmental phenotypes and their role in activating direct and indirect flight muscles. However, some of the genes interacting with *sog* can affect sensory neurons as well. For example, *trio* is also present in sensory neurons and is capable of modifying chemosensation (ARYA *et al.* 2015). Other *sog* variants that had epistatic interactions with marginal variants in *CG42671* (formerly *CG18490* and *CG34240*) and *ppk23*—discussed below, two genes with known or putative roles in developing the peripheral nervous system (PNS).

In addition to neuromuscular genes, we validated genes involved in patterning the PNS. One of the Bonferroni variants from the additive screen mapped to *Down Syndrome Cell Adhesion Molecule 4 (Dscam4)*; human ortholog *DSCAM*). DSCAMs are a conserved family of extracellular, immunoglobulin proteins that promote cell-cell adhesion. They are

found in complex (type IV) dendrite arborization neurons that promote dendritic target recognition and dendrite self-avoidance in the developing PNS (DOS SANTOS *et al.* 2015) and in the brain and central nervous system (CNS) (NEVES *et al.* 2004; ZHAN *et al.* 2004). Type IV dendritic arborization neurons transduce signals from sensory neurons (e.g. photoreceptors, chemosensors, and mechanosensors), to the CNS (STOCKER 1994; SMITH AND SHEPHERD 1996; NEVES *et al.* 2004; TADROS *et al.* 2016). *Dscams* are expressed differentially and combinatorially in different neurons, which allows them to create highly interconnected neural circuits (NEVES *et al.* 2004). They also work with other cell-cell adhesion proteins, like cadherins, in patterning the nervous system. *Cadherin-N* (*CadN* or *N-cad*) interacts with *Dscam2* and *Dscam4* in patterning olfactory receptor neurons (ORN), like *Or46a* (significant additive hit) and *Or59c* (significant epistatic hit with *ppk23*) (HUMMEL *et al.* 2003; HUMMEL AND ZIPURSKY 2004; SOBA *et al.* 2007; TADROS *et al.* 2016). Given their importance in patterning sensory neuron circuits and strong significance in the additive screen, we independently validated *Dscam4* and *CadN* using two separate insertional mutants for each. Both pairs of insertional mutants in both genes were significant, though the direction of effect was reversed, reiterating how cis-regulatory regions can differentially affect genes' expression levels. Our double validation for each supports a greater level of confidence in *Dscam4* and *CadN* as modifiers of the peripheral nervous system important for flight performance.

We validated two other dendrite patterning genes that also help to form sensory organs on the wing and body that contribute to proprioception: *furry* (*fry*; human homolog FRYL) and *Sno oncogene* (*Snoo* or *dSno*; human homolog SKI). These two conserved

proteins are expressed along the same types of sensory neurons as Dscams and cadherins that promote dendrite field patterning, dendrite self-avoidance, and development of sensory organs (EMOTO *et al.* 2004). *fry* assists Dscams and cadherins in dendritic tiling of chemosensors (olfaction or gustation) and mechanosensors (proprioception) (EMOTO *et al.* 2004; SOBA *et al.* 2007; MATSUBARA *et al.* 2011) that directly connect to sensory microchaete (hairs or bristles) organized along the wing and body in specific patterns (CONG *et al.* 2001). Meanwhile, *Snoo* interacts with the wingless pathway (QUIJANO *et al.* 2010; FISCHER *et al.* 2012), and is an important antagonist of *Medea* (*Med* or *dSmad4*; human homolog *Smad4*)—an important regulatory of the BMP-to-activin- $\beta$  pathway (TAKAESU *et al.* 2006). *Snoo* is known to modify wing shape (TAKAESU *et al.* 2006), dendritic tiling, and the development of sensory organs (microchate and campaniform sensilla) on the wing (QUIJANO *et al.* 2010; LUO 2017). These sensory organs play different roles; wing chaete can function as chemosensors (olfaction and gustation) and mechanosensors (STOCKER 1994; FURMAN AND BUKHARINA 2008), while campaniform sensilla measure strain on the deformed wing blade (DICKINSON 1990; DICKINSON *et al.* 1997; AINSLEY *et al.* 2003; YAMASHITA *et al.* 2018). Together, these sensory organs aid in proprioception of flight (LEHMANN AND BARTUSSEK 2017) and delineate a direct connection between the role of proper development of the wings' sensory organs and the proper development of the neural circuitry connecting them to the CNS in modifying flight performance.

We functionally validated two candidate genes with only tangential evidence of their function that we are naming *flapper* (*flap*, formerly *CG11073*) and *flippy* (*flip*, formerly

CG9766). *flapper* is expressed in the peripodial epithelium cells of the eye, leg, and wing imaginal discs (FIRTH AND BAKER 2007). It is expressed at very high levels during 16-18 hours of embryogenesis, pupariation (CASAS-VILA *et al.* 2017) and in the head, eyes, and carcass in the adult stage (CHINTAPALLI *et al.* 2007a). It was previously identified as a candidate gene in a screen for modifiers of circadian rhythm (HARBISON *et al.* 2019) and was significantly upregulated in flies bred for aggressive behavior (DIERICK AND GREENSPAN 2006), but both studies failed to functionally validate the gene. *flapper* was also implicated in the downregulation of amyloid- $\beta$  peptides (PAGE *et al.* 2012) and in late life fecundity (DURHAM *et al.* 2014) suggesting it may play a basic role in development that affects several phenotypes. Accordingly, we hypothesize it plays some role in patterning neural circuitry of sensory neurons on the cuticle and eyes, and facilitates neural circuit assembly in the brain. The other gene, *flippy* (human homolog *FANK1*), is pleiotropic with important roles in neuroanatomical development (MUMMERY-WIDMER *et al.* 2009; NEUMULLER *et al.* 2011) and sperm development (BROWN *et al.* 2014). It is important in the development of trichogen cells, which are precursors to the chaete flies use for mechanosensation. In humans, *FANK1* plays roles in spermatogenesis and apoptosis, and is a putative evolutionary target of balancing selection (ZHENG *et al.* 2007; DEGIORGIO *et al.* 2014). Given *flippy*'s pleiotropic role in neurodevelopment and gametogenesis, it may also be under stabilizing selection brought about by contrasting selective pressures for neural function and fitness.

Finally, qualitative observations of differentially performing DGRP lines support a role for proprioception as a modifier of flight performance. High-speed videos of strong,

intermediate, and weak lines show strong lines react quicker to an abrupt free fall and are better at controlling their descent than the intermediate fliers, and much more than weak fliers. This direct evidence corroborates with the validation screen and inferential association analyses to support a role for natural variants in genes that affect 1) sensory neural circuit connectivity, 2) development and function of neuromuscular junctions, and 3) the integration of these two onto wings of varying morphologies for modifying flight performance in a natural population.

*Important implications for acid sensing ion channels in flight performance and neural function flight*

Pickpocket genes encode a conserved group of degenerin/epithelial sodium channels (DEG/ENaC) that function as non-voltage gated, amiloride-sensitive cation channels (ADAMS *et al.* 1998). They are found in the brain, thoracic ganglion (LU *et al.* 2012; THISTLE *et al.* 2012), neuromuscular junctions (BEN-SHAHAR 2011; THISTLE *et al.* 2012), and trachea (LIU *et al.* 2003), though pickpocket family genes are most commonly found along type IV dendrite arborization sensory neurons that connect chemo- or mechanosensory organs to the CNS (GRUEBER *et al.* 2003; EMOTO *et al.* 2004; KUO *et al.* 2005; SOBA *et al.* 2007; MATSUBARA *et al.* 2011; THISTLE *et al.* 2012; GORCZYCA *et al.* 2014; NG *et al.* 2019) on the head, legs, and wings (PAUKERT *et al.* 2004; BEN-SHAHAR 2011; LU *et al.* 2012; ZELLE *et al.* 2013; MAUTHNER *et al.* 2014; JEONG *et al.* 2016). Chemosensing microchaete can contain olfactory receptor neurons (ORN), gustatory receptor neurons (GRN), and ionotropic receptors (IR), which are useful for foraging and pheromone detection (FRYE AND DICKINSON 2004b; PAUKERT *et al.* 2004; SHERMAN



AND DICKINSON 2004; TAYLOR AND KRAPP 2007; BEN-SHAHAR 2011; LU *et al.* 2012; ZELLE *et al.* 2013; MAUTHNER *et al.* 2014; JEONG *et al.* 2016; LEHMANN AND BARTUSSEK 2017). In this study, we identified six pickpocket genes (*ppk1*, *ppk8*, *ppk9*, *ppk10*, *ppk12*, *ppk23*), 10 gustatory receptors (*Gr10a*, *Gr10b*, *Gr28b*, *Gr36b*, *Gr36c*, *Gr39a*, *Gr59a*, *Gr59d*, *Gr61a*, *Gr64a*), 12 olfactory receptors and binding proteins (*Or24a*, *Or45a*, *Or46a*, *Or49a*, *Or59b*, *Or59c*, *Or67d*, *Or71a*, *Or85d*, *Obp8a*, *Obp28a*, *Obp47a*), and 13 ionotropic receptors (*Ir41a*, *Ir47a*, *Ir47b*, *Ir51a*, *Ir56b*, *Ir56c*, *Ir56d*, *Ir60d*, *Ir60f*, *Ir62a*, *Ir64a*, *Ir67b*, *Ir75d*) from the additive, marginal, epistatic, and network approaches. *Or85d* was identified from the 2<sup>nd</sup> most significant additive variant and only non-synonymous SNP that passed a Bonferroni threshold in the additive search. And yet, despite a combined 41 pickpocket, gustatory receptor, olfactory receptor, and ionotropic receptor genes, only six (*ppk10*, *ppk12*, *Gr59d*, *Or24a*, *Ir41a*, and *Ir60d*) overlapped with an olfactory screen testing for genetic associations across 14 odors (ARYA *et al.* 2015). Accordingly, we hypothesize a more nuanced role for these chemosensors in aiding proprioception during flight.

The magnitude of significant marginal variants and epistatic interactions that mapped to *ppk23* suggests this ion transporter has a much more interconnected role in the genetic architecture of flight performance than previously thought. *ppk23* is a modifier of flies' ability to track odors during free flight, but not a modifier of odorless flight (HOUOT *et al.* 2017). Our results support a role for *ppk23* in modifying flight, along with all but eight (*Or46a*, *Or49a*, *Or85d*, *Gr36b*, *Gr36c*, *Ir60d*, *Ir60f*, *ppk10*) of the 41 previously listed pickpocket and chemoreceptor genes that *ppk23* interacted with. Like *sog*, *ppk23* is

likely a central modifier of performance based on the number of epistatic interactions with variants mapping to genes identified in the marginal variant screen (*A2bp1/Rbfox1*, *cv-c*, *Fad2*, *CG9313*, *CG10936*, *CG42741*, *Rgk1*, *sog*, *Src64B*, *twi*, *Ten-a*). Some of these play roles in sensory signal processing (*A2bp1/Rbfox1*, *CG9313*, *CG10936*, *Fad2*, *Rgk1*), neuron growth (*sog* and *Src64b*), neuromuscular junction development (*cv-c*, *Src64b*, *Ten-a*), and transcription factors (*A2bp1/Rbfox1*, *CG42741*, *twi*) (JIN *et al.* 2016; SHUKLA *et al.* 2017), several of which had significant epistatic interactions of their own. Of these, *CG10936* is proposed to be involved in sensory perception (JIN *et al.* 2016), but has limited annotations otherwise. Our work supports this hypothesized function. *ppk23*, in addition to these interactions, is known to modulate physiology and lifespan (GENDRON *et al.* 2014), broadening its canonical roles in chemo- and mechanosensation. Taken together, *ppk23* likely has strong connections to many systems beyond detection of stimulation that have deeper connections to organismal biology.

The interconnectedness of *ppk23* also provides clues about the sexual dimorphism observed in flight. While males generally outperform females, likely due to differences in weight, sex failed to explain ~25% of the variation between the two groups. Like most pickpocket family genes, *ppk23* is well established as an important factor in chemosensation, pheromone detection, and courtship (LU *et al.* 2012; THISTLE *et al.* 2012; GORCZYCA *et al.* 2014)—highly sex-specific phenotypes. One of *ppk23*'s epistatic interactions mapped to *fruitless* (*fru*; human homolog *ZBTB24*), a transcription factor responsible for sex-specific neural phenotypes involved in courtship and pheromone

detection (KIMURA *et al.* 2005) that co-localizes with *ppk23* differentially between sexes, on the leg and wing microchaete (BEN-SHAHAR 2011; LU *et al.* 2012; THISTLE *et al.* 2012; PAVLOU AND GOODWIN 2013; GENDRON *et al.* 2014). In addition to the PNS, *ppk23* and *fru* have sex-specific co-localization patterns in the thoracic ganglion. This cluster of neurons central to the “escape” response, allowing for ultra-fast processing of and response to flight-associated cues (STRAUSFELD 2009; LEHMANN AND BARTUSSEK 2017). Males show more connections between *ppk23* and *fru* in the thoracic ganglion, and co-localization in neurons crossing the midline between the two sides of the anterior-most, pro-thoracic ganglion (LU *et al.* 2012; THISTLE *et al.* 2012). *fru* is also expressed in vMS2 motor neurons connecting the thoracic ganglion to the flight musculature, likely involved in courtship song generation and aggression behaviors (EWING 1979; YU *et al.* 2010). The connection between sensory neurons, *ppk23*, *fru*, and motor neurons involved in wing motion draw a clear connection between a potential mechanism delineating the sex-difference phenotype we observed. Given the prior connections between *ppk23*, *sog*, and the epistatic interactions between them that annotate to sensory neurons and motor neuron neuromuscular junctions, there are likely other important connections underlying the ability of flies to process proprioceptive signals that are relayed directly to the flight musculature during our assay that have yet to be uncovered. Some of these connections may lie in the genes identified using PEGASUS\_flies’ for the sex-difference analysis, like *doublesex (dsx)*, an interactor of *fru* and *ppk1* in patterning sex-specific neural networks for courtship; *dissatisfaction (dsf)*, a modifier of courtship behavior (FINLEY *et al.* 1997b; YU *et al.* 2010; REZAVAL *et al.* 2012; SHIRANGI *et al.* 2016); and several other genes: *blue cheese (bchs)*, *Ccn*, *CG13506*, *defective proboscis*

*extension response 6 (dpr6), pollux (plx), sidekick (sdk), eiger (egr)* (FINLEY *et al.* 1997a; BILLETTER *et al.* 2006; PAVLOU AND GOODWIN 2013; DOS SANTOS *et al.* 2015). Further study of these genes may yield promising insights into the sex-differences we observed in flight performance, as well as sex-specific behavioral traits.

#### *A proposed model for understanding the genetic architecture of flight performance*

Flight performance is likely an epiphenomenon of several interconnected complex traits. While we are unable to identify every modifier, we likely identified the main components of the genetic architecture. Accordingly, we propose the following model to synthesize our findings (Figure 4C).

Epidermal growth factor receptor is a key gene in a canonical developmental pathway. It can affect wing morphology, sensory organ development, and neurodevelopment, on its own and through the BMP signaling pathway. Proper development of these structures and circuits enables well-connected sensory neurons to receive external stimuli regarding proprioception. These signals are transduced through the thoracic ganglion, with sex-specific differences potentially modulated through *ppk23*, *fru*, and *dsx*. The thoracic ganglion processes these signals and activates motor neurons, which innervate the direct (control) and indirect (power) flight musculature at neuron muscular junctions. Activating these muscles allows the properly developed wings to flap and generate lift.

Implications for BMP signaling and pickpocket genes in neuroinjury and neurodegeneration

The complexity of congenital, neurodegenerative diseases lies in the mix of genetic elements with very modest effect size. Association screens with *Drosophila* present a compelling model for identifying these sources of variation, especially in neuron-centric traits (CARBONE *et al.* 2016; CHOW AND REITER 2017; LAVOY *et al.* 2018; MACKAY AND HUANG 2018). Our results present a strong link between flight performance and BMP signaling—a proposed candidate pathway for therapeutic interventions in several neurodegenerative diseases (BAYAT *et al.* 2011; PINTO *et al.* 2013; DESHPANDE *et al.* 2016). Mutations in *thickveins* (*tkv*) human homologs *BMPR1A* and *BMPR1B* are linked to familial Alzheimer’s Disease (KANG *et al.* 2014), while mutants of *Superoxide dismutase 1* (*dSOD1*; human homolog *SOD1*) associated with Amyotrophic Lateral Sclerosis (ALS) can be rescued by activators of BMP signaling expressed in proprioceptive and motor neurons (HELD *et al.* 2019). Our validation of the BMP antagonist *Snoo* confirms BMP signaling plays a role in flight performance. Given the number of epistatic interactions between *ppk23* and BMP signaling genes, it is very likely our data uncovers important modifiers of the BMP pathway that affect neurodysfunction in humans.

In addition to BMP signaling, we propose an expanded role for *ppk23*, and pickpocket family genes more generally, in neurobiology and neurodysfunction therapeutics. Acid Sensing Ion Channel (ASIC) family genes, the human homolog of the pickpocket family, can function as neuronal damage sensors. They detect drops in pH around neurons,

often caused injury, damage, and dysfunction, which can elicit an inflammation response (HUANG *et al.* 2015b; ORTEGA-RAMIREZ *et al.* 2017). These channels are found all over the brain and spinal column, supporting a functional and protective role following traumatic brain injury (concussion) and cerebral ischemia (stroke) (XIONG AND XU 2012; HUANG *et al.* 2015b). They are also identified as a potential target for genetic and/or pharmacological interventions of neurodegeneration and neuroinflammation (ORTEGA-RAMIREZ *et al.* 2017). Accordingly, our results break ground in identifying candidate genetic interactions that might be useful for such interventions.

### Acknowledgements

We thank P. Nakka for her guidance through PEGASUS and F. Lemieux for maintaining *Drosophila* stocks. We are grateful for critical feedback from M. Tatar and T. Roberts. This research was funded by National Institutes of Health grant GM067862 (to DMR). The authors declare no conflict of interest.

### Author contributions

ANS, JAM, and DMR conceived and designed the study. ANS performed validation crosses, while ANS and JAM collected data. ANS performed the statistical analyses guidance from SR and LC. ANS and SAS designed and implemented PEGASUS\_flies. ANS and DMR wrote the manuscript.

## Supplemental Results

### Establishing an empirically defined significance threshold

While the Bonferroni significance threshold is conservative, the conventional  $P = 1E-5$  threshold might be considered lax. Accordingly, we simulated two sets of genotype-phenotype matrices; one set “shuffled” the genotype-phenotype matrix while the other set randomly “subsampling” 150 of the 197 lines.

The significance threshold for each sex-based phenotype in each simulation was determined by taking the 5<sup>th</sup> percentile of the most significant  $P$ -value across 1000 permutations (DOERGE AND CHURCHILL 1996). Despite these efforts, the resulting significance thresholds were even more stringent than the Bonferroni (Table S18) and resulted in only one variant (2R\_2718036\_DEL) mapping to *CG15236* and *CG34215* in the shuffled sex-difference set. *CG15236*'s function is not well known, but it is expressed during embryogenesis and pupariation in the developing brain and central nervous system and putatively affects the wing veins (KRUPP *et al.* 2005; VONESCH *et al.* 2016). *CG34215* is less understood, though it is expressed at varying levels throughout developmental and adult stages (DOS SANTOS *et al.* 2015) and contains a single domain Von Willebrand factor type C domain—thought to play a role in anti-viral capabilities (CHEN *et al.* 2011).

## Literature Cited

- Adams, C. M., M. G. Anderson, D. G. Motto, M. P. Price, W. A. Johnson *et al.*, 1998 Ripped pocket and pickpocket, novel *Drosophila* DEG/ENaC subunits expressed in early development and in mechanosensory neurons. *Journal of Cell Biology* 140: 143-152.
- Ainsley, J. A., J. M. Pettus, D. Bosenko, C. E. Gerstein, N. Zinkevich *et al.*, 2003 Enhanced locomotion caused by loss of the *Drosophila* DEG/ENaC protein pickpocket1. *Current Biology* 13: 1557-1563.
- Albert, F. W., and L. Kruglyak, 2015 The role of regulatory variation in complex traits and disease. *Nature Reviews Genetics* 16: 197-212.
- Allan, D. W., S. E. St Pierre, I. Miguel-Aliaga and S. Thor, 2003 Specification of neuropeptide cell identity by the integration of retrograde BMP signaling and a combinatorial transcription factor code. *Cell* 113: 73-86.
- Arya, G. H., M. M. Magwire, W. Huang, Y. L. Serrano-Negrón, T. F. C. Mackay *et al.*, 2015 The Genetic Basis for Variation in Olfactory Behavior in *Drosophila melanogaster*. *Chemical Senses* 40: 233-243.
- Ashburner, M., C. A. Ball, J. A. Blake, D. Botstein, H. Butler *et al.*, 2000 Gene Ontology: tool for the unification of biology. *Nature Genetics* 25: 25-29.
- Babcock, D. T., and B. Ganetzky, 2014 An Improved Method for Accurate and Rapid Measurement of Flight Performance in *Drosophila*. *Jove-Journal of Visualized Experiments*.
- Ball, R. W., M. Warren-Paquin, K. Tsurudome, E. H. Liao, F. Elazzouzi *et al.*, 2010 Retrograde BMP Signaling Controls Synaptic Growth at the NMJ by Regulating Trio Expression in Motor Neurons. *Neuron* 66: 536-549.
- Battlay, P., P. B. Leblanc, L. Green, N. R. Garud, J. M. Schmidt *et al.*, 2018 Structural Variants and Selective Sweep Foci Contribute to Insecticide Resistance in the *Drosophila* Genetic Reference Panel. *G3-Genes Genomes Genetics* 8: 3489-3497.
- Bayat, V., M. Jaiswal and H. J. Bellen, 2011 The BMP signaling pathway at the *Drosophila* neuromuscular junction and its links to neurodegenerative diseases. *Current Opinion in Neurobiology* 21: 182-188.
- Bellen, H. J., R. W. Levis, Y. He, J. W. Carlson, M. Evans-Holm *et al.*, 2011a The *Drosophila* gene disruption project: progress using transposons with distinctive site-specificities. *Genetics: genetics*. 111.126995.
- Bellen, H. J., R. W. Levis, Y. C. He, J. W. Carlson, M. Evans-Holm *et al.*, 2011b The *Drosophila* Gene Disruption Project: Progress Using Transposons With Distinctive Site Specificities. *Genetics* 188: 731-U341.
- Ben-Shahar, Y., 2011 Sensory Functions for Degenerin/Epithelial Sodium Channels (DEG/ENaC), pp. 1-26 in *Advances in Genetics, Vol 76*, edited by T. Friedmann, J. C. Dunlap and S. F. Goodwin.
- Billeter, J. C., A. Villella, J. B. Allendorfer, A. J. Dornan, M. Richardson *et al.*, 2006 Isoform-specific control of male neuronal differentiation and behavior in *Drosophila* by the fruitless gene. *Current Biology* 16: 1063-1076.



- Boyle, E. A., Y. I. Li and J. K. Pritchard, 2017 An Expanded View of Complex Traits: From Polygenic to Omnigenic. *Cell* 169: 1177-1186.
- Brockington, M., Y. Yuva, P. Prandini, S. C. Brown, S. Torelli *et al.*, 2001 Mutations in the fukutin-related protein gene (FKRP) identify limb girdle muscular dystrophy 2I as a milder allelic variant of congenital muscular dystrophy MDC1C. *Human Molecular Genetics* 10: 2851-2859.
- Brodsky, A. K., 1994 *The evolution of insect flight*. Oxford University Press.
- Brown, J. B., N. Boley, R. Eisman, G. E. May, M. H. Stoiber *et al.*, 2014 Diversity and dynamics of the *Drosophila* transcriptome. *Nature* 512: 393-399.
- Browning, B. L., and S. R. Browning, 2016 Genotype Imputation with Millions of Reference Samples. *American Journal of Human Genetics* 98: 116-126.
- Browning, S. R., and B. L. Browning, 2007 Rapid and accurate haplotype phasing and missing-data inference for whole-genome association studies by use of localized haplotype clustering. *American Journal of Human Genetics* 81: 1084-1097.
- Carbon, S., E. Douglass, N. Dunn, B. Good, N. L. Harris *et al.*, 2019 The Gene Ontology Resource: 20 years and still GOing strong. *Nucleic Acids Research* 47: D330-D338.
- Carbone, M. A., A. Yamamoto, W. Huang, R. A. Lyman, T. B. Meadors *et al.*, 2016 Genetic architecture of natural variation in visual senescence in *Drosophila*. *Proceedings of the National Academy of Sciences of the United States of America* 113: E6620-E6629.
- Casas-Vila, N., A. Bluhm, S. Sayols, N. Dinges, M. Dejung *et al.*, 2017 The developmental proteome of *Drosophila melanogaster*. *Genome Research* 27: 1273-1285.
- Cheatle Jarvela, A. M., and V. F. Hinman, 2015 Evolution of transcription factor function as a mechanism for changing metazoan developmental gene regulatory networks. *EvoDevo* 6: 3.
- Chen, Y. H., X. T. Jia, L. Zhao, C. Z. Li, S. A. Zhang *et al.*, 2011 Identification and functional characterization of Dicer2 and five single VWC domain proteins of *Litopenaeus vannamei*. *Developmental and Comparative Immunology* 35: 661-671.
- Chintapalli, V. R., J. Wang and J. A. Dow, 2007a Using FlyAtlas to identify better *Drosophila melanogaster* models of human disease. *Nature genetics* 39: 715-720.
- Chintapalli, V. R., J. Wang and J. A. T. Dow, 2007b Using FlyAtlas to identify better *Drosophila melanogaster* models of human disease. *Nature Genetics* 39: 715-720.
- Chow, C. Y., K. J. P. Kelsey, M. F. Wolfner and A. G. Clark, 2016 Candidate genetic modifiers of retinitis pigmentosa identified by exploiting natural variation in *Drosophila*. *Human Molecular Genetics* 25: 651-659.
- Chow, C. Y., and L. T. Reiter, 2017 Etiology of Human Genetic Disease on the Fly. *Trends in Genetics*.

- Chow, C. Y., M. F. Wolfner and A. G. Clark, 2013 Large Neurological Component to Genetic Differences Underlying Biased Sperm Use in *Drosophila*. *Genetics* 193: 177-185.
- Cong, J. L., W. Geng, B. He, J. C. Liu, J. Charlton *et al.*, 2001 The furry gene of *Drosophila* is important for maintaining the integrity of cellular extensions during morphogenesis. *Development* 128: 2793-2802.
- Consortium, T. A. o. G. R., 2020 Alliance of Genome Resources Portal: unified model organism research platform. *Nucleic acids research* 48: D650-D658.
- Crawford, L., P. Zeng, S. Mukherjee and X. Zhou, 2017 Detecting epistasis with the marginal epistasis test in genetic mapping studies of quantitative traits. *Plos Genetics* 13.
- Crossman, S. H., S. J. Streichan and J. P. Vincent, 2018 EGFR signaling coordinates patterning with cell survival during *Drosophila* epidermal development. *Plos Biology* 16.
- Cruz, C., A. Glavic, M. Casado and J. F. de Celis, 2009 A Gain-of-Function Screen Identifying Genes Required for Growth and Pattern Formation of the *Drosophila melanogaster* Wing. *Genetics* 183: 1005-1026.
- Danecek, P., A. Auton, G. Abecasis, C. A. Albers, E. Banks *et al.*, 2011 The variant call format and VCFtools. *Bioinformatics* 27: 2156-2158.
- Das, J., and H. Y. Yu, 2012 HINT: High-quality protein interactomes and their applications in understanding human disease. *Bmc Systems Biology* 6.
- DeGiorgio, M., K. E. Lohmueller and R. Nielsen, 2014 A Model-Based Approach for Identifying Signatures of Ancient Balancing Selection in Genetic Data. *Plos Genetics* 10.
- Deshpande, M., Z. Feiger, A. K. Shilton, C. C. Luo, E. Silverman *et al.*, 2016 Role of BMP receptor traffic in synaptic growth defects in an ALS model. *Molecular Biology of the Cell* 27: 2898-2910.
- Dickinson, M. H., 1990 COMPARISON OF ENCODING PROPERTIES OF CAMPANIFORM SENSILLA ON THE FLY WING. *Journal of Experimental Biology* 151: 245-261.
- Dickinson, M. H., S. Hannaford and J. Palka, 1997 The evolution of insect wings and their sensory apparatus. *Brain Behavior and Evolution* 50: 13-24.
- Dickinson, M. H., and M. S. Tu, 1997 The function of dipteran flight muscle. *Comparative Biochemistry and Physiology a-Physiology* 116: 223-238.
- Dierick, H. A., and R. J. Greenspan, 2006 Molecular analysis of flies selected for aggressive behavior. *Nature Genetics* 38: 1023-1031.
- Doerge, R. W., and G. A. Churchill, 1996 Permutation Tests for Multiple Loci Affecting a Quantitative Character. *Genetics* 142: 285-294.
- dos Santos, G., A. J. Schroeder, J. L. Goodman, V. B. Strelets, M. A. Crosby *et al.*, 2015 FlyBase: introduction of the *Drosophila melanogaster* Release 6 reference genome assembly and large-scale migration of genome annotations. *Nucleic Acids Research* 43: D690-D697.

- Drummond, D. R., E. S. Hennessey and J. C. Sparrow, 1991 CHARACTERIZATION OF MISSENSE MUTATIONS IN THE ACT88F GENE OF DROSOPHILA-MELANOGASTER. *Molecular & General Genetics* 226: 70-80.
- Durham, M. F., M. M. Magwire, E. A. Stone and J. Leips, 2014 Genome-wide analysis in *Drosophila* reveals age-specific effects of SNPs on fitness traits. *Nature Communications* 5.
- Eden, E., D. Lipson, S. Yagev and Z. Yakhini, 2007 Discovering motifs in ranked lists of DNA sequences. *Plos Computational Biology* 3: 508-522.
- Eden, E., R. Navon, I. Steinfeld, D. Lipson and Z. Yakhini, 2009 GOrilla: a tool for discovery and visualization of enriched GO terms in ranked gene lists. *Bmc Bioinformatics* 10.
- Edwards, J. S., 1997 The evolution of insect flight: Implications for the evolution of the nervous system. *Brain Behavior and Evolution* 50: 8-12.
- Elgin, S., and D. Miller, 1978 Special techniques for tissue isolation and injection. II. Mass rearing of flies and mass production and harvesting of embryos. *Genetics and biology of Drosophila*.
- Emoto, K., Y. He, B. Ye, W. B. Grueber, P. N. Adler *et al.*, 2004 Control of dendritic branching and tiling by the tricornered-kinase/furry signaling pathway in *Drosophila* sensory neurons. *Cell* 119: 245-256.
- Ennos, A. R., 1989 COMPARATIVE FUNCTIONAL-MORPHOLOGY OF THE WINGS OF DIPTERA. *Zoological Journal of the Linnean Society* 96: 27-47.
- Ewing, A. W., 1979 NEUROMUSCULAR BASIS OF COURTSHIP SONG IN DROSOPHILA - ROLE OF THE DIRECT AND AXILLARY WING MUSCLES. *Journal of Comparative Physiology* 130: 87-93.
- Fernandes, I., and F. Schock, 2014 The nebulin repeat protein Lasp regulates I-band architecture and filament spacing in myofibrils. *Journal of Cell Biology* 206: 559-572.
- Finley, K. D., B. J. Taylor, M. Milstein and M. McKeown, 1997a dissatisfaction, a gene involved in sex-specific behavior and neural development of *Drosophila melanogaster*. *Proceedings of the National Academy of Sciences of the United States of America* 94: 913-918.
- Finley, K. D., B. J. Taylor, M. Milstein and M. McKeown, 1997b dissatisfaction, a gene involved in sex-specific behavior and neural development of *Drosophila melanogaster*. *Proceedings of the National Academy of Sciences* 94: 913-918.
- Firth, L. C., and N. E. Baker, 2007 Spitz from the retina regulates genes transcribed in the second mitotic wave, peripodial epithelium, glia and plasmatocytes of the *Drosophila* eye imaginal disc. *Developmental Biology* 307: 521-538.
- Fischer, S., F. Bayersdorfer, E. Harant, R. Reng, S. Arndt *et al.*, 2012 fussel (fuss) - A Negative Regulator of BMP Signaling in *Drosophila melanogaster*. *Plos One* 7.
- Fontaine, B., D. Sassoon, M. Buckingham and J.-P. Changeux, 1988 Detection of the nicotinic acetylcholine receptor alpha - subunit mRNA by in situ hybridization at neuromuscular junctions of 15 - day - old chick striated muscles. *The EMBO Journal* 7: 603-609.

- Frise, E., A. S. Hammonds and S. E. Celniker, 2010 Systematic image-driven analysis of the spatial *Drosophila* embryonic expression landscape. *Molecular Systems Biology* 6.
- Frye, M. A., and M. H. Dickinson, 2004a Closing the loop between neurobiology and flight behavior in *Drosophila*. *Current Opinion in Neurobiology* 14: 729-736.
- Frye, M. A., and M. H. Dickinson, 2004b Motor output reflects the linear superposition of visual and olfactory inputs in *Drosophila*. *Journal of Experimental Biology* 207: 123-131.
- Fuerst, P. G., and R. W. Burgess, 2009 Adhesion molecules in establishing retinal circuitry. *Current Opinion in Neurobiology* 19: 389-394.
- Furman, D., and T. Bukharina, 2008 How *Drosophila melanogaster* forms its mechanoreceptors. *Current genomics* 9: 312-323.
- Gaudet, P., M. S. Livstone, S. E. Lewis and P. D. Thomas, 2011 Phylogenetic-based propagation of functional annotations within the Gene Ontology consortium. *Briefings in Bioinformatics* 12: 449-462.
- Gendron, C. M., T. H. Kuo, Z. M. Harvanek, B. Y. Chung, J. Y. Yew *et al.*, 2014 *Drosophila* Life Span and Physiology Are Modulated by Sexual Perception and Reward. *Science* 343: 544-548.
- Gorczyca, D. A., S. Younger, S. Meltzer, S. E. Kim, L. Cheng *et al.*, 2014 Identification of Ppk26, a DEG/ENaC Channel Functioning with Ppk1 in a Mutually Dependent Manner to Guide Locomotion Behavior in *Drosophila*. *Cell Reports* 9: 1446-1458.
- Grueber, W. B., B. Ye, A. W. Moore, L. Y. Jan and Y. N. Jan, 2003 Dendrites of distinct classes of *Drosophila* sensory neurons show different capacities for homotypic repulsion. *Current Biology* 13: 618-626.
- Grumblin, G., V. Strelets and C. FlyBase, 2006 FlyBase: anatomical data, images and queries. *Nucleic Acids Research* 34: D484-D488.
- Hacker, U., U. Grossniklaus, W. J. Gehring and H. Jackle, 1992 DEVELOPMENTALLY REGULATED DROSOPHILA GENE FAMILY ENCODING THE FORK HEAD DOMAIN. *Proceedings of the National Academy of Sciences of the United States of America* 89: 8754-8758.
- Haight, S. E., S. S. Salvi, M. Sevdali, M. Stark, D. Goulding *et al.*, 2010 *Drosophila* indirect flight muscle specific Act88F actin mutants as a model system for studying congenital myopathies of the human ACTA1 skeletal muscle actin gene. *Neuromuscular Disorders* 20: 363-374.
- Harbison, S. T., S. Kumar, W. Huang, L. J. McCoy, K. R. Smith *et al.*, 2019 Genome-Wide Association Study of Circadian Behavior in *Drosophila melanogaster*. *Behavior Genetics* 49: 60-82.
- Held, A., P. Major, A. Sabin, R. A. Reenan, D. Lipscombe *et al.*, 2019 Circuit Dysfunction in SOD1-ALS Model First Detected in Sensory Feedback Prior to Motor Neuron Degeneration Is Alleviated by BMP Signaling. *Journal of Neuroscience* 39: 2347-2364.
- Hevia, C. F., A. Lopez-Varea, N. Esteban and J. F. de Celis, 2017 A Search for Genes Mediating the Growth-Promoting Function of TGF beta in the *Drosophila melanogaster* Wing Disc. *Genetics* 206: 231-249.

- Hewes, R. S., and P. H. Taghert, 2001 Neuropeptides and neuropeptide receptors in the *Drosophila melanogaster* genome. *Genome research* 11: 1126-1142.
- Houot, B., V. Gigot, A. Robichon and J. F. Ferveur, 2017 Free flight odor tracking in *Drosophila*: Effect of wing chemosensors, sex and pheromonal gene regulation. *Scientific Reports* 7.
- Hu, Y., I. Flockhart, A. Vinayagam, C. Bergwitz, B. Berger *et al.*, 2011a An integrative approach to ortholog prediction for disease-focused and other functional studies. *BMC bioinformatics* 12: 357.
- Hu, Y. H., I. Flockhart, A. Vinayagam, C. Bergwitz, B. Berger *et al.*, 2011b An integrative approach to ortholog prediction for disease-focused and other functional studies. *Bmc Bioinformatics* 12.
- Huang, W., M. A. Carbone, M. M. Magwire, J. A. Peiffer, R. F. Lyman *et al.*, 2015a Genetic basis of transcriptome diversity in *Drosophila melanogaster*. *Proceedings of the National Academy of Sciences* 112: E6010-E6019.
- Huang, W., A. Massouras, Y. Inoue, J. Peiffer, M. Ramia *et al.*, 2014 Natural variation in genome architecture among 205 *Drosophila melanogaster* Genetic Reference Panel lines. *Genome Research* 24: 1193-1208.
- Huang, W., S. Richards, M. A. Carbone, D. H. Zhu, R. R. H. Anholt *et al.*, 2012 Epistasis dominates the genetic architecture of *Drosophila* quantitative traits. *Proceedings of the National Academy of Sciences of the United States of America* 109: 15553-15559.
- Huang, Y., N. Jiang, J. Li, Y. H. Ji, Z. G. Xiong *et al.*, 2015b Two aspects of ASIC function: Synaptic plasticity and neuronal injury. *Neuropharmacology* 94: 42-48.
- Hummel, T., M. L. Vasconcelos, J. C. Clemens, Y. Fishilevich, L. B. Vosshall *et al.*, 2003 Axonal targeting of olfactory receptor neurons in *Drosophila* is controlled by *Dscam*. *Neuron* 37: 221-231.
- Hummel, T., and L. Zipursky, 2004 Afferent induction of olfactory glomeruli requires N-cadherin. *Neuron* 42: 77-88.
- Inlow, J. K., and L. L. Restifo, 2004 Molecular and comparative genetics of mental retardation. *Genetics* 166: 835-881.
- Jeong, Y. T., S. M. Oh, J. Shim, J. T. Seo, J. Y. Kwon *et al.*, 2016 Mechanosensory neurons control sweet sensing in *Drosophila*. *Nature Communications* 7.
- Jin, M., S. Aibar, Z. Q. Ge, R. Chen, S. Aerts *et al.*, 2016 Identification of novel direct targets of *Drosophila* *Sine oculis* and *Eyes absent* by integration of genome-wide data sets. *Developmental Biology* 415: 157-167.
- Kang, M. J., T. J. Hansen, M. Mickiewicz, T. J. Kaczynski, S. Fye *et al.*, 2014 Disruption of Axonal Transport Perturbs Bone Morphogenetic Protein (BMP) - Signaling and Contributes to Synaptic Abnormalities in Two Neurodegenerative Diseases. *Plos One* 9.
- Kao, S. Y., E. Nikonova, K. Ravichandran and M. L. Spletter, 2019 Dissection of *Drosophila melanogaster* Flight Muscles for Omics Approaches. *Jove-Journal of Visualized Experiments*.
- Karr, T. L., 2007 Fruit flies and the sperm proteome. *Human Molecular Genetics* 16: R124-R133.

- Kimura, K. I., M. Ote, T. Tazawa and D. Yamamoto, 2005 Fruitless specifies sexually dimorphic neural circuitry in the *Drosophila* brain. *Nature* 438: 229-233.
- Kofler, R., and C. Schlötterer, 2012 Gowinda: unbiased analysis of gene set enrichment for genome-wide association studies. *Bioinformatics* 28: 2084-2085.
- Kozopas, K. M., and R. Nusse, 2002 Direct flight muscles in *Drosophila* develop from cells with characteristics of founders and depend on DWnt-2 for their correct patterning. *Developmental Biology* 243: 312-325.
- Krupp, J. J., L. E. Yaich, R. J. Wessells and R. Bodmer, 2005 Identification of genetic loci that interact with cut during *Drosophila* wing-margin development. *Genetics* 170: 1775-1795.
- Kuo, C. T., L. Y. Jan and Y. N. Jan, 2005 Dendrite-specific remodeling of *Drosophila* sensory neurons requires matrix metalloproteases, ubiquitin-proteasome, and ecdysone signaling. *Proceedings of the National Academy of Sciences of the United States of America* 102: 15230-15235.
- Langfelder, P., and S. Horvath, 2008 WGCNA: an R package for weighted correlation network analysis. *BMC Bioinformatics* 9: 559.
- Lavoy, S., V. G. Chittoor-Vinod, C. Y. Chow and I. Martin, 2018 Genetic Modifiers of Neurodegeneration in a *Drosophila* Model of Parkinson's Disease. *Genetics* 209: 1345-1356.
- Lehmann, F. O., and J. Bartussek, 2017 Neural control and precision of flight muscle activation in *Drosophila*. *Journal of Comparative Physiology a-Neuroethology Sensory Neural and Behavioral Physiology* 203: 1-14.
- Lehmann, F. O., and M. H. Dickinson, 1997 The changes in power requirements and muscle efficiency during elevated force production in the fruit fly *Drosophila melanogaster*. *Journal of Experimental Biology* 200: 1133-1143.
- Liu, L., W. A. Johnson and M. J. Welsh, 2003 *Drosophila* DEG/ENaC pickpocket genes are expressed in the tracheal system, where they may be involved in liquid clearance. *Proceedings of the National Academy of Sciences of the United States of America* 100: 2128-2133.
- Liu, X. Y., Y. I. Li and J. K. Pritchard, 2019 Trans Effects on Gene Expression Can Drive Omnigenic Inheritance. *Cell* 177: 1022-+.
- Lobell, A. S., R. R. Kaspari, Y. L. S. Negron and S. T. Harbison, 2017 The Genetic Architecture of Ovariole Number in *Drosophila melanogaster*: Genes with Major, Quantitative, and Pleiotropic Effects. *G3-Genes Genomes Genetics* 7: 2391-2403.
- Lu, B. K., A. LaMora, Y. S. Sun, M. J. Welsh and Y. Ben-Shahar, 2012 ppk23-Dependent Chemosensory Functions Contribute to Courtship Behavior in *Drosophila melanogaster*. *Plos Genetics* 8.
- Luo, K., 2017 Signaling cross talk between TGF- $\beta$ /Smad and other signaling pathways. *Cold Spring Harbor perspectives in biology* 9: a022137.
- Mackay, T. F., and W. Huang, 2018 Charting the genotype–phenotype map: lessons from the *Drosophila melanogaster* Genetic Reference Panel. *Wiley Interdisciplinary Reviews: Developmental Biology* 7.

- Mackay, T. F. C., S. Richards, E. A. Stone, A. Barbadilla, J. F. Ayroles *et al.*, 2012 The *Drosophila melanogaster* Genetic Reference Panel. *Nature* 482: 173-178.
- Manolio, T. A., F. S. Collins, N. J. Cox, D. B. Goldstein, L. A. Hindorff *et al.*, 2009 Finding the missing heritability of complex diseases. *Nature* 461: 747-753.
- Marcus, J. M., 2001 The development and evolution of crossveins in insect wings. *Journal of Anatomy* 199: 211-216.
- Mardahl-Dumesnil, M., and V. M. Fowler, 2001 Thin filaments elongate from their pointed ends during myofibril assembly in *Drosophila* indirect flight muscle. *Journal of Cell Biology* 155: 1043-1053.
- Matsubara, D., S. Y. Horiuchi, K. Shimono, T. Usui and T. Uemura, 2011 The seven-pass transmembrane cadherin Flamingo controls dendritic self-avoidance via its binding to a LIM domain protein, Espinas, in *Drosophila* sensory neurons. *Genes & Development* 25: 1982-1996.
- Maughan, D. W., and I. O. Vigoreaux, 1999 An integrated view of insect flight muscle: Genes, motor molecules, and motion. *News in Physiological Sciences* 14: 87-92.
- Mauthner, S. E., R. Y. Hwang, A. H. Lewis, Q. Xiao, A. Tsubouchi *et al.*, 2014 Balboa Binds to Pickpocket In Vivo and Is Required for Mechanical Nociception in *Drosophila* Larvae. *Current Biology* 24.
- McCarthy, M. I., G. R. Abecasis, L. R. Cardon, D. B. Goldstein, J. Little *et al.*, 2008 Genome-wide association studies for complex traits: consensus, uncertainty and challenges. *Nature Reviews Genetics* 9: 356-369.
- McClellan, J., and M. C. King, 2010 Genetic Heterogeneity in Human Disease. *Cell* 141: 210-217.
- Metaxakis, A., S. Oehler, A. Klinakis and C. Savakis, 2005a Minos as a genetic and genomic tool in *Drosophila melanogaster*. *Genetics*.
- Metaxakis, A., S. Oehler, A. Klinakis and C. Savakis, 2005b Minos as a genetic and genomic tool in *Drosophila melanogaster*. *Genetics* 171: 571-581.
- Montgomery, S. L., D. Vorojeikina, W. Huang, T. F. C. Mackay, R. R. H. Anholt *et al.*, 2014 Genome-Wide Association Analysis of Tolerance to Methylmercury Toxicity in *Drosophila* Implicates Myogenic and Neuromuscular Developmental Pathways. *Plos One* 9.
- Montooth, K. L., J. H. Marden and A. G. Clark, 2003 Mapping determinants of variation in energy metabolism, respiration and flight in *Drosophila*. *Genetics* 165: 623-635.
- Mummery-Widmer, J. L., M. Yamazaki, T. Stoeger, M. Novatchkova, S. Bhalerao *et al.*, 2009 Genome-wide analysis of Notch signalling in *Drosophila* by transgenic RNAi. *Nature* 458: 987-U959.
- Murali, T., S. Pacifico, J. K. Yu, S. Guest, G. G. Roberts *et al.*, 2011 DroID 2011: a comprehensive, integrated resource for protein, transcription factor, RNA and gene interactions for *Drosophila*. *Nucleic Acids Research* 39: D736-D743.
- Nakka, P., B. J. Raphael and S. Ramachandran, 2016 Gene and Network Analysis of Common Variants Reveals Novel Associations in Multiple Complex Diseases. *Genetics* 204: 783-+.

- Neely, G. G., A. Hess, M. Costigan, A. C. Keene, S. Goulas *et al.*, 2010 A Genome-wide Drosophila Screen for Heat Nociception Identifies alpha 2 delta 3 as an Evolutionarily Conserved Pain Gene. *Cell* 143: 628-638.
- Negre, N., C. D. Brown, L. J. Ma, C. A. Bristow, S. W. Miller *et al.*, 2011 A cis-regulatory map of the Drosophila genome. *Nature* 471: 527-531.
- Neumuller, R. A., C. Richter, A. Fischer, M. Novatchkova, K. G. Neumuller *et al.*, 2011 Genome-Wide Analysis of Self-Renewal in Drosophila Neural Stem Cells by Transgenic RNAi. *Cell Stem Cell* 8: 580-593.
- Neves, G., J. Zucker, M. Daly and A. Chess, 2004 Stochastic yet biased expression of multiple Dscam splice variants by individual cells. *Nature Genetics* 36: 240-246.
- Ng, R., S. S. Salem, S. T. Wu, M. L. Wu, H. H. Lin *et al.*, 2019 Amplification of Drosophila Olfactory Responses by a DEG/ENaC Channel. *Neuron* 104: 947-+.
- Nguyen, M. U., J. Kwong, J. Chang, V. G. Gillet, R. M. Lee *et al.*, 2016 The extracellular and cytoplasmic domains of syndecan cooperate postsynaptically to promote synapse growth at the Drosophila neuromuscular junction. *PloS one* 11.
- Nongthomba, U., S. Pasalodos-Sanchez, S. Clark, J. D. Clayton and J. C. Sparrow, 2001 Expression and function of the Drosophila ACT88F actin isoform is not restricted to the indirect flight muscles. *Journal of muscle research and cell motility* 22: 111-119.
- O'Connor, M. B., D. Umulis, H. G. Othmer and S. S. Blair, 2006 Shaping BMP morphogen gradients in the Drosophila embryo and pupal wing. *Development* 133: 183-193.
- Okada, H., H. A. Ebhardt, S. C. Vonesch, R. Aebersold and E. Hafen, 2016 Proteome-wide association studies identify biochemical modules associated with a wing-size phenotype in *Drosophila melanogaster*. *Nature Communications* 7.
- Oleksiak, M. F., G. A. Churchill and D. L. Crawford, 2002 Variation in gene expression within and among natural populations. *Nature genetics* 32: 261.
- Ortega-Ramirez, A., R. Vega and E. Soto, 2017 Acid-Sensing Ion Channels as Potential Therapeutic Targets in Neurodegeneration and Neuroinflammation. *Mediators of Inflammation*.
- Page, R. M., A. Munch, T. Horn, P. H. Kuhn, A. Colombo *et al.*, 2012 Loss of PAFAH1B2 Reduces Amyloid-beta Generation by Promoting the Degradation of Amyloid Precursor Protein C-Terminal Fragments. *Journal of Neuroscience* 32: 18204-18214.
- Paukert, M., S. Sidi, C. Russell, M. Siba, S. W. Wilson *et al.*, 2004 A family of acid-sensing ion channels from the zebrafish - Widespread expression in the central nervous system suggests a conserved role in neuronal communication. *Journal of Biological Chemistry* 279: 18783-18791.
- Paul, L., S. H. Wang, S. N. Manivannan, L. Bonanno, S. Lewis *et al.*, 2013 Dpp-induced Egfr signaling triggers postembryonic wing development in *Drosophila*. *Proceedings of the National Academy of Sciences of the United States of America* 110: 5058-5063.
- Pavlou, H. J., and S. F. Goodwin, 2013 Courtship behavior in *Drosophila melanogaster*: towards a 'courtship connectome'. *Current Opinion in Neurobiology* 23: 76-83.



- Pinto, C., P. Cardenas, N. Osses and J. P. Henriquez, 2013 Characterization of Wnt/beta-catenin and BMP/Smad signaling pathways in an in vitro model of amyotrophic lateral sclerosis. *Frontiers in Cellular Neuroscience* 7.
- Pitchers, W., J. Nye, E. J. Marquez, A. Kowalski, I. Dworkin *et al.*, 2019 A Multivariate Genome-Wide Association Study of Wing Shape in *Drosophila melanogaster*. *Genetics* 211: 1429-1447.
- Purcell, S., B. Neale, K. Todd-Brown, L. Thomas, M. A. R. Ferreira *et al.*, 2007 PLINK: A tool set for whole-genome association and population-based linkage analyses. *American Journal of Human Genetics* 81: 559-575.
- Quijano, J. C., M. J. Stinchfield, B. Zerlanko, Y. Y. Gibbens, N. T. Takaesu *et al.*, 2010 The Sno Oncogene Antagonizes Wingless Signaling during Wing Development in *Drosophila*. *Plos One* 5.
- Reyna, M. A., M. D. M. Leiserson and B. J. Raphael, 2018 Hierarchical HotNet: identifying hierarchies of altered subnetworks. *Bioinformatics* 34: 972-980.
- Rezaval, C., H. J. Pavlou, A. J. Dornan, Y. B. Chan, E. A. Kravitz *et al.*, 2012 Neural Circuitry Underlying *Drosophila* Female Postmating Behavioral Responses. *Current Biology* 22: 1155-1165.
- Schindelin, J., I. Arganda-Carreras, E. Frise, V. Kaynig, M. Longair *et al.*, 2012 Fiji: an open-source platform for biological-image analysis. *Nature Methods* 9: 676-682.
- Sherman, A., and M. H. Dickinson, 2004 Summation of visual and mechanosensory feedback in *Drosophila* flight control. *Journal of Experimental Biology* 207: 133-142.
- Shirangi, T. R., A. M. Wong, J. W. Truman and D. L. Stern, 2016 Doublesex Regulates the Connectivity of a Neural Circuit Controlling *Drosophila* Male Courtship Song. *Developmental Cell* 37: 533-544.
- Shukla, J. P., G. Deshpande and L. S. Shashidhara, 2017 Ataxin 2-binding protein 1 is a context-specific positive regulator of Notch signaling during neurogenesis in *Drosophila melanogaster*. *Development* 144: 905-915.
- Sibilia, M., R. Kroismayr, B. M. Lichtenberger, A. Natarajan, M. Hecking *et al.*, 2007 The epidermal growth factor receptor: from development to tumorigenesis. *Differentiation* 75: 770-787.
- Smith, S. A., and D. Shepherd, 1996 Central afferent projections of proprioceptive sensory neurons in *Drosophila* revealed with the enhancer-trap technique. *Journal of Comparative Neurology* 364: 311-323.
- Soba, P., S. Zhu, K. Emoto, S. Younger, S. J. Yang *et al.*, 2007 *Drosophila* sensory neurons require Dscam for dendritic self-avoidance and proper dendritic field organization. *Neuron* 54: 403-416.
- Spletter, M. L., C. Barz, A. Yeroslaviz, C. Schonbauer, I. R. S. Ferreira *et al.*, 2015 The RNA-binding protein Arrest (Bruno) regulates alternative splicing to enable myofibril maturation in *Drosophila* flight muscle. *Embo Reports* 16: 178-191.
- Stocker, R. F., 1994 THE ORGANIZATION OF THE CHEMOSENSORY SYSTEM IN *DROSOPHILA-MELANOGASTER* - A REVIEW. *Cell and Tissue Research* 275: 3-26.

- Strausfeld, N. J., 2009 Brain and optic lobes, pp. 121-130 in *Encyclopedia of Insects*. Elsevier.
- Tadros, W., S. W. Xu, O. Akin, C. H. Yi, G. J. E. Shin *et al.*, 2016 Dscam Proteins Direct Dendritic Targeting through Adhesion. *Neuron* 89: 480-493.
- Takaesu, N. T., C. Hyman-Walsh, Y. Ye, R. G. Wisotzkey, M. J. Stinchfield *et al.*, 2006 dSno facilitates Baboon signaling in the Drosophila brain by switching the affinity of Medea away from Mad and toward dSmad2. *Genetics* 174: 1299-1313.
- Taylor, G. K., and H. G. Krapp, 2007 Sensory systems and flight stability: what do insects measure and why? *Advances in insect physiology* 34: 231-316.
- Thistle, R., P. Cameron, A. Ghorayshi, L. Dennison and K. Scott, 2012 Contact chemoreceptors mediate male-male repulsion and male-female attraction during Drosophila courtship. *Cell* 149: 1140-1151.
- Ueda, A., and C. F. Wu, 2009 Effects of Social Isolation on Neuromuscular Excitability and Aggressive Behaviors in Drosophila: Altered Responses by Hk and gsts1, Two Mutations Implicated in Redox Regulation. *Journal of Neurogenetics* 23: 378-394.
- Ugur, B., K. C. Chen and H. J. Bellen, 2016 Drosophila tools and assays for the study of human diseases. *Disease Models & Mechanisms* 9: 235-244.
- Vannoy, C. H., W. Xiao, P. J. Lu, X. Xiao and Q. L. Lu, 2017 Efficacy of Gene Therapy Is Dependent on Disease Progression in Dystrophic Mice with Mutations in the FKRP Gene. *Molecular Therapy-Methods & Clinical Development* 5: 31-42.
- Vonesch, S. C., D. Lamparter, T. F. C. Mackay, S. Bergmann and E. Hafen, 2016 Genome-Wide Analysis Reveals Novel Regulators of Growth in Drosophila melanogaster. *PLOS Genetics* 12: e1005616.
- Watanabe, K., S. Stringer, O. Frei, M. U. Mirkov, C. de Leeuw *et al.*, 2019 A global overview of pleiotropy and genetic architecture in complex traits. *Nature Genetics* 51: 1339-+.
- Weitkunat, M., and F. Schnorrer, 2014 A guide to study Drosophila muscle biology. *Methods* 68: 2-14.
- Wharton, K. A., and M. Serpe, 2013 Fine-tuned shuttles for bone morphogenetic proteins. *Current Opinion in Genetics & Development* 23: 374-384.
- Wittkopp, P. J., B. K. Haerum and A. G. Clark, 2004 Evolutionary changes in cis and trans gene regulation. *Nature* 430: 85-88.
- Xiong, Z. G., and T. L. Xu, 2012 The role of ASICs in cerebral ischemia. *Wiley Interdisciplinary Reviews: Membrane Transport and Signaling* 1: 655-662.
- Yamagata, M., and J. R. Sanes, 2008 Dscam and Sidekick proteins direct lamina-specific synaptic connections in vertebrate retina. *Nature* 451: 465-U466.
- Yamashita, S., T. Takigahira and K. H. Takahashi, 2018 Genome-wide association analysis of host genotype and plastic wing morphological variation of an endoparasitoid wasp *Asobara japonica* (Hymenoptera: Braconidae). *Genetica* 146: 313-321.
- Yu, J. K., S. Pacifico, G. Z. Liu and R. L. Finley, 2008 DroiD: the Drosophila Interactions Database, a comprehensive resource for annotated gene and protein interactions. *Bmc Genomics* 9.

- Yu, J. Y., M. I. Kanai, E. Demir, G. Jefferis and B. J. Dickson, 2010 Cellular Organization of the Neural Circuit that Drives *Drosophila* Courtship Behavior. *Current Biology* 20: 1602-1614.
- Yu, K., M. A. Sturtevant, B. Biehs, V. Francois, R. W. Padgett *et al.*, 1996 The *Drosophila* decapentaplegic and short gastrulation genes function antagonistically during adult wing vein development. *Development* 122: 4033-4044.
- Zelle, K. M., B. K. Lu, S. C. Pyfrom and Y. Ben-Shahar, 2013 The Genetic Architecture of Degenerin/Epithelial Sodium Channels in *Drosophila*. *G3-Genes Genomes Genetics* 3: 441-450.
- Zhan, X. L., J. C. Clemens, G. Neves, D. Hattori, J. J. Flanagan *et al.*, 2004 Analysis of Dscam diversity in regulating axon guidance in *Drosophila* mushroom bodies. *Neuron* 43: 673-686.
- Zheng, Z., H. Zheng and W. Yan, 2007 Fank1 is a testis-specific gene encoding a nuclear protein exclusively expressed during the transition from the meiotic to the haploid phase of spermatogenesis. *Gene Expression Patterns* 7: 777-783.
- Zhou, S. S., T. V. Morozova, Y. N. Hussain, S. E. Luoma, L. McCoy *et al.*, 2016 The Genetic Basis for Variation in Sensitivity to Lead Toxicity in *Drosophila melanogaster*. *Environmental Health Perspectives* 124: 1062-1070.
- zur Lage, P., F. G. Newton and A. P. Jarman, 2019 Survey of the Ciliary Motility Machinery of *Drosophila* Sperm and Ciliated Mechanosensory Neurons Reveals Unexpected Cell-Type Specific Variations: A Model for Motile Ciliopathies. *Frontiers in Genetics* 10.

**Table 1. Six additive variants surpassed the Bonferroni significance threshold.**

These variants represented all four sex-based phenotypes and were typically near the minor allele frequency (MAF) > 0.05 limit. All but one mapped to a gene in *Drosophila* (Dmel), and three had human orthologs (Hsap). Additionally, two SNPs mapped to transcription factor binding sites (TFBS) and a silencer region.

Variant	MAF	Annotation		
		Gene (Dmel)	Gene (Hsap)	Regulatory Region
2R_17433667_SNP	0.05128	<i>Egfr</i> (intron)	EGFR	TFBS ( <i>bcd, da, dl, gt, hb, kni, Med, prd, sna, tll, twi, disco, Trl</i> )
2R_2718036_DEL	0.05641	<i>CG15236</i> (intron) <i>CG34215</i> (downstream, 764 bp)	- -	-
3L_8237821_SNP	0.0829	<i>Dscam4</i> (intron)	DSCAM	-
3R_20907854_SNP	0.06557	<i>fd96Ca</i> (upstream, 552bp)	FOXB1/ FOXB2	TFBS ( <i>dl</i> ) Silencer ( <i>HDAC</i> )
3R_4379159_SNP	0.05263	<i>Or85d</i> (non-synonymous, C277Y)	-	-
3R_9684126_SNP	0.1514	-	-	-

**Table 2. Aggregated gene and variant counts by sex-based phenotype for each analysis.** Each analysis identified different genetic modifiers (variants, genes, networks). For each analysis, the different variant-, gene-, and network-based analyses identified separate genetic features associated with flight performance.

<b>Additive analysis</b>				
	<b>Male</b>	<b>Female</b>	<b>Sex-Average</b>	<b>Sex-Different</b>
Bonferroni variants ( $P \leq 2.63 \cdot 10^{-8}$ )	1	4	3	1
Bonferroni MinSNP genes ( $P \leq 2.63 \cdot 10^{-8}$ )	1	4	3	2
Conventional variants ( $P \leq 1.00 \cdot 10^{-5}$ )	68	85	85	16
Conventional MinSNP genes ( $P \leq 1 \cdot 10^{-5}$ )	56	73	69	11
<b>Marginal analysis</b>				
	<b>Male</b>	<b>Female</b>	<b>Sex-Average</b>	<b>Sex-Different</b>
Bonferroni Variants ( $P \leq 2.56 \cdot 10^{-8}$ )	7	13	62	0
MinSNP Genes ( $P \leq 2.56 \cdot 10^{-8}$ )	5	7	21	0
<b>Epistatic analysis</b>				
	<b>Male</b> ( $P \leq 3.75 \cdot 10^{-9}$ )	<b>Female</b> ( $P \leq 2.02 \cdot 10^{-9}$ )	<b>Sex-Average</b> ( $P \leq 4.24 \cdot 10^{-10}$ )	<b>Sex-Different</b>
Paired Primary Variants	1	5	18	0
Paired Primary Genes	1	2	6	0
Paired Secondary Variants	42	2188	6139	0
Paired Secondary Genes	28	1061	2419	0
<b>Whole gene analysis</b>				
	<b>Male</b>	<b>Female</b>	<b>Sex-Average</b>	<b>Sex-Different</b>
Bonferroni ( $P \leq 3.01 \cdot 10^{-6}$ )	23	29	25	23
<b>Network analysis</b>				
	<b>All sex-based phenotypes</b>			
Sub-Networks	9			

Supplemental tables 1-18 are available online:

- <https://doi.org/10.26300/v4rm-sa82>

Supplemental files 1-3 are available online:

1. <https://doi.org/10.26300/dwvm-vt70>
2. <https://doi.org/10.26300/317y-p682>
3. <https://doi.org/10.26300/xcrh-c744>
4. <https://doi.org/10.26300/qhc7-dp70>

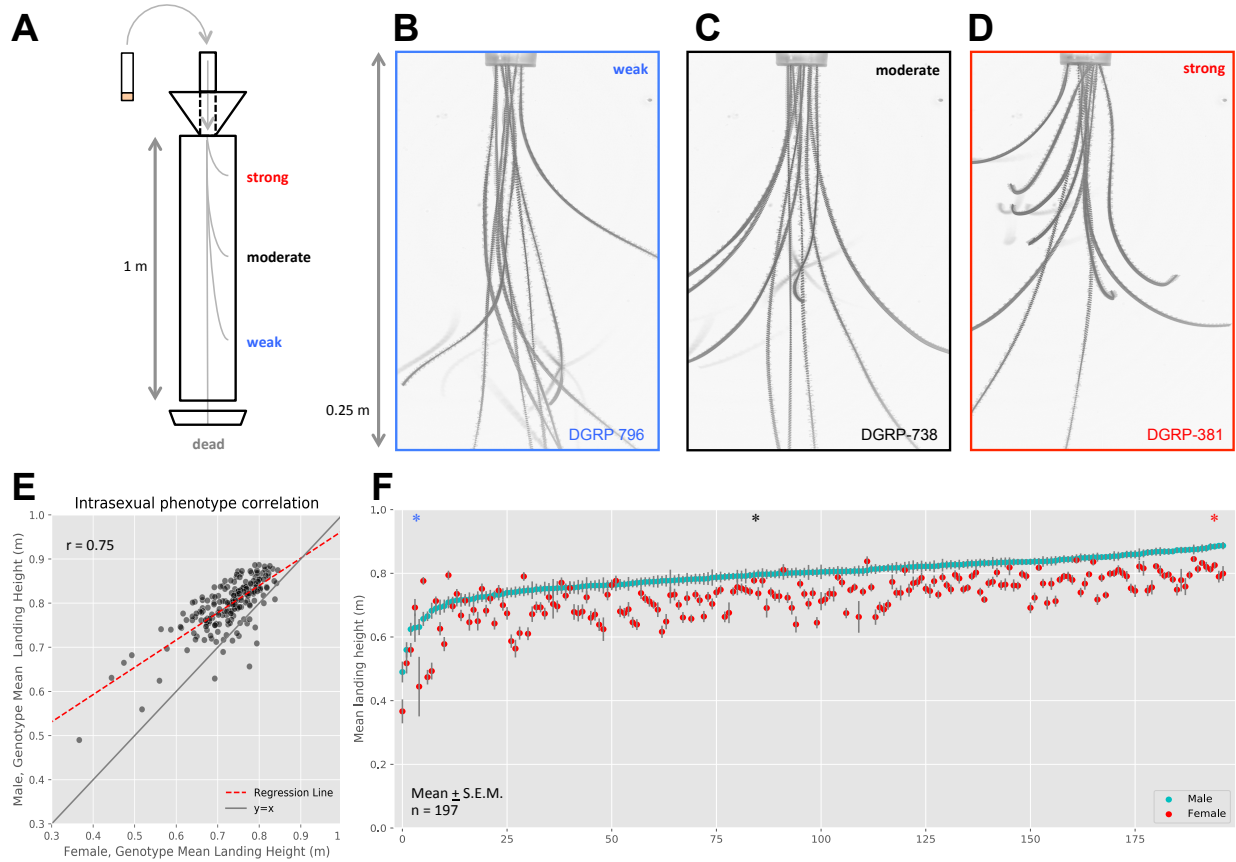


**Figure 1. DGRP lines show differences in flight performance across lines.** (A) Flight performance assay measures the average landing height of flies as they fall through a flight column. Vials of flies are sent down the top chute and abruptly stop at the bottom, ejecting flies into a meter-long column. Falling flies will instinctively right themselves and fly to the periphery, doing so at different times depending on their performance ability. (B-D) Collapsed z-stacks of high-speed video frames from the top quarter of the flight column illustrate these performance differences in (B) weak, (C) intermediate, and (D) strong genotypes. (E) There is sexual dimorphism within genotypes (deviation of red dashed regression line from  $y = x$  solid gray line), though sexes are well correlated ( $r = 0.75$ ,  $n = 197$ ). (F) Sexually dimorphic performances are also viewable in the distribution of performances for each male (cyan) and female (red) genotype pair (mean  $\pm$  S.E.M.). Sex-genotype pairs are sorted in order of increasing male mean landing height. Genotype performances for genotypes in B-D are indicated on the distribution with the corresponding color-coded asterisk (\*) above the respective genotype position.

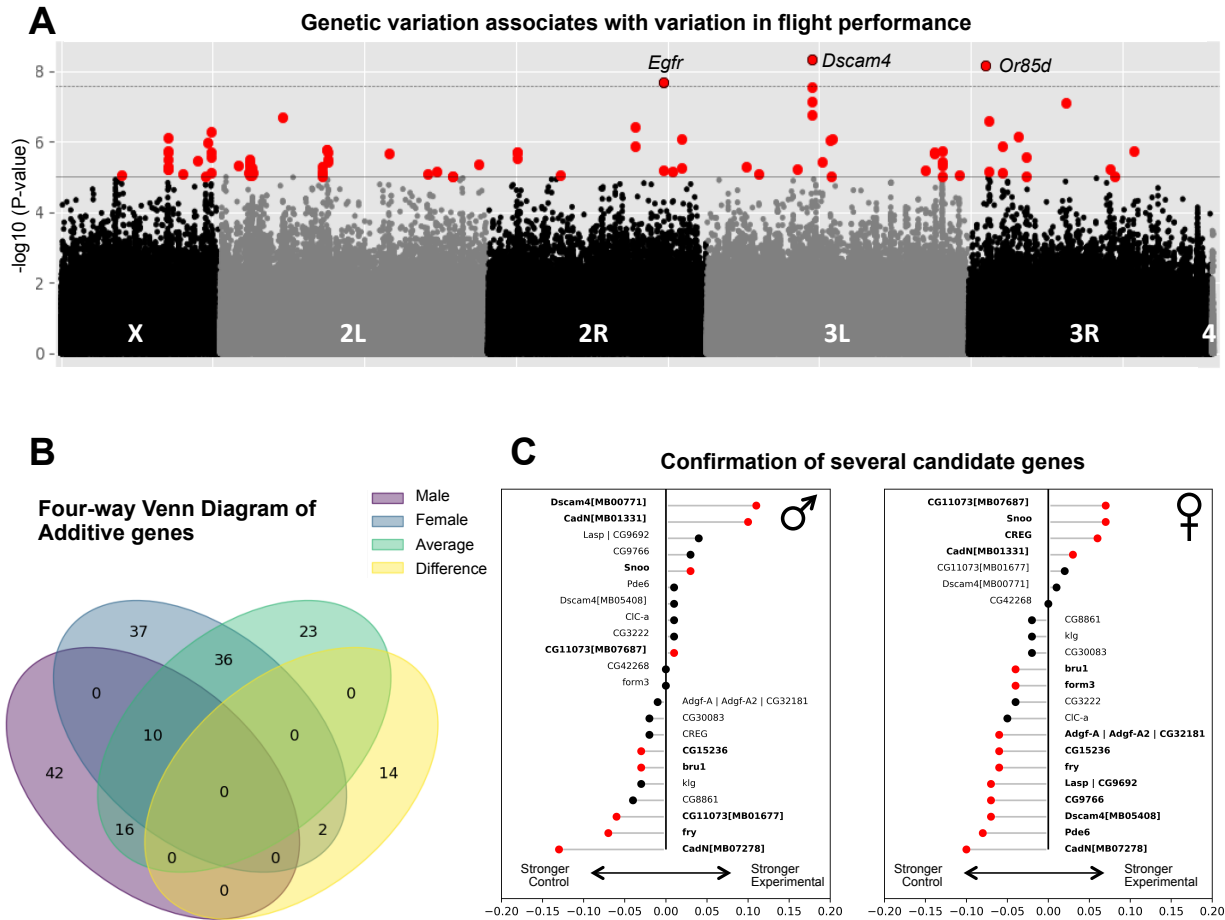


**Figure 2. Variation in flight performance associated with several additive variants, some of which were functionally validated.** (A) An additive screen for genetic variants identified several variants that exceeded the traditional DGRP ( $P \leq 1E-5$ ) threshold (gray line). These points (red points) were spread throughout the genome on all but chromosome 4. Sex-average variants pictured, though other sex-based phenotypes had similar profiles. (B) Approximately half of all variants were shared with at least one other sex-based analysis, while the other half of all variants was exclusive to a single analysis. (C) Candidate genes were selected based on the genes that the most significant variants mapped to. Both sexes were tested for flight performance. Validated genes were determined if there was a significant difference between experimental lines homozygous for an insertional mutant in the candidate gene and their background control lines lacking the insertional mutant (red points, Mann-Whitney-U test,  $P \leq 0.05$ ). Very significant candidate genes (*CadN*, *CG11073/flapper*, and *Dscam4*) each had two independent validation lines.



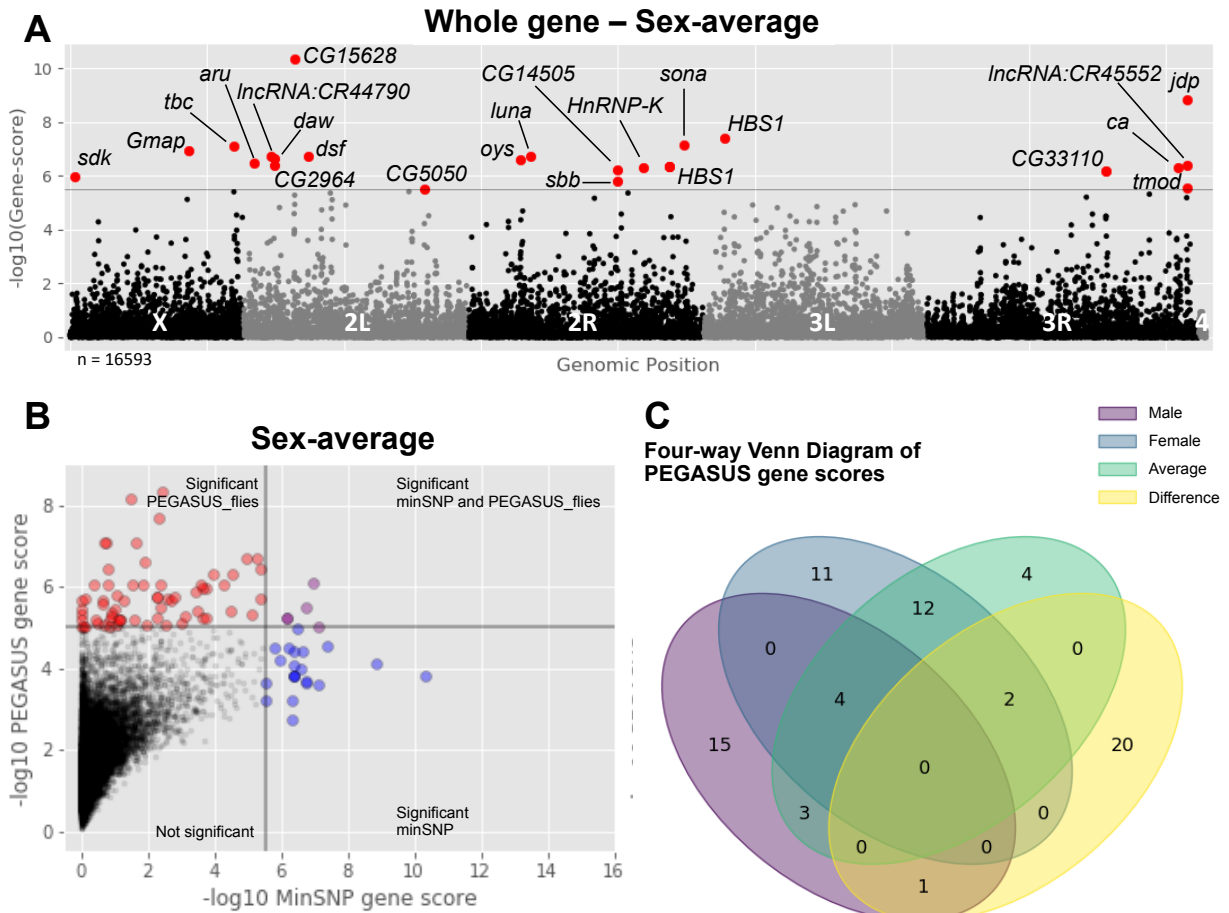


**Figure 3. PEGASUS\_flies identifies different genetic modifiers than the additive screen.** (A) PEGASUS\_flies results plotted as a Manhattan plot. For the sex-average phenotype, several genes (red points, labeled with gene symbol) exceed a strict Bonferroni significance threshold (gray dashed line,  $P \leq 3.43E-6$ ) identified several genes. (B) PEGASUS\_flies prioritizes genetic modifiers of moderate effect, taking into account linkage blocks and gene length. Significant PEGASUS\_flies (red) compared against genes significant under a minSNP approach for additive variants (blue) have very little overlap between the two sets (purple). (C) Many of the genes PEGASUS\_flies identifies are unique to a sex-based phenotype, though the sex-average genes were generally found in other analyses.

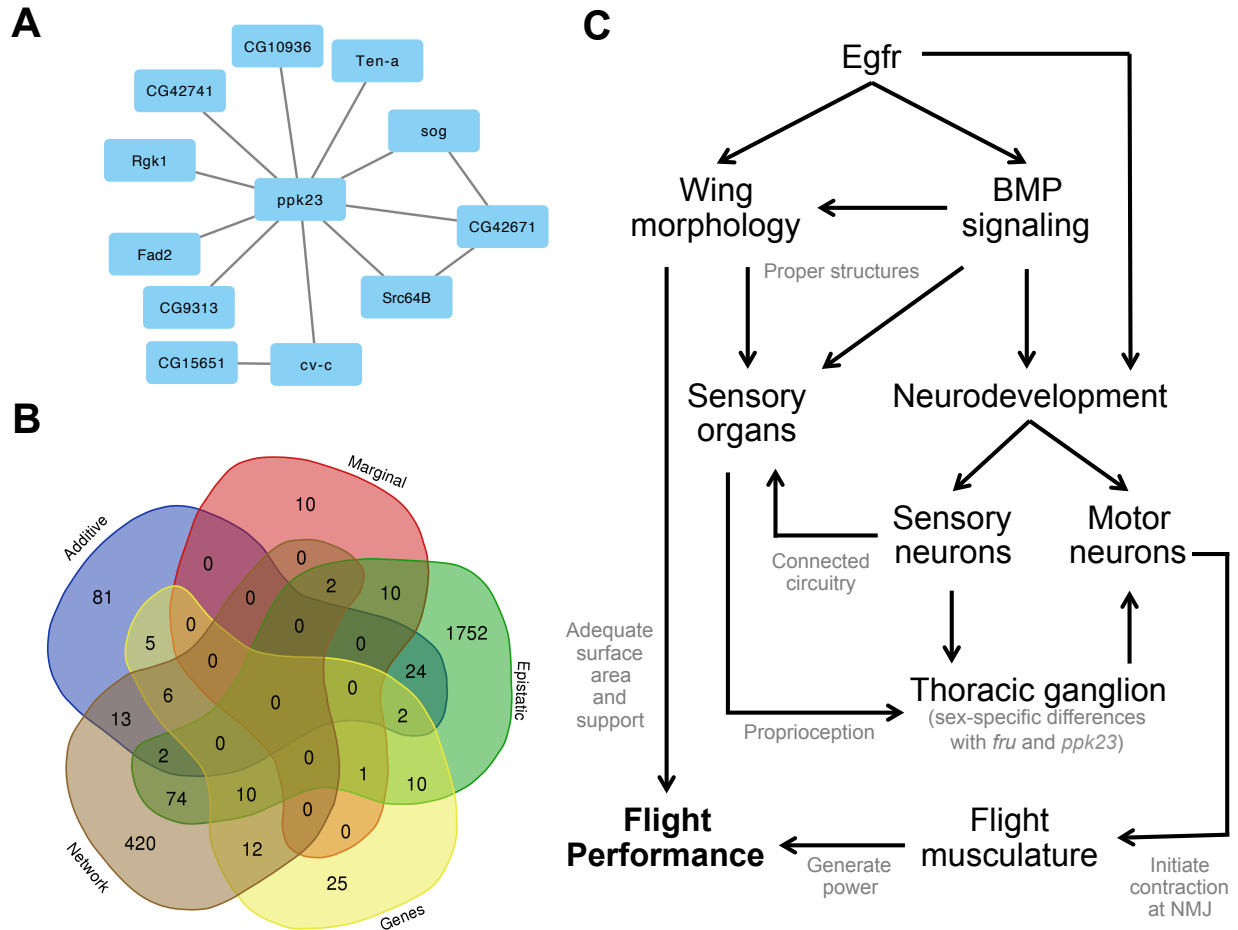


**Figure 4. Flight performance is a larger complex trait comprised of several smaller traits.** (A) The genetic architecture of epistatically interacting genes generally coordinated through *ppk23*. A few other genes mapped to from marginal variants had epistatic interactions with marginal variants in *ppk23*. (B) Genes or genes mapped to from variants across different analyses were not identified in more than three analyses. Roughly half or more genes were unique to each analysis. (C) Flight performance has a complex genetic architecture, with the key developmental gene *Egfr* and BMP signaling pathway contributing to wing and neurodevelopment. These processes are both important for structuring the sensory organs that enable the fly to use mechanosensory channels for proprioception. Signals from the sensory organs on the wing, head, and body travel to the brain and thoracic ganglion, which sends signals through the motor neurons to the direct and indirect flight musculature that is also differentially assembled and innervated to generate power and control the wing angle during flight.

## Flight performance repeatability

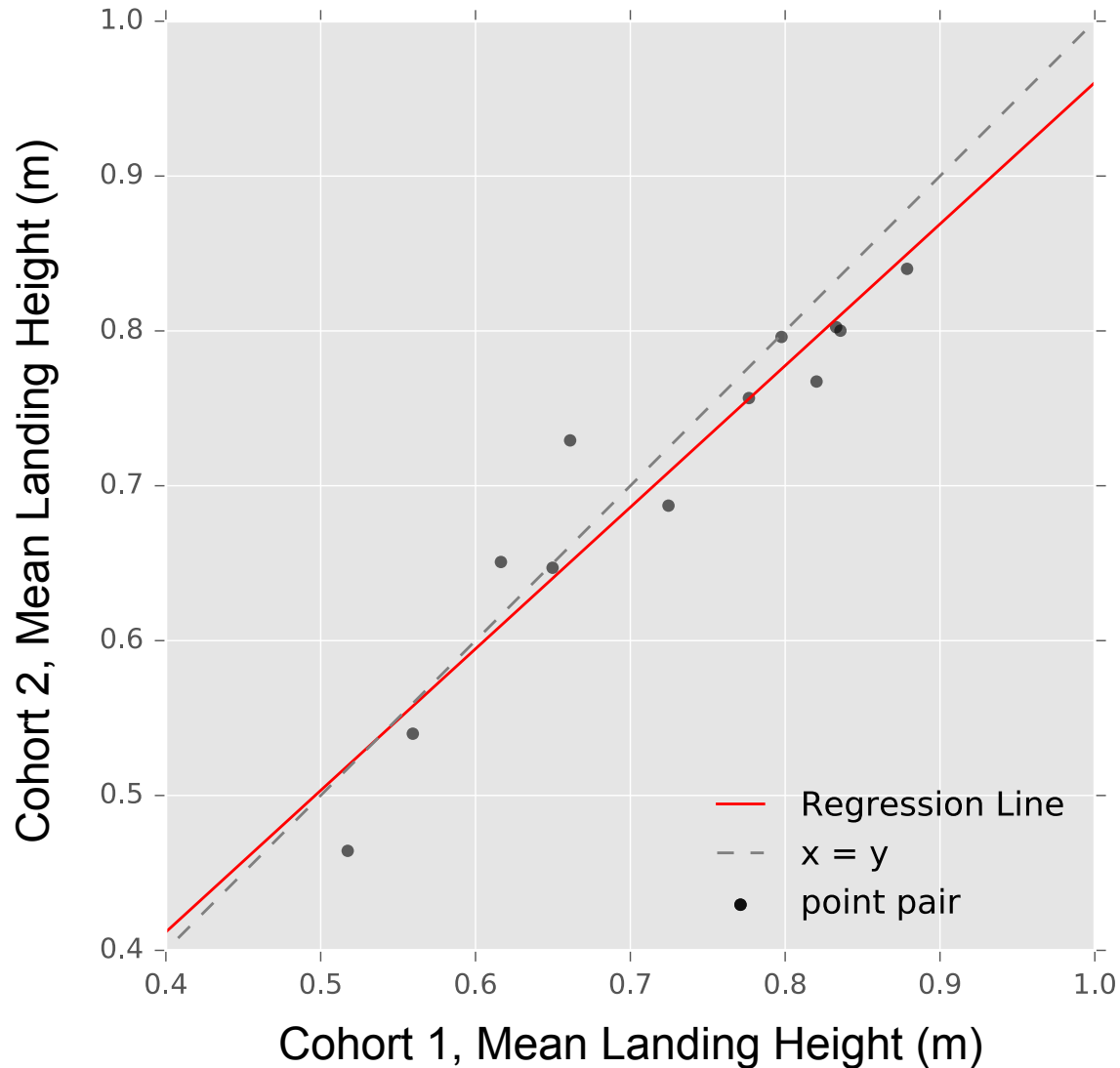


**Figure S1. DGRP lines' mean flight performance is highly repeatable across generations.** Set of genotypes ( $n = 12$ ) reared 10 generations apart show very strong agreement ( $r = 0.95$ ) in mean flight performance scores. The regression line (red line) through the point pairs (black points) has nearly the same slope and y-intercept as the  $x = y$  line (gray dashed line).

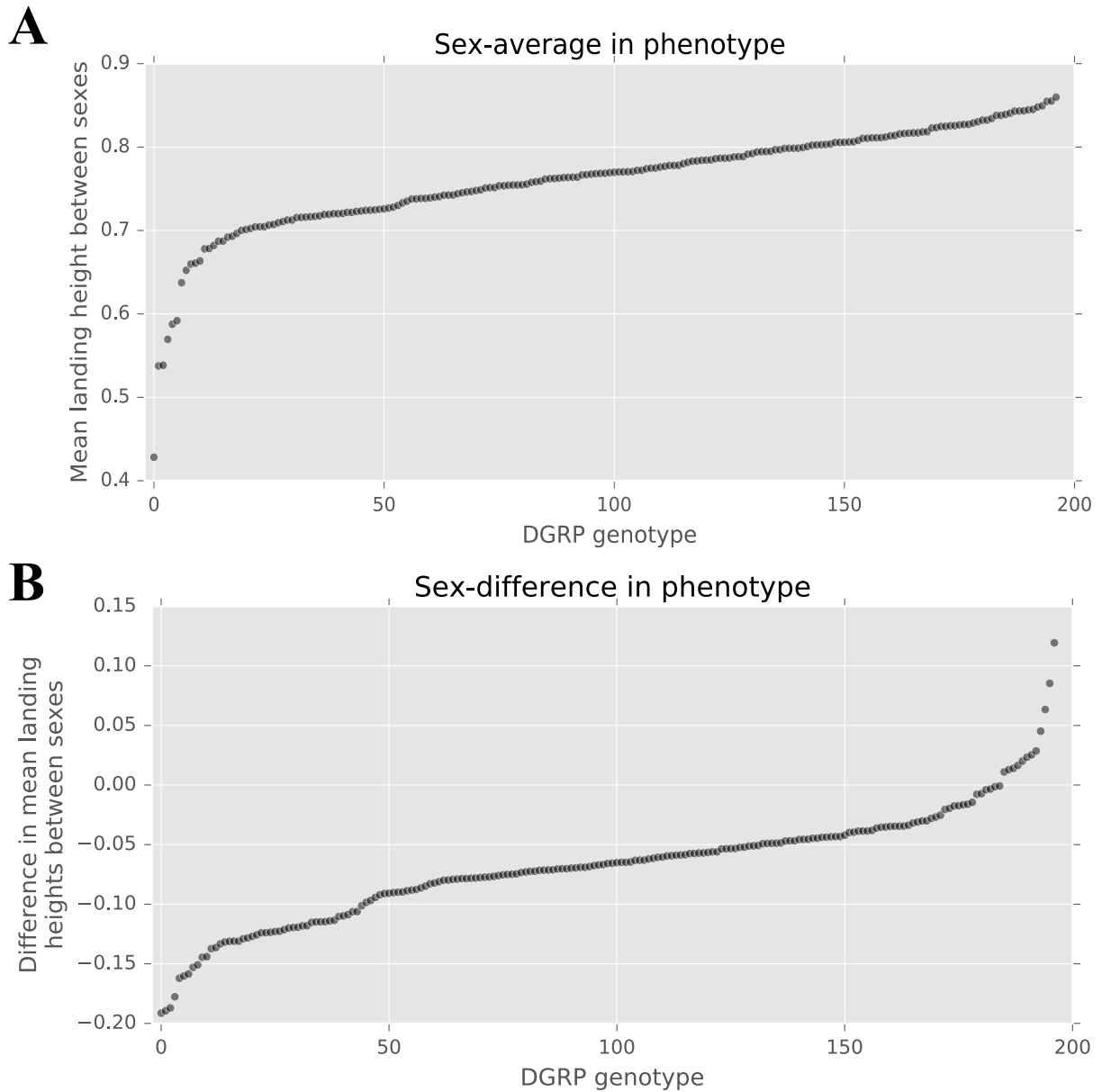


**Figure S2. Sex-average and sex-difference phenotypic distributions are amenable to an association study.** Distribution in mean landing height (m) for (A) sex-average and (B) sex-difference phenotypes suggest ample phenotypic variation exists to run an association study. Each plot is sorted in order of increasing phenotype score, independent of one another.

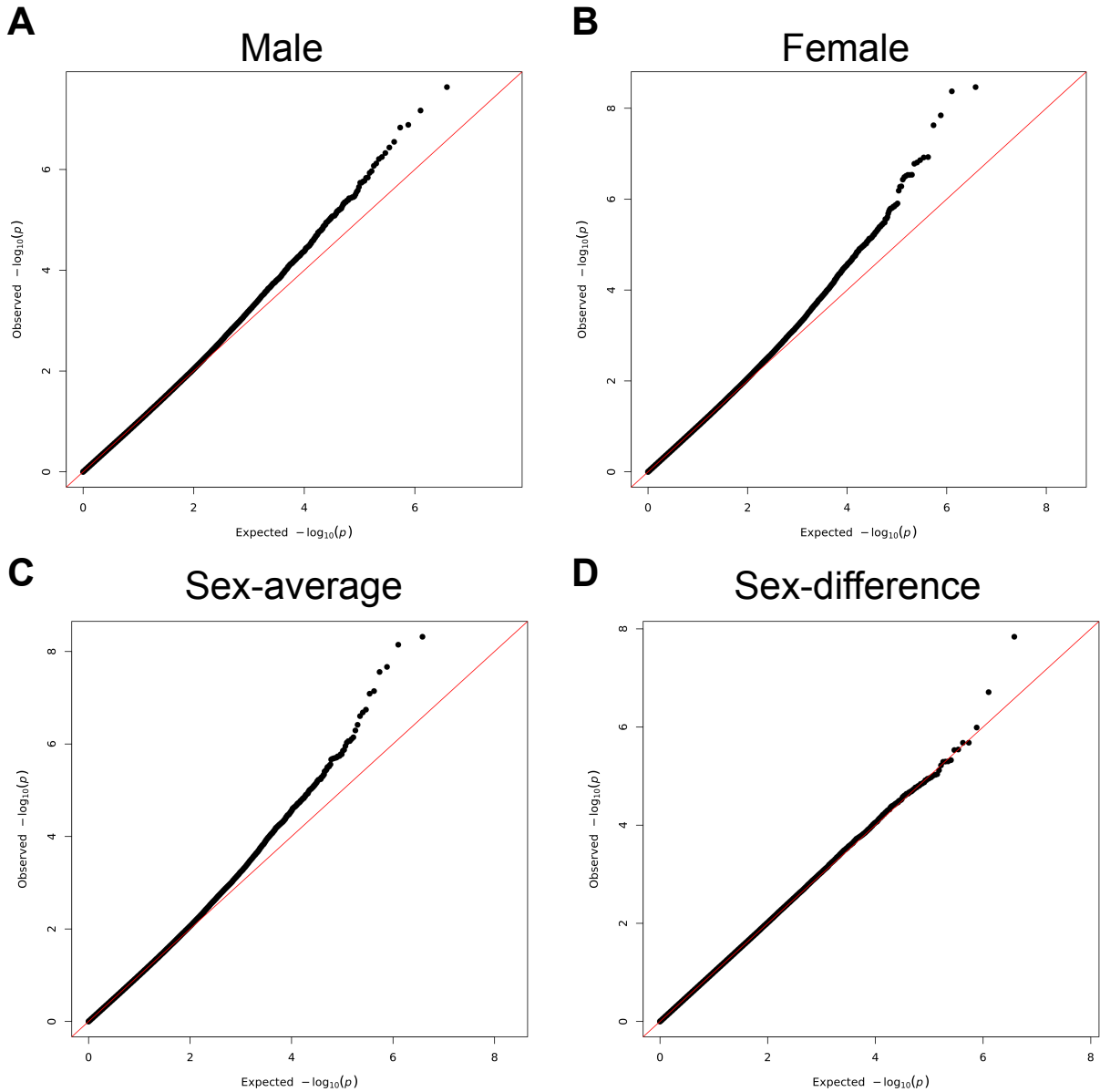


**Figure S3. QQ-plots show enrichment for some additive variants across each of the sex-based phenotypes.** Plots comparing the theoretical vs. observed  $P$ -value distribution across (A) males, (B) females, (C) sex-average, and (D) sex-difference phenotypes. Red line denotes  $y = x$ .

## Linkage heatmap of top hits

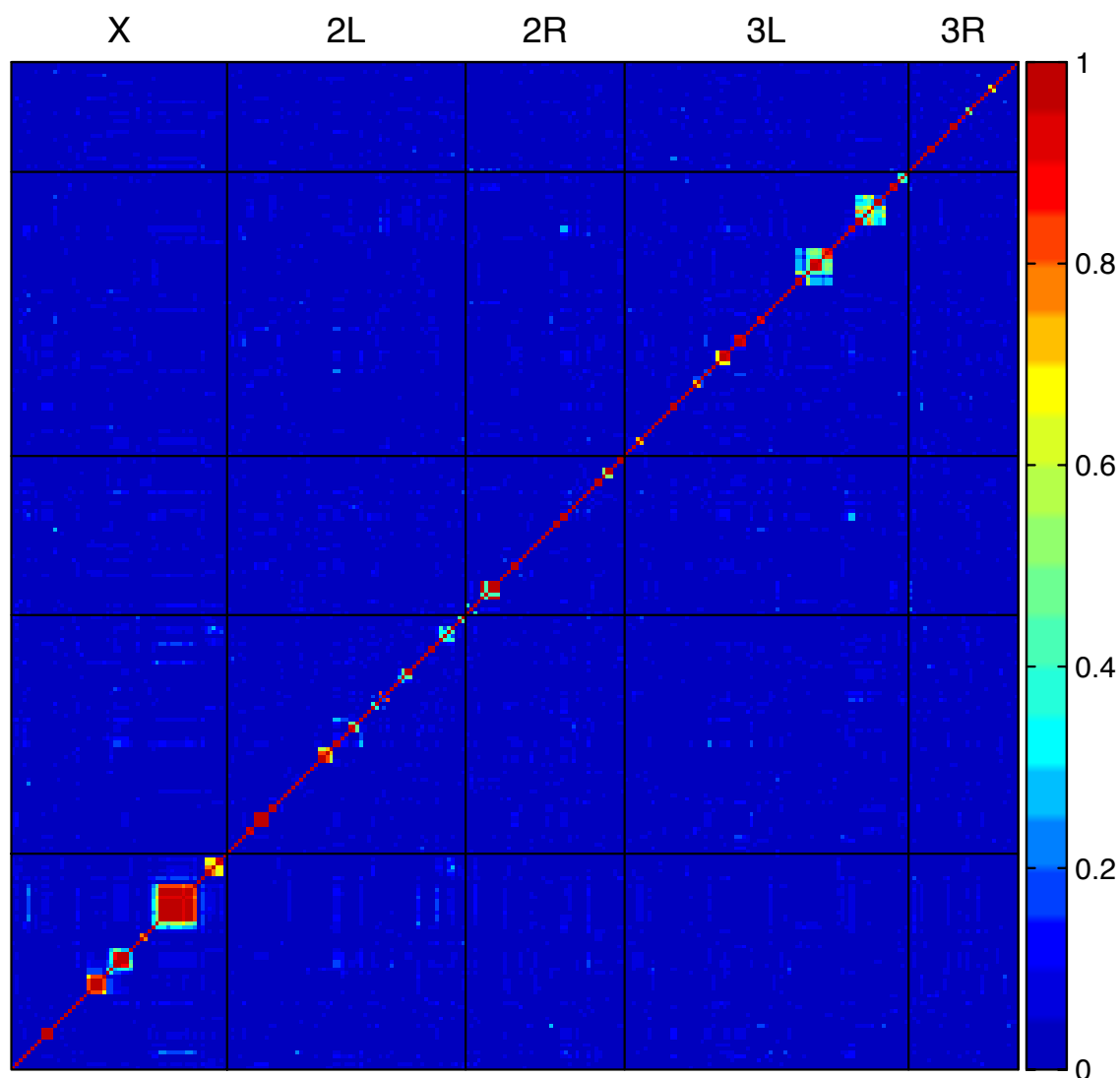


**Figure S4. Top additive associations are spaced throughout the genome.** Top additive variants, those reported in DGRP2 webserver file with the `top.annot` suffix, are largely free of linkage blocks. There is a larger block on X, corresponding with 10 variants that map to intronic and one synonymous coding site in *CG32506*. The heat component corresponds with likelihood of being in a linkage block from less (0 - blue) to more likely (1 - red).

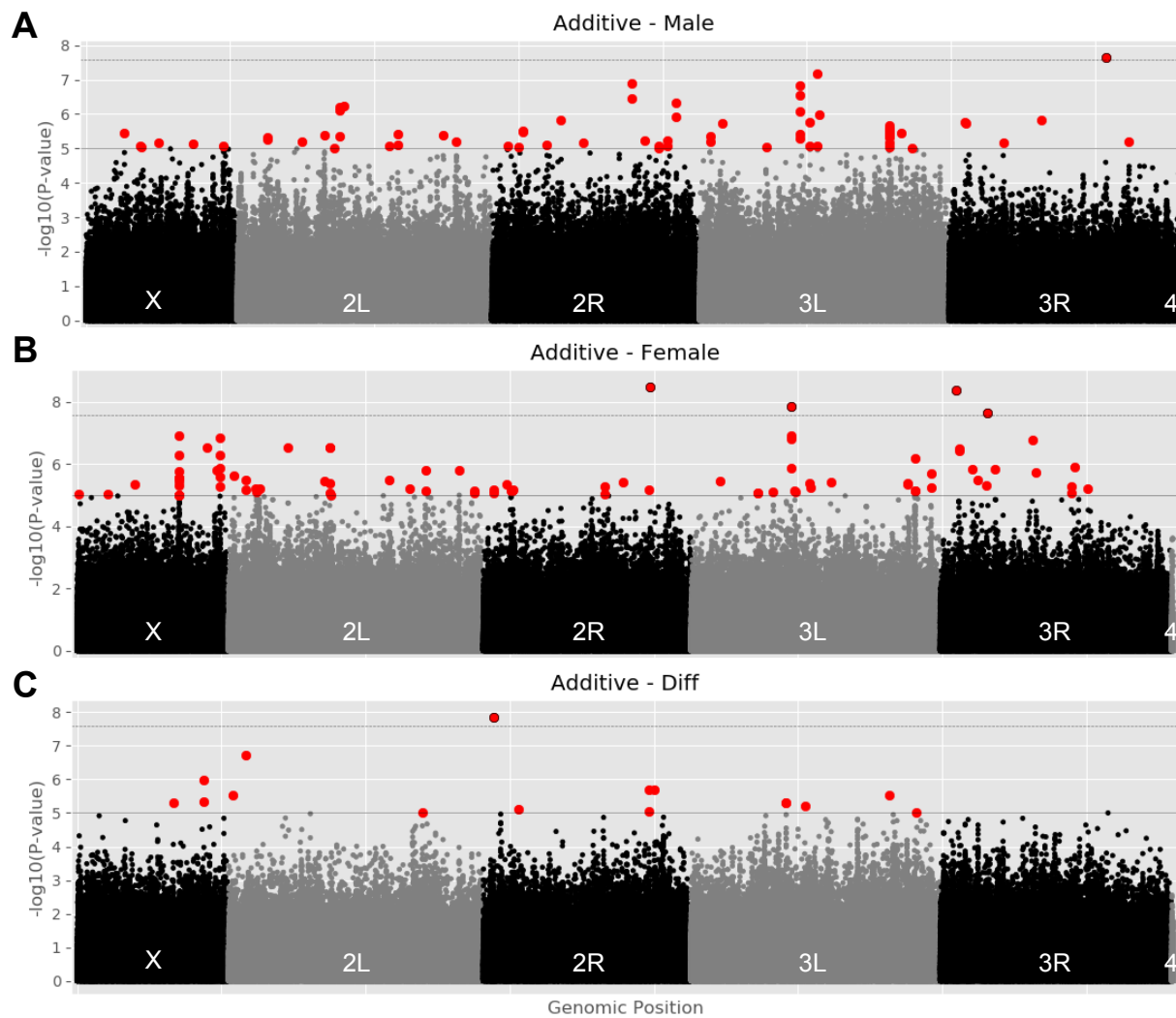


**Figure S5. Additional sex-based phenotype Manhattan plots for additive analysis.** (A) Males, (B) females, and (C) sex-difference phenotypes all have significant additive variants pass a traditional DGRP threshold ( $P \leq 1E-5$ , gray solid line, red points), and at least one variant pass a Bonferroni threshold ( $P \leq 2.63E-8$ , gray dashed line, red dot with black outline). Variants are arranged in order of relative genomic position by chromosome and plotted by the  $-\log_{10}$  of the  $P$ -value. The sex-average is displayed in text.

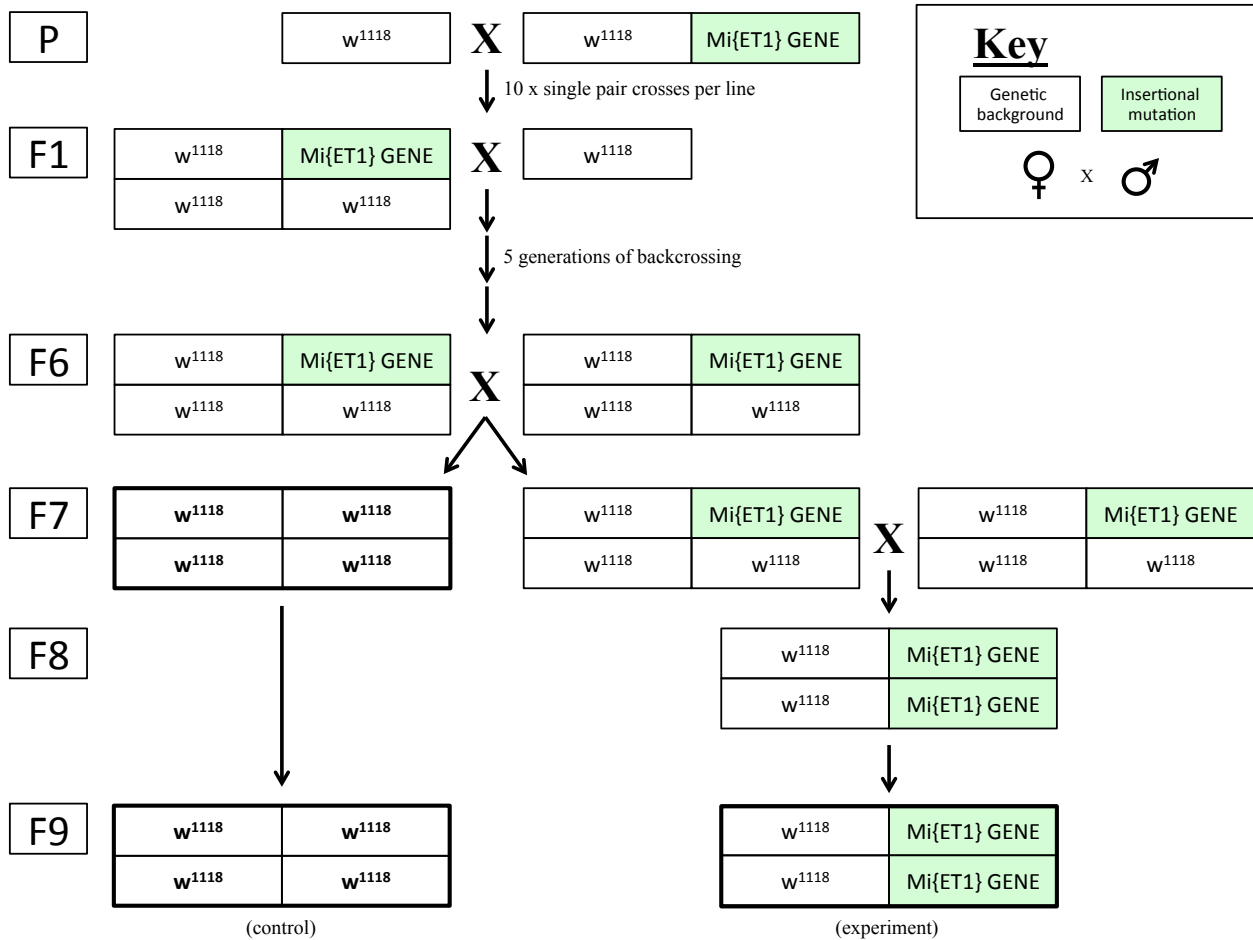


**Figure S6.** Genetic crosses performed for deriving experimental and control stocks used to validate candidate genes. All crosses are represented with females on the left and males on the right. Ten single pair crosses of a female genetic control, either  $w^{1118}$  (pictured) or  $y[1] w[67c23]$ , in white boxes were crossed with the respective *Mi{ET1}* insertional mutant line in green boxes. After the initial cross, heterozygous flies were backcrossed to the respective genetic control for five generations. In the sixth generation, single pairs of heterozygous flies were crossed. Progeny without the  $Avic\backslash GFP^{E.3xP3}$  marker were collected as homozygous nulls, while several vials of putatively homozygous mutants (no progeny without marker) were crossed again to confirm genotype. Stocks were monitored for two additional generations to confirm mutant carrier status before a homozygous mutant stock was selected as an experimental line.



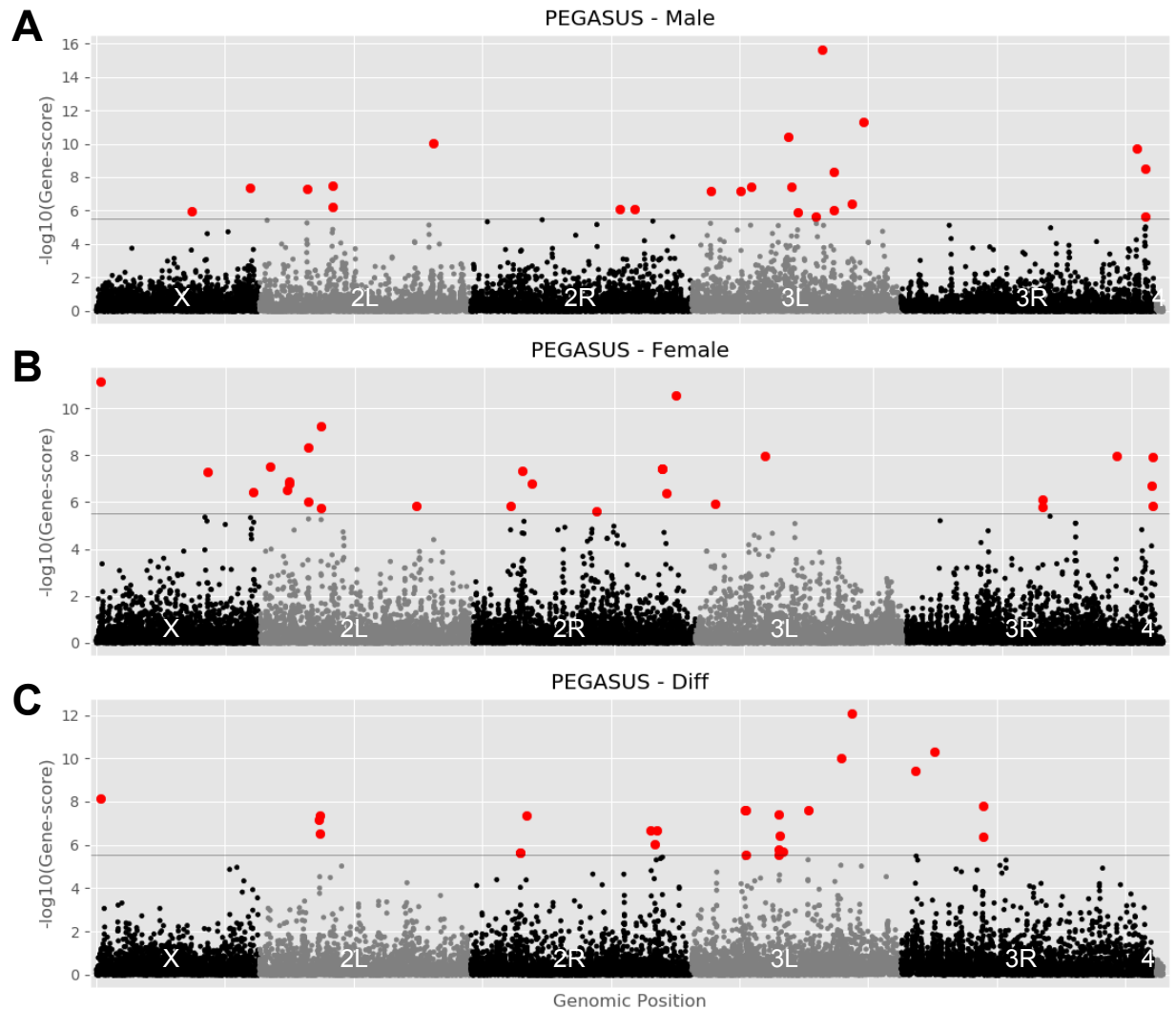


**Figure S7. Significant whole genes are distributed throughout the genome and sex-based phenotypes.** Whole gene analyses conducted with PEGASUS\_flies for (A) males, (B) females, and (C) sex-difference phenotypes showed enrichment for significant whole genes across these three, and the sex-average (displayed in text). Each dot represents a whole gene, ordered by position across the chromosomes and plotted as the  $-\log_{10}$  of the gene-score. Points above the Bonferroni threshold ( $P \leq 3.03 \times 10^{-6}$ , gray line) are colored in red.

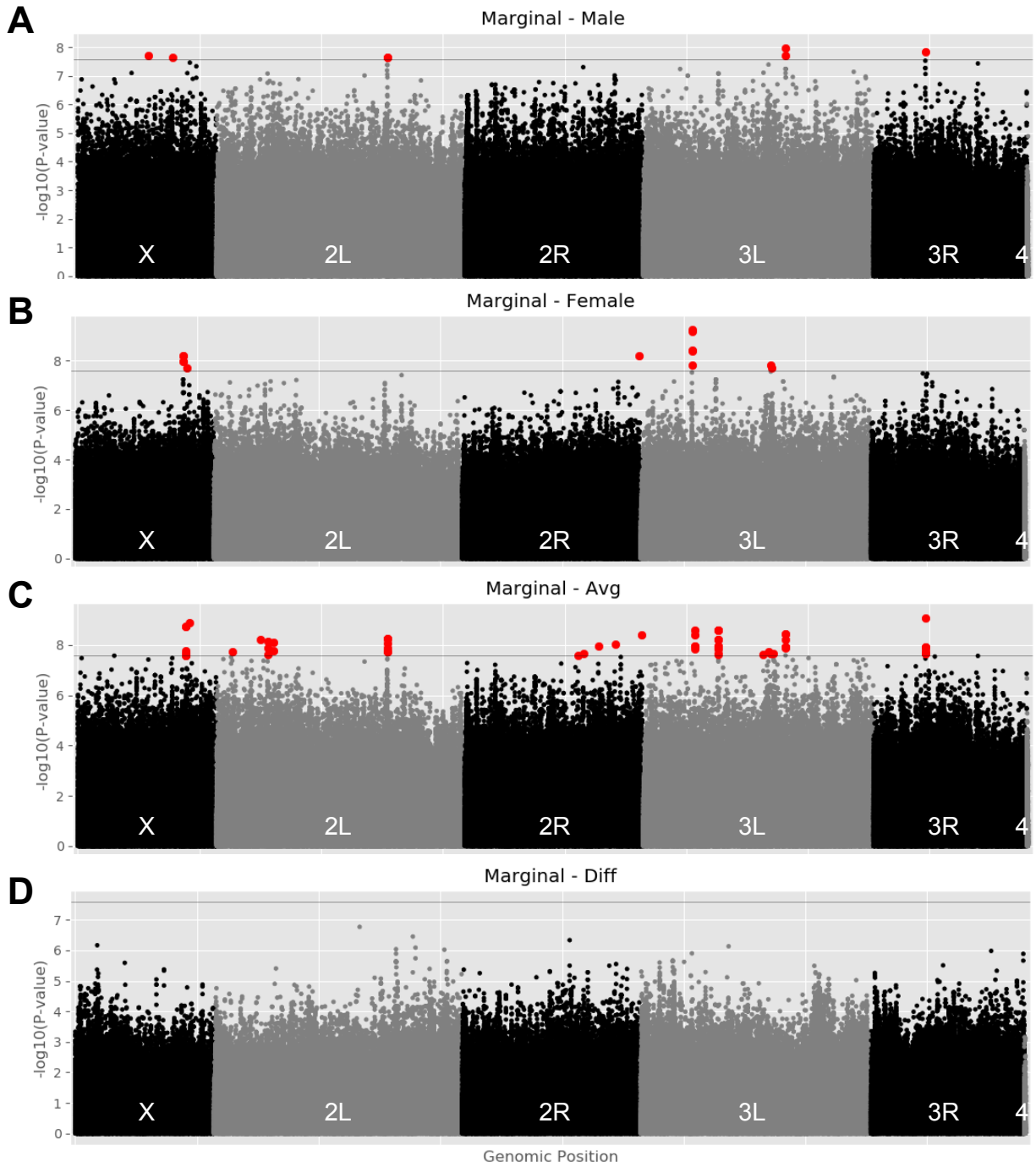


**Figure S8. Significant marginal variants are unevenly distributed across sex-based phenotypes.** (A) Males had very few significant variants pass a Bonferroni threshold ( $P \leq 2.56E-8$ , gray solid line, red points), while (B) females had more and (C) sex-average had the most. (D) Sex-difference had no significant marginal variants. Variants are arranged in order of relative genomic position by chromosome and significance scores  $-\log_{10}$  transformed.

**Consensus module—trait relationships across  
Female Expression and Male Expression**

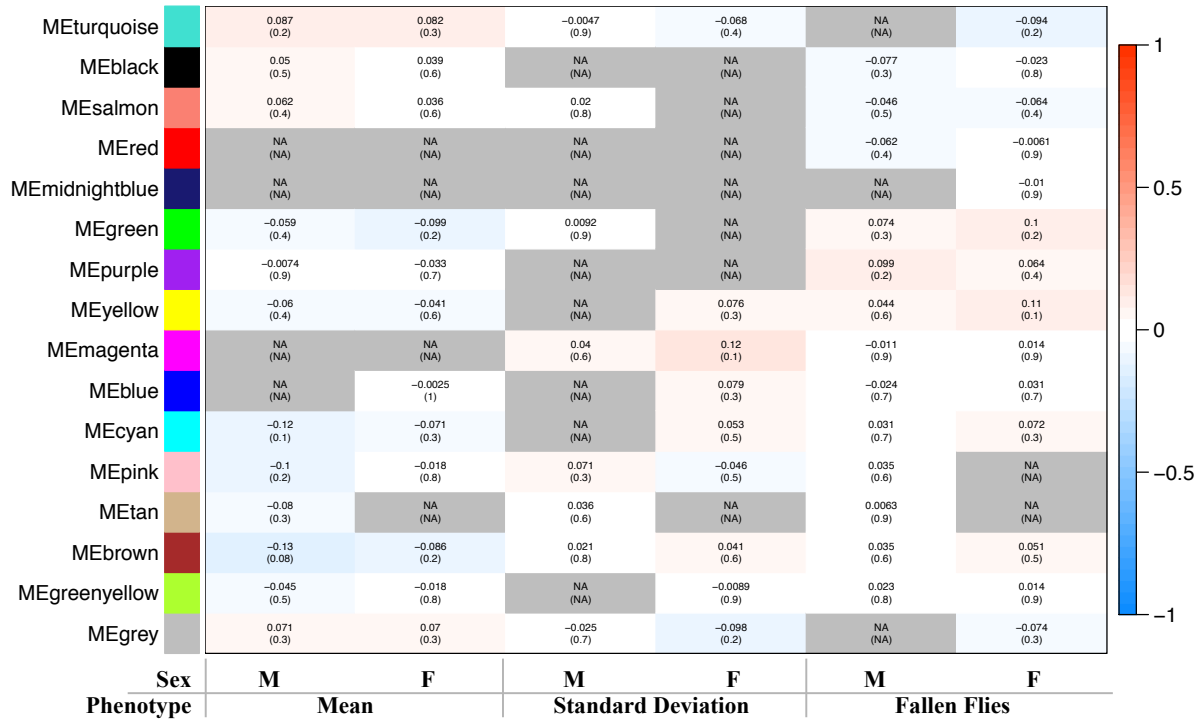


**Figure S9. Trait-relationship correlation matrix shows no correlation between measured phenotypes and young adult transcriptome.** Neither sexes' mean landing height, standard deviation in landing height, or proportion of flies that fell through the column (fallen) were significant with a cluster of similarly expressed genes in a Weighted Gene Co-expression Network Analysis (WGCNA). Colored modules on the left represent WGCNA-generated clusters of genes and the color of each table cell corresponds with the magnitude of correlation coefficient (top number in cell). The bottom number in each cell is the significance of the correlation. No clusters were significantly correlated with any sex-phenotype combination.

## **Chapter 2**

### *The Genetic Architecture of Robustness for Flight Performance in Drosophila*

Adam N. Spierer and David M. Rand

Modified from submission to *Evolution* (in prep)

## Abstract

A central challenge of quantitative genetics is to partition phenotypic variation into genetic and non-genetic components. While external environmental factors are traditionally considered the most important sources of non-genetic variation, developmental noise resulting in developmental instability can also contribute significantly to phenotypic variation within and among genetically identical individuals. Accordingly, more robust traits have more consistent phenotypes, resulting from developmental stability buffering against stochastic developmental processes. The genetics of robustness are poorly understood, though evidence points to genetic factors that promote developmental stability, as well as leverage developmental noise to create more interconnected neural networks. Accordingly, we sought to expand the understanding of robustness by performing an association study on a previously studied, whole organism trait: flight performance. Using 197 of the *Drosophila* Genetic Reference Panel (DGRP) lines, we surveyed whole genes and variants from additive, marginal, and epistatic analyses that associated with the genetic architecture of robustness for flight performance. Of the 1229 genes we identified, many had annotations for developmental and neurodevelopmental processes and a sizable fraction of genes were identified from associations that differed between sexes. Additionally, many genes were pleiotropic, with several annotated for fitness-associated traits (e.g. gametogenesis and courtship). Our results corroborate with a previous study for genetic modifiers of micro-environmental variation, and have sizable overlap with studies for modifiers of wing morphology, embryonic central nervous system development, and courtship behavior. These results point to an important and shared role for genetic modifiers of robustness affecting development and behavior.

## Introduction

Evolution acts on the genetic variation underlying phenotypic variation among individuals and populations. While many research programs focus on understanding genetic factors that contribute to phenotypic variation, fewer focus on non-genetic factors. The phenomenon of non-genetic (micro-environmental) variation describes the phenotypic variation that occurs in the absence of genetic variation, best studied in the genetically identical individuals. Non-genetic variation can arise from external (environmental) or internal (developmental) factors. Phenotypic variation caused by environmental factors (e.g. temperature) can result in phenotypic plasticity. Plastic phenotypes are considered canalized or robust if they are resilient (consistent) when faced with external factors (KLINGENBERG 2019). Robustness can also refer to a phenotype's ability to resist internal factors and stressors. Here, developmental instability, caused by developmental noise in stochastic molecular processes (e.g. important transcripts or signals in very low abundance), can lead greater phenotypic variation (ALBAYRAK *et al.* 2016; SCHOR *et al.* 2017; KLINGENBERG 2019) that is separate from phenotypic plasticity.

Depending on the affected developmental process, developmental instability can alter an organism's developmental trajectory. This phenomenon is observable as phenotypic variation across genetically identical individuals (MORGANTE *et al.* 2015; VOGT 2015), such as deviations from bilateral symmetry (fluctuating asymmetry) (VALEN 1962; SOTO *et al.* 2008), which are hypothesized to be negatively associated with fitness (QUINTO-SANCHEZ *et al.* 2018; LAJUS *et al.* 2019). Buffering systems exist to maintain phenotypic

robustness in the presence of these stressors. Some proteins, like chaperonins (HSP90), buffer against noise and stress by maintaining a protein's structure (RUTHERFORD AND LINDQUIST 1998; CHEN AND WAGNER 2012). Similarly, the mitochondrial unfolded protein response is associated with maintaining homeostasis and promoting longevity (PELLEGRINO *et al.* 2013; JOVAISAITE *et al.* 2014). Other proteins, like certain neurodevelopmental cell-cell adhesion molecules (DSCAMs and teneurins), leverage developmental noise to create more robust neural networks, which can drive repeatable non-genetic phenotypic variation in behavioral responses (AYROLES *et al.* 2015; HIESINGER AND HASSAN 2018; HONEGGER AND DE BIVORT 2018). Organisms also co-opt non-genetic phenotypic to their advantage; the parthenogenic, marbled crayfish exhibits phenotypic variation in several life history traits, which may ultimately serve as a bet hedging strategy for colonizing different environments (VOGT *et al.* 2008; HIESINGER AND HASSAN 2018).

Genes that modulate a system's ability to resist developmental noise or a stressor are hypothesized evolutionary targets (WAGNER 2008; VOGT 2015; MENEZES *et al.* 2018). This suggests non-genetic phenotypic variation can be affected by genetic variation, though the genetic factors affecting non-genetic variation are not well understood. One approach leverages phenotypic variation for trait robustness across genetically identical individuals in a Genome Wide Association Study (GWAS) framework. Previous studies demonstrate this strategy's feasibility and are successful in identifying genetic modifiers of robustness (KAIN *et al.* 2012; AYROLES *et al.* 2015; MORGANTE *et al.* 2015; MENEZES *et al.* 2018; ROMAN *et al.* 2018).

Accordingly, we sought to contribute to the elucidation of these genetic factors by studying a highly functional life history trait: flight performance. We turned to the *Drosophila* Genetic Reference Panel (DGRP) lines, a collection of 205 genetically distinct and inbred lines of *D. melanogaster* that represent a snapshot of natural variation in a wild population (MACKAY *et al.* 2012; HUANG *et al.* 2014). Using a flight column to test flies' ability to react and respond to an abrupt drop (BENZER 1973; BABCOCK AND GANETZKY 2014), we tested 197 DGRP lines for their mean-normalized standard deviation (coefficient of variation) in flight performance. For this study, the coefficient of variation serves as a proxy for understanding phenotypic robustness for groups of genetically identical individuals, which we used to identify additive, marginal, and epistatic variants, as well as whole genes, across four sex-based phenotypes (males, females, and the average (sex-average) and difference (sex-difference) between sexes). We also successfully validated several candidate genes (*bru1*, *CadN*, *CG15236*, *CG32181/Adgf-A/Adgf-A2*, *CG3222*, *CG9766*, *CREG*, *Dscam4*, *flapper*, *Form3*, *fry*, *Lasp/CG9692*, *Pde6*, *Snoo*), which also validated roles in affecting overall flight performance (SPIERER *et al.* 2020). Our results broaden the genetic modifiers of phenotypic robustness to include many genes with general and specific developmental and neurodevelopmental roles, several of which overlap with a previous screen for micro-environmental plasticity (MORGANTE *et al.* 2015), as well as screens for wing morphology (PITCHERS *et al.* 2019) and courtship behaviors (TURNER *et al.* 2013; GAERTNER *et al.* 2015). Our results support a role for several genetic modifiers



contributing to phenotypic robustness, and they identify novel associations between known and unknown genetic modifiers affecting non-genetic phenotypic variation.

## Methods

### *Drosophila Stocks and Husbandry*

197 *Drosophila* Genetic Reference Panel (DGRP) lines (HUANG *et al.* 2014) and 24 stocks used in the validation experiment were obtained from Bloomington *Drosophila* Stock Center (Table S1; <https://bdsc.indiana.edu/>). Flies were grown on a standard cornmeal media (MOSSMAN *et al.* 2016) at 25° under a 12h:12h light-dark cycle. Two to three days post-eclosion, they were sorted by sex under light CO<sub>2</sub> anesthesia and given five days to recover before assaying flight performance.

### *Flight performance assay*

We tested approximately 100 flies of each sex from 197 DGRP genotypes (Table S1) using a refined protocol (BABCOCK AND GANETZKY 2014) for measuring flight performance (BENZER 1973). For each sex-genotype combination, groups of 20 flies in five glass vials were knocked down, uncorked, and rapidly inverted down a fixed length chute. The vials traveled until they reached a stop, at which point flies were ejected into a 100 cm long by 13.5 cm wide tube. Freefalling flies instinctively attempt to right themselves and land. A transparent acrylic sheet coated in TangleTrap adhesive lined the inside of the tube and immobilized flies at their respective landing height. The sheet, was removed, pinned to a white poster board, and photographed using a Raspberry Pi (model 3 B+) and PiCamera (V2). The positional coordinates were extracted using ImageJ/FIJI's `Find Maxima` feature with options for a light background and noise tolerance of 30 (SCHINDELIN *et al.* 2012). The distributions of landing heights for each sex-genotype combination were used to calculate the mean and standard deviation.

The coefficient of variation, or the mean-normalized standard deviation, was used as the final phenotype value to represent robustness.

### Genome wide association mapping

Robustness phenotypes (Table S2) were submitted to the DGRP2 webserver for the additive association analysis (<http://dgrp2.gnets.ncsu.edu/>) (MACKAY *et al.* 2012; HUANG *et al.* 2014), which returned association results for four sex-based phenotypes: males, females, average between sexes (sex-average) and difference between sexes (sex-difference). We analyzed 1,901,174 common variants (minor allele frequency  $\geq 0.05$ ) using a mixed effect model to account for *Wolbachia* infection status and presence of five major inversions. Since certain inversions covaried with the robustness phenotype (Table S3), only significance scores from a linear mixed model accounting for *Wolbachia* status and the presence of five major inversions were considered.

### Validating candidate genes

Candidate genes (Table S1B) were selected if they were identified from variants identified in the sex-average additive variant screen for mean landing height and if there were publicly available lines containing a *Minos* enhancer trap ( *Mi{ET1}* ) mutational insertion (METAXAKIS *et al.* 2005) generated by the *Drosophila* Gene Disruption Project (BELLEN *et al.* 2011). Experimental and control lines were derived from common isoparental crosses for each candidate gene stock backcrossed five times to the respective  $w^{1118}$  or  $y^1w^{67c23}$  background. Isoparental crosses between the resulting heterozygous offspring were partitioned for absence (control line) or presence

(experimental line) of the construct. Experimental lines were verified for homozygosity if all progeny contained the insertion after several rounds of culturing. Validations were conducting in the flight performance assay described above. The distributions in landing heights were assessed for significance if they passed a  $P \leq 0.05$  significance threshold in a Kolmogorov-Smirnov test comparing control and mutant genotypes.

### Calculating gene-score significance

Gene-level significance scores (gene-score) were determined using `PEGASUS_flies` (SPIERER *et al.* 2020), a *Drosophila*-optimized method for the human-based platform Precise, Efficient Gene Association Score Using SNPs (PEGASUS) (NAKKA *et al.* 2016). This analysis calculates gene-scores for each gene as a test of whether the distribution of additive variants within a gene (accounting for linkage disequilibrium) deviates from a null chi-squared distribution. Variants from the additive association screen were considered and mapped onto gene annotations and linkage disequilibrium files available with the `PEGASUS_flies` package—derived initially from the DGRP2 webserver.

### Screening for epistatic interactions

Marginal variants, corresponding with variants more likely to interact with other variants, were identified using MArginal ePlstasis Test (MAPIT) (CRAWFORD *et al.* 2017). This approach uses a linear mixed modeling framework to test the marginal effect of each variant against a focal phenotype. MAPIT requires a complete genotype-phenotype matrix so the DGRP genome was imputed for missing variants using BEAGLE 4.1

(BROWNING AND BROWNING 2007; BROWNING AND BROWNING 2016) and filtered for  $MAF \geq 0.05$  using VCFtools (v.0.1.16) (DANECEK *et al.* 2011).

MAPIT was run using the `Davies` method on the DGRP2 webserver's adjusted phenotype scores, 1,952,233 imputed and filtered variants (File S1), and relatedness and covariate status files available on the DGRP2 webserver (<http://dgrp2.gnets.ncsu.edu/data.html>). Marginal effect  $P$ -values for each sex-based phenotype (File S2) were filtered for a Bonferroni threshold ( $P \leq 2.56e-8$ ) and served as a focused subset for targeted pairwise epistasis testing against the unimputed variants ( $n = 1,901,174$ ). Epistatic interactions were calculated using the `–epistasis` test in a `–set-by-all` framework in PLINK (v.1.90) (PURCELL *et al.* 2007). Significant epistatic interactions were considered if they passed a Bonferroni threshold:  $0.05 / (n \times 1901174 \text{ variants})$ , where `n` represents the number of significant marginal variants tested in a sex-specific subset (Table 2).

### Annotating FBgn and orthologs

FB5.57 annotations for FlyBase gene numbers (FBgn) were converted to FB\_2020\_01 annotations using the FlyBase tool `Upload/Convert IDs` (THURMOND *et al.* 2019).

Updated FBgn (Dmel) were mapped to human orthologs (Hsap) using the *Drosophila* RNAi Stock Center (DRSC) Integrative Ortholog Prediction Tool (DIOPT)(Hu *et al.* 2011) tool, with the additional filtering parameter: "Return only best match when there is more than one match per input gene or protein." Annotations for various genes without a citation were done so with auto-generated summaries and unreferenced descriptors of

genes' functions, expression profiles, and orthologs from FlyBase (GRUMBLING *et al.* 2006; DOS SANTOS *et al.* 2015). These descriptors were compiled from data supplied by the Gene Ontology Consortium (ASHBURNER *et al.* 2000; CARBON *et al.* 2019), the Berkeley *Drosophila* Genome Project (FRISE *et al.* 2010), FlyAtlas (CHINTAPALLI *et al.* 2007), The Alliance of Genome Resources Consortium (CONSORTIUM 2020), modENCODE (DOS SANTOS *et al.* 2015), *Drosophila* RNAi Screening Center (DRSC) Integrative Ortholog Prediction Tool (DIOPT) (HU *et al.* 2011), and Phylogenetic Annotation and INference Tool (PAINT) (GAUDET *et al.* 2011).

#### Data availability

All phenotype data required to run the outlined analyses are available in the Supplement or using the DGRP2 webserver (<http://dgrp2.gnets.ncsu.edu/>).

## Results and Discussion

We sought to identify the genetic modifiers of robustness in a whole organism phenotype: flight performance. Using the *Drosophila* Genetic Reference Panel (DGRP) lines, we identified several additive, marginal, and epistatic variants, as well as whole genes that associate with genotypes' robustness in response to a flight challenge. In the sections that follow we describe the variant-based, gene-based, and epistatic analyses in turn. Results and discussion of findings are combined to avoid redundancy and facilitate interpretation.

### Variation in flight performance across the DGRP

We screened 197 DGRP lines (Table S1) for their flight ability in response to an abrupt drop (Figure 1A). Qualitative observations made in a previous study of strong, intermediate, and weak genotypes in the flight assay suggests stronger fliers react faster and with better coordination than weaker fliers (SPIERER *et al.* 2020). The mean and standard deviation in landing height were calculated for each sex-genotype combination, along with the mean-normalized standard deviation (coefficient of variation), which served as our metric for robustness (Figure S1; Table S3). Genotypes that have a lower coefficient of variation (more consistent) are more robust for flight performance (KLINGENBERG 2019). On average, flight performance was more robust in males than females (males: 0.17 A.U.  $\pm$  0.055 SD vs. females: 0.22 A.U.  $\pm$  0.075 SD; Figures 1B and S2) and it was related between sexes ( $r = 0.55$ ; Figure 1C). This observation suggests robustness of flight performance is sexually dimorphic and that we expect to see differences in the genetic architecture between sexes.

Robustness of flight performance was not significantly correlated with any of the DGRP2 webserver's datasets for either sex (Table S3), suggesting it is a unique trait. To study this trait more in depth, we took distinct approaches to identify the additive, marginal, and epistatic variants that associated with robustness in flight performance, as well as an approach that identified whole genes (Table 1). Each approach is targeted to identify different feature types in the overall genetic architecture.

#### Several variants of large effect associate with robustness in flight performance

We performed a Genome Wide Association Study (GWAS) to calculate the significance of variants' additive effects, and subsequently whole gene significance scores. We analyzed the effects of 1,901,174 common variants ( $MAF \geq 0.05$ ) across for four sex-based phenotypes (males, females, the sex-average, and sex-difference; Figures 1D and S3-5). Two of the major inversions covaried with our phenotype scores (Table S4), so we used a mixed model to account for *Wolbachia* infection status, presence of inversions, and polygenic relatedness.

Under the Bonferroni threshold ( $P \leq 2.63E-8$ ), eight variants were significant for either the male, female, or sex-average analysis, but not sex-difference (Tables 2-4; Table S5). Three of these variants (2R\_17433667\_SNP, 3R\_4379159\_SNP, 3R\_9684126\_SNP) were also significant additive variants passing a Bonferroni threshold in the screen for mean landing height in flight performance (SPIERER *et al.* 2020). These variants mapped to *Epidermal Growth Factor Receptor* (*Egfr*; human



homolog *EGFR*), *Odorant receptor 85d (Or85d)* and an intergenic region on chromosome 3R, respectively. *Egfr* is a tyrosine kinase receptor involved in several developmental and homeostatic processes. It is a known source of natural variants that can modify wing shape and affect flight performance (PAUL *et al.* 2013; PITCHERS *et al.* 2019). This intronic variant also mapped to a region with several annotated early embryonic transcription factor binding sites (TFBS; *bcd, da, dl, gt, hb, kni, Med, prd, sna, tll, twi, disco, Trl*) (NEGRE *et al.* 2011). Disrupted regulation of dose-sensitive developmental patterning signals (like those involving *Egfr*) can create developmental noise (ALBAYRAK *et al.* 2016). Since this process would likely happen early in development, it can cause disrupt signal gradient-dependent cell differentiation and amplify during ontogeny. Accordingly, *Egfr* signaling may be an important factor contributing to developmental instability, which typically manifests as decreased robustness for a given trait (HIESINGER AND HASSAN 2018; KLINGENBERG 2019). Since the TFBS annotations only cover embryogenesis (NEGRE *et al.* 2011), it is possible this site is acted on by other transcription factors later during development and homeostasis. Next, the non-synonymous variant in *Or85d*, an odorant receptor expressed on the antennae and maxillary palp (COUTO *et al.* 2005), results in a cytosine to tyrosine transition (C277Y). This site is highly conserved (Figure S6) (SIEPEL *et al.* 2005; SIEPEL AND HAUSSLER 2005) citation, though analysis with the PROVEAN webtool (CHOI AND CHAN 2015) suggests this mutation is neutral (scored -2.312 with -2.5 as deleterious). Our previous screen for mean landing height in flight performance identified an outsized role for several chemosensory receptors, like *Or85d*, as putative mediators of proprioception. Finally, the intergenic region lacked any embryonic TFBS annotations,

suggesting it may interact with transcription factors or epigenetic factors later during development or homeostasis. The remaining Bonferroni additive variants mapped to genes that were also identified from additive Bonferroni variants in the mean flight performance screen (*Dscam4* and *flapper*) or were otherwise strongly significant (*Snoo*). All three of these genes have known or hypothesized roles in developing robust neural circuits (QUIJANO *et al.* 2010; TADROS *et al.* 2016; SPIERER *et al.* 2020). The identification of these genes in both screens suggests they have a dual role in affecting genotypes' ability and variability in flight performance.

We also took a less conservative approach and used the traditional DGRP association threshold ( $P \leq 1E-5$ ). Here, we identified 163 unique, significant variants (Table S5), 18 of which mapped to coding regions (Table 4). These include a novel transcriptional start site (CG43707) in a gene affecting muscle architecture and flight performance (SCHNORRER *et al.* 2010) and six non-synonymous SNPs (CG12517, CG13794, CG34215, *Or85d*, *Spn*, *Tif-IA*). Some of these affect neural phenotypes, like the olfactory receptor *Or85d* and CG13794, a neurotransmitter (COUTO *et al.* 2005; ROMERO-CALDERON *et al.* 2007), while others affected multiple traits (pleiotropic). CG12517 and *Tif-IA* are involved in the stress response of the fat body and insulin-based metabolism, respectively, and both are involved in development of the germline (YATSU *et al.* 2008; TOOTLE *et al.* 2011; TSUZUKI *et al.* 2012; GHOSH *et al.* 2014). *Spn* (*Spinophilin*; human homolog *PPP1R9A*), a pre-synaptic regulator of neurons (MUHAMMAD *et al.* 2015), affects flight performance (SCHNORRER *et al.* 2010), male aggression (EDWARDS *et al.* 2009), odor response (SAMBANDAN *et al.* 2006), and is also

found in sperm (WASBROUGH *et al.* 2010). These annotations represent a broader trend in our data, where neural and pleiotropic genes play an important role in the genetic architecture of robustness of flight performance.

Variation in protein coding regions is often overshadowed by variation in non-coding (presumably regulatory) regions across the genetic architecture of many complex traits (BOYLE *et al.* 2017). Similarly, the majority of variants in the additive and subsequent analyses were highly enriched for intergenic and non-coding regions, with most mapping to non-coding regions within 1kb of a gene (Table 4). Many of these genes had annotations for flight (*neto*) and locomotion (*Mbs*, *sbb*, *Syt1*, *Ten-a*, *Tmc*, *Trim9*). There were also several annotations for genes affecting flies' ability to process external stimuli, like light (*Bsg*, *bun*, *cdm*, *chn*, *CNMaR*, *Egfr*, *Lar*, *Mbs*, *Miga*, *Moe*, *Nrg*, *pnt*, *sbb*, *Trim9*), chemicals (*Dyrk2*, *Egfr*, *Ir48c*, *Ir92a*, *MiP*, *mtgo*, *Or85d*, *Ten-a*, *vn*), touch (*brv2* and *Tmc*) and sound (*nrv3*). Certain structures, such as chaete and wing hairs (*chn*, *ds*, *fry*, *kmr*, *Mbs*, *pyd*, *Snoo*), are responsible for chemo- and mechanosensation, which are connected to the central nervous system through properly assembled neural networks (*CG44153*, *chn*, *Dscam4*, *fry*, *Nrg*, *shot*, *Snoo*, *Spn*, *Tmc*) that transduce signals using neurotransmitters (*ChAT*, *CG13794*, *Syt1*, *Sytbeta*, *VACHT*). These signals are processed in the brain and ganglia, and can pass out to motor neurons and neuromuscular junctions (*cdm*, *ChAT*, *Lar*, *Neto*, *nmo*, *Nrg*, *Ptp10D*, *Sdc*, *Syt1*, *Ten-a*) to activate muscles (*bru1*, *bves*, *Casp52*, *chn*, *Lasp*, *Neto*, *pnt*, *Pyk*, *shot*, *ths*, *vn*) for an appropriate response. In flight, the indirect flight muscles generate power by deforming the thoracic cuticle (*ckd*, *CrebA*, *Eip75B*) to move the well-developed wing structures

(*ds, Egfr, fry, Mbs, Mrtf, nmo, pnt, pyd, sbb, shot, vn*) (DICKINSON *et al.* 1997; FRYE AND DICKINSON 2004; DICKINSON *et al.* 2005; FONTAINE *et al.* 2009), while the direct flight muscles perform finer adjustments to change the angle of the wing. Regulation for many of these processes occurs through trans-regulatory elements (*bru1, bun, bur, CG8312, chinmo, chn, CrebA, Eip75B, fry, Hers, mammo, Moe, Mrtf, mxt, otp, pnt, RpL21, sbb, Sfmmt, Tif-1A, toc, Zasp52*) that are generally active during development (ASHBURNER *et al.* 2000; GRUMBLING *et al.* 2006; GAUDET *et al.* 2011; DOS SANTOS *et al.* 2015; CARBON *et al.* 2019). Several genes are pleiotropic and are found in the testes or involved in spermatogenesis (*Bsg, CG9692, Lar, Lasp, mammo, toc, vn*), found in ovaries or involved in oogenesis (*bun, CG12517, Egfr, Eip75B, Lar, Mbs, Sfmmt*), and required for sex identity (*chinmo* and *Mip*). These genes represent a number of developmental and functional processes affecting flight performance, which may also provide an explanation for the observed sexual dimorphism. Annotations for these genes' functions were compiled from auto-generated summaries and Gene Ontology (GO) terms available through FlyBase (DOS SANTOS *et al.* 2015; THURMOND *et al.* 2019) and are available for all genes found in the current study as a master lookup table (Table S10).

*Functional validation of candidate genes supports a role for neurodevelopment affecting robustness of flight performance*

We functionally validated several genes' roles in affecting robustness of flight performance. Using the candidate genes identified from the mean landing height screen, we tested for differences in the distribution of landing heights for using a Kolmogorov-Smirnov test. We validated 11 single genes (*bru1, CadN, flippy (CG9766)*,

CG15236, *CREG*, *Dscam4*, *flapper* (CG11073), *form3*, *fry*, *Pde6*, and *Snoo*), and two constructs that fell in multiple genes (*Adgf-A/Adgf-A2/CG32181* and *CG9692/Lasp*) (Figures 2 and S7; Table S6). These genes were also validated in the mean flight performance screen, indicating these genes likely play dual roles modifying the ability and variability of flight performance.

#### Analyses of whole-gene effects identifies distinct factors affecting robustness

A conventional minSNP approach deems a gene significant if its most significant variant passes a significance threshold. However, this approach is biased toward longer genes (many neural genes can exceed 100kb (KING *et al.* 2013; SUGINO *et al.* 2014; GABEL *et al.* 2015)) and does not account for linkage between sites. To counteract these biases, we employed *PEGASUS\_flies* (SPIERER *et al.* 2020), a *Drosophila* version of the human-focused *PEGASUS* platform (NAKKA *et al.* 2016), to assess a whole gene's significance. Because this method takes a more holistic approach, testing the distribution of variants in a gene against a null chi-squared distribution, it can detect significant genes that would be missed otherwise in a minSNP approach.

Using *PEGASUS\_flies*, we identified 45 unique genes (Table S7) across all four sex-based phenotypes that passed a Bonferroni threshold ( $P \leq 3.43E-6$ ; Figures 3A and S8). Two were present in the additive screen (*nmo* and *Sdc*) and accompany 27 other genes (*ana3*, *barc*, *Br140*, *caps*, *CG5921*, *CG5937*, *CG12163*, *CG44774*, *Crz*, *ct*, *ctrip*, *Dop2R*, *Dys*, *ena*, *ham*, *Nckx30C*, *Oct-TyR*, *olf186-F*, *PsGEF*, *Ptp4E*, *rad*, *rodgi*, *row*, *tou*, *TLL5*, *tutl*, *wde*) with annotations for neurodevelopment and function. Some genes

also affected muscle, chaete, or general development (*caps*, CG5937, CG31635, CG32521, CG3277, CG43333), while others facilitated gametogenesis or promoted reproductive success (*ana3*, CG1632, CG5937, CG12163, CG44774, *CHES-1-like*, *Crz*, *ct*, *Dop2R*, *Dys*, *ena*, *Gbs-70E*, *PsGEF*, *tou*, *wde*). These results largely corroborated the annotations from the genes in the additive search and expanded the number of genetic variants that associate with robustness in flight performance.

#### Association of marginal variants with robustness in flight performance

Complex traits derive much of their complexity from the epistatic, or pairwise, interactions that act as a context-specific effectors (HUANG *et al.* 2012). However, traditional epistasis analyses face large computational and statistical hurdles. We circumvent these limitations by focusing our search for pairwise epistatic interactions with MArginal ePIstasis Test (MAPIT) (CRAWFORD *et al.* 2017). This linear mixed modeling approach identifies marginal variants, which represent genetic hubs as they are more likely to have epistatic interactions other variants. Using this informed set of marginal variants, we can perform a set-by-all epistasis search, rather than testing all possible combinations. Doing so, we identified 104 significant marginal variants exceeding a Bonferroni threshold ( $P \leq 2.56E-8$ ; Figures 2B and S8) that mapped to 66 genes across all sex-based phenotypes (Table 5). Most variants mapped to intergenic or non-coding regions, underscoring the importance of gene regulation in modifying phenotype (MACKAY AND HUANG 2018). But of the coding variants, one (2R\_15214612\_SNP) mapped a putatively neutral (-0.403 PROTEAN score) (CHOI AND CHAN 2015) non-synonymous site in GTPase *Rad*, *Gem/Kir family member 1* (*Rgk1*;

human homolog *RRAD*) in the sex-average analysis. *Rgk1* is pleiotropic, with roles in central nervous system development, olfactory-based learning (MURAKAMI *et al.* 2017), sperm, muscle, and generalized developmental (KARR 2007; SCHNORRER *et al.* 2010). This variant had no epistatic interactions, but four other variants in *Rgk1* (2R\_15202880\_SNP, 2R\_15202883\_SNP, 2R\_15212327\_DEL, and 2R\_15212584\_DEL) had epistatic interactions with *PKC- $\delta$*  and *ush* in the sex-difference epistasis screen.

Among the 66 marginal minSNP genes, seven (*Bx*, *CG9313*, *CG15651*, *CG9171*, *PKC- $\delta$ /*Pkcdelta**, *jvl*, *ush*) were identified from 19 marginal variants that had epistatic interactions. In total, 6313 epistatic interactions passed sex-specific significance thresholds, and mapped to 1081 genes (Table 2)—the largest set of genes identified in any analysis. Interestingly, several of the marginal genes (identified from marginal variants) had epistatic interactions with other marginal genes (marginal-marginal epistatic interactions; Figure 4A), suggesting a highly interconnected genetic architecture underlies robustness for flight performance. Broadly, epistatic interactions were enriched for neurodevelopment and general development. There are too many epistatic interactions to comprehensively describe below (Table S8), so we will instead focus on the marginal variants that mapped to genes and some of their noteworthy epistatic interactions.

Many marginal variants in female and sex-average epistasis analyses map to pleiotropic genes

While the male marginal variant mapped to an intergenic region, there were several marginal genes identified from the female and sex-average analyses that were also pleiotropic. Among these was *Beadex* (*Bx*; human homolog *LMO1*), a LIM-only protein that interacts with other LIM-homeodomain proteins. It is known to interact with *apterous* (*ap*) in the wing discs, where *ap* contributes to wing morphogenesis and neuronal pathfinding (MILAN *et al.* 1998). *Bx* is also involved in dorsoventral patterning of the wing blade, the hypothesized wing blade axis that other studies have identified as the main driver of morphological variation (MUNOZ-MUNOZ *et al.* 2016; PITCHERS *et al.* 2019). *CG9171* (human homolog *B4GAT1*) is a glucuronosyltransferase predicted to localize to the Golgi and perform O-linked mannosylation. It is known to affect flight performance (SCHNORRER *et al.* 2010) and has a putative role in muscular dystrophy (BUYSEE *et al.* 2013). Similarly, *CG15651* (human homolog *FKRP*) is also predicted to affect O-linked mannosylation in the Golgi complex and is linked to muscular dystrophy as well (BROCKINGTON *et al.* 2001). The marginal variant associated with *CG15651* also overlapped with *CG9313*, a axonemal outer arm dynein intermediate chain involved in sperm mobility and audiosensation in the Johnston's organ (ZUR LAGE *et al.* 2019). Finally, a marginal variant mapped to *javelin-like* (*jvl*), important for actin and microtubule organization, mechanosensing macrochaete formation, muscle formation in flight, and oogenesis (TILNEY *et al.* 2003; SCHNORRER *et al.* 2010).



Just like these genes, their epistatic interactors also map to genes broadly affecting wing morphology, muscle development, neural circuit assembly and neuronal function, and interestingly, sex-related behaviors and sex-specific tissues (Table S8).

### Epistatic interactions associating with the sex-difference phenotype

The marginal variants in the sex-difference epistasis search had four times as many epistatic interactions as the next closest sex-based phenotype (females). *Protein Kinase C- $\delta$*  (*PKC- $\delta$*  or *Pkdc*; human homologs *PRKCD* and *PRKCQ*) drove this trend, accounting for over half (3211 of 6313) of all epistatic interactions in our study, some of which were with variants in other marginal genes (Figure 3C), suggesting a more central and interconnected role within the genetic network. *PKC- $\delta$*  is a member of the Protein Kinase C family and is known to modulate flies' ability to learn from their environment, especially during flight (COLOMB AND BREMBS 2016; GETAHUN *et al.* 2016; GOROSTIZA *et al.* 2016). Flies' inability to learn from proprioceptive cues corresponds increased variation in their flight path (HESSELBERG AND LEHMANN 2009; LEHMANN AND BARTUSSEK 2017), similar to what we observe.

Of the genes identified from epistatic variants, six had annotations for flight (*Gem3*, *flii*, *klar*, *Neto*, *SERCA*, *Tbh*) and several others were involved in learning and memory, which is likely facilitated by genes modulating dendritic and synaptic growth, via cell-cell adhesion (*bdl*, *beat-Vc*, *CadN*, *caps*, *Ccn*, *CG34353*, *CG4333*, *CG44153*, *cora*, *Dscam3*, *ed*, *Fam21*, *glec*, *kirre*, *Lac*, *Lar*, *Nlg1*, *sli*, *Ten-a*, *Tig*, *tkv*, *trio*, *uzip*). Importantly, the presence of three specific families of cell-cell adhesion genes identified

here, and in other analyses, has a greater importance in varying behavioral phenotypes. Down Syndrome Cell Adhesion Molecules (DSCAM; *Dscam3* and *Dscam4*), cadherins (*Cad87A*, *CadN*, *CadN2*), and teneurin (*Ten-a*) family genes play roles in growth and patterning of complex (type IV) dendritic arborization neurons, commonly found in the peripheral and central nervous systems (HONG *et al.* 2012; KISE AND SCHMUCKER 2013; LI *et al.* 2020). They contribute to differential wiring of diverse neural networks through dendritic self-avoidance (KISE AND SCHMUCKER 2013) in the brain, sensory organs of the wing, and many other areas (NAGAI AND MIZUNO 2014). *Ten-a* was previously identified and validated in a screen for individuality in locomotor handedness (AYROLES *et al.* 2015), and we validated *CadN* and *Dscam4* in the present study for their contribution to robustness of flight performance. These genes' role in modulating phenotypic variation through differential circuit assembly is hypothesized to function as a bet-hedging strategy (HIESINGER AND HASSAN 2018; HONEGGER AND DE BIVORT 2018); a select group of genes or variants can generate greater behavioral variation, which might boost populations' ability to survive a selection bottleneck. Accordingly, the identification of these gene families in the sex-difference screen supports a role for differential neural wiring affecting the sexual dimorphism observed in robustness of flight performance.

Another marginal variant from the sex-difference epistasis screen was the developmental transcription factor *u-shaped* (*ush*; human homolog *ZFPM1*), which mediates neurodevelopment and thoracic (FROMENTAL-RAMAIN *et al.* 2010). It also regulates *scute* (*sc*), which has roles in the sex-determination pathway (WRISCHNIK *et al.* 2003), and both *sc* and *achaete* (*a/ac*) in the SC-A complex that contributes to

development of mechanosensating chaete and sensory organs on the wing (SKEATH AND CARROLL 1991; CUBADDA *et al.* 1997). As expected, many of the genes *ush* interacted with had annotations for gravitaxis and locomotion (*CASK*, *CG34353*, *dnc*, *InR*, *ITP*, *mid1*, *Neto*, *nmo*, *Syn2*, *unc-104*), sensory organ development (*aPKC*, *CG9313*, *DI*, *dpr1*, *dpr9*, *dpr10*, *fry*, *fz*, *Gyc88E*, *mew*, *mib*, *rdgA*), dendrite morphogenesis and self-avoidance (*acj6*, *CadN*, *Cbp53E*, *Cont*, *cv-c*, *fru*, *fry*, *hdc*, *mAChR-B*, *Mob2*, *mtt*, *Nedd4*, *Prosap*, *pum*, *shn*, *Tm1*, *unc-104*), and learning and memory (*aPKC*, *CASK*, *cher*, *dnc*, *gom*, *klg*, *lillo*, *Mob2*, *Nep4*, *Rkg1*, *pum*, *scrib*, *sNPF-R*, *teq*). There were also epistatic interactions with genes annotated for courtship behaviors (*Btk29A*, *CASK*, *dnc*, *fru*, *gom*, *Rkg1*). In particular, *fruitless (fru)* was identified in the previous flight performance screen as an epistatic interactor with *ppk23* (SPIERER *et al.* 2020). *fru* also genetically interacts with *doublesex (dsx)*, identified in our previous screen from the whole gene approach, where they pattern sex-specific circuits along the neurons that connect leg and wing chaete (functioning as contact chemosensors for pheromone detection) to the thoracic ganglion (flight control center) and brain, and out along motor neurons to the flight musculature (for visual flagging and courtship song) (YU *et al.* 2010; PAVLOU AND GOODWIN 2013; SHIRANGI *et al.* 2016).

#### *Flight and courtship share morphological structures and genetic modifiers*

Genes involved in courtship and robustness of flight performance may play more of a shared role than previously thought. In addition to the genes associated with the sex-difference epistasis screen, we also identified *factor of interpulse interval (fipi)* in the sex-average marginal variant screen. *fipi*, which regulates the intervals of courtship

song (FEDOTOV *et al.* 2018), was also previously identified in an independent screen for micro-environmental variation (MORGANTE *et al.* 2015), supporting a role for genes affecting trait canalization also affecting courtship and flight. With respect to courtship-specific traits, we identified several genes shared with other DGRP courtship screens, including (*CG1358* and *Dif*) (TURNER *et al.* 2013) and (*bru-3*, *CG13024*, *CG42784*, *Fur1*, *shot*, *SKIP*, *Ubx*, *wuc*) (GAERTNER *et al.* 2015). From these screens, *Dscam* (*Dscam1* vs. *Dscam3* and *Dscam4*) and Beat family (*beat-Ib* and *beat-IIIc* vs. *beat-IIb*, *beat-VI*, and *beat-Vc*). In addition to these, we also identified several genes with annotations for sex determination, courtship behavior, and sex-specific neural patterning (*Alh*, *bab1*, *Btk29A*, *CASK*, *chinmo*, *dnc*, *dysb*, *fipi*, *fru*, *gom*, *lov*, *Mip*, *Nrg*, *Sh*, *Tbh*), as well as many genes that had dual roles in somatic and germ development. Enrichment for these genes leads us to hypothesize that pleiotropic genes associated with courtship, and fitness in general, may also contribute to variation in robustness of flight performance.

We base this hypothesis on the observation that many of the morphological structures and neural circuits that promote flight performance are also important for courtship. In flight, well-structured wings are important for generating lift (MARCUS 2001) and chaete are important for proprioception (FURMAN AND BUKHARINA 2008; QUIJANO *et al.* 2010), while courtship requires wings for visual flagging and courtship song (SADAF *et al.* 2015) and chaete for chemosensing pheromones (THISTLE *et al.* 2012; PAVLOU AND GOODWIN 2013). Similarly, neural circuits that innervate the dual chemo- and mechanosensory chaete require strong neural networks wired with type IV dendritic arborization neurons.

Differential neural patterning by Dscams and other cell-cell adhesion molecules (cadherins and teneurins) ensure these circuits are well connected to the CNS (HONG *et al.* 2012). These circuits can also differ between sexes; *fru* and *dsx* co-localize to many of these sensory and CNS neurons, which can have important implications in differential detection of pheromones and courtship behaviors (YU *et al.* 2010; PAVLOU AND GOODWIN 2013). These differentiated circuits extend to the brain and thoracic ganglion (flight control center) and out along motor neurons and neuromuscular junctions that innervate the direct (fine motor movement) and indirect (power generating) flight muscles.

Since flight and courtship are both important for wildtype flies, and courtship behaviors differ between sexes, selection for genes that modify these behaviors can become caught in an evolutionary tug-of-war. When contrasting evolutionary forces act individual variants or genes, it can create intralocus sexual dimorphism or conflict. Here, what is beneficial for one sex may be neutral or disadvantageous for the other. This phenomenon is observed in insects in the context of locomotor performance, courtship behavior, and fitness (BERGER *et al.* 2014; BERGER *et al.* 2016). In studies where male flies were allowed to genetically “win” the sex conflict and evolve, males have increased locomotor activity (LONG AND RICE 2007), wing morphological variation (ABBOTT *et al.* 2010), and fitness increased, while females are all decreased.

Variation in wing morphology is an important phenotype in the context of trait robustness because it is sensitive to factors that buffer against developmental noise and serves as a strong proxy for developmental stability (SOTO *et al.* 2008; KLINGENBERG

2019), and hypothesized to be under stabilizing selection (MUNOZ-MUNOZ *et al.* 2016; SZTEPANACZ *et al.* 2017). Reduced genetic variation may play a larger role in their system as a bet hedging strategy, similar to those used in neural wiring. If a select group of genes shared between traits have some ability to create more phenotypic variation in a system, then populations may still have phenotypic variation on the other end of a genetic bottleneck (HIESINGER AND HASSAN 2018). This strategy in parthenogenetic crayfish supports a role for genes with the ability to generate phenotypic variation in the absence of genetic variation, and their ability to colonize new ecological niches speaks to the success of this strategy (VOGT *et al.* 2008).

#### *Genetic architecture of robustness is comprised of different types of modifiers*

Each analysis we conducted sheds light on different areas of the genetic architecture (Table 1). The additive variant analysis identified single variants with larger effects on the phenotype, while the whole gene analysis identified genes of moderate effect based on the distribution of additive variants in a gene. The marginal variant analysis identified single variants that were more likely to interact with other variants, while the epistasis analysis identified those specific interactions. Of the variant-based analyses, all additive variants were exclusive, though the marginal variants and epistatic interactions had some overlap, as expected (Figure 4B), demonstrating the importance of using multiple analytical methods to uncover the larger genetic architecture. When mapping these variants to genes, all analyses identified genes that were shared with at least two other analyses (Figure 4C). This result suggests that genes contain different types of variants

that affect separate facets of the genetic architecture. For a complete list of all genes identified in this study and which analysis they were present in, see Table S10.

#### Overlap between robustness and other DGRP studies

Genes and variants shared between the present study and other studies sheds light on how the genetic architecture of complex traits in general may share some of the same modifiers. Comparison the screens for variants associating with overall flight performance (mean) against robustness for flight performance (coefficient of variation), we consistently identified approximately 15-20% overlap between variants and their mapped genes (Figure 4D-H; Table S10). However, we found no overlap between whole gene analyses (Figure 4I). Together, these results suggest that while certain main features of the genetic architecture are shared between traits, they have largely separate genetic architectures.

Similarly, we found commonalities between robustness in flight performance and other DGRP studies conducted beyond the flight phenotype. In particular, a micro-environmental plasticity screen for startle response, resistance to starvation, and chill coma recovery (MORGANTE *et al.* 2015) shared 37 genes (*Bsg25D*, *CARPB*, *CG17716*, *CG31690*, *CG32767*, *CG33981*, *CG4168*, *CG42322*, *CG42324*, *CG43901*, *CG5853*, *Diap1*, *dpr6*, *dpr8*, *E2f1*, *ed*, *Eip63E*, *FAM21*, *fipi*, *fred*, *fru*, *IA-2*, *Lac*, *Lmpt*, *lncRNA:CR32773*, *lncRNA:iab8*, *Moe*, *mtgo*, *nub*, *Pde9*, *PsGEF*, *Ptp99A*, *pum*, *Pvf3*, *rdgA*, *Rgk3*, *Src64B*) and a wing morphology screen (PITCHERS *et al.* 2019) shared 16 genes (*bru1*, *Bx*, *CG1358*, *CG14926*, *Con*, *dally*, *dar1*, *Dgk*, *ds*, *Dys*, *Egfr*, *Lar*, *luna*, *pip*,

*RhoGEF64C, Sp1*). The overlap between these studies suggests that modifiers of robustness for flight performance also impact other traits, raising the importance of further studying variance-based phenotypes.



## **Conclusions**

High-speed videos of flight trajectories elicited in the abrupt drop of the flight performance screen qualitatively show that stronger and more robust genotypes react and respond faster than their counterparts. Because neural-intensive traits (reaction time, proprioception, and reaction) play prominent roles in modulating flight performance, this study likely identifies genetic modifiers of neural circuits and function more so than modifiers of wing morphology that have functional impacts on flight. However, these modifiers of wing morphology serve as a strong lens for understanding genes that may impact developmental stability, and by extension robustness. We present results from four analyses in four sex-based phenotypes surveying different facets of the genetic architecture. Several of the variants were shared between sexes, though many more differed between them. Future studies should consider evaluating both the mean and coefficient of variation for their focal phenotype to better understand modifiers affecting robustness in a specific complex trait, as well as robustness in complex traits more generally. In doing so, higher-order, multivariate analyses can be conducted across DGRP studies to survey common trends in genetic modifiers across the genetic architecture that may share a common basis.

## **Acknowledgements**

We thank Faye Lemieux for her assistance with fly husbandry and Jim A. Mossman for his assistance collecting data.

## Literature Cited

- Abbott, J. K., S. Bedhomme and A. K. Chippindale, 2010 Sexual conflict in wing size and shape in *Drosophila melanogaster*. *Journal of Evolutionary Biology* 23: 1989-1997.
- Albayrak, C., C. A. Jordi, C. Zechner, J. Lin, C. A. Bichsel *et al.*, 2016 Digital Quantification of Proteins and mRNA in Single Mammalian Cells. *Molecular Cell* 61: 914-924.
- Albert, F. W., and L. Kruglyak, 2015 The role of regulatory variation in complex traits and disease. *Nature Reviews Genetics* 16: 197-212.
- Ashburner, M., C. A. Ball, J. A. Blake, D. Botstein, H. Butler *et al.*, 2000 Gene Ontology: tool for the unification of biology. *Nature Genetics* 25: 25-29.
- Ayroles, J. F., S. M. Buchanan, C. O'Leary, K. Skutt-Kakaria, J. K. Grenier *et al.*, 2015 Behavioral idiosyncrasy reveals genetic control of phenotypic variability. *Proceedings of the National Academy of Sciences of the United States of America* 112: 6706-6711.
- Babcock, D. T., and B. Ganetzky, 2014 An Improved Method for Accurate and Rapid Measurement of Flight Performance in *Drosophila*. *Jove-Journal of Visualized Experiments*.
- Bellen, H. J., R. W. Levis, Y. C. He, J. W. Carlson, M. Evans-Holm *et al.*, 2011 The *Drosophila* Gene Disruption Project: Progress Using Transposons With Distinctive Site Specificities. *Genetics* 188: 731-U341.
- Benzer, S., 1973 Genetic dissection of behavior. *Scientific American* 229: 24-37.
- Berger, D., E. C. Berg, W. Widegren, G. Arnqvist and A. A. Maklakov, 2014 Multivariate intralocus sexual conflict in seed beetles. *Evolution* 68: 3457-3469.
- Berger, D., T. You, M. R. Minano, K. Grieshop, M. I. Lind *et al.*, 2016 Sexually antagonistic selection on genetic variation underlying both male and female same-sex sexual behavior. *Bmc Evolutionary Biology* 16.
- Boyle, E. A., Y. I. Li and J. K. Pritchard, 2017 An Expanded View of Complex Traits: From Polygenic to Omnigenic. *Cell* 169: 1177-1186.
- Breuker, C. J., J. S. Patterson and C. P. Klingenberg, 2006 A Single Basis for Developmental Buffering of *Drosophila* Wing Shape. *Plos One* 1.
- Brockington, M., Y. Yuva, P. Prandini, S. C. Brown, S. Torelli *et al.*, 2001 Mutations in the fukutin-related protein gene (FKRP) identify limb girdle muscular dystrophy 2I as a milder allelic variant of congenital muscular dystrophy MDC1C. *Human Molecular Genetics* 10: 2851-2859.
- Browning, B. L., and S. R. Browning, 2016 Genotype Imputation with Millions of Reference Samples. *American Journal of Human Genetics* 98: 116-126.
- Browning, S. R., and B. L. Browning, 2007 Rapid and accurate haplotype phasing and missing-data inference for whole-genome association studies by use of localized haplotype clustering. *American Journal of Human Genetics* 81: 1084-1097.
- Buyse, K., Riemersma, M., Powell, G., van Reeuwijk, J., Chitayat, D., Roscioli, T., Kamsteeg, E.-J., van den Elzen, C., van Beusekom, E. and Blaser, S. (2013).

- Missense mutations in  $\beta$ -1, 3-N-acetylglucosaminyltransferase 1 (B3GNT1) cause Walker–Warburg syndrome. *Human Molecular Genetics* 22: 1746-1754.
- Carbon, S., E. Douglass, N. Dunn, B. Good, N. L. Harris *et al.*, 2019 The Gene Ontology Resource: 20 years and still GOing strong. *Nucleic Acids Research* 47: D330-D338.
- Chintapalli, V. R., J. Wang and J. A. T. Dow, 2007 Using FlyAtlas to identify better *Drosophila melanogaster* models of human disease. *Nature Genetics* 39: 715-720.
- Choi, Y., and A. P. Chan, 2015 PROVEAN web server: a tool to predict the functional effect of amino acid substitutions and indels. *Bioinformatics* 31: 2745-2747.
- Colomb, J., and B. Brembs, 2016 PKC in motoneurons underlies self learning, a form of motor learning in *Drosophila*. *PeerJ* 4.
- Consortium, T. A. o. G. R., 2020 Alliance of Genome Resources Portal: unified model organism research platform. *Nucleic acids research* 48: D650-D658.
- Couto, A., M. Alenius and B. J. Dickson, 2005 Molecular, anatomical, and functional organization of the *Drosophila* olfactory system. *Current Biology* 15: 1535-1547.
- Crawford, L., P. Zeng, S. Mukherjee and X. Zhou, 2017 Detecting epistasis with the marginal epistasis test in genetic mapping studies of quantitative traits. *Plos Genetics* 13.
- Cubadda, Y., P. Heitzler, R. P. Ray, M. Bourouis, P. Ramain *et al.*, 1997 u-shaped encodes a zinc finger protein that regulates the proneural genes *achaete* and *scute* during the formation of bristles in *Drosophila*. *Genes & Development* 11: 3083-3095.
- Danecek, P., A. Auton, G. Abecasis, C. A. Albers, E. Banks *et al.*, 2011 The variant call format and VCFtools. *Bioinformatics* 27: 2156-2158.
- Dickinson, M., G. Farman, M. Frye, T. Bekyarova, D. Gore *et al.*, 2005 Molecular dynamics of cyclically contracting insect flight muscle in vivo. *Nature* 433: 330-333.
- Dickinson, M. H., S. Hannaford and J. Palka, 1997 The evolution of insect wings and their sensory apparatus. *Brain Behavior and Evolution* 50: 13-24.
- dos Santos, G., A. J. Schroeder, J. L. Goodman, V. B. Strelets, M. A. Crosby *et al.*, 2015 FlyBase: introduction of the *Drosophila melanogaster* Release 6 reference genome assembly and large-scale migration of genome annotations. *Nucleic Acids Research* 43: D690-D697.
- Eanes, W. F., T. J. S. Merritt, J. M. Flowers, S. Kumagai, E. Sezgin *et al.*, 2006 Flux control and excess capacity in the enzymes of glycolysis and their relationship to flight metabolism in *Drosophila melanogaster*. *Proceedings of the National Academy of Sciences of the United States of America* 103: 19413-19418.
- Edwards, A. C., L. Zwarts, A. Yamamoto, P. Callaerts and T. F. Mackay, 2009 Mutations in many genes affect aggressive behavior in *Drosophila melanogaster*. *BMC biology* 7: 29.
- Fedotov, S. A., J. V. Bragina, N. G. Besedina, L. V. Danilenkova, E. A. Kamysheva *et al.*, 2018 Gene CG15630 (*fipi*) is involved in regulation of the interpulse interval in *Drosophila* courtship song. *Journal of Neurogenetics* 32: 15-26.

- Fisher, D. N., M. Brachmann and J. B. Burant, 2018 Complex dynamics and the development of behavioural individuality. *Animal Behaviour* 138: E1-E6.
- Fontaine, E. I., F. Zabala, M. H. Dickinson and J. W. Burdick, 2009 Wing and body motion during flight initiation in *Drosophila* revealed by automated visual tracking. *Journal of Experimental Biology* 212: 1307-1323.
- Frise, E., A. S. Hammonds and S. E. Celniker, 2010 Systematic image-driven analysis of the spatial *Drosophila* embryonic expression landscape. *Molecular Systems Biology* 6.
- Fromental-Rainin, C., N. Taquet and P. Rainin, 2010 Transcriptional interactions between the pannier isoforms and the cofactor U-shaped during neural development in *Drosophila*. *Mechanisms of Development* 127: 442-457.
- Frye, M. A., and M. H. Dickinson, 2004 Closing the loop between neurobiology and flight behavior in *Drosophila*. *Current Opinion in Neurobiology* 14: 729-736.
- Furman, D., and T. Bukharina, 2008 How *Drosophila melanogaster* forms its mechanoreceptors. *Current genomics* 9: 312-323.
- Gabel, H. W., B. Kinde, H. Stroud, C. S. Gilbert, D. A. Harmin *et al.*, 2015 Disruption of DNA-methylation-dependent long gene repression in Rett syndrome. *Nature* 522: 89-U221.
- Gaertner, B. E., E. A. Ruedi, L. J. McCoy, J. M. Moore, M. F. Wolfner *et al.*, 2015 Heritable Variation in Courtship Patterns in *Drosophila melanogaster*. *G3-Genes Genomes Genetics* 5: 531-539.
- Gaudet, P., M. S. Livstone, S. E. Lewis and P. D. Thomas, 2011 Phylogenetic-based propagation of functional annotations within the Gene Ontology consortium. *Briefings in Bioinformatics* 12: 449-462.
- Getahun, M. N., M. Thoma, S. Lavista-Llanos, I. Keesey, R. A. Fandino *et al.*, 2016 Intracellular regulation of the insect chemoreceptor complex impacts odour localization in flying insects. *Journal of Experimental Biology* 219: 3428-3438.
- Ghosh, A., E. J. Rideout and S. S. Grewal, 2014 TIF-1A-Dependent Regulation of Ribosome Synthesis in *Drosophila* Muscle Is Required to Maintain Systemic Insulin Signaling and Larval Growth. *Plos Genetics* 10.
- Gorostiza, E. A., J. Colomb and B. Brembs, 2016 A decision underlies phototaxis in an insect. *Open Biology* 6.
- Grumbling, G., V. Strelets and C. FlyBase, 2006 FlyBase: anatomical data, images and queries. *Nucleic Acids Research* 34: D484-D488.
- Hesselberg, T., and F. O. Lehmann, 2009 The role of experience in flight behaviour of *Drosophila*. *Journal of Experimental Biology* 212: 3377-3386.
- Hiesinger, P. R., and B. A. Hassan, 2018 The Evolution of Variability and Robustness in Neural Development. *Trends in Neurosciences* 41: 577-586.
- Holmbeck, M. A., J. R. Donner, E. Villa-Cuesta and D. M. Rand, 2015 A *Drosophila* model for mito-nuclear diseases generated by an incompatible interaction between tRNA and tRNA synthetase. *Disease models & mechanisms* 8: 843-854.
- Honegger, K., and B. de Bivort, 2018 Stochasticity, individuality and behavior. *Current Biology* 28: R8-R12.

- Hong, W. Z., T. J. Mosca and L. Q. Luo, 2012 Teneurins instruct synaptic partner matching in an olfactory map. *Nature* 484: 201-+.
- Hu, Y. H., I. Flockhart, A. Vinayagam, C. Bergwitz, B. Berger *et al.*, 2011 An integrative approach to ortholog prediction for disease-focused and other functional studies. *Bmc Bioinformatics* 12.
- Huang, W., A. Massouras, Y. Inoue, J. Peiffer, M. Ramia *et al.*, 2014 Natural variation in genome architecture among 205 *Drosophila melanogaster* Genetic Reference Panel lines. *Genome Research* 24: 1193-1208.
- Huang, W., S. Richards, M. A. Carbone, D. H. Zhu, R. R. H. Anholt *et al.*, 2012 Epistasis dominates the genetic architecture of *Drosophila* quantitative traits. *Proceedings of the National Academy of Sciences of the United States of America* 109: 15553-15559.
- Kain, J. S., C. Stokes and B. L. de Bivort, 2012 Phototactic personality in fruit flies and its suppression by serotonin and white. *Proceedings of the National Academy of Sciences of the United States of America* 109: 19834-19839.
- Karr, T. L., 2007 Fruit flies and the sperm proteome. *Human Molecular Genetics* 16: R124-R133.
- King, I. F., C. N. Yandava, A. M. Mabb, J. S. Hsiao, H. S. Huang *et al.*, 2013 Topoisomerases facilitate transcription of long genes linked to autism. *Nature* 501: 58-+.
- Kise, Y., and D. Schmucker, 2013 Role of self-avoidance in neuronal wiring. *Current Opinion in Neurobiology* 23: 983-989.
- Klingenberg, C. P., 2019 Phenotypic Plasticity, Developmental Instability, and Robustness: The Concepts and How They Are Connected. *Frontiers in Ecology and Evolution* 7.
- Lajus, D. L., P. V. Golovin, A. O. Yurtseva, T. S. Ivanova, A. S. Dorgham *et al.*, 2019 Fluctuating asymmetry as an indicator of stress and fitness in stickleback: a review of the literature and examination of cranial structures. *Evolutionary Ecology Research* 20.
- Lehmann, F. O., and J. Bartussek, 2017 Neural control and precision of flight muscle activation in *Drosophila*. *Journal of Comparative Physiology a-Neuroethology Sensory Neural and Behavioral Physiology* 203: 1-14.
- Li, J. F., S. Han, H. J. Li, N. D. Udeshi, T. Svinkina *et al.*, 2020 Cell-Surface Proteomic Profiling in the Fly Brain Uncovers Wiring Regulators. *Cell* 180: 373-+.
- Long, T. A. F., and W. R. Rice, 2007 Adult locomotory activity mediates intralocus sexual conflict in a laboratory-adapted population of *Drosophila melanogaster*. *Proceedings of the Royal Society B-Biological Sciences* 274: 3105-3112.
- Ludwig, W., 1932 *Das rechts-links-problem im tierreich und beim menschen: mit einem anhang rechts-links-merkmale der pflanzen*. Springer-Verlag.
- Mackay, T. F., and W. Huang, 2018 Charting the genotype–phenotype map: lessons from the *Drosophila melanogaster* Genetic Reference Panel. *Wiley Interdisciplinary Reviews: Developmental Biology* 7.
- Mackay, T. F. C., S. Richards, E. A. Stone, A. Barbadilla, J. F. Ayroles *et al.*, 2012 The *Drosophila melanogaster* Genetic Reference Panel. *Nature* 482: 173-178.

- Manolio, T. A., F. S. Collins, N. J. Cox, D. B. Goldstein, L. A. Hindorff *et al.*, 2009 Finding the missing heritability of complex diseases. *Nature* 461: 747-753.
- Marcus, J. M., 2001 The development and evolution of crossveins in insect wings. *Journal of Anatomy* 199: 211-216.
- Menezes, B. F., J. Salces-Ortiz, H. Muller, N. Burlet, S. Martinez *et al.*, 2018 An attempt to select non-genetic variation in resistance to starvation and reduced chill coma recovery time in *Drosophila melanogaster*. *Journal of Experimental Biology* 221.
- Metaxakis, A., S. Oehler, A. Klinakis and C. Savakis, 2005 Minos as a genetic and genomic tool in *Drosophila melanogaster*. *Genetics* 171: 571-581.
- Milan, M., F. J. Diaz-Benjumea and S. M. Cohen, 1998 Beadex encodes an LMO protein that regulates Apterous LIM-homeodomain activity in *Drosophila* wing development: a model for LMO oncogene function. *Genes & Development* 12: 2912-2920.
- Montgomery, S. L., D. Vorojeikina, W. Huang, T. F. C. Mackay, R. R. H. Anholt *et al.*, 2014 Genome-Wide Association Analysis of Tolerance to Methylmercury Toxicity in *Drosophila* Implicates Myogenic and Neuromuscular Developmental Pathways. *Plos One* 9.
- Montooth, K. L., J. H. Marden and A. G. Clark, 2003 Mapping determinants of variation in energy metabolism, respiration and flight in *Drosophila*. *Genetics* 165: 623-635.
- Morgante, F., P. Sorensen, D. A. Sorensen, C. Maltecca and T. F. C. Mackay, 2015 Genetic Architecture of Micro-Environmental Plasticity in *Drosophila melanogaster*. *Scientific Reports* 5.
- Mossman, J. A., L. M. Biancani, C. T. Zhu and D. M. Rand, 2016 Mitonuclear Epistasis for Development Time and Its Modification by Diet in *Drosophila*. *Genetics* 203: 463-+.
- Muhammad, K., S. Reddy-Alla, J. H. Driller, D. Schreiner, U. Rey *et al.*, 2015 Presynaptic spinophilin tunes neurexin signalling to control active zone architecture and function. *Nature Communications* 6.
- Munoz-Munoz, F., V. P. Carreira, N. Martinez-Abadias, V. Ortiz, R. Gonzalez-Jose *et al.*, 2016 *Drosophila* wing modularity revisited through a quantitative genetic approach. *Evolution* 70: 1530-1541.
- Murakami, S., M. Minami-Ohtsubo, R. Nakato, K. Shirahige and T. Tabata, 2017 Two Components of Aversive Memory in *Drosophila*, Anesthesia-Sensitive and Anesthesia-Resistant Memory, Require Distinct Domains Within the Rgk1 Small GTPase. *Journal of Neuroscience* 37: 5496-5510.
- Nagai, T., and K. Mizuno, 2014 Multifaceted roles of Furry proteins in invertebrates and vertebrates. *Journal of Biochemistry* 155: 137-146.
- Nakka, P., B. J. Raphael and S. Ramachandran, 2016 Gene and Network Analysis of Common Variants Reveals Novel Associations in Multiple Complex Diseases. *Genetics* 204: 783-+.
- Negre, N., C. D. Brown, L. J. Ma, C. A. Bristow, S. W. Miller *et al.*, 2011 A cis-regulatory map of the *Drosophila* genome. *Nature* 471: 527-531.

- Paul, L., S. H. Wang, S. N. Manivannan, L. Bonanno, S. Lewis *et al.*, 2013 Dpp-induced Egfr signaling triggers postembryonic wing development in *Drosophila*. *Proceedings of the National Academy of Sciences of the United States of America* 110: 5058-5063.
- Pavlou, H. J., and S. F. Goodwin, 2013 Courtship behavior in *Drosophila melanogaster*: towards a 'courtship connectome'. *Current Opinion in Neurobiology* 23: 76-83.
- Pitchers, W., J. Nye, E. J. Marquez, A. Kowalski, I. Dworkin *et al.*, 2019 A Multivariate Genome-Wide Association Study of Wing Shape in *Drosophila melanogaster*. *Genetics* 211: 1429-1447.
- Purcell, S., B. Neale, K. Todd-Brown, L. Thomas, M. A. R. Ferreira *et al.*, 2007 PLINK: A tool set for whole-genome association and population-based linkage analyses. *American Journal of Human Genetics* 81: 559-575.
- Quijano, J. C., M. J. Stinchfield, B. Zerlanko, Y. Y. Gibbens, N. T. Takaesu *et al.*, 2010 The Sno Oncogene Antagonizes Wingless Signaling during Wing Development in *Drosophila*. *Plos One* 5.
- Quinto-Sanchez, M., F. Munoz-Munoz, J. Gomez-Valdes, C. Cintas, P. Navarro *et al.*, 2018 Developmental pathways inferred from modularity, morphological integration and fluctuating asymmetry patterns in the human face. *Scientific Reports* 8.
- Roman, A. C., J. Vicente-Page, A. Perez-Escudero, J. M. Carvajal-Gonzalez, P. M. Fernandez-Salguero *et al.*, 2018 Histone H4 acetylation regulates behavioral inter-individual variability in zebrafish. *Genome Biology* 19.
- Romero-Calderon, R., R. M. Shome, A. F. Simon, R. W. Daniels, A. DiAntonio *et al.*, 2007 A screen for neurotransmitter transporters expressed in the visual system of *Drosophila melanogaster* identifies three novel genes. *Developmental Neurobiology* 67: 550-569.
- Sadaf, S., O. V. Reddy, S. P. Sane and G. Hasan, 2015 Neural Control of Wing Coordination in Flies. *Current Biology* 25: 80-86.
- Sambandan, D., A. Yamamoto, J. J. Fanara, T. F. C. Mackay and R. R. H. Anholt, 2006 Dynamic genetic interactions determine odor-guided behavior in *Drosophila melanogaster*. *Genetics* 174: 1349-1363.
- Schindelin, J., I. Arganda-Carreras, E. Frise, V. Kaynig, M. Longair *et al.*, 2012 Fiji: an open-source platform for biological-image analysis. *Nature Methods* 9: 676-682.
- Schnorrer, F., C. Schonbauer, C. C. H. Langer, G. Dietzl, M. Novatchkova *et al.*, 2010 Systematic genetic analysis of muscle morphogenesis and function in *Drosophila*. *Nature* 464: 287-291.
- Schor, I. E., J. F. Degner, D. Harnett, E. Cannavo, F. P. Casale *et al.*, 2017 Promoter shape varies across populations and affects promoter evolution and expression noise. *Nature Genetics* 49: 550-+.
- Shirangi, T. R., A. M. Wong, J. W. Truman and D. L. Stern, 2016 Doublesex Regulates the Connectivity of a Neural Circuit Controlling *Drosophila* Male Courtship Song. *Developmental Cell* 37: 533-544.
- Shorter, J., C. Couch, W. Huang, M. A. Carbone, J. Peiffer *et al.*, 2015 Genetic architecture of natural variation in *Drosophila melanogaster* aggressive behavior.

- Proceedings of the National Academy of Sciences of the United States of America 112: E3555-E3563.
- Siepel, A., G. Bejerano, J. S. Pedersen, A. S. Hinrichs, M. M. Hou *et al.*, 2005 Evolutionarily conserved elements in vertebrate, insect, worm, and yeast genomes. *Genome Research* 15: 1034-1050.
- Siepel, A., and D. Haussler, 2005 Phylogenetic hidden Markov models, pp. 325-351 in *Statistical methods in molecular evolution*. Springer.
- Skeath, J. B., and S. B. Carroll, 1991 REGULATION OF ACHAETE-SCUTE GENE-EXPRESSION AND SENSORY ORGAN PATTERN-FORMATION IN THE DROSOPHILA WING. *Genes & Development* 5: 984-995.
- Soto, I. M., V. P. Carreira, E. M. Soto and E. Hasson, 2008 Wing morphology and fluctuating asymmetry depend on the host plant in cactophilic *Drosophila*. *Journal of Evolutionary Biology* 21: 598-609.
- Spierer, A. N., J. A. Mossman, S. A. Smith, L. Crawford, S. Ramachandran and D. M. Rand, 2020. Chapter 1: Natural variation in the regulation of neurodevelopmental genes modifies flight performance in *Drosophila*. 1-74.
- Sugino, K., C. M. Hempel, B. W. Okaty, H. A. Arnson, S. Kato *et al.*, 2014 Cell-Type-Specific Repression by Methyl-CpG-Binding Protein 2 Is Biased toward Long Genes. *Journal of Neuroscience* 34: 12877-12883.
- Sujkowski, A., A. N. Spierer, T. Rajagopalan, B. Bazzell, M. Safdar *et al.*, 2018 Mitonuclear interactions modify *Drosophila* exercise performance. *Mitochondrion*.
- Sztepanacz, J. L., K. McGuigan and M. W. Blows, 2017 Heritable Micro-environmental Variance Covaries with Fitness in an Outbred Population of *Drosophila serrata*. *Genetics* 206: 2185-2198.
- Tadros, W., S. W. Xu, O. Akin, C. H. Yi, G. J. E. Shin *et al.*, 2016 Dscam Proteins Direct Dendritic Targeting through Adhesion. *Neuron* 89: 480-493.
- Thistle, R., P. Cameron, A. Ghorayshi, L. Dennison and K. Scott, 2012 Contact chemoreceptors mediate male-male repulsion and male-female attraction during *Drosophila* courtship. *Cell* 149: 1140-1151.
- Thurmond, J., J. L. Goodman, V. B. Strelets, H. Attrill, L. S. Gramates *et al.*, 2019 FlyBase 2.0: the next generation. *Nucleic Acids Research* 47: D759-D765.
- Tilney, L. G., P. S. Connelly, L. Ruggiero, K. A. Vranich and G. M. Guild, 2003 Actin filament turnover regulated by cross-linking accounts for the size, shape, location, and number of actin bundles in *Drosophila* bristles. *Molecular Biology of the Cell* 14: 3953-3966.
- Tootle, T. L., D. Williams, A. Hubb, R. Frederick and A. Spradling, 2011 *Drosophila* Eggshell Production: Identification of New Genes and Coordination by Pxt. *Plos One* 6.
- Tsuzuki, S., M. Ochiai, H. Matsumoto, S. Kurata, A. Ohnishi *et al.*, 2012 *Drosophila* growth-blocking peptide-like factor mediates acute immune reactions during infectious and non-infectious stress. *Scientific Reports* 2.
- Turner, T. L., P. M. Miller and V. A. Cochrane, 2013 Combining Genome-Wide Methods to Investigate the Genetic Complexity of Courtship Song Variation in *Drosophila melanogaster*. *Molecular Biology and Evolution* 30: 2113-2120.



- Valen, L. V., 1962 A study of fluctuating asymmetry. *Evolution* 16: 125-142.
- Vogt, G., 2015 Stochastic developmental variation, an epigenetic source of phenotypic diversity with far-reaching biological consequences. *Journal of Biosciences* 40: 159-204.
- Vogt, G., M. Huber, M. Thiemann, G. van den Boogaart, O. J. Schmitz *et al.*, 2008 Production of different phenotypes from the same genotype in the same environment by developmental variation. *Journal of Experimental Biology* 211: 510-523.
- Wagner, A., 2008 Robustness and evolvability: a paradox resolved. *Proceedings of the Royal Society B-Biological Sciences* 275: 91-100.
- Wasbrough, E. R., S. Dorus, S. Hester, J. Howard-Murkin, K. Lilley *et al.*, 2010 The *Drosophila melanogaster* sperm proteome-II (DmSP-II). *Journal of proteomics* 73: 2171-2185.
- Wrischnik, L. A., J. R. Timmer, L. A. Megna and T. W. Cline, 2003 Recruitment of the proneural gene *scute* to the *Drosophila* sex-determination pathway. *Genetics* 165: 2007-2027.
- Yatsu, J., M. Hayashi, M. Mukai, K. Arita, S. Shigenobu *et al.*, 2008 Maternal RNAs encoding transcription factors for germline-specific gene expression in *Drosophila* embryos. *International Journal of Developmental Biology* 52: 913-923.
- Yu, J. Y., M. I. Kanai, E. Demir, G. Jefferis and B. J. Dickson, 2010 Cellular Organization of the Neural Circuit that Drives *Drosophila* Courtship Behavior. *Current Biology* 20: 1602-1614.
- Zhu, C. T., P. Ingelmo and D. M. Rand, 2014 GxGxE for Lifespan in *Drosophila*: Mitochondrial, Nuclear, and Dietary Interactions that Modify Longevity. *Plos Genetics* 10.
- zur Lage, P., F. G. Newton and A. P. Jarman, 2019 Survey of the Ciliary Motility Machinery of *Drosophila* Sperm and Ciliated Mechanosensory Neurons Reveals Unexpected Cell-Type Specific Variations: A Model for Motile Ciliopathies. *Frontiers in Genetics* 10.

**Table 1. Different approaches uncover different types of genetic modifiers affecting the focal phenotype.** No single screen will identify all modifiers; so four overlapping approaches were conducted to better survey the genetic architecture of robustness of flight performance.

<b>Screen type</b>	<b>Target modifier type</b>	<b>Analysis platform</b>
Additive	Variants of large effect	DGRP2 webservice/FastLMM
Marginal	Interconnected variants	MAPIT
Epistatic interactions	Connections between variants	PLINK
Whole gene	Genes of moderate effect	PEGASUS_flies

**Table 2. Eight additive variants passed the Bonferroni threshold.** In the additive approach, eight variants passed the strict Bonferroni significance threshold ( $P \leq 2.63E-8$ ). These common variants were typically near the Minor Allele Frequency (MAF) threshold of 0.05. Nearly all variants mapped to genes, three of which had human homologs. Non-coding variants mapped to introns or upstream of the gene's coding region, however three variants also contained transcription factor binding sites (TFBS) annotated active during the embryonic stage (NEGRE *et al.* 2011).

Variant	MAF	Variant type	Annotation		
			Gene symbol		Embryonic TFBS
			Dmel	Hsap	
2L_7949902_SNP	0.053	Intron	<i>Snoo</i>	<i>SKI</i>	
2L_7949906_SNP	0.053	Intron	<i>Snoo</i>	<i>SKI</i>	-
2R_17433667_SNP	0.051	Intron	<i>Egfr</i>	<i>EGFR</i>	<i>bcd, da, dl, gt, hb, kni, Med, prd, sna, tll, twi, disco, Trl</i>
2R_17987191_SNP	0.067	Upstream (152 bp)	<i>flapper</i>	-	<i>dl</i>
2R_17987203_SNP	0.062	Upstream (164 bp)	<i>flapper</i>	-	<i>dl</i>
3L_8237797_DEL	0.084	Intron	<i>Dscam4</i>	<i>DSCAM</i>	-
3R_4379159_SNP	0.053	Non-synonymous	<i>Or85d</i>	-	-
3R_9684126_SNP	0.15	Intergenic		-	-

**Table 3. Each analysis and sex-based phenotype identified varying enrichment for genetic modifiers.** (A) Additive loci (variants and the genes they map to) at Bonferroni and traditional DGRP GWAS thresholds differ in enrichment by an order of magnitude. (B) Marginal variants mapped to several genes, and were tested for (C) epistatic interactions. Marginal variants were only tested for epistatic interactions if they passed  $MAF \geq 0.05$  in the unimputed genome. Finally, (D) whole genes were identified consistently across all sex-based phenotypes

<b>(A) Additive Loci</b>				
	<b>Male</b>	<b>Female</b>	<b>Sex-Average</b>	<b>Sex-Different</b>
Variants (Bonferroni; $P \leq 2.63e-8$ )	2	5	4	0
Genes (Bonferroni; $P \leq 2.63e-8$ )	1	3	3	0
Variants (Traditional DGRP; $P \leq 1.00e-5$ )	75	76	76	21
Genes (Traditional DGRP; $P \leq 1.00e-5$ )	49	62	58	17
<b>(B) Marginal Loci</b>				
	<b>Male</b>	<b>Female</b>	<b>Sex-Average</b>	<b>Sex-Different</b>
Variants (Bonferroni; $P \leq 2.56e-8$ )	1	53	19	45
Genes (Bonferroni; $P \leq 2.56e-8$ )	0	30	11	32
<b>(C) Epistatic Loci</b>				
	<b>Male</b> ( $P \leq 2.63E-8$ )	<b>Female</b> ( $P \leq 5.06E-10$ )	<b>Sex-Average</b> ( $P \leq 1.34e-9$ )	<b>Sex-Different</b> ( $P \leq 5.90e-10$ )
Paired Primary Variants	1	7	3	8
Paired Primary Genes	0	3	1	2
Paired Secondary Variants	20	428	611	2019
Paired Secondary Genes	13	193	243	763
<b>(D) Gene-scores</b>				
	<b>Male</b>	<b>Female</b>	<b>Sex-Average</b>	<b>Sex-Different</b>
Whole genes (Bonferroni; $P \leq 3.43E-6$ )	10	22	20	10

**Table 4. Significant variants are non-uniformly distributed across site classes.** Variants mapped to several site classes in the genome. Across all variant-based analyses, intergenic (variants lacking FBgn annotations) and genic (sites with FBgn annotations) sites were both represented. Some genic variants mapped to multiple FBgn (Genic—mapped). These genic variants mapped to 12 different site classes.

<b>Site class</b>	<b>Additive</b> ( $P \leq 2.63E-8$ )	<b>Additive</b> ( $P \leq 1E-5$ )	<b>Marginal</b> ( $P \leq 2.56E-8$ )	<b>Epistatic</b> (variable)
<b>Intergenic</b>	1	25	21	608
<b>Genic—unique</b>	7	138	66	2443
<b>Genic—mapped</b>				
	7	217	97	3275
Novel start site	0	1	0	9
Splice site region	0	0	0	1
Codon change plus codon insertion	0	0	0	2
Codon deletion	0	0	0	1
Non-synonymous coding	1	6	1	81
Exon (candidate region)	0	3	1	61
Synonymous coding	0	8	7	238
Upstream	2	47	9	462
Downstream	0	24	15	592
Intron	4	121	62	1683
5' UTR	0	1	0	50
3' UTR	0	6	2	95

**Table 5. Summary of top marginal variants, representing these variants more likely to interact with other variants, significant for robustness for flight performance.** Reported top variant IDs that pass a Bonferroni threshold ( $P \leq 2.56E-8$ ) and map within 1kb of a gene. Variants tied in significance are listed on separate lines and if their variant type is different, are accompanied with a vertical bar (|). The number of variants (#) identified overall for each FlyBase gene numbers (FBgn) are listed with the respective *D. melanogaster* (Dmel) gene symbol and predicted *H. sapiens* (Hsap) ortholog. If multiple genes mapped to the same intron, then rows within a cell correspond for variant type, #, Dmel, and Hsap. The sex is listed in bold for the reported *P*-value, and if another sex-based phenotype was also significant past the Bonferroni threshold, then it is listed in the default style. See Table S9 for a complete list of significant marginal variants.

ID	Variant Type	#	FBgn	Dmel	Hsap	Sex	P-value
2L_13665283_SNP	UPSTREAM	2	FBgn0028527	<i>CG18507</i>	<i>TMEM268</i>	A	1.30E-08
2L_15118901_SNP	DOWNSTREAM UPSTREAM	1 1	FBgn0001978 FBgn0264435	<i>stc</i> <i>lncRNA:CR43853</i>	<i>NFX1</i>	F	2.20E-09
2L_17858284_SNP	INTRON	1	FBgn0262018	<i>CadN2</i>	CDH family	D	8.41E-09
2L_18376890_SNP	INTRON	1	FBgn0000636	<i>Fas3</i>	<i>NECTIN3</i>	D	2.64E-09
2L_18405116_INS 2L_18405122_SNP	DOWNSTREAM	3	FBgn0265680	<i>lncRNA:CR44487</i>		D	9.82E-09
2L_3813243_SNP	INTRON	1	FBgn0031573	<i>CG3407</i>		D	9.04E-09
2L_4744991_SNP	INTRON	2	FBgn0031627	<i>fipi</i>	<i>NCAM1 &amp; 2</i>	A & F	3.20E-09
2L_520870_SNP 2L_520873_SNP 2L_520875_SNP	INTRON	4	FBgn0003963	<i>ush</i>	<i>ZFPM1</i>	D	1.85E-08
2L_5789592_SNP	INTRON	4	FBgn0031738	<i>CG9171</i>	<i>B4GAT1</i>	F	1.28E-09
2L_6255045_SNP	INTRON UPSTREAM	2 1	FBgn0053531 FBgn0031791	<i>Ddr</i> <i>AANATL2</i>	<i>DDR2</i>	D	1.54E-08
2L_6837786_SNP	SYNONYMOUS_CODING	1	FBgn0051632	<i>sens-2</i>	<i>GFI1B</i>	F	2.54E-08
2R_15214612_SNP	NON_SYNONYMOUS_CODING	2	FBgn0264753	<i>Rgk1</i>	<i>RRAD</i>	A & F	6.62E-09
2R_16329683_SNP	INTRON	1	FBgn0086604	<i>side-VIII</i>		D	7.25E-09
2R_16871314_SNP	DOWNSTREAM UTR_3_PRIME	1 1	FBgn0034567 FBgn0034566	<i>CG15651</i> <i>CG9313</i>	<i>FKRP</i> <i>DNAI1</i>	A	1.12E-08
2R_17237364_SNP	INTRON	1	FBgn0034624	<i>CG17974</i>	<i>R3HDML</i>	F	2.32E-08
2R_17881811_SNP	INTRON	1	FBgn0085399	<i>CG34370</i>		D	2.56E-08
2R_18317818_SNP	DOWNSTREAM	1	FBgn0034730	<i>ppk12</i>	<i>ASIC2</i>	F	7.95E-09
2R_18901796_SNP	INTRON	1 1	FBgn0261705 FBgn0003900	<i>CG42741</i> <i>twi</i>	<i>KLF8</i> <i>TWIST1</i>	A & F	2.20E-16
2R_18942230_SNP	UPSTREAM	1	FBgn0265187	<i>Fatp2</i>	<i>SLC27A4</i>	F	1.58E-08
2R_9370228_SNP	INTRON DOWNSTREAM	1	FBgn0000119	<i>arr</i> <i>cbc</i>	<i>LRP6</i> <i>CLP1</i>	F	1.68E-08
2R_9482083_SNP	SYNONYMOUS_CODING	1	FBgn0033859	<i>fand</i>	<i>XAB2</i>	F	7.24E-09
3L_10477242_SNP	INTRON	1	FBgn0052062	<i>Rbfox1</i>	<i>RBFOX1</i>	D	1.09E-08
3L_11307007_SNP	DOWNSTREAM	1	FBgn0036153	<i>CG7573</i>	<i>ZMPSTE24</i>	F	2.52E-09
3L_12128004_SNP   3L_12128115_SNP	INTRON   SYNONYMOUS_CODING	2	FBgn0036254	<i>CG5645</i>	<i>KRI1</i>	A & F	9.17E-09
3L_12261406_SNP	SYNONYMOUS_CODING	1	FBgn0052100	<i>CG32100</i>		F	6.15E-09
3L_12816254_SNP	SYNONYMOUS_CODING	1	FBgn0260965	<i>CG42588</i>	<i>GTF3C2</i>	D	1.26E-08
3L_14984696_SNP	UTR_3_PRIME UPSTREAM	1 1	FBgn0002778	<i>mnd</i> <i>Zip71B</i>	<i>SLC7A7</i> <i>SLC39A5</i>	D	1.52E-08

3L_15528436_SNP	UPSTREAM	1	FBgn0004396	<i>CrebA</i>	<i>CREB3L2</i>	D	1.23E-08
3L_15606096_SNP	UPSTREAM	2	FBgn0036520	<i>CG13449</i>		D	9.44E-09
3L_15606096_SNP 3L_15606118_SNP	DOWNSTREAM	2	FBgn0259236	<i>comm3</i>		D	9.44E-09
3L_18652370_SNP	INTRON	1	FBgn0036801	<i>MYPT-75D</i>	<i>PPP1R16A &amp; B</i>	F	2.22E-08
3L_2124762_SNP	INTRON	1	FBgn0052311	<i>zormin</i>		F	7.36E-09
3L_4614543_SNP	INTRON	8	FBgn0262733	<i>Src64B</i>	<i>SRC</i>	A & F	2.20E-16
3L_6787706_SNP	DOWNSTREAM	1	FBgn0086680	<i>vvl</i>	<i>POU3F2 - 4</i>	F	2.33E-08
3R_10255142_DEL	INTRON	1	FBgn0285955	<i>cv-c</i>	<i>DLC1</i>	F	1.59E-08
3R_10571744_SNP	INTRON DOWNSTREAM	1	FBgn0263929 FBgn0038257	<i>jvl</i> <i>smp-30</i>	<i>RGN</i>	F	9.67E-09
3R_10653019_SNP	INTRON	1	FBgn0266756	<i>btsz</i>	<i>SYTL4</i>	F	1.76E-08
3R_14535017_SNP 3R_14535554_SNP	INTRON	2 2	FBgn0000303 FBgn0270928	<i>ChAT</i> <i>VAcHT</i>	<i>CHAT</i> <i>SLC18A3</i>	D	3.35E-09
3R_1760833_SNP	INTRON	2	FBgn0083949	<i>side-III</i>	<i>NPHS1</i>	D	7.73E-09
3R_17798817_DEL	INTRON	1	FBgn0264490	<i>Eip93F</i>	<i>LCOR &amp; LCORL</i>	D	2.24E-08
3R_19043498_SNP	INTRON	1	FBgn0262975	<i>cnc</i>	<i>NFE2L1 &amp; 2</i>	D	2.12E-09
3R_20094952_SNP	INTRON	1	FBgn0011225	<i>jar</i>	<i>MYO6</i>	D	2.09E-08
3R_20997431_SNP 3R_20997437_SNP 3R_20997471_SNP	INTRON	3	FBgn0083946	<i>lobo</i>	<i>DRC7</i>	D	8.66E-09
3R_21094714_SNP	INTRON EXON DOWNSTREAM	1 1 1	FBgn0266741 FBgn0039307 FBgn0263002	<i>asRNA:CR45214</i> <i>CR13656</i> <i>CR43310</i>		D	2.33E-08
3R_21260509_SNP	INTRON	2	FBgn0004509	<i>Fur1</i>	<i>FURIN</i>	D	5.14E-09
X_12027308_INS	INTRON	1	FBgn0267001	<i>Ten-a</i>	<i>TENM3</i>	D	2.39E-08
X_12327550_SNP	INTRON	4	FBgn0259680	<i>Pkcdelta</i>	<i>PRKCD</i>	D	4.83E-09
X_15377082_DEL	INTRON	1	FBgn0030648	<i>CG6340</i>	<i>RSRC2</i>	D	4.09E-09
X_17611389_INS	INTRON	1	FBgn0261570	<i>raskol</i>	<i>DAB2IP &amp; RASAL2</i>	F	9.23E-09
X_18221352_SNP	SYNONYMOUS_CODING	1	FBgn0030913	<i>CG6123</i>		A & F	8.99E-09
X_18460258_SNP	INTRON DOWNSTREAM	1 1	FBgn0265598 FBgn0052546	<i>Bx</i> <i>tRNA:Pro-CGG-2-1</i>	<i>LMO1</i>	F	8.77E-09
X_4690532_SNP	DOWNSTREAM	1	FBgn0029728	<i>CG2861</i>		D	1.74E-08
X_5716556_SNP	INTRON	1	FBgn0029814	<i>CG15765</i>		F	1.90E-08
X_5868574_DEL	INTRON	1	FBgn0029830	<i>Grip</i>	<i>GRIP1</i>	F	2.48E-08
X_8085024_SNP	INTRON	1	FBgn0261873	<i>sdt</i>	<i>MPP5</i>	D	1.26E-08

Supplemental tables 1-10 are available online:

- <https://doi.org/10.26300/nfaa-m737>

Supplemental files 1-2 are available online:

1. <https://doi.org/10.26300/yfm8-9383>
2. <https://doi.org/10.26300/cxjw-6q95>



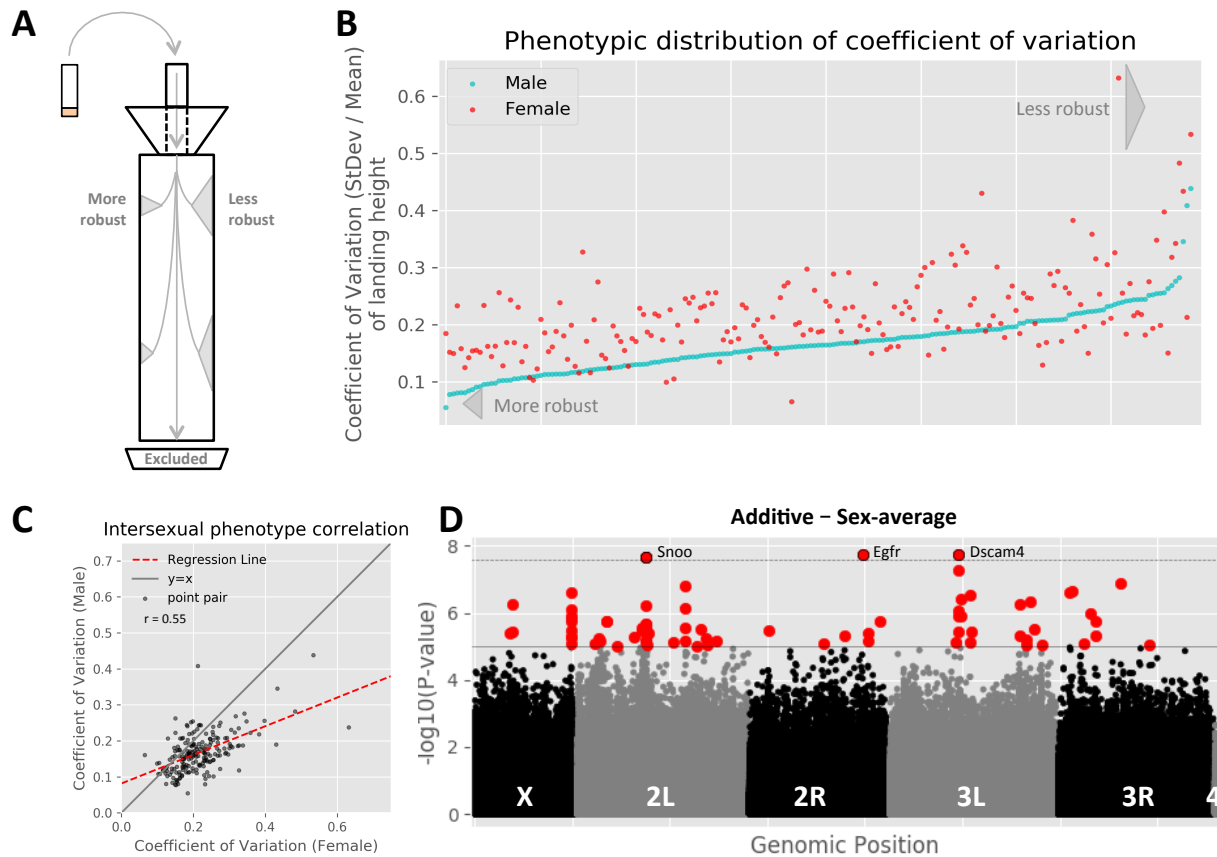


**Figure 1. The *Drosophila* Genetic Reference Panel lines demonstrate variation for robustness in flight performance across genotypes and sexes.** (A) Flies were assayed for flight performance using a meter-long flight column (BABCOCK AND GANETZKY 2014). The coefficient of variation (mean-normalized standard deviation) is a proxy for robustness; more robust genotypes have less variation in landing height around the mean. Flies that passed through the column were excluded from the analysis. (B) The phenotypic distribution of sex-genotype pairs, ordered by increasing male score, demonstrates the DGRP lines have variation in their robustness for flight performance. Genotypes demonstrated phenotypic variation for robustness in both sexes. (C) Males were generally more robust than females, though the two were related ( $r = 0.55$ ; regression line in red). Sexual dimorphism is observed by the intersection of the regression line and  $y = x$  line (gray). (D) Additive variants in the sex-average analysis, visualized as a function of the  $-\log_{10}$  of variants'  $P$ -value illustrates several variants (red) passed the traditional DGRP significance threshold ( $P \leq 1E-5$ ; gray solid line), and three (red with black outline) passed Bonferroni significance threshold ( $P \leq 2.63E-8$ , gray dashed line). Variants that did not pass the significance threshold are colored in black or gray by chromosome.

## Functional validation of candidate genes

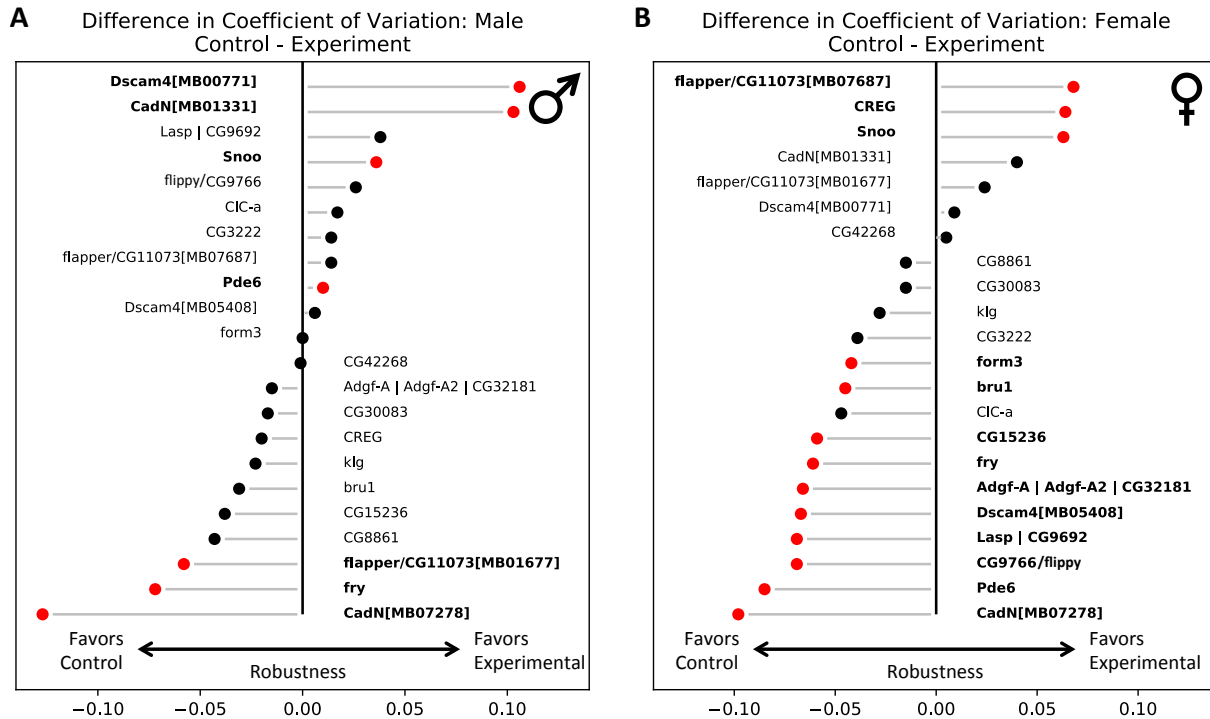


**Figure 2. Several genes validated for robustness of flight performance.** Flies homozygous for *Mi{ET1}* insertion constructs inserted in candidate genes (experiment) were tested against their background control (control). Comparisons between control and experiment lines were assessed for significance using a Klotz-Smirnov test ( $P \leq 0.05$ ; red points and bold text). Values to the left of the midline suggest control genotypes were more robust than experimental lines, while the opposite is true for values to the right of the line. (A) Seven constructs were significant in males, (B) while 13 were significant in females. Some candidate genes were tested more than once (*CadN*, *Dscam4*, and *flapper*) because they were strongly significant in the sex-average additive association screen. Separate constructs are denoted by a suffix containing a `MB` code.

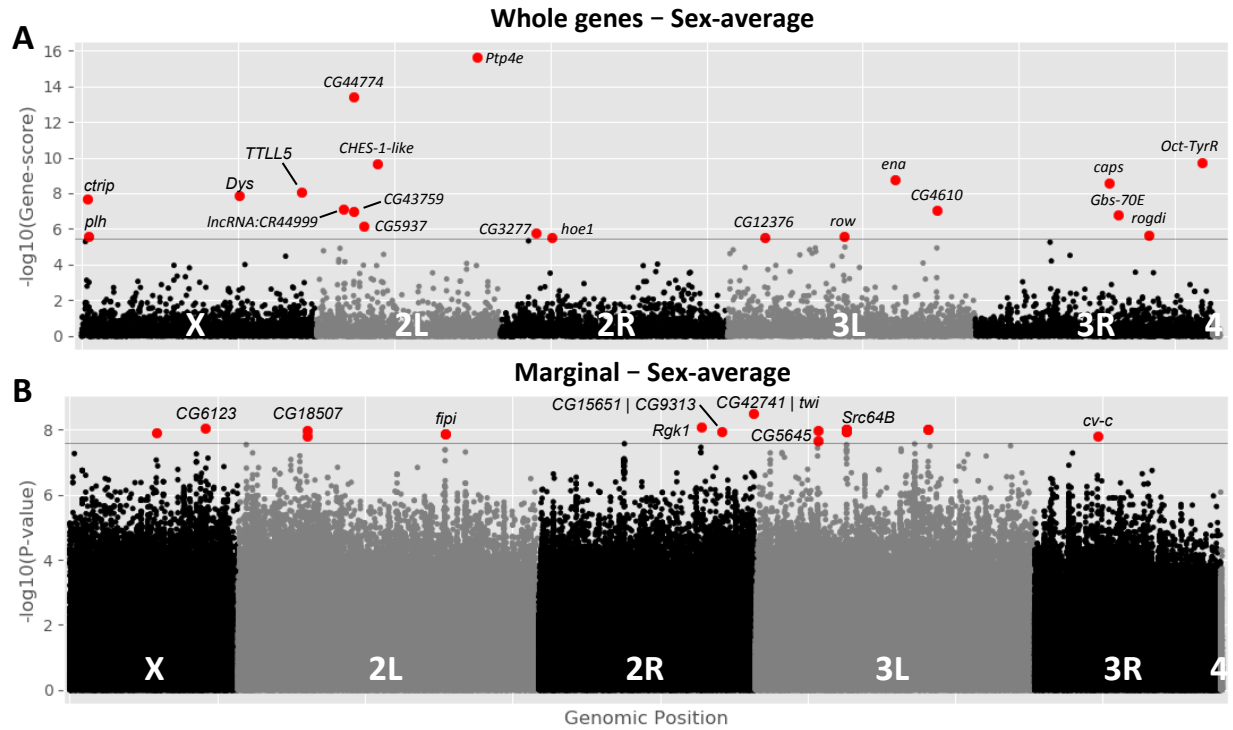


**Figure 3. Several genetic variants positively associate with flight performance across different types of analyses.** (A) Manhattan plot for sex-average whole gene analysis suggests several genes (red) were significant above a Bonferroni threshold ( $P \leq 3.43E-6$ , gray line). (B) Manhattan plot for sex-average marginal analysis suggests several variants (red) were significant above a Bonferroni threshold ( $P \leq 2.56E-8$ , gray line). For each plot, points are arranged by relative chromosome (genomic) position and all points are  $-\log_{10}$  transformed.

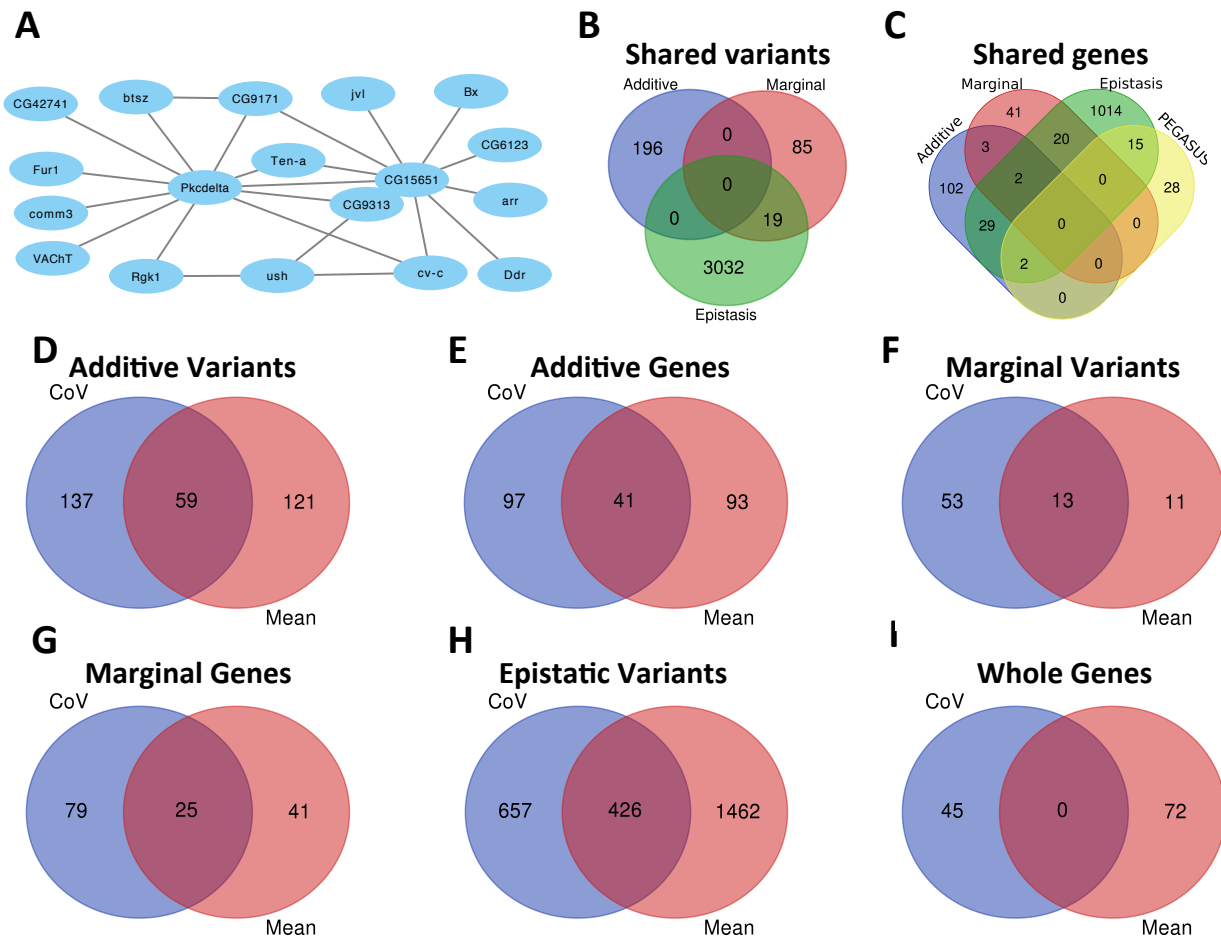


**Figure 4. Robustness of flight performance is comprised of an interconnected genetic architecture.** (A) There were several interactions between genes identified from marginal variants. In particular, *PKC- $\delta$*  had the greatest number of interactions with other marginal genes, while *CG15651* and *CG9313* were next. There was a marginal variant that overlapped with *CG15651* and *CG9313*, so all edges connecting to *CG15651* also connect to *CG9313*, however there was an independent variant in *CG9313* that did not overlap with *CG15651* that interacted in the sex-difference screen with *PKC- $\delta$*  and *ush*. Intergenic regions that also interacted with genic marginal variants are not displayed. (B) For the additive, marginal, and epistatic variants identified, additive variants were unique, while marginal and epistatic variants had some overlap. This overlap was expected since the marginal variants served as a subset in searching for epistatic variants. (C) Genes and genes mapped from variants had some overlap between analyses, though most genes were unique to a single analysis. When comparing variants and unique genes across (D-E) additive, marginal (F-G), and epistatic (H) analyses, there was roughly 15-20% overlap between the shared group and all those identified. However, there was no overlap between the (I) whole genes identified using *PEGASUS\_flies*.

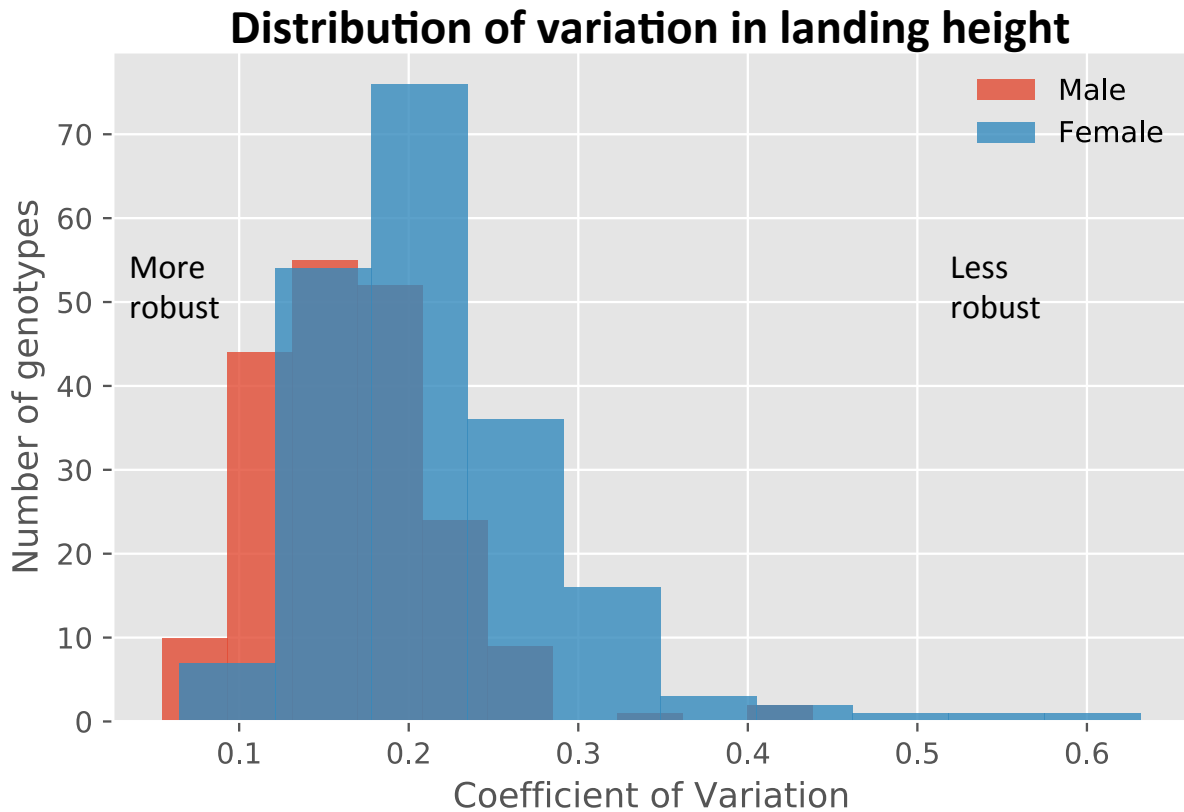


**Figure S1. Coefficient of variation is near-normally distributed across sexes.**

Genotypes' coefficient of variation is a measure of the standard deviation divided by the mean, representing a normalized measure of variation across genotypes. The distribution for each sex (males more so) was near-normally distributed, though there was a tail to the distribution favoring greater coefficients of variations. Lower coefficients of variation correspond with a greater degree of robustness for flight performance.

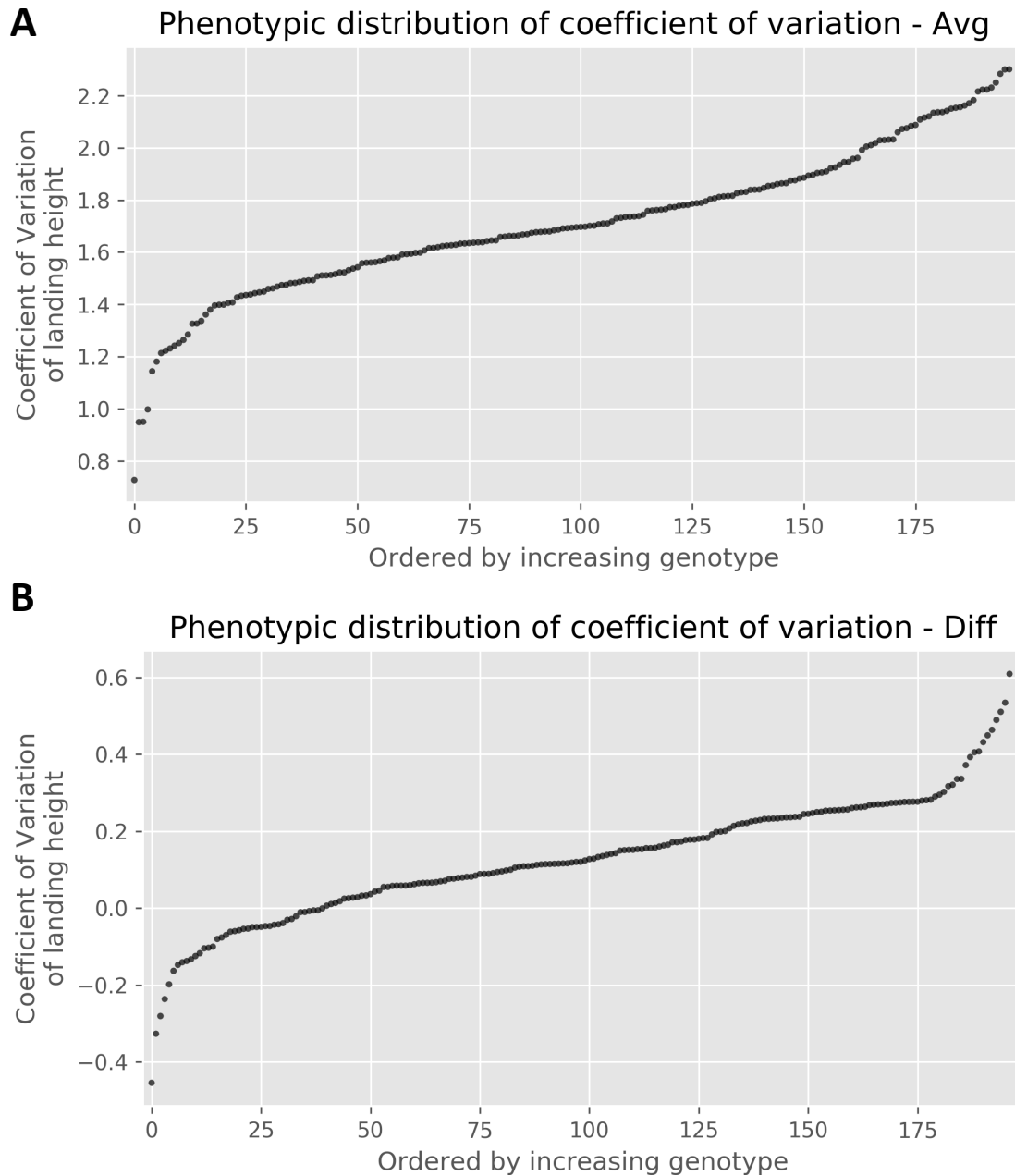


**Figure S2. Phenotypic distributions for sex-average and sex-difference phenotypes.** (A) Sex-average and (B) sex-difference phenotypes exhibit phenotypic variation for the coefficient of variation in flight performance. Each distribution is independently arranged by increasing phenotype score. The sex-difference scores represent females – males.

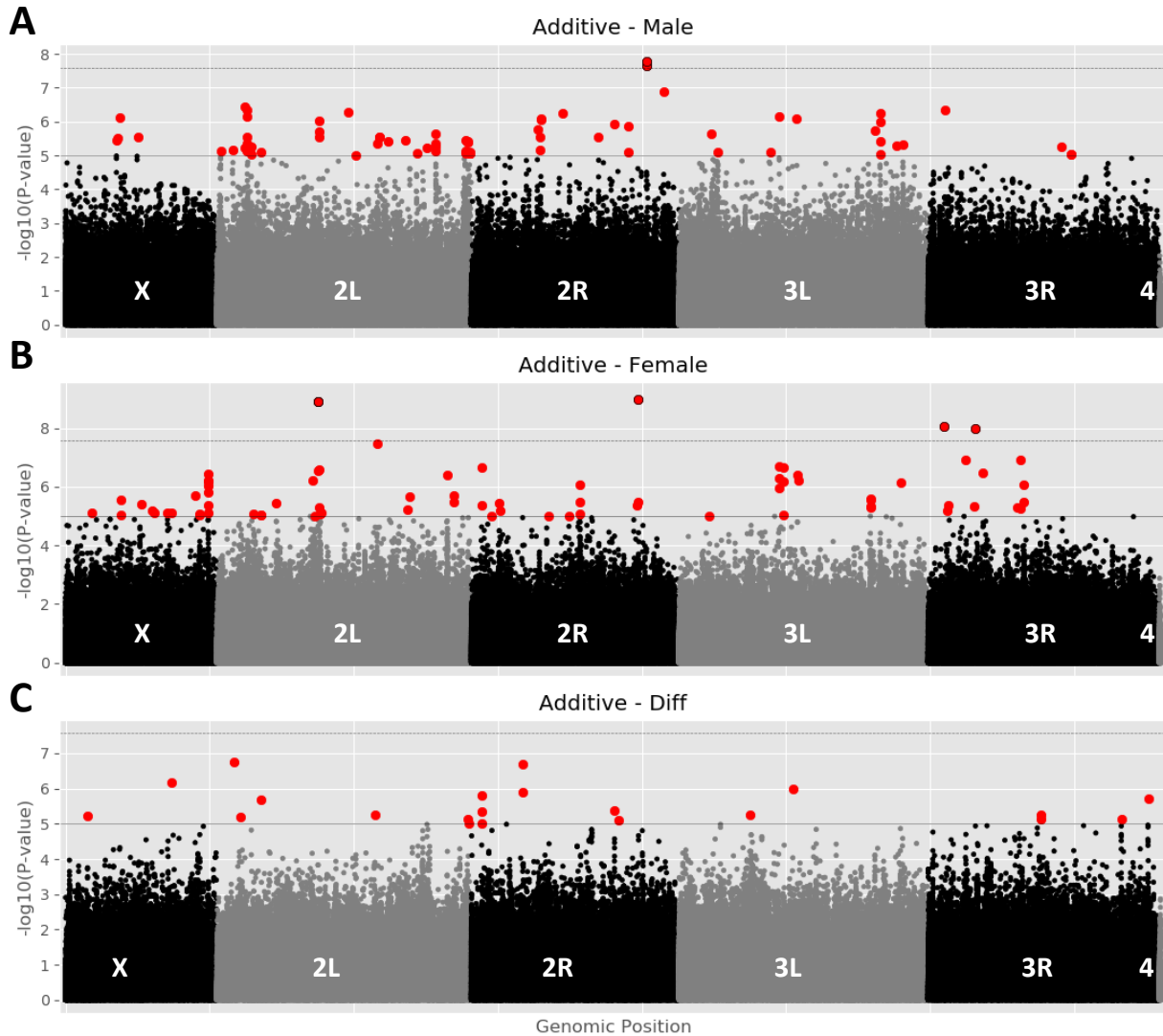


**Figure S3. Significant variants in additive analysis by sex-based phenotype.** Several additive variants were identified across the (A) male, (B) female, and (C) sex-difference phenotypes. Variants that passed a traditional DGRP significance threshold ( $P \leq 1E-5$ ; gray solid line) are in red, while those that passed a Bonferroni threshold ( $P \leq 2.63E-8$ ; gray dashed line) are red with black outline. Points ordered by their relative position across each chromosome (labeled) and plotted against the  $-\log_{10}$  of their significance score.

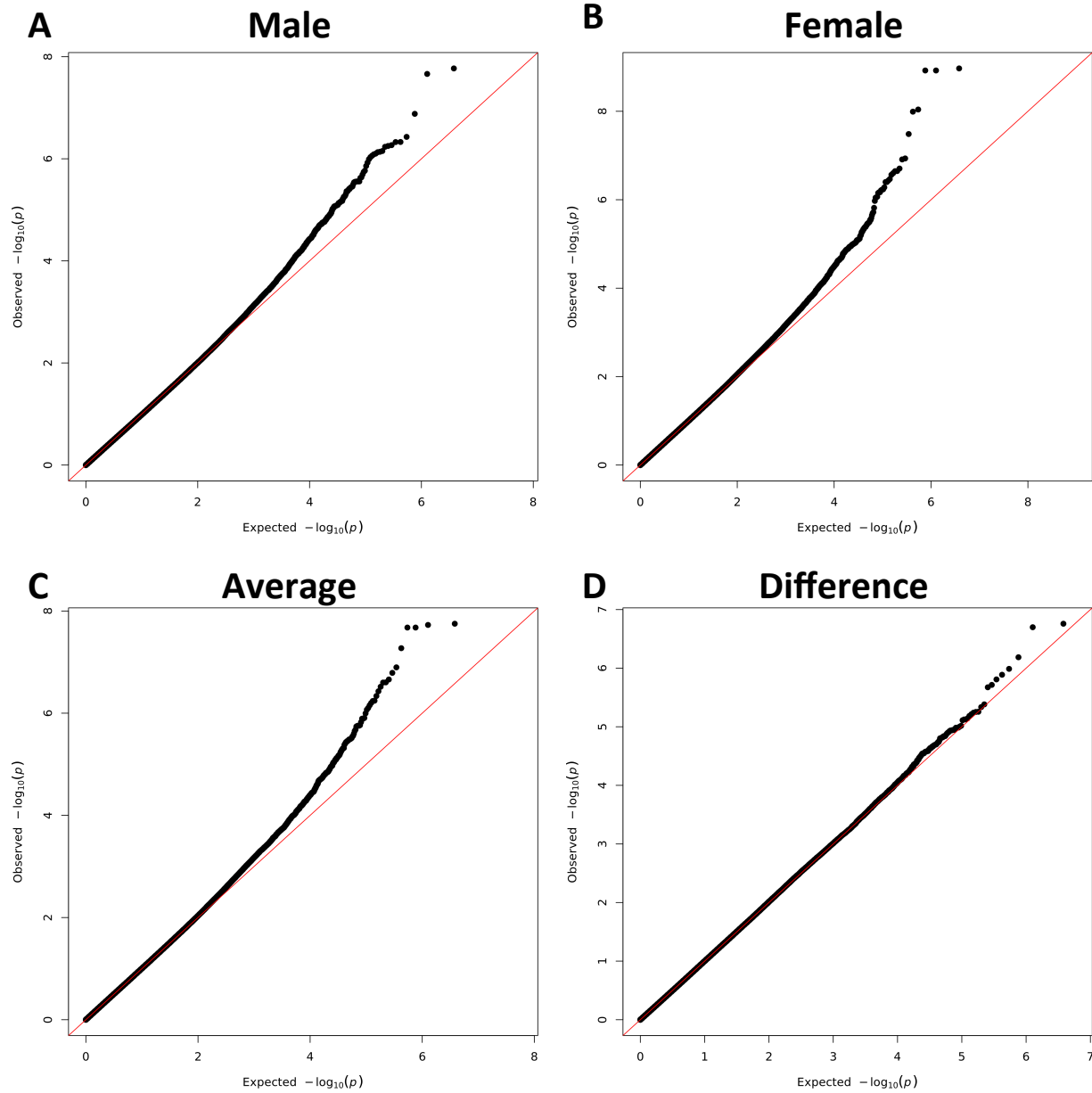


**Figure S4. Quantile-quantile (QQ) plots suggest several additive variants associate with robustness in flight performance.** QQ-plots illustrating the distribution in observed vs. expected  $P$ -values for the (A) male, (B) female, and (C) sex-average phenotypes, and (D) sex-difference phenotypes. These plots suggest each sex-based phenotype has several significant variants based on the deviation from the red line representing a 1:1 (expected : observed) relationship.



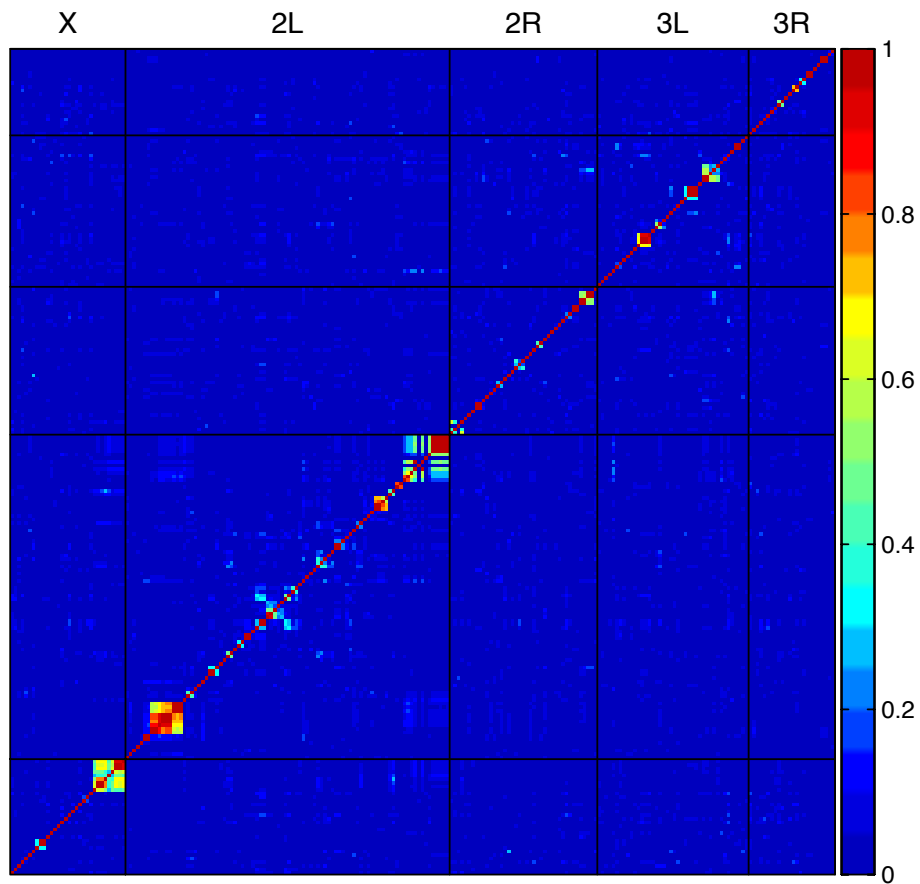


**Figure S5. Significant additive variants are broadly distributed across the genome.** Heat map illustrating the chromosomal location of each of the DGRP2 webserver's putative `top hits` (returned from DGRP2 webserver) colored from decreasing (blue, 0) to increasing (red, 1) linkage score. Most variants were distributed throughout all but chromosome 4, with some variants in linkage blocks (multicolored squares).

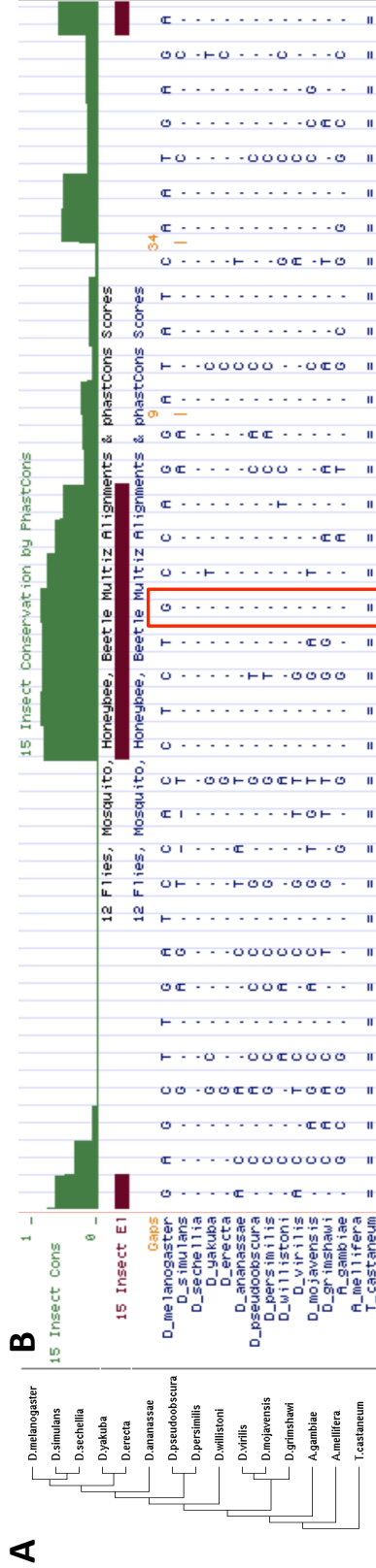


**Figure S6. Non-synonymous variant (3R\_4379159\_SNP) in Odorant receptor 85d lies in a strongly conserved region across several insect species.** (A) Phylogeny of 15 insect taxa includes several members of the *Drosophilidae* family, as well as members of the order *Diptera*. (B) This variant (red box) encodes a moderate missense mutation (tGc/tAc; C277Y) of unknown function. However, the high level of conservation among the 15 lineages hints at the site's importance, despite a putatively neutral (-2.312, -2.5 is deleterious) PROVEAN score (CHOI AND CHAN 2015). Images were acquired from UCSC Genome Browser (<http://genome.ucsc.edu/>).

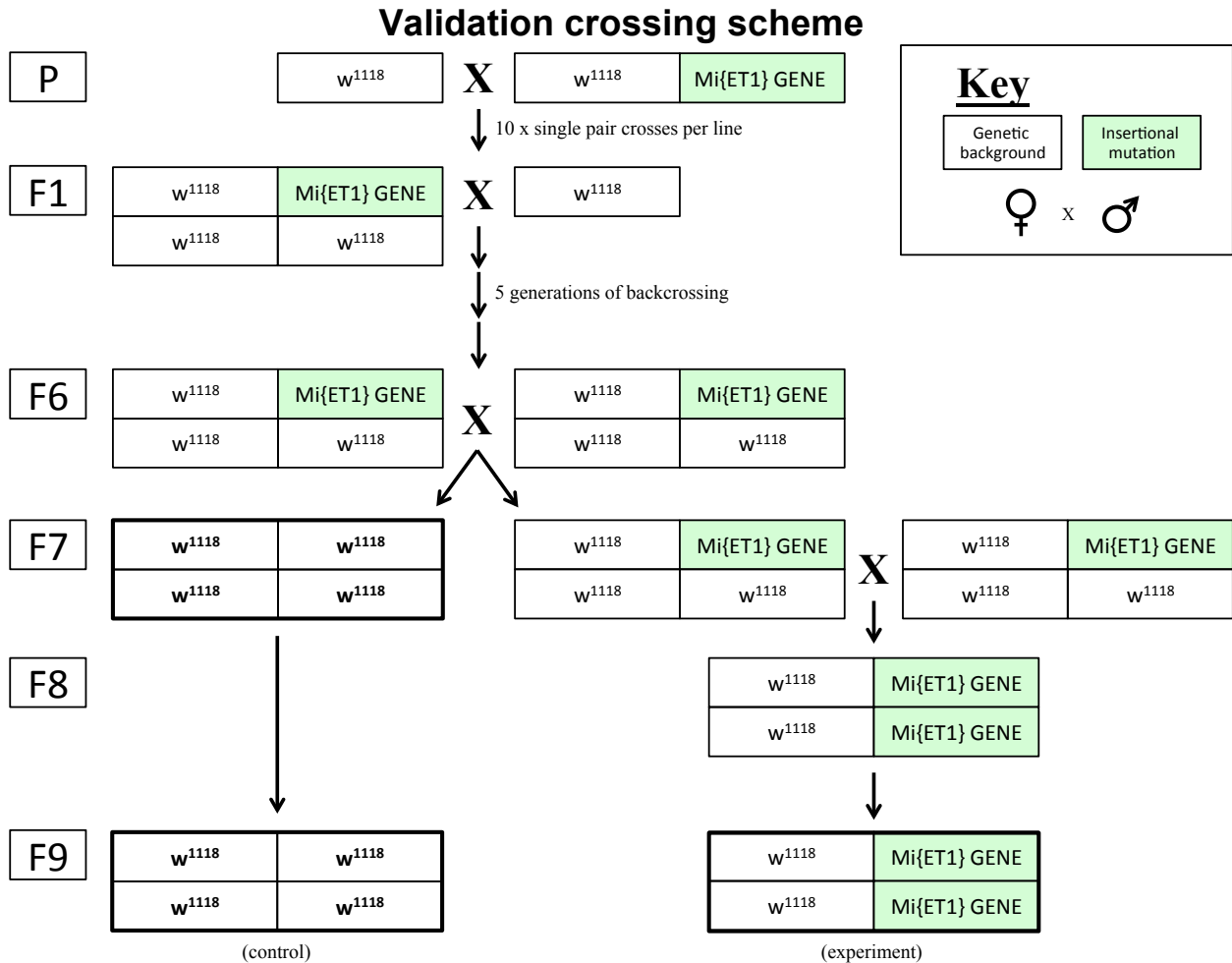


**Figure S7. *Drosophila* crossing scheme used to generate control and experimental lines for candidate gene validation.** All crosses take place between females on the left and males on the right. White boxes represent the background control line, either  $w^{1118}$  (or  $y^{1w67c23}$ ), while green boxes represent the construct. The first generation cross generated females heterozygous for the construct, which were then backcrossed for five consecutive generations to the respective background control line. Isoparental crosses between heterozygotes for the construct were screened for flies without the construct (control) or heterozygous/homozygous for the construct. The latter group was self-crossed within the same vial and the resulting crosses that contained no flies without the reporter were deemed homozygous for the construct (experiment). Both control and experiment lines were maintained for 2 generations to confirm their genotype before testing. Figure reproduced with permission (SPIERER *et al.* 2020).

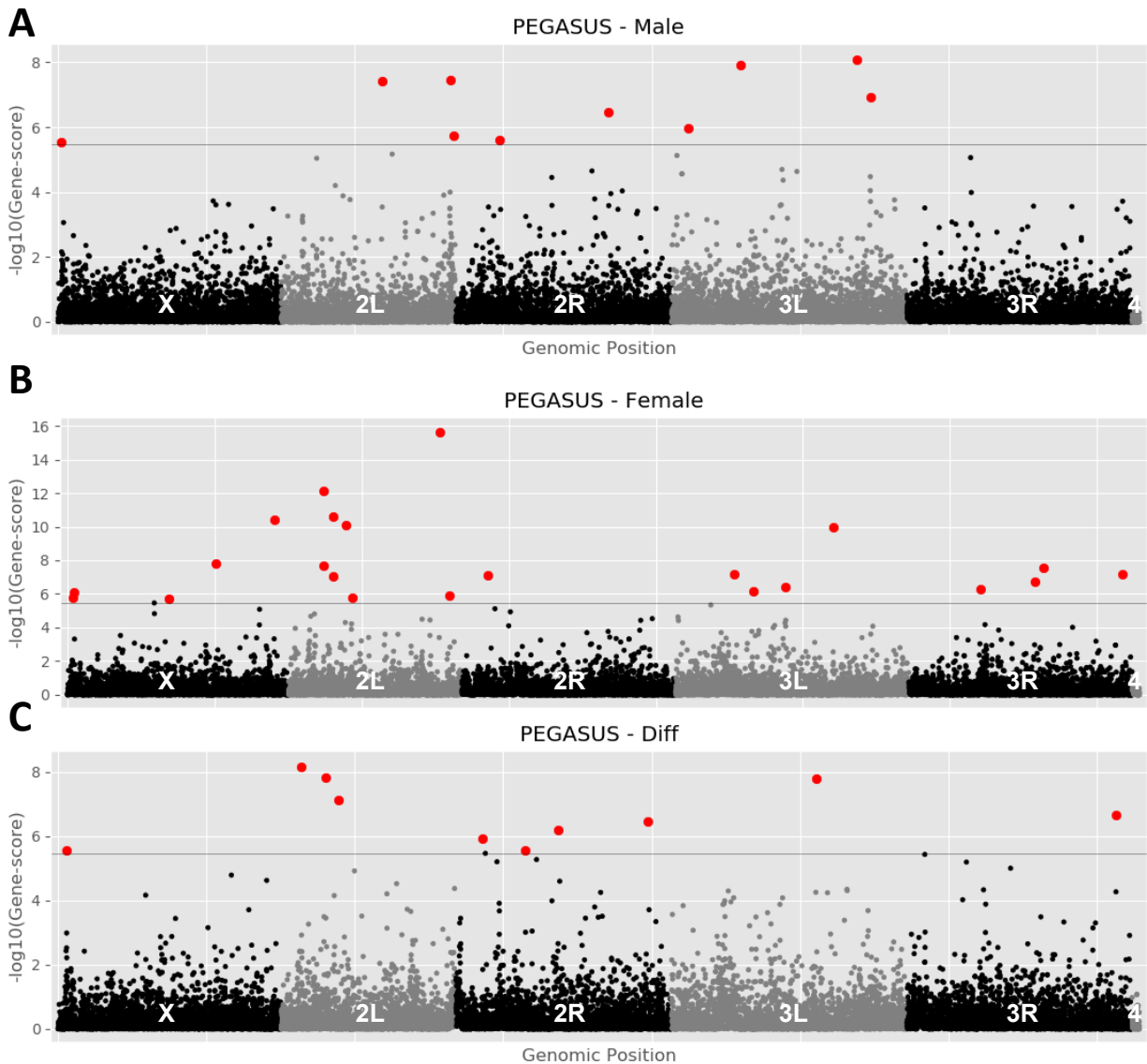


**Figure S8. Several whole genes were identified across each sex-based phenotype using PEGASUS\_flies.** In total, 45 unique genes were found in (A) males, (B) females, (C) and sex-difference. Significant genes (red points) passed the Bonferroni threshold ( $P \leq 3.43 \times 10^{-6}$ ; gray line), while the remaining did not (black and gray). Points are arranged in order of relative position on each chromosome (labeled), and plotted against the  $-\log_{10}$  of their significance score.

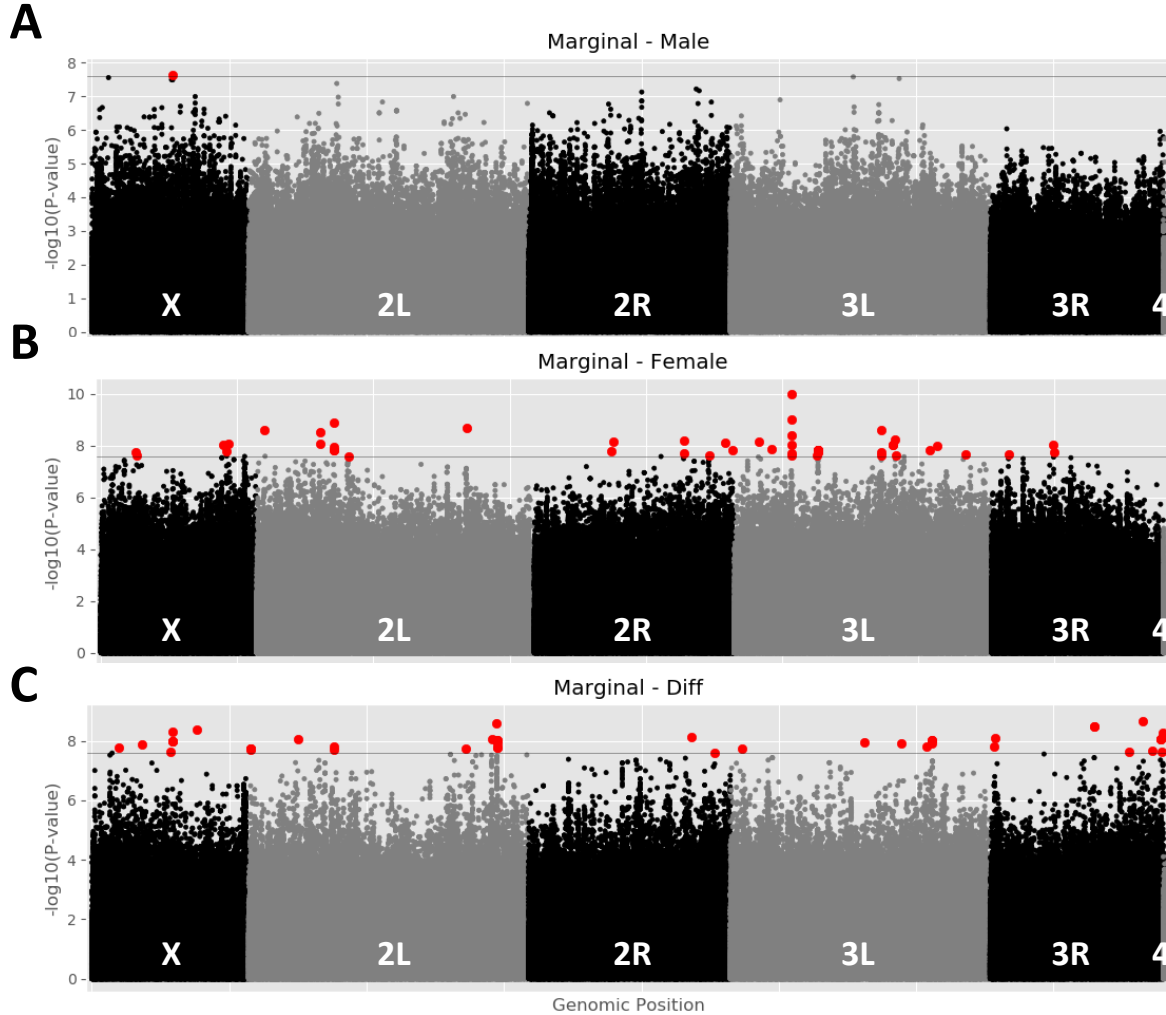


**Figure S9. Significant marginal variants were identified across each sex-based phenotype.** Several marginal variants were identified across the (A) male, (B) female, and (C) sex-difference phenotypes. Significant variants (red) passed a Bonferroni threshold ( $P \leq 2.56 \times 10^{-8}$ ; gray solid line), while those that did not are colored in black or gray. Points are ordered by their relative genomic position and their significance score  $-\log_{10}$  transformed.

## **Chapter 3**

### *Mito-Nuclear Interactions Modify Drosophila Exercise Performance*

Alyson Sujkowski, Adam N. Spierer, Thiviya Rajagopalan, Brian Bazzell,  
Maryam Safdar, Dinko Imsirovic, Robert Arking, David M. Rand, and Robert Wessells

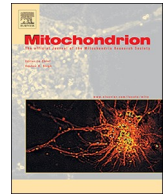
Modified from submission to *Mitochondrion* (2019)



ELSEVIER

Contents lists available at ScienceDirect

## Mitochondrion

journal homepage: [www.elsevier.com/locate/mito](http://www.elsevier.com/locate/mito)Mito-nuclear interactions modify *Drosophila* exercise performanceAlyson Sujkowski<sup>a</sup>, Adam N. Spierer<sup>b</sup>, Thiviya Rajagopalan<sup>a</sup>, Brian Bazzell<sup>a</sup>, Maryam Safdar<sup>a</sup>, Dinko Imsirovic<sup>a</sup>, Robert Arking<sup>c</sup>, David M. Rand<sup>b</sup>, Robert Wessells<sup>a,\*</sup><sup>a</sup> Department of Physiology, Wayne State University, Detroit, MI, United States<sup>b</sup> Department of Ecology and Evolutionary Biology, Brown University, Providence, RI, United States<sup>c</sup> Department of Biological Sciences, Wayne State University, Detroit, MI, United States

## ARTICLE INFO

## Keywords:

*Drosophila*  
Exercise  
Mitochondrial  
Nuclear  
Interaction

## ABSTRACT

Endurance exercise has received increasing attention as a broadly preventative measure against age-related disease and dysfunction. Improvement of mitochondrial quality by enhancement of mitochondrial turnover is thought to be among the important molecular mechanisms underpinning the benefits of exercise. Interactions between the mitochondrial and nuclear genomes are important components of the genetic basis for variation in longevity, fitness and the incidence of disease. Here, we examine the effects of replacing the mitochondrial genome (mtDNA) of several *Drosophila* strains with mtDNA from other strains, or from closely related species, on exercise performance. We find that mitochondria from flies selected for longevity increase the performance of flies from a parental strain. We also find evidence that mitochondria from other strains or species alter exercise performance, with examples of both beneficial and deleterious effects. These findings suggest that both the mitochondrial and nuclear genomes, as well as interactions between the two, contribute significantly to exercise capacity.

## 1. Introduction

Endurance exercise is increasingly recognized as an intervention that profoundly reduces the incidence of multiple important age-related diseases, including cancer, diabetes, and cognitive decline (Cassilhas et al., 2016; Thomas et al., 2017; Zanuso et al., 2017). Despite the pervasive benefits of exercise, the molecular mechanisms driving these effects are only just beginning to be understood. One important mechanism mediating the effects of endurance exercise is thought to be maintenance of mitochondrial integrity and quality (Bo et al., 2010; Kang et al., 2013; Laker et al., 2014b).

Mitochondrial dysfunction increases with age in humans (Dai et al., 2012) and model organisms (Kang et al., 2013; Owusu-Ansah et al., 2013), leading to reduced respiratory function, and increased accumulation of reactive oxygen species (Chan et al., 2010). These deficits have been associated with increased incidence of cardiovascular (Liang and Kobayashi, 2015) and neurodegenerative (Moran et al., 2012) diseases, as well as general metabolic dysfunction (Ziegler et al., 2015).

Endurance training has long been known to stimulate mitochondrial biogenesis (Irrcher et al., 2003). More recently, it has become clear that training also improves mitochondrial quality (Yan et al., 2012), and this improvement is dependent on induction of mitophagy (Venditti et al.,

2013). This mechanism appears to be broadly conserved, as it has been observed in both vertebrate (Booth et al., 2015) and invertebrate (Laker et al., 2014b) models.

Effective mitochondrial activity depends on cooperative function between proteins encoded by the nuclear and mitochondrial genomes (Rand et al., 2004; Tranah, 2011). Coordination between the products of these genomes is essential for proper function under normal conditions, or during stressful conditions such as endurance exercise (Ryan and Hoogenraad, 2007). While endurance exercise has been observed to induce substantial changes to chronic expression of nuclear genes (Coffey and Hawley, 2007; Sujkowski et al., 2015), less is known about the coordination of these changes with the mitochondrial genome.

Substantial individual variation in the response to identical endurance exercise paradigms exists within the human population (Bouchard et al., 2012; Puthuchery et al., 2011) and between strains of model organisms (Britton and Koch, 2001; Mendez et al., 2016). With increasing interest in personalized genomic approaches to medicine, understanding the genetic bases of this individual variation is an important goal. One important source of this variation could be interactions between the mitochondrial and nuclear genomes. Here, we seek to gain greater understanding of the contributions of the mitochondrial and nuclear genomes to exercise adaptation using unique populations

\* Corresponding author.

E-mail address: [rwessell@med.wayne.edu](mailto:rwessell@med.wayne.edu) (R. Wessells).<https://doi.org/10.1016/j.mito.2018.11.005>

Received 2 March 2018; Received in revised form 19 October 2018; Accepted 3 November 2018

1567-7249/ © 2018 Elsevier B.V. and Mitochondria Research Society. All rights reserved.

of “mito-switch” *Drosophila*. These lines harbor mitochondria from exogenous fly lines of three types: (1) a line selected for greater longevity over many generations, (2) different strains of *Drosophila melanogaster*, (3) other species from the *Drosophila* genus.

Using a negative geotaxis-based paradigm for endurance exercise (Piazza et al., 2009a; Tinkerhess et al., 2012a), we assessed the baseline speed, endurance, flight and cardiac performance of wild-type *Drosophila*. We then compared them to flies with an identical nuclear genome, but different mitochondrial genomes (hereafter mitotypes or mtDNAs). We further compared the ability of each combination of mitotype/nucleotype to adapt to 3 weeks of chronic endurance exercise.

We find that mitochondria derived from longevity-selected flies were able to confer substantial performance improvements on their original parental line. Mitochondria from exogenous strains or from other *Drosophila* species had complex and variable effects, with both mitotype and nucleotype having significant effects on most assays. These results are consistent with the ideas that both the mitochondrial and nuclear genomes, as well as interactions between the two, play important roles in determining exercise capacity.

## 2. Materials and methods

### 2.1. *Drosophila* stocks and maintenance

$w^{1118}$  and *OregonR* were obtained from the Bloomington *Drosophila* stock center (BDSC). *Ra*, *La*, *RaLa*<sub>(m)</sub>, and *LaRa*<sub>(m)</sub> were described in (Arking, 1987; Soh et al., 2007). *OreR*<sub>(m)</sub>; *OreR*, *sil*<sub>(m)</sub>; *OreR*, *sm21*<sub>(m)</sub>; *OreR*, *Zim53*<sub>(m)</sub>; *OreR*,  $w^{1118}$ ;  $w^{1118}$ , *sil*<sub>(m)</sub>;  $w^{1118}$ , *sm21*<sub>(m)</sub>;  $w^{1118}$ , *OreR*<sub>(m)</sub>;  $w^{1118}$ , *Zim53*<sub>(m)</sub>;  $w^{1118}$ , and *Zim53*<sub>(m)</sub>; *Zim53*, hereafter referred to as the ‘mitoswitch’ lines, were described in (Zhu et al., 2014). Note that the *RaLa*<sub>(m)</sub> and *LaRa*<sub>(m)</sub> stocks list the nuclear genomes first and the mtDNA (m) second, whereas the ‘mitoswitch lines list the mtDNA (m) first and the nuclear genome second, separated by a semicolon (e.g., *OreR*<sub>(m)</sub>;  $w^{1118}$ ). Flies were cultured and housed on standard 10% sucrose 10% yeast medium at 25 °C, 50% humidity under 12 h light/dark cycle. All stocks were confirmed by PCR to be Wolbachia-free at the time of measurement.

### 2.2. Exercise training

Exercise training was performed as in Piazza et al. (2009a). Briefly, cohorts of at least 880 male flies were collected under light CO<sub>2</sub> anesthesia within 2 h of eclosion and separated into vials of 20. Flies were then further divided into 2 cohorts of at least 440 flies designated “exercised” or “unexercised”. Every morning prior to training, both exercised and unexercised cohorts were flipped onto fresh vials of 10% sucrose, 10% yeast food. Unexercised flies were treated identically to exercised siblings, but had a foam stopper placed low in the vial during exercise training to prevent running while on the exercise apparatus. The exercise device drops the fly vials every 15 s in order to repetitively induce negative geotaxis. Exercised flies are free to run to the top of the vial. A program of gradually increasing daily exercise generates significant improvements in mobility (Damschroder et al., 2018).

### 2.3. Climbing speed

Each day prior to exercise training, flies were assessed for climbing performance using a rapid iterative negative geotaxis (RING) assay as in Gargano et al. (2005). Flies were transferred to individual polypropylene vials in a RING apparatus and allowed to equilibrate for 1 min. Negative geotaxis was elicited by sharply rapping the RING apparatus four times in rapid succession. The positions of the flies were captured in digital images taken 2 s after eliciting the behavior. Images were analyzed using ImageJ (Bethesda, MD). The relative distance climbed by each fly was converted into quadrants using Microsoft Excel. The performance of 20 flies was calculated as the average of four

consecutive trials to generate a single datum. Flies were tested longitudinally 5 times per week for 3–5 weeks to assess decline in negative geotaxis speed with age. Data were further consolidated into pre- and post-training performance normalized to the starting climbing index of each individual cohort. Summary histograms are presented as the average climbing speed of a single cohort during week 1, and after 3 weeks of endurance training. Between assessments, flies were returned to food vials and housed until the following RING test. Statistical tests and modeling are described in *Statistical Analyses*.

### 2.4. Endurance

Climbing endurance was measured using the fatigue assay described previously (Damschroder et al., 2018; Tinkerhess et al., 2012a). At least eight vials of 20 flies from each cohort were subjected to the fatigue assay at two time points. Before exercise, flies are tested once on day 5 of adulthood. The cohort is then split into exercised and unexercised groups and tested again on day 25 of adulthood. For each assessment, the flies were placed on the Power Tower exercise machine and made to climb until they were fatigued, or no longer responded to the negative geotaxis stimulus. Monitored continuously, a vial of flies was visually determined to be “fatigued” when five or fewer flies could climb higher than 1 cm after three consecutive drops. A minimum of 8 vials containing 20 flies each was used for each fatigue assessment with each vial plotted as a single datum. Summary histograms are presented as the average runspan of a single cohort during week 1, and after 3 weeks of endurance training. Each experiment was performed in duplicate or triplicate, and runspans were scored blindly when possible. The time from the start of the assay to the time of fatigue was recorded for each vial, and the data analyzed using log-rank analysis in GraphPad Prism (San Diego, CA, USA). In addition, two-way ANOVA was performed in R (R, 2016) comparing genotype x training and nucleotype x mitotype for exercised and unexercised cohorts for all orthogonal experimental groups. Additional log-rank analyses were performed in Prism. Tables and graphs depict a single, representative cohort.

### 2.5. Pacing

At the conclusion of the training period, 25-day old flies were removed from the study and subjected to electrical pacing as in Wessells et al. (2004). Briefly, flies are placed between two electrodes touching conductive jelly spread over the electrodes and the heart is paced with a square wave stimulator at 40 V and 6 Hz for 30 s. The percentage of fly hearts that responded to pacing with either fibrillation or arrest was recorded as “% failure”. Percent failure is a marker for stress sensitivity and characteristically declines with age (Piazza et al., 2009b; Wessells and Bodmer, 2004). Endurance exercise reduces cardiac failure rate across ages in trained male *Drosophila* (Piazza et al., 2009a; Sujkowski et al., 2015). Pacing experiments were performed in duplicate with  $n \geq 68$  for all pacing experiments. Data were analyzed using chi-squared tests for probabilities with Yates' continuity correction. Tables and graphs depict a single, representative cohort.

### 2.6. Flight performance

Flight analysis was performed on day 25 after training was complete. Flight was analyzed as in Sujkowski et al. (2015). Triplicate cohorts of at least 71 flies were exercise trained in narrow vials housing groups of 20 age-matched siblings. Acrylic sheeting with paintable adhesive was placed in the flight tube, and fly cohorts were ejected into the apparatus to record flight performance and subsequent landing height after release. Fly cohorts were introduced to the flight tester one vial at a time using a gravity-dependent drop tube in order to reduce variability. After a full cohort of flies was captured on the adhesive, the sheeting was removed to a white surface in order to photograph landing height of each fly. Flies with damaged wings were censored from final



analysis to control for mechanical stress not related to training performance. Images were analyzed using ImageJ. Landing height graphs depict mean  $\pm$  SD with Tukey *post-hoc* test between all pairwise comparisons. Asterisks indicate significantly different groups. Tables represent 2-way ANOVA factoring nucleotype  $\times$  training in all genotypes, and mitotype  $\times$  nucleotype in trained and untrained groups separately. Tables and graphs depict a single, representative cohort.

### 2.7. Lysotracker

Similar to cardiac pacing and flight, Lysotracker staining of adult fat bodies was performed as in Sujkowski et al. on day 25 (Sujkowski et al., 2012). Adult flies separated by treatment were dissected, ventral side up, in room temperature PBS. Partially dissected flies with their fat bodies exposed were rinsed  $1\times$  in fresh PBS. Lysotracker green (Molecular Probes, Eugene, OR) was diluted to  $0.01\ \mu\text{M}$  in PBS and applied to dissected preps for 30 s. Samples were washed 3 times in fresh PBS. Stained fat bodies were subsequently removed and mounted in Vectashield reagent (Vector Laboratories, Burlingame, CA, USA). Confocal work was done at the Microscopy, Imaging and Cytometry Resources Core at Wayne State University, School of Medicine on a Zeiss Laser Scanning LSM 780 (Jena, Germany) using a  $40\times$  oil immersion objective. Images were analyzed using ImageJ (Bethesda, MD). 10 samples were analyzed for each sample and duplicate biological cohorts were assessed for each group. Lysotracker graphs depict mean  $\pm$  SEM with Tukey *post-hoc* test between all pairwise comparisons. Asterisks indicate significantly different groups. Tables represent 2-way ANOVA factoring nucleotype  $\times$  training in all genotypes, and mitotype  $\times$  nucleotype in trained and untrained groups separately. Tables and graphs depict a single, representative cohort.

### 2.8. Citrate synthase activity

Triplicate biological replicates of 8 age-matched adult male flies of each genotype were homogenized in  $400\ \mu\text{L}$  ice-cold Cellytic M buffer (Sigma Catalog Number C2978). Protein concentration of each sample was determined using BCA (Pierce BCA Protein Assay Kit (ThermoFisher cat. 23,225) according to manufacturer's protocol with the following modification: The volume of homogenate pipetted from each biological replicate was reduced from  $20\ \mu\text{L}$  to  $5\ \mu\text{L}$  per well in order to stay within range of the standard curve. Sample volumes were adjusted so all had equal protein. Citrate Synthase activity was determined using the assay kit according to protocol (Sigma Catalog number CS0720). Briefly, an assay mix of  $176\ \mu\text{L}$   $1\times$  assay buffer,  $2\ \mu\text{L}$   $10\ \text{mM}$  DNTB,  $2\ \mu\text{L}$   $30\ \text{mM}$  AcCoA and  $10\ \mu\text{L}$  sample was added per well and read on a kinetic program at  $412\ \text{nm}$  every 30 s for 4 min and 30 s to determine baseline.  $10\ \mu\text{L}$   $10\ \text{mM}$  Oxaloacetate (made fresh in  $1\times$  assay buffer) was added to all wells, and the plate was read again as described above. Change in slope was calculated to determine activity/min/mg of total protein.

### 2.9. Statistical analyses

The negative geotaxis (Climbing Speed) data were analyzed using mixed effect models in the R statistical package. The data reported in Table 1 were based on four replicate vials of 20 flies for each genotype. Each vial was quantified for climbing on successive days as repeated measures. While individual flies were not quantified, the proportion of flies in each vial was quantified on successive days, so the vial is the unit of repeated measure. Because there were very few deaths in each vial, this is a more appropriate way to capture variation due to Age than to treat it as a survivorship analysis.

Statistical analyses followed two general three-way models:

Climbing Index  $\sim G + T + A + G\times T + G\times A + T\times A + G\times T\times A + \text{error}$ , where G, T and A are the terms in the model for Genotype, Treatment (Exercised vs. Unexercised) and Age (different days as shown

in Fig. 1), respectively, plus all interaction terms.

We also separated the Nuclear and mtDNA components of Genotype in additional models that were run separately on the Exercised and Unexercised treatments:

Climbing Index  $\sim N + M + A + N\times M + N\times A + M\times A + N\times M\times A + \text{error}$ , where N, M and A are the terms in the model for Nuclear genotype, mtDNA genotype and Age, respectively, plus all interaction terms.

To correct for the autocorrelation structure across the repeated measures of the Age effect in these three-way models, we used the R libraries *car* and *nlme*, and the *gls* and *lme* functions, with the autocorrelation correction as “`correlation = corAR1(form = ~ Age | ReplicateVial)`”. This treats the replicate vials as random effects with a lag time of 1, which captures the successive days of climbing analyses. A unique auto correlation value was estimated for each model and data set using the ACF function in R: `ACF(model, form = ~1 | ReplicateVial)`. The Results were summarized using the `anova(model)` and `Anova(model)` functions, which display F-values and Chi-Square tests, for analyses of variance, and deviance, respectively. The values reported for the analysis of deviance quantify the effects of comparing a fixed effect model to the model with the random effect of replicate vial corrected for autocorrelation. The R scripts describing these analyses are provided in the Supplemental material, and are modified from those reported by S. Mangiafico ([http://rcompanion.org/handbook/I\\_09.html](http://rcompanion.org/handbook/I_09.html)).

Statistical analyses for the data presented in Figs. 3, 6 and 7 followed the same strategy with very similar models. The Ra/La lines are a matched set of genotypes where each mtDNA is represented on each Nuclear genome, so tests of Genotype can be partitioned orthogonally for tests of Nuclear  $\times$  mtDNA interactions.

The mitoswitch lines include 10 genotypes, three of which are original isofemale lines (OreR,  $w^{1118}$  and Zim 53), and the  $w^{1118}$  mtDNA and the Zim53 nuclear genome are not paired with all other genotypes. Thus analyses were of two types: ANOVAs among the 10 Genotypes testing for interactions with Training effects, and ANOVAs for a subset of eight genotypes where four mtDNAs (*D. melanogaster* mtDNA OreR and Zim53, and *D. simulans* mtDNAs *sm21* and *sil*) are each paired with the two nuclear genomes (*D. melanogaster* OreR or  $w^{1118}$ ). For these eight mitonuclear genotypes three-way ANOVAs were possible to test for Nuclear  $\times$  mtDNA  $\times$  Training interactions. Finally, within the eight orthogonal mitoswitch genotypes, two-way ANOVAs were performed separately for the Unexercised and Exercised samples, testing for Nuclear  $\times$  mtDNA interactions.

Mitoswitch lines are analyzed twice in Table 2, once with only one repetition for each type, and another time with multiple repetitions of three groups pooled in the model. Thus, the degrees of freedom for each term does not change between the two analyses, but the total residual DF does. Both analyses gave qualitatively similar results.

For each phenotype, the following models were run in the R statistical package, using the `aov` and `lm` functions, and reporting results using the `summary(model)` and `Anova(model)` commands. Type II sum of squares were reported, but in most cases the data sets were balanced.

For the Ra/La and 10 mitoswitch lines, the following general 2-way model was tested.

Phenotype  $\sim G + T + G\times T + \text{error}$

For the orthogonal Ra/La and 8 mitoswitch lines, the following 3-way model was tested:

Phenotype  $\sim N + M + T + N\times M + N\times T + M\times T + N\times M\times T + \text{error}$

And within either the Unexercised or Exercised samples of flies, the following 2-way model was tested:

Phenotype  $\sim N + M + N\times M + \text{error}$

In these models, G = the term for genotype (i.e., joint mito-nuclear

**Table 1**  
Repeated measures analysis of climbing speed by genotype, training and age.

Ra/La		Analysis of variance			Analysis of Deviance	
Combined	Term in models	DF	F-value	p-value	Chisq	Pr(> Chisq)
	(Intercept)	1	21,709.05	< 0.0001		
	Genotype	3	30.75	< 0.0001	92.24	< 2.2E-16
	Training	1	23.60	< 0.0001	23.60	1.184E-06
	Age	1	1842.70	< 0.0001	1842.70	< 2.2E-16
	Genotype:Training	3	14.99	< 0.0001	44.98	9.344E-10
	Genotype:Age	3	34.56	< 0.0001	103.67	< 2.2E-16
	Training:Age	1	8.35	0.0041	8.35	0.0038662
	Genotype:Training:Age	3	6.46	0.0003	19.37	0.0002298
	Residuals	400				
<b>Unexercised</b>		<b>DF</b>	<b>F-value</b>	<b>p-value</b>	<b>Chisq</b>	<b>Pr(&gt; Chisq)</b>
	(Intercept)	1	9584.20	< 0.0001		
	Nuclear	1	0.01	0.9237	0.01	9.236E-01
	mtDNA	1	99.86	< 0.0001	99.85	< 2.2E-16
	Age	1	1009.07	< 0.0001	1009.07	< 2.2E-16
	Nuclear:mtDNA	1	0.09	0.763	0.09	7.627E-01
	Nuclear:Age	1	5.54	0.0195	5.54	1.855E-02
	mtDNA:Age	1	64.36	< 0.0001	64.36	1.038E-15
	Nuclear:mtDNA:Age	1	10.89	0.0011	10.89	0.0009668
	Residuals	200				
<b>Exercised</b>		<b>DF</b>	<b>F-value</b>	<b>p-value</b>	<b>Chisq</b>	<b>Pr(&gt; Chisq)</b>
	(Intercept)	1	12,346.02	< 0.0001		
	Nuclear	1	23.20	< 0.0001	23.20	1.464E-06
	mtDNA	1	5.15	0.0244	5.14	0.023317
	Age	1	837.15	< 0.0001	837.15	< 2.2E-16
	Nuclear:mtDNA	1	4.69	0.0316	4.69	0.030367
	Nuclear:Age	1	26.95	< 0.0001	26.95	2.09E-07
	mtDNA:Age	1	7.24	0.0077	7.24	7.115E-03
	Nuclear:mtDNA:Age	1	6.59	0.011	6.59	1.023E-02
	Residuals	200				
<b>Percent Change (Fig. 2A)</b>		<b>DF</b>	<b>F-value</b>	<b>Sum Sq</b>	<b>Pr(&gt; F)</b>	
	Nuclear	1	0.44	8.1	0.51	
	mtDNA	1	228.22	4225.8	< 2.2E-16	
	Nuclear:mtDNA	1	80.22	1485.3	1.62E-13	
	Residuals	76		1407.20		
Residual standard error: 4.303 on 76 degrees of freedom						
Multiple R-squared: 0.8025,						
Adjusted R-squared: 0.7947						
F-statistic: 103 on 3 and 76 DF, p-value: < 2.2e-16						
<b>Mitoswitch</b>			<b>Analysis of variance</b>		<b>Analysis of Deviance</b>	
<b>10 Genotypes</b>	<b>Term in models</b>	<b>DF</b>	<b>F-value</b>	<b>p-value</b>	<b>Chisq</b>	<b>Pr(&gt; Chisq)</b>
	(Intercept)	1	25,807.94	< 0.0001		
	Genotype	9	16.45	< 0.0001	157.34	< 2.2E-16
	Training	1	0.88	0.3485	0.88	3.483E-01
	Age	1	2900.16	< 0.0001	2900.16	< 2.2E-16
	Genotype:Training	9	1.31	0.228	11.68	2.322E-01
	Genotype:Age	9	9.70	< 0.0001	87.27	5.725E-15
	Training:Age	1	3.20	0.074	3.19	7.388E-02
	Genotype:Training:Age	9	0.55	0.8362	4.98	8.365E-01
	Residuals	1864				
<b>8 Genotypes</b>		<b>DF</b>	<b>F-value</b>	<b>p-value</b>	<b>Chisq</b>	<b>Pr(&gt; Chisq)</b>
	(Intercept)	1	20,061.80	< 0.0001		
	Genotype	7	19.73	< 0.0001	147.09	< 2.2E-16
	Training	1	0.32	0.5708	0.32	5.707E-01
	Age	1	2224.39	< 0.0001	2224.39	< 2.2E-16
	Genotype:Training	7	1.20	0.2997	8.32	3.053E-01
	Genotype:Age	7	11.98	< 0.0001	83.88	2.217E-15
	Training:Age	1	2.48	0.1156	2.48	1.154E-01
	Genotype:Training:Age	7	0.56	0.7905	3.90	7.907E-01
	Residuals	1488				
<b>Unexercised</b>		<b>DF</b>	<b>F-value</b>	<b>p-value</b>	<b>Chisq</b>	<b>Pr(&gt; Chisq)</b>
	(Intercept)	1	11,351.95	< 0.0001		
	Nuclear	1	42.20	< 0.0001	45.40	1.606E-11
	mtDNA	3	4.03	0.0074	11.09	1.127E-02
	Age	1	1389.44	< 0.0001	1390.81	< 2.2E-16
	Nuclear:mtDNA	3	3.33	0.0193	9.96	1.889E-02
	Nuclear:Age	1	7.90	0.0051	7.76	5.354E-03
	mtDNA:Age	3	6.65	0.0002	19.96	1.730E-04
	Nuclear:mtDNA:Age	3	8.46	< 0.0001	25.38	1.286E-05
	Residuals	744				

(continued on next page)

Table 1 (continued)

Ra/La			Analysis of variance		Analysis of Deviance	
Combined	Term in models	DF	F-value	p-value	Chisq	Pr(> Chisq)
<b>Exercised</b>		<b>DF</b>	<b>F-value</b>	<b>p-value</b>	<b>Chisq</b>	<b>Pr(&gt; Chisq)</b>
	(Intercept)	1	8986.16	< 0.0001		
	Nuclear	1	47.05	< 0.0001	50.14	1.435E-12
	mtDNA	3	5.25	0.0014	16.08	1.090E-03
	Age	1	905.04	< 0.0001	906.61	< 2.2E-16
	Nuclear:mtDNA	3	6.74	0.0002	20.44	1.379E-04
	Nuclear:Age	1	11.16	0.0009	11.18	8.281E-04
	mtDNA:Age	3	4.42	0.0043	13.25	4.119E-03
	Nuclear:mtDNA:Age	3	4.17	0.0061	12.50	5.855E-03
	Residuals	744				
<b>Percent Change (Fig. 2D&amp;E)</b>		<b>DF</b>	<b>F-value</b>	<b>Sum Sq</b>	<b>Pr(&gt; F)</b>	
	Nuclear	1	149.20	1439.8	< 2.2E-16	
	mtDNA	3	130.93	3790.4	< 2.2E-16	
	Nuclear:mtDNA	3	99.53	2881.4	< 2.2E-16	
	Residuals	152		1466.8		

Residual standard error: 3.106 on 152 degrees of freedom  
Multiple R-squared: 0.8469,  
Adjusted R-squared: 0.8398  
F-statistic: 120.1 on 7 and 152 DF, p-value: < 2.2e-16

genotype), T = the term for Training (Unexercised vs. Exercised) and M = the term for mtDNA (either Ra or La mtDNA), or one of the four mtDNAs from *D. melanogaster* or *D. simulans* stated above.

In each case, we test the hypothesis that Genotype, Training regimen, or Nuclear or mtDNA genotype explains significant levels of variation across treatments. Of additional interest is the strength of the interaction terms in these models, as they reflect the consistency, or context-dependence, of the main experimental variables we built in to this overall experiment.

It should be noted that the data in Fig. 3 appear as a time-course of survivorship format, but the data actually represent an attrition profile across 8 replicate vials, due to fatigue over time. As such, the vials were independent and were not treated as repeated measurements. Replicate sets of 8 vials of 20 flies for each genotype and Training treatment were subjected to climbing assays over the course of a given day. When fewer than 5 flies in a vial showed climbing activity, the time that vial was marked as ‘fatigued’ was taken as the response variable. Each ‘curve’ in Fig. 3 has 8 points on it, representing the 8 initial vials and the time each one failed to climb. These time point data were normally distributed across the data set, and were treated as independent data observations in the ANOVAs described above.

ANOVAs are reported in Tables 1 and 2, with the Ra/La lines and mitoswitch lines shown separately. Test results report Sum of Squares (Type II), F-value, and P-value, with the R-squared and associated degrees of freedom.

## 2.10. Data and reagent availability

All raw data and reagents will be made available to other researchers upon request.

## 3. Results

### 3.1. Longitudinal climbing performance

*La* flies are selectively bred for longevity from their parental *Ra* line (Arking, 2001; Arking et al., 2002; Arking et al., 1996). *RaLa*<sub>(m)</sub> and *LaRa*<sub>(m)</sub> flies are reciprocal isogenic lines containing heterologous mitonuclear combinations, with the nucleotide indicated first followed immediately by mitotype, as indicated by the subscript (*m*) (Soh et al., 2007).

*La* flies perform better than *Ra* flies in an acute test of climbing speed measured longitudinally across 5 weeks as reported previously

(2-way ANOVA, genotype effect,  $p < 0.0001$ ) (Fig. 1A) (Piazza et al., 2009a; Sujkowski et al., 2015). In all genotypes, climbing performance declines normally with age, but *Ra* flies respond to exercise with increased climbing speed relative to age-matched, unexercised siblings as previously observed (2-way ANOVA, exercise effect,  $p \leq 0.0273$ ). In contrast, age-matched *La* cohorts receive no further training benefit (Fig. 1A), also observed previously (Sujkowski et al., 2015). *LaRa*<sub>(m)</sub> flies improve negative geotaxis speed in comparison to unexercised controls with exercise training (2-way ANOVA, exercise effect,  $p < 0.0001$ ) (Fig. 1B). Similar to *La* flies, *RaLa*<sub>(m)</sub> lines show a reduced decline in negative geotaxis speed with age, resulting in enhanced climbing speed compared to *Ra* with or without training (2-way ANOVA, genotype effect,  $p < 0.0001$ ) (Fig. 1B, compare 1A to 1B).

The next lines tested were three wild type strains of *D. melanogaster* with their own mtDNA (*Oregon R*,  $w^{1118}$  and *Zimbabwe 53*), as well as additional mito-switched lines with one of several types of mtDNA placed on to the *Oregon R* (*OreR*) or  $w^{1118}$  nuclear chromosomal backgrounds. Mitochondria were either from *D. simulans* (*sil*-from a Hawaii strain, or *sm21*-from strain C167.4 which is the *sil* haplotype) or from *D. melanogaster* (*OreR*,  $w^{1118}$ , or *Zimbabwe*, (*Zim53*)). These lines are notated with the mitotype first, indicated by a subscript (*m*), followed by the nucleotype (Zhu et al., 2014). Both *OreR* and  $w^{1118}$  wild type flies improve negative geotaxis speed across ages with endurance exercise (2-way ANOVA, exercise effect,  $p \leq 0.0030$ ,  $p \leq 0.0280$ , respectively), but *OreR* flies perform comparatively better and decline less rapidly with age than  $w^{1118}$ , independent of training status (2-way ANOVA, genotype effect,  $p < 0.0001$ ) (Fig. 1C).

*OreR* flies with *sil* mitochondria (e.g., *sil*<sub>(m)</sub>;*OreR*) increase negative geotaxis speed across ages with endurance training (2-way ANOVA, exercise effect,  $p \leq 0.0081$ ), but do not reach improvement equivalent to *OreR* with matched mitochondria (2-way ANOVA, exercise effect,  $p < 0.0001$ , genotype effect  $p < 0.0001$ ) (Fig. 1D), *OreR* with *sm21* mitochondria, however, receive no benefit from exercise training, and even become a little slower (2-way ANOVA, exercise effect,  $p \leq 0.0276$ ) (Fig. 1E).  $w^{1118}$  flies with *sil* mitochondria reduce speed with exercise but surpass performance of trained  $w^{1118}$  flies whether exercised or not after day 25 (2-way ANOVA, exercise effect,  $p < 0.0001$ , genotype effect  $p < 0.0001$ ) (Fig. 1F).  $w^{1118}$  flies with *sm21* mitochondria also fail to improve climbing speed with training but resemble untrained  $w^{1118}$  flies at young ages (2-way ANOVA, genotype effect,  $p = 0.2526$ ) and climb slightly better than wild-type untrained flies after day 20 (2-way ANOVA, genotype effect,  $p \leq 0.0471$ ) (Fig. 1G). However,  $w^{1118}$  flies with *OreR* mitochondria respond to exercise with increased speed,

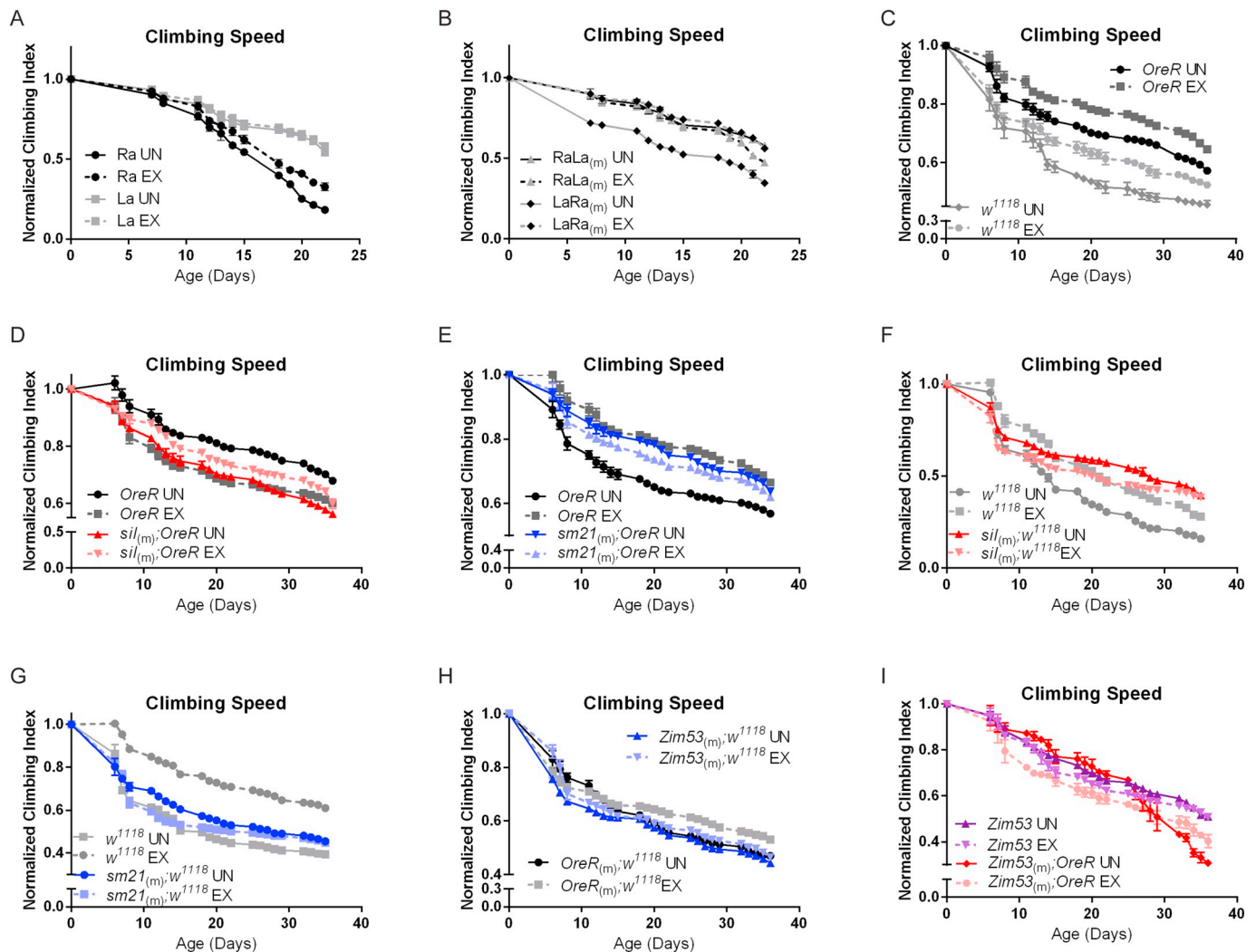


**Fig. 1. Mito-nuclear interactions differentially modulate climbing speed during endurance exercise** (A) Exercised (EX) *Ra* flies are protected against declining negative geotaxis speed with age compared to unexercised (UN) siblings. *La* flies have higher negative geotaxis speed than *Ra*. (B) Exercised *LaRa<sub>(m)</sub>* flies are protected against declining negative geotaxis speed with age compared to unexercised siblings. *RaLa<sub>(m)</sub>* flies have higher negative geotaxis speed than *LaRa<sub>(m)</sub>*. (C) Both exercised *OreR* and *w<sup>1118</sup>* flies are protected against declining negative geotaxis speed and *OreR* flies perform better than *w<sup>1118</sup>* flies whether exercised or not. (D) *sil<sub>(m)</sub>;OreR* flies are protected against declining negative geotaxis speed compared to unexercised siblings, but do not reach performance equal to exercised *OreR* flies. (E) *sm21<sub>(m)</sub>;OreR* flies do not enhance negative geotaxis speed with training, and resemble trained *OreR* lines. (F) *sil<sub>(m)</sub>;w<sup>1118</sup>* lines reduce climbing speed with exercise in weeks 2–4 relative to unexercised siblings, but climb faster than trained *w<sup>1118</sup>* flies after day 25. (G) Exercised *sm21<sub>(m)</sub>;w<sup>1118</sup>* flies reduce climbing speed in weeks 2 and 3 compared to untrained siblings, and perform better than untrained *w<sup>1118</sup>* flies in weeks 3 and 4. Climbing speed does not reach performance of trained *w<sup>1118</sup>* flies with matched nuclear and mtDNA. (H) *OreR<sub>(m)</sub>;w<sup>1118</sup>* flies are protected against declining negative geotaxis speed with age compared to unexercised siblings, but *Zim53<sub>(m)</sub>;w<sup>1118</sup>* lines are not. (I) Unexercised *Zim53<sub>(m)</sub>;OreR* flies have increased climbing speed in the first 3 weeks of adulthood before a rapid decline in performance. Exercised *Zim53<sub>(m)</sub>;OreR* flies climb significantly more slowly than unexercised siblings until week 5. *Zim53* flies do not improve climbing speed with exercise training.  $n \geq 100$  for all climbing experiments. Graphs are representative of a single repetition of at least duplicate cohorts. Error bars indicate SEM. ANOVAs reporting main and interaction effects are presented in Table 1.

similar to *OreR* (2-way ANOVA, exercise effect,  $p \leq 0.0120$ ) (Fig. 1H), while *w<sup>1118</sup>* flies with *Zim53* mitochondria had a modest response to exercise in week 1 only (2-way ANOVA, exercise effect,  $p < 0.0001$ ) (Fig. 1H). Similarly, *Zim53 melanogaster* with their own mtDNA do not improve climbing speed with exercise, indeed performing worse at some individual time points (2-way ANOVA, exercise effect,  $p \leq 0.0478$ ) and *OreR* flies with *Zim53* mitochondria also reduce climbing speed with training (2-way ANOVA, exercise effect,  $p < 0.0001$ ) (Fig. 1I).

In order to better visualize the response to exercise, independent of differences in starting speed or changes with age, we graphed the difference between the speed of exercised and unexercised flies (from Fig. 1) of the same subtype, at both the beginning and end of the exercise protocol. On day 5 of adulthood, *La* flies have higher negative

geotaxis scores in an acute test of climbing speed than age-matched *Ra* flies (ANOVA with Tukey *post-hoc* test,  $p = 0.0014$ ) (Fig. 2A), as previously reported (Piazza et al., 2009a; Sujkowski et al., 2015). Day-5 climbing speed of *RaLa<sub>(m)</sub>* flies is statistically indistinguishable from *La* cohorts of the same age, while *LaRa<sub>(m)</sub>* flies resemble *Ra* cohorts (Fig. 2A). We next subjected *Ra*, *La*, *RaLa<sub>(m)</sub>* and *LaRa<sub>(m)</sub>* flies to our 3-week ramped endurance training protocol (Piazza et al., 2009a; Tinkerhess et al., 2012a). Exercised *Ra* flies increase climbing speed 12% relative to unexercised control *Ra* flies (Fig. 2B). *La* flies, which have a much higher baseline speed, do not gain further additive benefit from training (Fig. 2B). *LaRa<sub>(m)</sub>* flies show greater improvement in climbing speed than *RaLa<sub>(m)</sub>* cohorts after exercise (Fig. 2B).

Thus, the unexercised speed of these lines is strongly predicted by their mitotype, while nucleotype also has a significant effect (Table 1).

**Table 2**  
ANOVAs of Endurance by Genotype and Training.<sup>a</sup>

Ra/La					
Combined	Term in models	DF	Sum Sq	F-value	Pr(> F)
	Genotype	3	741,754	140.68	< 2E-16
	Training	1	102,800	58.49	2.940E-10
	Genotype:Training	3	106,176.00	20.14	5.590E-09
	Residuals	56	98,422.00		
Residual standard error: 41.92 on 56 degrees of freedom Multiple R-squared: 0.9062, Adjusted R-squared: 0.8945 F-statistic: 77.28 on 7 and 56 DF, p-value: < 2.2e-16					
	<b>Term in models</b>	<b>DF</b>	<b>Sum Sq</b>	<b>F-value</b>	<b>Pr(&gt; F)</b>
	Nuclear	1	18,057	10.2739	0.00233
	mtDNA	1	717,197	408.0703	< 2.2E-16
	Training	1	102,800	58.4913	2.94E-10
	Nuclear:mtDNA	1	6500	3.6986	0.05955
	Nuclear:Training	1	3379	1.9223	0.1711
	mtDNA:Training	1	97,266	55.3423	6.05E-10
	Nuclear:mtDNA:Training	1	5532	3.1474	0.08149
	Residuals	98,422	56		
Residual standard error: 41.92 on 56 degrees of freedom Multiple R-squared: 0.9062, Adjusted R-squared: 0.8945					
<b>Unexercised</b>	<b>Term in models</b>	<b>DF</b>	<b>Sum Sq</b>	<b>F-value</b>	<b>Pr(&gt; F)</b>
	Nuclear	1	2907	2.408	0.1319
	mtDNA	1	671,351	556.0972	< 2E-16
	Nuclear:mtDNA	1	20	0.0162	0.8997
	Residuals	28	33,803		
Residual standard error: 34.75 on 28 degrees of freedom Multiple R-squared: 0.9523, Adjusted R-squared: 0.9471 F-statistic: 186.2 on 3 and 28 DF, p-value: < 2.2e-16					
<b>Exercised</b>	<b>Term in models</b>	<b>DF</b>	<b>Sum Sq</b>	<b>F-value</b>	<b>Pr(&gt; F)</b>
	Nuclear	1	18,528	8.0284	0.008445
	mtDNA	1	143,113	62.0122	1.41E-08
	Nuclear:mtDNA	1	12,013	5.2051	0.030326
	Residuals	28	64,619		
Residual standard error: 48.04 on 28 degrees of freedom Multiple R-squared: 0.7288, Adjusted R-squared: 0.6997 F-statistic: 25.08 on 3 and 28 DF, p-value: 4.36e-08					
Mitoswitch					
<sup>a</sup> Single replicate	Term in models	DF	Sum Sq	F-value	Pr(> F)
	Genotype	9	1,970,323	17.65	< 2E-16
	Training	1	122,047	9.8396	0.002082
	Genotype:Training	9	341,335	3.0577	0.002254
	Residuals	140	1,736,515		
Residual standard error: 111.4 on 140 degrees of freedom Multiple R-squared: 0.5836, Adjusted R-squared: 0.5271 F-statistic: 10.33 on 19 and 140 DF, p-value: < 2.2e-16					
	<b>Term in models</b>	<b>DF</b>	<b>Sum Sq</b>	<b>F-value</b>	<b>Pr(&gt; F)</b>
	Genotype	9	2,937,788	25.7026	< 2E-16
	Training	1	297,622	23.4348	2.688E-06
	Genotype:Training	9	408,360	3.5727	0.0004016
	Residuals	188	2,387,600		
Residual standard error: 112.7 on 188 degrees of freedom Multiple R-squared: 0.6041, Adjusted R-squared: 0.5641 F-statistic: 15.1 on 19 and 188 DF, p-value: < 2.2e-16					
<sup>a</sup> Multiple replicate	<b>Term in models</b>	<b>DF</b>	<b>Sum Sq</b>	<b>F-value</b>	<b>Pr(&gt; F)</b>
	Genotype	12	3,003,960	19.8597	< 2.2E-16
	Training	1	297,622	23.6071	2.54E-06
	Genotype:Training	12	435,446	2.8785	0.001167
	Residuals	182	2,294,342		
Residual standard error: 112.3 on 182 degrees of freedom Multiple R-squared: 0.6196,					

(continued on next page)

Table 2 (continued)

Mitoswitch					
<sup>a</sup> Single replicate	Term in models	DF	Sum Sq	F-value	Pr(> F)
Adjusted R-squared: 0.5673 F-statistic: 11.86 on 25 and 182 DF, p-value: < 2.2e-16					
<b>Combined</b>	<b>Term in models</b>	<b>DF</b>	<b>Sum Sq</b>	<b>F-value</b>	<b>Pr(&gt; F)</b>
	Genotype	17	1,260,238	13.2686	2.29E-12
	Training	1	52,124	3.8416	0.05248
	Genotype:Training	7	288,620	3.0388	0.005787
	Residuals	112	1,519,660		
Residual standard error: 116.5 on 112 degrees of freedom Multiple R-squared: 0.513, Adjusted R-squared: 0.4478 F-statistic: 7.866 on 15 and 112 DF, p-value: 8.66e-12					
<b>Combined</b>	<b>Term in models</b>	<b>DF</b>	<b>Sum Sq</b>	<b>F-value</b>	<b>Pr(&gt; F)</b>
	Nuclear	1	1,110,981	81.8801	5.16E-15
	mtDNA	3	30,103	0.7395	0.530637
	Training	1	52,124	3.8416	0.5248
	Nuclear:mtDNA	3	119,154	2.9272	0.036869
	Nuclear:Training	1	245	0.018	0.8934
	mtDNA:Training	3	70,392	1.7293	0.165052
	Nuclear:mtDNA:Training	3	217,983	5.3552	0.001751
	Residuals	112	1,519,660		
Residual standard error: 116.5 on 112 degrees of freedom Multiple R-squared: 0.513, Adjusted R-squared: 0.4478 F-statistic: 7.866 on 15 and 112 DF, p-value: 8.66e-12					
<b>Unexercised</b>	<b>Term in models</b>	<b>DF</b>	<b>Sum Sq</b>	<b>F-value</b>	<b>Pr(&gt; F)</b>
	Nuclear	1	539,123	48.6235	3.83E-09
	mtDNA	3	80,235	2.4121	0.7632
	Nuclear:mtDNA	3	314,700	9.4609	3.75E-05
	Residuals	56	620,912		
Residual standard error: 105.3 on 56 degrees of freedom Multiple R-squared: 0.6007, Adjusted R-squared: 0.5508 F-statistic: 12.03 on 7 and 56 DF, p-value: 2.952e-09					
<b>Exercised</b>	<b>Term in models</b>	<b>DF</b>	<b>Sum Sq</b>	<b>F-value</b>	<b>Pr(&gt; F)</b>
	Nuclear	1	572,103	35.6471	1.70E-07
	mtDNA	3	20,260	0.4208	0.7388
	Nuclear:mtDNA	3	22,437	0.466	0.7072
	Residuals	56	898,748		

Residual standard error: 126.7 on 56 degrees of freedom.

Multiple R-squared: 0.4062, Adjusted R-squared: 0.332.

F-statistic: 5.472 on 7 and 56 DF, p-value: 7.959e-05.

<sup>a</sup> "Single replicate" analysis includes one cohort of 8 vials of each group performed at the same time. <sup>a</sup>"Multiple replicates" model includes all data from single replicate model plus an additional cohort of 8 vials for OreR, Zim53 and  $w^{1118}$  from Fig. 3. See methods for detailed description of statistical models.

Because flies with the *Ra* mitotype increase their speed after training to match the flies with the high-speed *La* mitotype (Figs. 1B, 2B), the effect of mitotype, and the nucleotype/mitotype interaction are only marginally significant after training (Table 1).

For the wild type and mitochondrial introgression strains, day 5 climbing speed was similar with the exception of *Zim53* wild type flies, which have increased negative geotaxis scores in comparison to all groups (ANOVA with Tukey *post-hoc* test,  $p \leq 0.0214$ ) (Fig. 2C). After 3 weeks of endurance exercise, both  $w^{1118}$  and *OreR* flies responded to training with increased climbing speed relative to unexercised control siblings (Fig. 2D, E). In contrast, none of the mitochondrial introgressed lines increased post-training climbing speed in either the  $w^{1118}$  (Fig. 2D) or *OreR* (Fig. 2E) nuclear backgrounds. Thus, the results fall into two classes, with wild-type lines robustly responding to exercise with increased speed, and mitoswitched lines showing a blunted or absent response. This suggests that mito-nuclear compatibility plays an important role in modifying exercise-induced speed increases. Consistent with this observation, the nuclear x mito effect was significant in exercised and unexercised groups (Table 1).

### 3.2. Endurance

Endurance was measured using a fatigue tolerance assay in which flies are placed on the exercise machine in vials of 20 and allowed to run to exhaustion (Tinkerhess et al., 2012a). Vials are scored as fatigued when fewer than 5 flies remain running and data are analyzed similarly to a survival curve, referred to here as "runspan". After 3 weeks of endurance exercise, trained *Ra* flies extended endurance in comparison to unexercised control *Ra* siblings (log-rank,  $p < 0.0001$ ) (Fig. 3A). *La* flies have enhanced post-training runspan whether exercised or not (log-rank, *Ra* UN vs *La* UN,  $p < 0.0001$ , *La* UN vs *La* EX,  $p = 0.6427$ ) (Fig. 3A), as previously observed (Sujkowski et al., 2015). *LaRa<sub>(m)</sub>* flies increase endurance after exercise training (log-rank,  $p < 0.0001$ ) (Fig. 3B) while *RaLa<sub>(m)</sub>* flies have high endurance whether exercised or not (log-rank, *LaRa<sub>(m)</sub>* UN vs *RaLa<sub>(m)</sub>* UN,  $p < 0.0001$ , *RaLa<sub>(m)</sub>* UN vs EX,  $p = 0.6136$ ) (Fig. 3B). Thus, endurance either before or after exercise correlates strongly with the mitotype in these lines (Table 2), although the nucleotype also becomes significant in the exercised cohorts (Table 2).

*OreR*,  $w^{1118}$  and *Zim53* flies with matched nuclear and mitochondrial DNA increase endurance after exercise training relative to age-matched, unexercised siblings (Fig. 3C, E, F, G, I). When *sm21* or *sil*

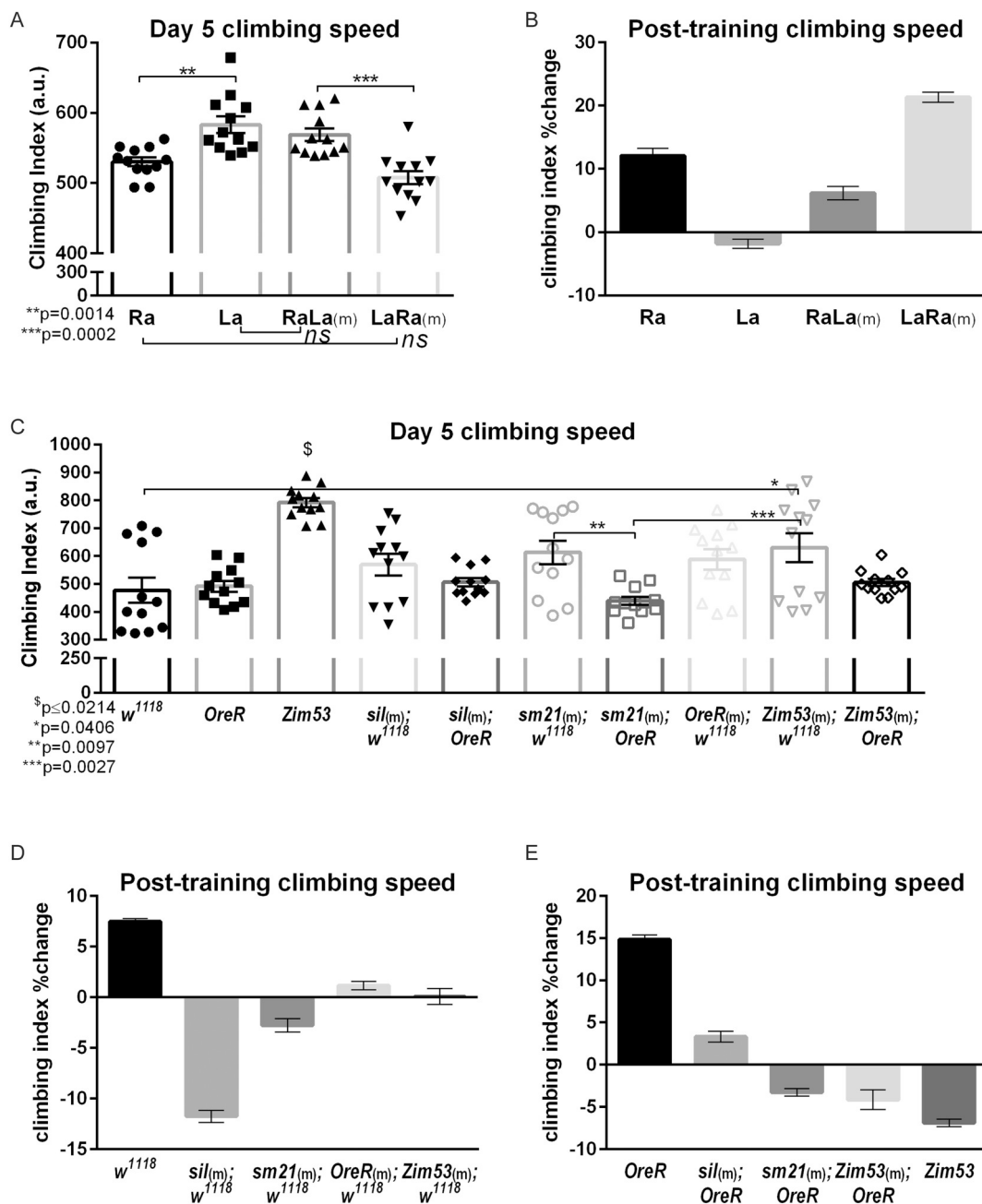


**Fig. 2. Acute climbing speed is affected by both nuclear and mitochondrial genotype in *Drosophila*** (A) *La* flies have higher climbing index in comparison to the parental *Ra* line at day 5 of adulthood. *RaLa*<sub>(m)</sub> flies have higher climbing index relative to *LaRa*<sub>(m)</sub> flies and perform similarly to *La* flies. *LaRa*<sub>(m)</sub> and *Ra* flies climb with similar speed ( $p = 0.3361$ ). (B) After exercise training, *Ra*, *RaLa*<sub>(m)</sub> and *LaRa*<sub>(m)</sub> flies all improve climbing speed in comparison to untrained control siblings. (C) At day 5 of adulthood, *w*<sup>1118</sup>, *OreR*, *sil*<sub>(m);w<sup>1118</sup>, *sil*<sub>(m);OreR</sub>, *sm21*<sub>(m);w<sup>1118</sup>, *sm21*<sub>(m);OreR</sub>, *OreR*<sub>(m);w<sup>1118</sup>, and *Zim53*<sub>(m);OreR</sub> lines climb with similar performance ( $p = 0.2320$ ), but *Zim53* climbing index is enhanced in comparison to each group. Additional statistically significant pairwise comparisons are indicated with brackets. Following endurance exercise, only *w*<sup>1118</sup> (D) and *OreR* (E) increase climbing speed across ages relative to untrained siblings.  $n \geq 100$  for all negative geotaxis experiments. Graphs are representative of a single repetition of at least duplicate cohorts for all experiments presented in the manuscript. Error bars indicate SEM. ANOVAs reporting main and interaction effects are presented in Table 1.</sub></sub></sub>

mitochondria are introduced into flies with *OreR* or *w*<sup>1118</sup> nucleotide, the exercise response was severely blunted (Fig. 3D–G). Flies with *w*<sup>1118</sup> nucleotide and *OreR* mitotype had baseline endurance similar to *OreR*, but did not improve with exercise (Fig. 3H). Flies with *w*<sup>1118</sup> nucleotide and *Zim53* mitotype responded to exercise with improved endurance (log-rank,  $p = 0.0094$ ), but both pre- and post-exercise endurance were similar to *w*<sup>1118</sup> and much lower than *Zim53* alone (compare Fig. 3H to 3C and I). By contrast, flies with *OreR* mitotype and *Zim53* mitotype had high endurance, similar to the parental *Zim53*, but did not improve with exercise, even showing reduced endurance after training (log-rank,

$p = 0.0090$ ) (Fig. 3I). The overall effect of nucleotide on endurance was much stronger than that of mitotype in the mitoswitch group (Table 2).

To better visualize exercise response independent of baseline endurance, we graphed the difference between maximum endurance of each line, before or after a three-week training program. The mitotype strongly predicted the endurance and the strength of the exercise effect in the closely related *Ra La* group (Fig. 4A, B), but nucleotide was a better predictor of endurance in the more divergent mitoswitch group (Fig. 4 C–E). This is likely due to the complex interaction between

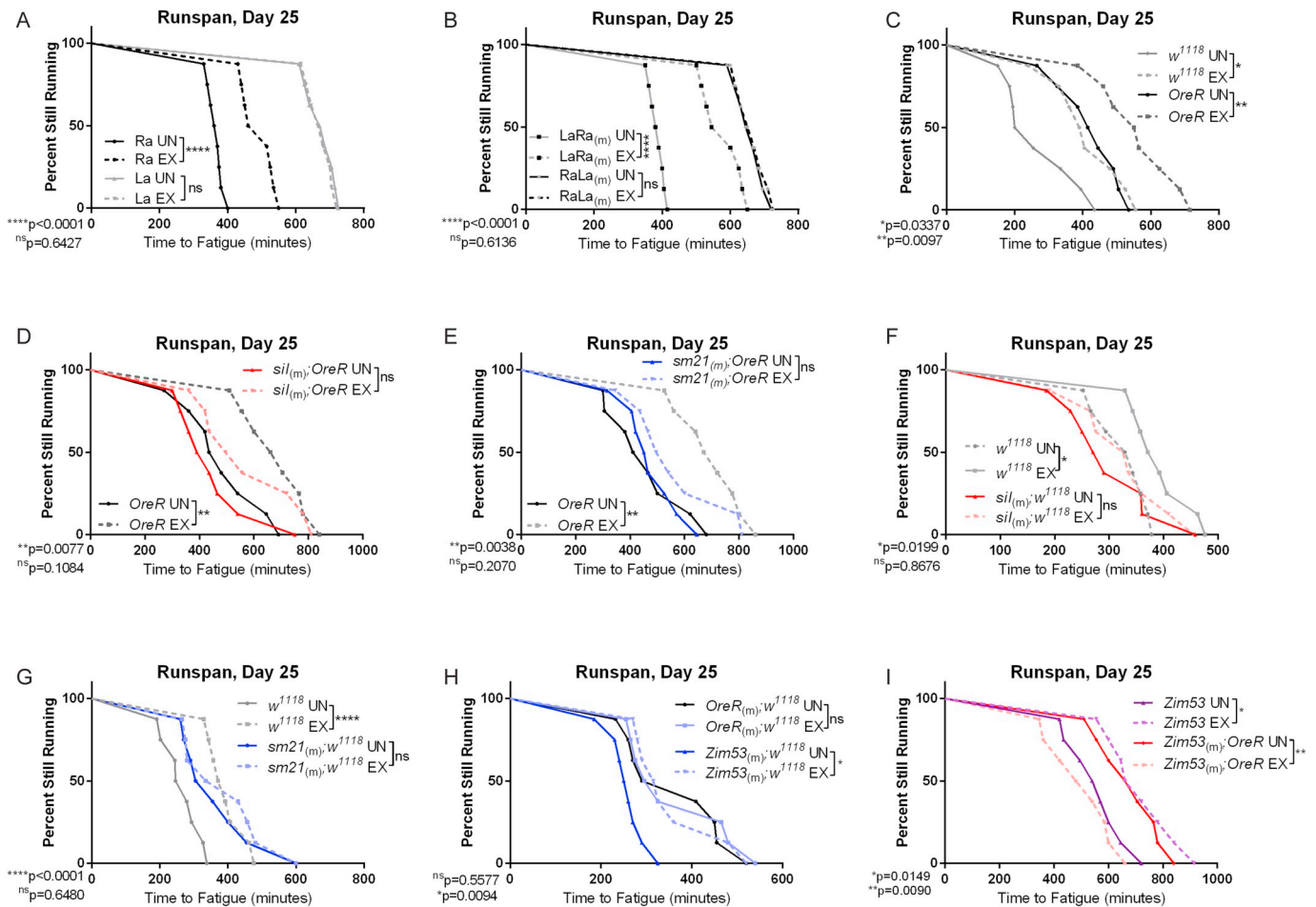


**Fig. 3. Exercise training increases endurance in *Drosophila* with matched nuclear and mitochondrial genotypes** (A) *Ra* flies increase endurance after exercise (EX) training. *La* flies have increased endurance in comparison to trained and untrained (UN) parental *Ra* flies, but do not receive further benefit from exercise. (B) *LaRa*<sub>(m)</sub> flies increase endurance after exercise training, while *RaLa*<sub>(m)</sub> flies have enhanced endurance independent of training status. (C) *w*<sup>1118</sup> and *OreR* flies have better endurance after exercise training, and untrained *OreR* flies have higher runspan than untrained *w*<sup>1118</sup> flies ( $p = 0.0103$ ), and trained *OreR* flies outperform trained *w*<sup>1118</sup> cohorts ( $p = 0.0150$ ). Neither *sil*<sub>(m);*OreR*</sub> (D) nor *sm21*<sub>(m);*OreR*</sub> (E) increase endurance with exercise training like *OreR* flies with matched nuclear and mtDNA. Similarly, *sil*<sub>(m);*w*<sup>1118</sup></sub> (F) and *sm21*<sub>(m);*w*<sup>1118</sup></sub> (G) do not improve endurance with exercise training like *w*<sup>1118</sup> flies (F,G). (H) *Zim53*<sub>(m);*w*<sup>1118</sup></sub> lines improve endurance with exercise training, but *OreR*<sub>(m);*w*<sup>1118</sup></sub> flies do not. (I) Untrained *Zim53*<sub>(m);*OreR*</sub> flies have greater endurance than trained siblings, but exercised *Zim53* flies improve endurance after exercise.  $n = 8$  vials of 20 flies for all endurance experiments. Graphs are representative of a single repetition of at least duplicate cohorts.  $p$ -values are determined by log-rank. ANOVAs reporting main and interaction effects are presented in Table 2.

mitotype and exercise, where some mitotypes appear deleterious and others appear beneficial. Taken together, these results suggest that both mitotype and nucleotype play important roles in modifying endurance during training, and the relative strength of each role is context dependent.

### 3.3. Cardiac performance

We have previously established that endurance exercise reduces cardiac failure in response to external electrical pacing (Piazza et al., 2009a; Sujkowski et al., 2015). External pacing is a cardiac stress assay that paces *Drosophila* hearts to twice their normal heart rate, then measures the percentage of flies that undergo arrest (Wessells and Bodmer, 2004), a phenotype that is highly age-dependent (Wessells et al., 2004) and acts as a marker for overall cardiac health. Failure rate in *OreR* and *w*<sup>1118</sup> flies is normal at day 25 of adulthood. Endurance exercise exerts a protective effect on both lines, reducing the percentage of cardiac failure rate in response to external pacing (Fig. 5A–D).

Flies with mitochondrial genotypes derived from *D. simulans* had varied responses to cardiac pacing following endurance exercise. *sil*<sub>(m);*OreR*</sub> flies did not improve cardiac performance with exercise training (Fig. 5A, Chi-squared = 0.1418,  $p = 0.706479$ ) Only

*sm21*<sub>(m);*OreR*</sub> flies reduced pacing-induced cardiac failure after exercise training. (Fig. 5B, Chi-squared = 13.7221,  $p = 0.0002$ ). Cardiac failure in *sil*<sub>(m);*w*<sup>1118</sup></sub> flies was higher than average independent of training status (Fig. 5C, Chi-squared = 5.6004,  $p = 0.0179$ ). *sm21*<sub>(m);*w*<sup>1118</sup></sub> did not receive any cardiac benefit from endurance exercise, but had baseline cardiac performance that resembled trained *w*<sup>1118</sup> control siblings whether exercised or not (Fig. 5D, Chi-squared = 0.2197,  $p = 0.6329$ ).

In contrast, flies with mitochondrial genotypes derived from *D. melanogaster* strains retained cardiac protection conferred by endurance training. Both *OreR*<sub>(m);*w*<sup>1118</sup></sub> and *Zim53*<sub>(m);*w*<sup>1118</sup></sub> lines reduced cardiac failure in response to pacing stress after exercise, (Chi-squared = 20.1719,  $p < 0.0001$ , Chi-squared = 5.7736,  $p = 0.0162$ , respectively). *Zim53* flies have a lower-than-average failure rate at day 25 of adulthood, and do not derive further benefit from exercise (Fig. 5F, compare to *OreR*, *w*<sup>1118</sup> EX) (*Zim53* UN vs *OreR* EX: Chi-squared = 0.1479,  $p = 0.7005$ , vs *w*<sup>1118</sup> EX: Chi-squared = 0.1841,  $p = 0.6679$ ) and *Zim53*<sub>(m);*OreR*</sub> have low cardiac failure rate whether exercised or not. (Fig. 5F, compare to *OreR*, *w*<sup>1118</sup> EX) (*Zim53*<sub>(m);*OreR*</sub> UN vs *OreR* EX: Chi-squared = 0.4705,  $p = 0.4927$ , vs *w*<sup>1118</sup> EX: Chi-squared = 3.5733,  $p = 0.0587$ ).

When considered across all lines tested in Fig. 5, both nucleotype



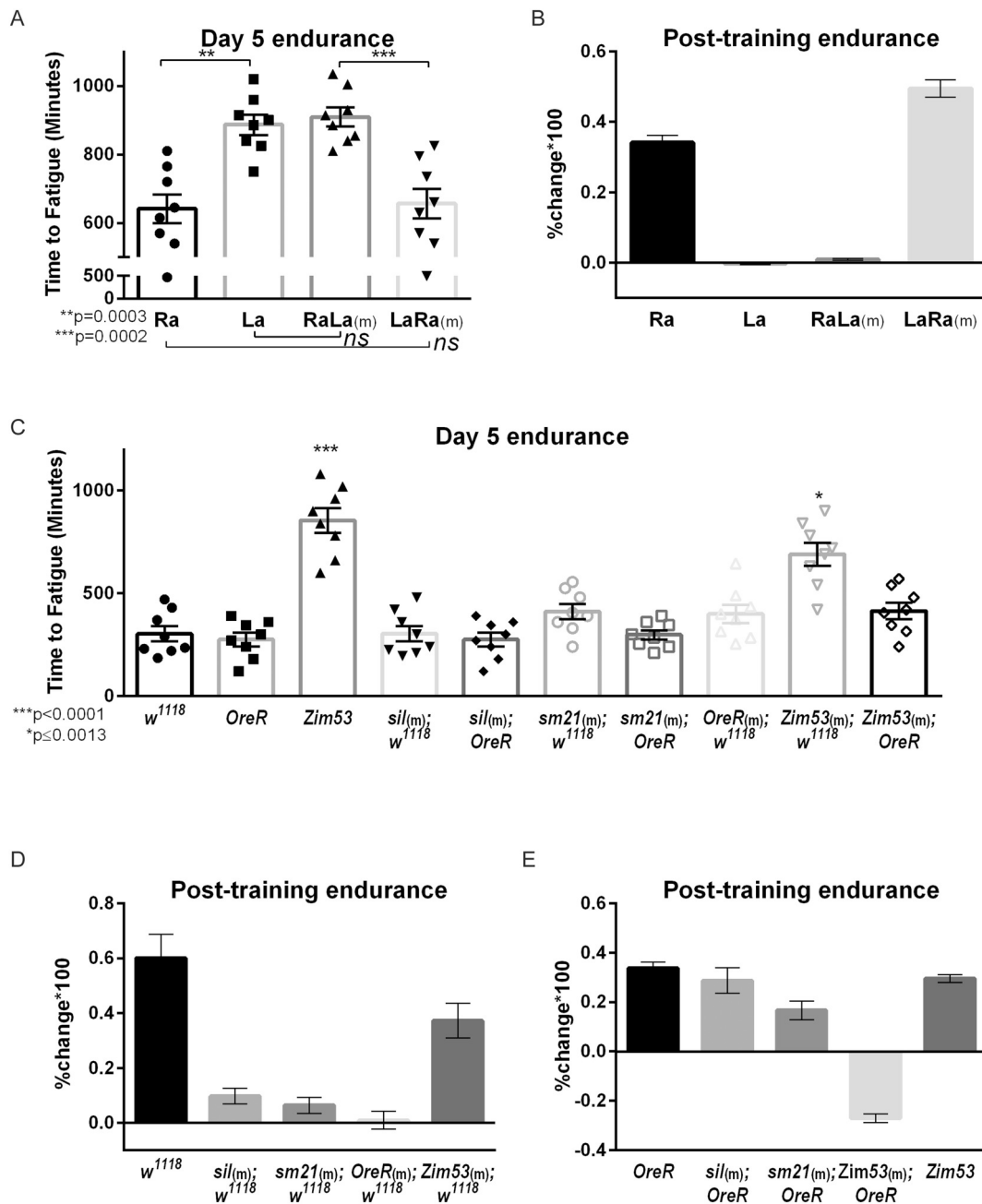


**Fig. 4. Exercise increases endurance independent of mito-nuclear mismatch** (A) *La* flies have increased endurance in comparison to the parental *Ra* line at day 5 of adulthood. *RaLa*(m) flies have better endurance than *LaRa*(m) flies and perform similarly to *La* flies ( $p = 0.9707$ ). *LaRa*(m) and *Ra* flies have equivalent endurance ( $p = 0.9909$ ). (B) After exercise training, *Ra* and *LaRa*(m) flies improve endurance compared to untrained cohorts. (C) At day 5 of adulthood, *w*<sup>1118</sup>, *OreR*, *sil*(m);*w*<sup>1118</sup>, *sil*(m);*OreR*, *sm21*(m);*w*<sup>1118</sup>, *sm21*(m);*OreR*, *OreR*(m);*w*<sup>1118</sup>, and *Zim53*(m);*OreR* lines have similar endurance ( $p = 0.1140$ ), but *Zim53*(m);*w*<sup>1118</sup> and *Zim53* have comparatively better endurance. Following endurance exercise, the majority of *w*<sup>1118</sup> (D) and *OreR* mitotypes (E) increase endurance in comparison to unexercised siblings, with the exception of *OreR*(m);*w*<sup>1118</sup> (D) and *Zim53*(m);*OreR* (E).  $n = 8$  vials of 20 for all endurance experiments. Graphs are representative of a single repetition of at least duplicate cohorts for all experiments presented in the manuscript. Error bars indicate SEM.

and mitotype had highly significant effects on cardiac pacing response (Table 3). The nucleotide had a stronger effect on post-training pacing response, although mitotype was also significant (Table 3). In general, these mitonuclear epistatic interactions are genotype-dependent. For example, the *sm21* mtDNA is responsive to training in the *OreR* nuclear background but not in the *w*<sup>1118</sup> nuclear background (Fig. 5B and D), but either of the *D. melanogaster* mtDNAs are responsive to training in the *w*<sup>1118</sup> nuclear background (Fig. 5E).

### 3.4. Flight performance

We have previously established that endurance training significantly improves flight index in wild-type *Drosophila* (Sujkowski et al., 2015). Both *OreR* and *w*<sup>1118</sup> lines increase flight performance with exercise training (Fig. 6A–D). Although *sil* mitotype flies in the *OreR* background do not improve landing height with exercise (Fig. 6A), *sil* mitotype flies in the *w*<sup>1118</sup> nuclear background have increased flight performance compared to the *w*<sup>1118</sup> nucleotide in both unexercised (ANOVA with Tukey *post-hoc* test,  $p = 0.0002$ ) and exercised (ANOVA with Tukey *post-hoc* test,  $p < 0.0001$ ) groups

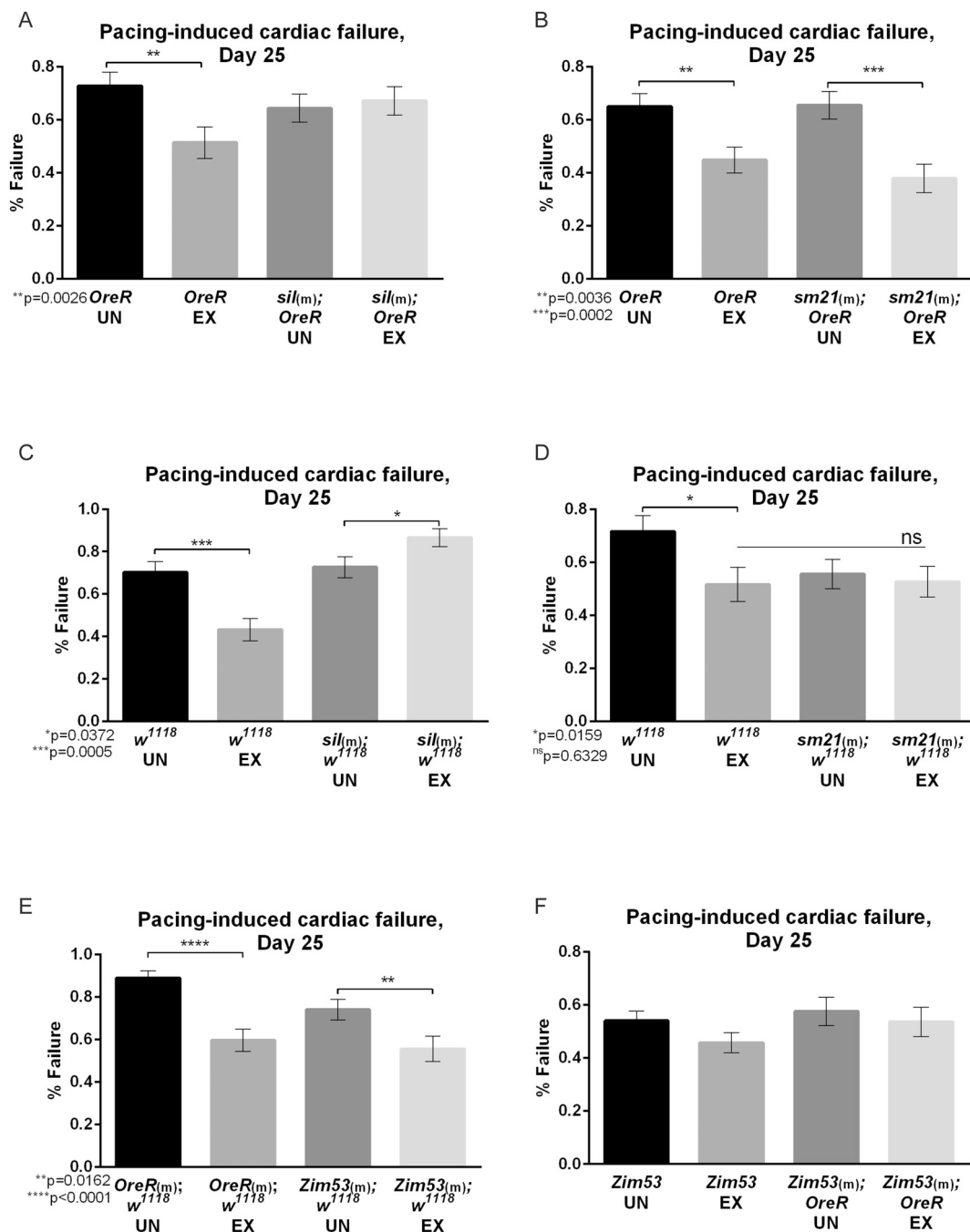


**Fig. 5. Mito-nuclear incompatibility negatively impacts cardiac health** (A) Exercise (EX) significantly reduces pacing-induced cardiac failure in *OreR* and *sm21(m);OreR* flies (B) in comparison to age-matched unexercised (UN) siblings, but *sil(m);OreR* flies (A) do not receive cardiac benefits from endurance exercise. (C) *sil(m);w<sup>1118</sup>* flies do not receive cardiac protection from endurance training and have unusually high pacing-induced cardiac failure rate. (D) *sm21(m);w<sup>1118</sup>* flies had significantly less cardiac failure than age-matched unexercised *w<sup>1118</sup>* flies whether exercised or not. Exercised *w<sup>1118</sup>* flies received cardiac protection from pacing-stress post-training (C, D). (E) Both *OreR(m);w<sup>1118</sup>* and *Zim53(m);w<sup>1118</sup>* flies had reduced cardiac failure compared to age-matched unexercised siblings and (F) *Zim53* and *Zim53(m);OreR* flies had low cardiac failure in response to pacing whether exercised or not.  $n \geq 67$  for all pacing experiments. Graphs are representative of a single repetition of at least duplicate cohorts.  $p$ -values generated by Chi-squared analysis, error bars indicate SEM. ANOVAs reporting main and interaction effects are presented in Table 3.

(Fig. 6C). Flies with the *sm21* mitotype fail to adapt to exercise training with increased landing height in either the *OreR* or *w<sup>1118</sup>* nuclear background (Fig. 6B, D). Neither *OreR(m);w<sup>1118</sup>* nor *Zim53(m);w<sup>1118</sup>* flies increase flight with exercise training (Fig. 6E). *Zim53* lines have strong, exercise-independent flight performance, and *Zim53(m);OreR* flies improve flight performance with exercise (Fig. 6F, ANOVA with Tukey *post-hoc* test,  $p < 0.0001$ ).

When mitoswitch groups were considered together, both nucleotype

and mitotype were significant, although the interaction (nucleotype-by-mitotype) was highly significant only in post-training flight (Table 3).

### 3.5. Lysosomal activity

Exercise training increases Lysotracker staining in adipose tissue of wild-type male flies (Sujkowski et al., 2015; Sujkowski et al., 2012). *sil(m);OreR*, *sm21(m);w<sup>1118</sup>* and *sil(m);w<sup>1118</sup>* do not increase fat body

**Table 3**  
Post-training assessment.

Pacing		Degrees of freedom	Chi-squared	n	P-value
Unexercised	Nucleotype	2	28.914	≥ 149	< 0.0001
	Mitotype	4	50.051		< 0.0001
Exercised	Nucleotype	2	23.799	≥ 79	< 0.0001
	Mitotype	4	30.802		< 0.0001
	Nucleotype	2	8.2195	≥ 72	< 0.0001
	Mitotype	4	43.839		0.01641

Flight		Degrees of freedom	Sum of squares	F-value	n
Pr(> F)					
0.5660228	Nuclear	1	202	0.3295	≥ 149
0.0045025	mtDNA	3	8028	4.3719	
	Training	1	20,947	34.2248	
	6.022E-09				
	Nuclear:m-tDNA	3	14,604	7.9535	
	2.913E-05				
	Nuclear:T-training	1	8534	13.9434	
	0.0001955				
mtDNA;Training	3	8348	4.5462	0.0035343	
Nu:mtDNA:Train	3	5976	3.2548	0.029496	
Residuals	1495	915,024			
Residuals: Sum of Squares: 915024					
Residual standard error: 24.74 on 1495 degrees of freedom					
Multiple R-squared: 0.06828, Adjusted R-squared: 0.05893					
F-statistic: 7.304 on 15 and 1495 DF, p-value: 8.681e-16					

Unexercised		Degrees of freedom	Sum of squares	F-value	n
Pr(> F)					
0.007478	Nucleotype	1	3425	7.1972	≥ 78
	Mitotype	3	6821	4.7787	
	0.002647				
Interaction	3	2712	1.9001	0.12208	
Residuals: Sum of Squares: 325936					
Residual standard error: 21.81 on 685 degrees of freedom					
Multiple R-squared: 0.03759, Adjusted R-squared: 0.02775					
F-statistic: 3.822 on 7 and 685 DF, p-value: 0.0004379					

Exercised		Degrees of freedom	Sum of squares	F-value	n
Pr(> F)					
0.004624	Nucleotype	1	5389	7.4103	≥ 71
	0.006624				
	Mitotype	3	9529	4.3676	
Interaction	3	17,868	8.1895	2.249E-05	
Residuals: Sum of Squares: 589088					
Residual standard error: 26.97 on 810 degrees of freedom					
Multiple R-squared: 0.05226, Adjusted R-squared: 0.04407					
F-statistic: 6.38 on 7 and 810 DF, p-value: 2.546e-07					

Lysotracker		Degrees of freedom	Sum of squares	F-value	n
Pr(> F)					
8.210E-12	Genotype	9	937.19	9.5159	20
1.011E-08	Training	1	395.15	36.1096	
< 2.2E-16	Interaction	9	1660.08	16.8558	

(continued on next page)

Table 3 (continued)

Lysotracker	Degrees of freedom	Sum of squares	F-value	n
Pr(> F)				
Residuals: Sum of Squares: 1969.73 Residual standard error: 3.308 on 180 degrees of freedom Multiple R-squared: 0.603, Adjusted R-squared: 0.5611 F-statistic: 14.39 on 19 and 180 DF, p-value: < 2.2e-16				
Unexercised	Degrees of freedom	Sum of squares	F-value	n
Pr(> F)				
0.02299	Nucleotype	1	44.88	10
6.457E-11	Mitotype	3	601.99	24.1345
2.939E-05	Interaction	3	231.09	9.2646
Residuals: Sum of Squares: 1718.27 Residual standard error: 3.454 on 144 degrees of freedom Multiple R-squared: 0.5799, Adjusted R-squared: 0.5361 F-statistic: 13.25 on 15 and 144 DF, p-value: < 2.2e-16				
Exercised	Degrees of freedom	Sum of squares	F-value	n
Pr(> F)				
0.0489765	Nucleotype	1	62.37	10
0.0002306	Mitotype	3	342.72	7.3464
4.649E-09	Interaction	3	870.84	18.6667
Residuals: Sum of Squares: 598.63 Residual standard error: 2.883 on 72 degrees of freedom Multiple R-squared: 0.5946, Adjusted R-squared: 0.5552 F-statistic: 15.09 on 7 and 72 DF, p-value: 5.763e-12				

lysosomal activity after exercise training as seen in exercised *OreR* and *w<sup>1118</sup>* flies with matched nuclear and mtDNA (Fig. 7A–C). Exercise-trained *sm21<sub>(m);w<sup>1118</sup></sub>* flies, however, upregulate fat body Lysotracker normally (Fig. 7D, ANOVA with Tukey *post-hoc* test,  $p = 0.0007$ ). *OreR<sub>(m);w<sup>1118</sup></sub>* have low fat body Lysotracker staining, and *Zim53<sub>(m);w<sup>1118</sup></sub>* flies also show atypical Lysotracker staining (Fig. 7G). *Zim53* and *Zim53<sub>(m);OreR</sub>* lines have low Lysotracker staining in adipose tissue whether or not they are exercise trained (Fig. 7F). Both mitotype and nucleotype had significant effects on Lysotracker staining, although mitotype was much stronger (Table 3).

### 3.5.1. Mitochondrial function

Because the effect of mitotype is strongest in the closely related *Ra* and *La* lines, we examined mitochondrial function in these lines before and after exercise. We were unable to detect significant differences that tracked with performance in pairwise comparisons for either ATP production, mtDNA/nuclear DNA ratio or in Complex II activity of isolated mitochondria (Supplemental Tables S1–S3). However, we found a strong difference in whole-fly citrate synthase activity between *Ra* and *La* mitotypes (Fig. 8). This difference was independent of nucleotype and was affected by training only in the *Ra* mitotype (Fig. 8), paralleling the climbing speed and endurance results (Figs. 1, 3).

Citrate synthase activity reflects increased TCA cycle activity and has been previously shown to increase in trained muscle of mammals (Ferreira et al., 2010; Li et al., 2011), without necessarily increasing mitochondrial number (Vigelson et al., 2014). Therefore, it seems plausible that increased citrate synthase activity in the *La* mitotype may have functional significance to the increased endurance of flies carrying this mitotype. Future work will be necessary to uncover the molecular

mechanism by which the activity of this nuclear-encoded enzyme is modified by mitotype.

In summary, mitotype played its strongest role in the closely related *Ra* and *La* lines, but was also significant in the more divergent mitoswitch lines. Among the more divergent lines, the *D. melanogaster* *Zim53* and *D. simulans sil* mitotypes demonstrate a clear influence on performance that the *D. simulans sm21* mitotype does not, despite the fact that *Zim53* and *sil* come from different species and *sm21* and *sil* are more similar in mtDNA sequence. This suggests that specific sequences within the mtDNA are likely to be important, as degree of divergence by itself does not fully explain the observed mitonuclear interactions. The upregulation of citrate synthase activity in a high-performance mitotype suggests that upregulation of TCA cycle activity is likely to be a key downstream effect of the relevant mtDNA sequences.

## 4. Discussion

### 4.1. Mitochondria and exercise training

Recent findings in several organisms, including humans (Irrcher et al., 2003; Powers et al., 2014; Yan et al., 2012), mice (Lantier et al., 2014; Lira et al., 2013; Matsakas et al., 2010), *Drosophila* (Laker et al., 2014b; Piazza et al., 2009a) and *C. elegans* (Laranjeiro et al., 2017; Restif et al., 2014) have supported the idea that chronic endurance exercise increases mitochondrial health. It has been previously observed that strains with nucleotype and mitotype derived from different progenitor strains have profound alterations in the dietary effects on longevity and development time in *Drosophila* (Mossman et al., 2016; Zhu et al., 2014) and on metabolism and aging in mice (Latorre-Pellicer

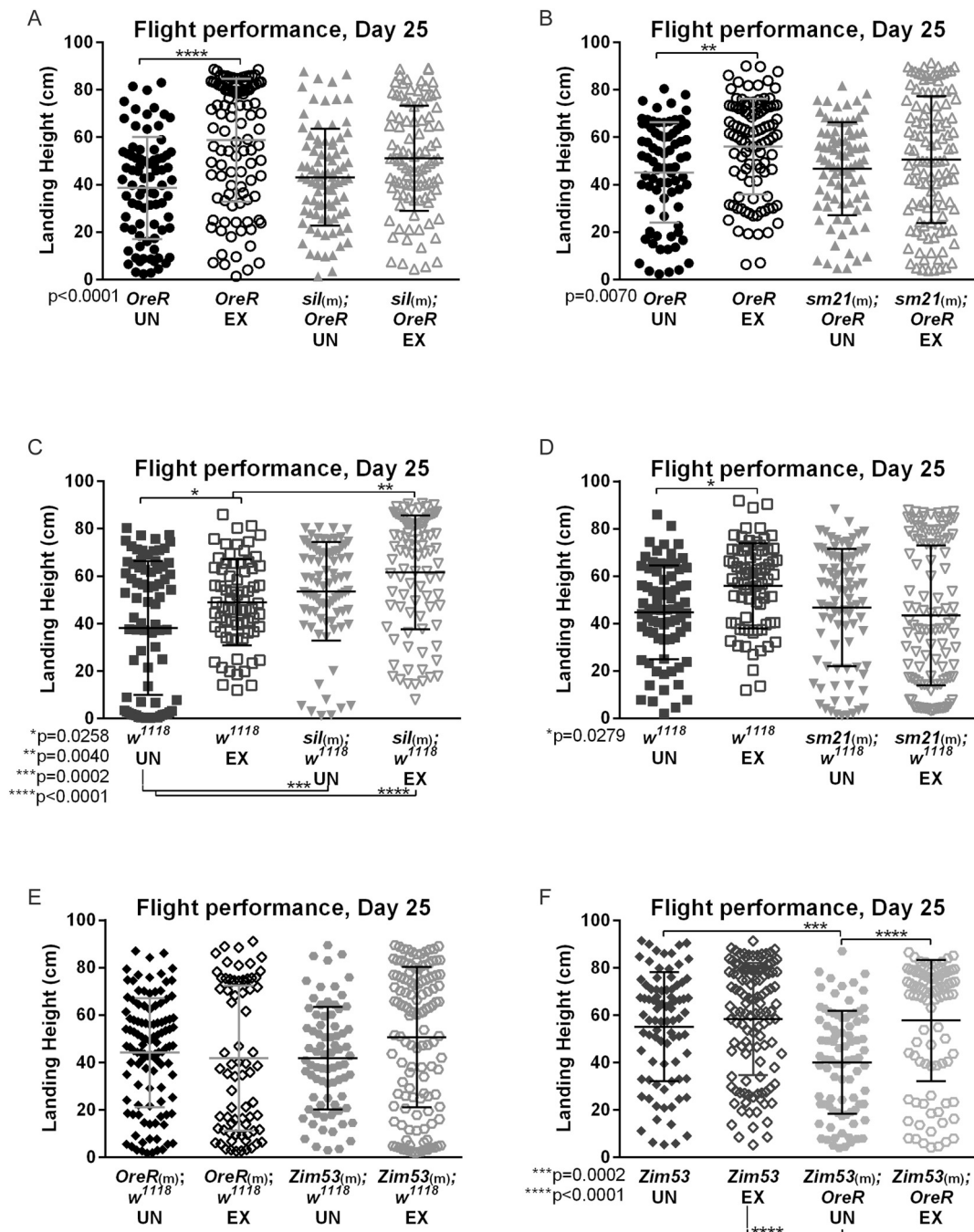


**Fig. 6. Enhancements in flight performance are weakly affected by mito-nuclear interactions (A–D)** Both *OreR* and *w<sup>1118</sup>* flies improve landing height after endurance exercise (EX). (A) *sil(m);OreR*, (B) *sm21(m);OreR*, and (D) *sm21(m);w<sup>1118</sup>* and fail to improve flight performance after endurance exercise. (C) *sil(m);w<sup>1118</sup>* flies have enhanced flight compared to trained and untrained (UN) *w<sup>1118</sup>* lines whether exercised or not. (E) Neither *OreR(m);w<sup>1118</sup>* nor *Zim53(m);w<sup>1118</sup>* flies increase flight performance after exercise training. *Zim53* flies have training-independent enhanced flight performance, and exercised *Zim53(m);OreR* flies increased landing height compared to unexercised control siblings.  $n \geq 71$  for all cohorts.  $p$ -values generated by ANOVA with Tukey *post-hoc* comparison, error bars indicate SD. Graphs are representative of a single repetition of at least duplicate cohorts. ANOVAs reporting main and interaction effects are presented in Table 3.

et al., 2016). Here, we examine the idea that replacement of mitochondria with exogenous mitochondria derived from other strains or other species would confer changes in exercise capacity.

The strains used have widely divergent baseline exercise capacities, with *La* having the highest and *w<sup>1118</sup>* the lowest among them. *Zim53* has an unusual profile, with a baseline capacity similar to *OreR*, but with a slower age-related decline that is not responsive to exercise training. Indeed, the *Zim53* group behaved as an outlier in almost every assay.

We find that exogenous mitochondria can, in fact, change the baseline capacity of a given strain (e.g. *RaLa(m)*). However, in other

cases, baseline capacity is unaltered by introduction of exogenous mitochondria (e.g. *OreR(m);w<sup>1118</sup>*). Despite their divergent baseline capacities, all the wild-type strains carrying their own mitochondria responded to exercise training with the characteristic changes to speed, endurance, etc.

We find a general trend that strains with exogenous mitotypes have a reduced quantitative response to exercise training in several assays, including speed, endurance, cardiac stress resistance, and adipose LysoTracker staining. The fact that exercise response is more negatively affected by exogenous mitochondria than baseline capacity suggests

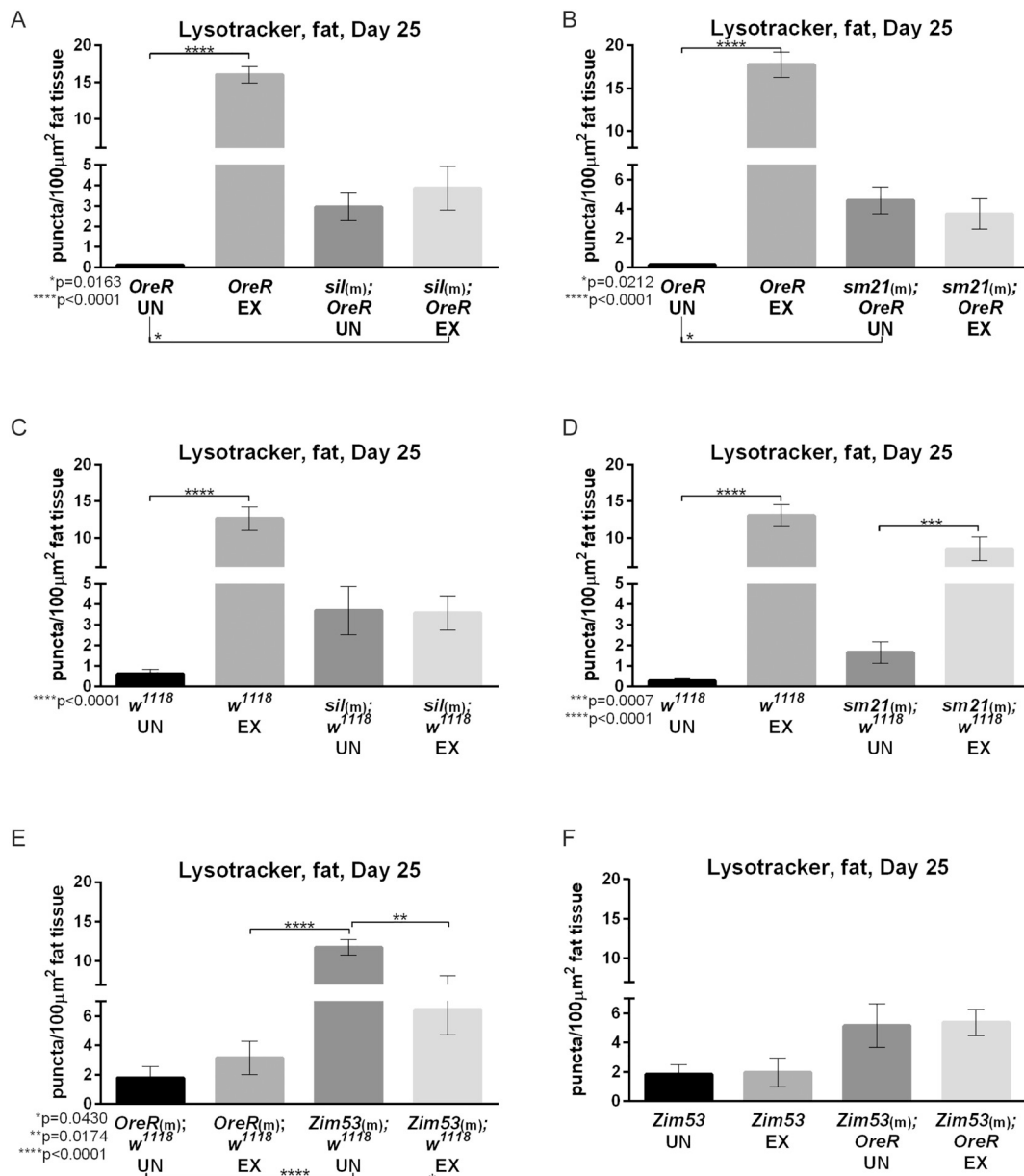


**Fig. 7. Mito-nuclear interactions strongly affect lysosomal activity in *Drosophila* fat body after endurance exercise** (A) *OreR* and *w<sup>1118</sup>* flies upregulate fat body lysosomal activity after endurance training (EX), but in *sil(m);OreR* (A), *sm21(m);OreR* (B), and *sil(m);w<sup>1118</sup>* flies (C) lysosomal activity in the fat body remains low. (D) Only *sm21(m);w<sup>1118</sup>* flies have increased fat body Lysotracker staining after endurance exercise. (E) Similarly, *OreR(m);w<sup>1118</sup>* and *Zim53(m);w<sup>1118</sup>* do not upregulate fat body lysosomal activity after exercise. In fact, Lysotracker is higher in unexercised (UN) *Zim53(m);w<sup>1118</sup>* flies than in exercised siblings. (F) *Zim53* and *Zim53(m);OreR* flies have low Lysotracker staining in the fat body whether exercised or not.  $n = 10$  for all cohorts.  $p$ -values generated by ANOVA with Tukey *post-hoc* comparison, error bars indicate SEM. Graphs are representative of a single repetition of at least duplicate cohorts. ANOVAs reporting main and interaction effects are presented in Table 3.

that mito-nuclear compatibility is an important factor during exercise adaptations. This seems to be the case even when baseline capacity is not altered. Because chronic exercise induces mitochondrial biogenesis and mitophagy, it is likely that incompatibilities that may be innocuous in sedentary animals are highlighted under conditions where mitochondria are undergoing active replication and fission. Consistent with this idea, variation in mitochondrial *tRNA* sequence has been identified as a molecular mechanism for mito-nuclear incompatibility in temperature adaptation (Hoekstra et al., 2013; Zhang et al., 2017).

Despite the evident importance of mitotype as a determinant of exercise capacity and response to exercise training, it is clear that the nuclear genome also has an important role to play. Microarrays have identified conserved pathways that are altered transcriptionally by

exercise in mice (Ort et al., 2007; Teran-Garcia et al., 2005) and *Drosophila* (Sujkowski et al., 2015). Furthermore, conserved single-gene candidates have been identified that are capable of conferring benefits of exercise, including *PGC1- $\alpha$*  (Diop et al., 2015; Tinkerhess et al., 2012b; Xiong et al., 2015), as well as invertebrate-specific factors, such as *Mthl-3* in *Drosophila* (Sujkowski et al., 2015). Epigenetic markers have also been linked to exercise, including markers that can be passed by maternal heredity in mice (Laker et al., 2014a).

Different assays clearly showed different sensitivity to mitotype and nucleotype across cohorts. For example, lysosomal activity was more sensitive to mitotype, whereas endurance in mitoswitch groups was more sensitive to nucleotype. The variety of effects clearly suggest that systemic adaptation to increased daily exercise involves multiple

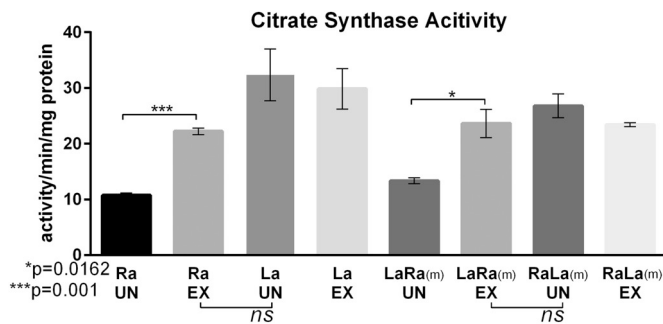


**Fig. 8. Citrate Synthase Specific Activity parallels climbing speed and endurance in closely-related *Ra* and *La* lines.** Trained *Ra* flies have higher citrate synthase activity than age-matched, untrained siblings. Untrained *La* flies have high citrate synthase activity that does not increase with training. *LaRa<sub>(m)</sub>* flies have increased citrate synthase activity after endurance training, similar to *Ra* flies, and *RaLa<sub>(m)</sub>* flies have citrate synthase activity similar to *La* lines independent of training status.  $n = 8$  flies for each cohort.  $p$ -values are generated by ANOVA with Bonferroni *post-hoc* comparison, error bars indicate SEM. Graph is representative of triplicate repetitions of triplicate biological cohorts.

interactions between the mitochondrial and nuclear genomes in various tissues. Thus, it seems clear that nuclear factors, mitochondrial factors, and the interactions between them are all of importance in driving the exercise response.

#### 4.2. Mitochondria from selected lines, wild strains and divergent species

The clearest effect of mitotype on exercise capacity and exercise response was seen in the lines derived from *Ra* and *La*. One potentially important difference between these lines and the others used in the study is that these lines share a common progenitor, as *La* was created by selection for longevity from the original *Ra* (Arking, 1987). Thus, they are more closely related than any other combination used here. Previous work has demonstrated that mitochondria from *La* flies predict the longevity of the line under dietary restriction (Soh et al., 2007), suggesting that mitochondrial genes, whether nuclear or mitochondrially encoded, are part of the selection effect. It is further notable that the introgression of a mtDNA from a different species (*D. simulans* mtDNA in *D. melanogaster* chromosomes) does not produce a consistently more dysfunctional fly genotype, as might be expected from the breakdown of a co-adapted mitonuclear genetic interaction. Most of the variation across mtDNAs in baseline performance or response to exercise was attributable to variation between mtDNA within a species (*Zim53* vs. *OreR*, or *sil* vs. *sm21*). These findings are consistent with fitness assays using many of these same mitonuclear genotypes (Montooth et al., 2010), and a larger set of independent mtDNA introgression strains (Mossman et al., 2016). The *sil* and *Zim53* mtDNAs were more likely to contribute beneficial effects, and there was some indication that this was more pronounced in the  $w^{1118}$  nuclear background, than in the *OreR* nuclear background (see Figs. 3, 4 and 6). This is consistent with other studies of mitonuclear epistatic interactions, where beneficial and deleterious combinations are common, but not predictable by the main effects of either nuclear or mitochondrial genome.

Microarray experiments demonstrated that 65% of the transcriptional changes between *Ra* and *La* are identical to the changes between *Ra* and exercised *Ra* (Sujkowski et al., 2015). Thus, the selection process that created the *La* line was inadvertently similar to the process of exercise-training. This raises the fascinating idea that introgressed mitochondria from the *La* line may be functionally equivalent to introducing mitochondria from an exercise-trained *Ra* back into a sedentary *Ra* fly. The common origin between the mitotype and nucleotype of the *RaLa<sub>(m)</sub>* and *LaRa<sub>(m)</sub>* may be reflected in better mitonuclear compatibility, allowing the effect of the mitochondria to be more clearly demonstrated.

#### 4.3. Gene x gene x environment interactions

Interactions between mitochondrial and nuclear genome have been demonstrated to play an important role in the response to dietary restriction (Mossman et al., 2016; Zhu et al., 2014) and hypoxia (Mossman et al., 2017) in *Drosophila*. Here, we find further evidence that major environmental changes, such as chronic endurance exercise, are dependent on interactions between the mitochondrial and nuclear genomes.

A growing body of literature has focused on individual differences in exercise response, both in model organisms (Britton and Koch, 2001; Koch et al., 2012; Mendez et al., 2016) and in humans (Bouchard et al., 2012; Puthuchery et al., 2011). While these differences are presumed to derive from genetics, relatively few conserved single genes have been identified that promote efficient exercise adaptations (Bostrom et al., 2013). Of those that have been identified, such as *PGC1- $\alpha$*  (Laker et al., 2014a; Tinkerhess et al., 2012b), a common thread is regulation of either mitochondrial biogenesis or autophagy/mitophagy. As these processes require cooperation between mitochondrial and nuclear genes, it seems likely that mito-nuclear interactions are an important factor in the efficiency of individual exercise adaptation across the animal kingdom. Given the increased interest in mitochondrial replacement therapy for the treatment of mtDNA-encoded disease, the unpredictable nature of the outcomes in these experiments indicates that further study is needed to identify the mechanisms underlying high-fitness mitonuclear interactions.

While great progress has been made using model organisms to better understand responses to diet (Mossman et al., 2016; Ort et al., 2007; Rera et al., 2011), the response to chronic activity is much less well understood. Like diet, exercise is an important environmental variable with broad effects on metabolism and physiology. Now that multiple exercise models have been developed in *Drosophila* (Mendez et al., 2016; Piazza et al., 2009a; Tinkerhess et al., 2012a) and *C. elegans* (Laranjeiro et al., 2017), the stage is set to better explore these interactions using the strengths of invertebrate genetics.

#### Acknowledgement

We gratefully acknowledge funding for this study provided by the NIH/NIA and NIH/NIGMS (1R01AG059683-02, 5R21AG055712-02 to RJW, and 2R01GM067862, 1R01AG027849 to DMR) and by an MDRC Pilot Award to RW.

#### References

- Arking, R., 1987. Successful selection for increased longevity in *Drosophila*: analysis of the survival data and presentation of a hypothesis on the genetic regulation of longevity. *Exp. Gerontol.* 22, 199–220.
- Arking, R., 2001. Gene expression and regulation in the extended longevity phenotypes of *Drosophila*. *Ann. N. Y. Acad. Sci.* 928, 157–167.
- Arking, R., Force, A.G., Dudas, S.P., Buck, S., Baker 3rd, G.T., 1996. Factors contributing to the plasticity of the extended longevity phenotypes of *Drosophila*. *Exp. Gerontol.* 31, 623–643.
- Arking, R., Buck, S., Novoseltev, V.N., Hwangbo, D.S., Lane, M., 2002. Genomic plasticity, energy allocations, and the extended longevity phenotypes of *Drosophila*. *Ageing Res. Rev.* 1, 209–228.
- Bo, H., Zhang, Y., Ji, L.L., 2010. Redefining the role of mitochondria in exercise: a dynamic remodeling. *Ann. N. Y. Acad. Sci.* 1201, 121–128.
- Booth, F.W., Rueggsegger, G.N., Toedebusch, R.G., Yan, Z., 2015. Endurance exercise and the regulation of skeletal muscle metabolism. *Prog. Mol. Biol. Transl. Sci.* 135, 129–151.
- Bostrom, P.A., Graham, E.L., Georgiadi, A., Ma, X.C., 2013. Impact of exercise on muscle and non-muscle organs. *IUBMB Life* 65, 845–850.
- Bouchard, C., Blair, S.N., Church, T.S., Earnest, C.P., Hagberg, J.M., Hakkinen, K., Jenkins, N.T., Karavirta, L., Kraus, W.E., Leon, A.S., Rao, D.C., Sarzynski, M.A., Skinner, J.S., Slentz, C.A., Rankinen, T., 2012. Adverse metabolic response to regular exercise: is it a rare or common occurrence? *PLoS One* 7, e37887.
- Britton, S.L., Koch, L.G., 2001. Animal genetic models for complex traits of physical capacity. *Exerc. Sport Sci. Rev.* 29, 7–14.
- Cassilhas, R.C., Tufik, S., de Mello, M.T., 2016. Physical exercise, neuroplasticity, spatial learning and memory. *Cell. Mol. Life Sci.* 73, 975–983.
- Chan, S.L., Wei, Z., Chigurupati, S., Tu, W., 2010. Compromised respiratory adaptation

- and thermoregulation in aging and age-related diseases. *Ageing Res. Rev.* 9, 20–40.
- Coffey, V.G., Hawley, J.A., 2007. The molecular bases of training adaptation. *Sports Med.* 37, 737–763.
- Dai, D.F., Rabinovitch, P.S., Ungvari, Z., 2012. Mitochondria and cardiovascular aging. *Circ. Res.* 110, 1109–1124.
- Damschroder, D., Cobb, T., Sujkowski, A., Wessells, R., 2018. *Drosophila* endurance training and assessment of its effects on systemic adaptations. *Bio-Protocol* 8.
- Diop, S.B., Bisharat-Kernizan, J., Birse, R.T., Oldham, S., Ocorr, K., Bodmer, R., 2015. PGC-1/spargel counteracts high-fat-diet-induced obesity and cardiac lipotoxicity downstream of TOR and brummer ATGL lipase. *Cell Rep.* 10, 1572–1584.
- Ferreira, J.C., Bacurau, A.V., Bueno Jr., C.R., Cunha, T.C., Tanaka, L.Y., Jardim, M.A., Ramires, P.R., Brum, P.C., 2010. Aerobic exercise training improves Ca<sup>2+</sup> handling and redox status of skeletal muscle in mice. *Exp. Biol. Med.* 235, 497–505.
- Gargano, J.W., Martin, I., Bhandari, P., Grotewiel, M.S., 2005. Rapid iterative negative geotaxis (RING): a new method for assessing age-related locomotor decline in *Drosophila*. *Exp. Gerontol.* 40, 386–395.
- Hoekstra, L.A., Siddiq, M.A., Montooth, K.L., 2013. Pleiotropic effects of a mitochondrial-nuclear incompatibility depend upon the accelerating effect of temperature in *Drosophila*. *Genetics* 195, 1129.
- Ircher, I., Adhithetty, P.J., Joseph, A.M., Ljubicic, V., Hood, D.A., 2003. Regulation of mitochondrial biogenesis in muscle by endurance exercise. *Sports Med.* 33, 783–793.
- Kang, C., Chung, E., Diffie, G., Ji, L.L., 2013. Exercise training attenuates aging-associated mitochondrial dysfunction in rat skeletal muscle: role of PGC-1 $\alpha$ . *Exp. Gerontol.* 48, 1343–1350.
- Koch, L.G., Britton, S.L., Wisloff, U., 2012. A rat model system to study complex disease risks, fitness, aging, and longevity. *Trends Cardiovasc. Med.* 22, 29–34.
- Laker, R.C., Lillard, T.S., Okutsu, M., Zhang, M., Hoehn, K.L., Connelly, J.J., Yan, Z., 2014a. Exercise prevents maternal high-fat diet-induced hypermethylation of the Pgc-1 $\alpha$  gene and age-dependent metabolic dysfunction in the offspring. *Diabetes* 63, 1605–1611.
- Laker, R.C., Xu, P., Ryall, K.A., Sujkowski, A., Kenwood, B.M., Chain, K.H., Zhang, M., Royal, M.A., Hoehn, K.L., Driscoll, M., Adler, P.N., Wessells, R.J., Saucerman, J.J., Yan, Z., 2014b. A novel MitoTimer reporter gene for mitochondrial content, structure, stress, and damage in vivo. *J. Biol. Chem.* 289, 12005–12015.
- Lantier, L., Fentz, J., Mounier, R., Leclerc, J., Treebak, J.T., Pehmoller, C., Sanz, N., Sakakibara, I., Saint-Amand, E., Rimbaud, S., Maire, P., Marette, A., Ventura-Clapier, R., Ferry, A., Wojtaszewski, J.F., Foretz, M., Viollet, B., 2014. AMPK controls exercise endurance, mitochondrial oxidative capacity, and skeletal muscle integrity. *FASEB J.* 28, 3211–3224.
- Laranjeiro, R., Harinath, G., Burke, D., Braeckman, B.P., Driscoll, M., 2017. Single swim sessions in *C. elegans* induce key features of mammalian exercise. *BMC Biol.* 15, 30.
- Latorre-Pellicer, A., Moreno-Loshuertos, R., Lechuga-Vieco, A.V., Sanchez-Cabo, F., Torroja, C., Acin-Perez, R., Calvo, E., Aix, E., Gonzalez-Guerra, A., Logan, A., Bernad-Miana, M.L., Romanos, E., Cruz, R., Cogliati, S., Sobrino, B., Carracedo, A., Perez-Martos, A., Fernandez-Silva, P., Ruiz-Cabello, J., Murphy, M.P., Flores, I., Vazquez, J., Enriquez, J.A., 2016. Mitochondrial and nuclear DNA matching shapes metabolism and healthy ageing. *Nature* 535, 561–565.
- Li, L., Muhlfeld, C., Niemann, B., Pan, R., Li, R., Hilfiker-Kleiner, D., Chen, Y., Rohrbach, S., 2011. Mitochondrial biogenesis and PGC-1 $\alpha$  deacetylation by chronic treadmill exercise: differential response in cardiac and skeletal muscle. *Basic Res. Cardiol.* 106, 1221–1234.
- Liang, Q., Kobayashi, S., 2015. Mitochondrial quality control in the diabetic heart. *J. Mol. Cell. Cardiol.* 95, 57–69.
- Lira, V.A., Okutsu, M., Zhang, M., Greene, N.P., Laker, R.C., Breen, D.S., Hoehn, K.L., Yan, Z., 2013. Autophagy is required for exercise training-induced skeletal muscle adaptation and improvement of physical performance. *FASEB J.* 27, 4184–4193.
- Matsakas, A., Mouisel, E., Amthor, H., Patel, K., 2010. Myostatin knockout mice increase oxidative muscle phenotype as an adaptive response to exercise. *J. Muscle Res. Cell Motil.* 31, 111–125.
- Mendez, S., Watanabe, L., Hill, R., Owens, M., Moraczewski, J., Rowe, G.C., Riddle, N.C., Reed, L.K., 2016. The treadWheel: a novel apparatus to measure genetic variation in response to gently induced exercise for *Drosophila*. *PLoS One* 11, e0164706.
- Montooth, K.L., Meiklejohn, C.D., Abt, D.N., Rand, D.M., 2010. Mitochondrial-nuclear epistasis affects fitness within species but does not contribute to fixed incompatibilities between species of *Drosophila*. *Evol.; Int. J. Organ. Evol.* 64, 3364–3379.
- Moran, M., Moreno-Lastres, D., Marin-Buera, L., Arenas, J., Martin, M.A., Ugalde, C., 2012. Mitochondrial respiratory chain dysfunction: implications in neurodegeneration. *Free Radic. Biol. Med.* 53, 595–609.
- Mossman, J.A., Biancani, L.M., Zhu, C.T., Rand, D.M., 2016. Mitonuclear epistasis for development time and its modification by diet in *Drosophila*. *Genetics* 203, 463–484.
- Mossman, J.A., Tross, J.G., Jourjine, N.A., Li, N., Wu, Z., Rand, D.M., 2017. Mitonuclear interactions mediate transcriptional responses to hypoxia in *Drosophila*. *Mol. Biol. Evol.* 34, 447–466.
- Ort, T., Gerwien, R., Lindborg, K.A., Diehl, C.J., Lemieux, A.M., Eisen, A., Henriksen, E.J., 2007. Alterations in soleus muscle gene expression associated with a metabolic endpoint following exercise training by lean and obese Zucker rats. *Physiol. Genomics* 29, 302–311.
- Owusu-Ansah, E., Song, W., Perrimon, N., 2013. Muscle mitohormesis promotes longevity via systemic repression of insulin signaling. *Cell* 155, 699–712.
- Piazza, N., Gosangi, B., Devilla, S., Arking, R., Wessells, R., 2009a. Exercise-training in young *Drosophila melanogaster* reduces age-related decline in mobility and cardiac performance. *PLoS One* 4, e5886.
- Piazza, N., Hayes, M., Martin, I., Duttaroy, A., Grotewiel, M., Wessells, R., 2009b. Multiple measures of functionality exhibit progressive decline in a parallel, stochastic fashion in *Drosophila* Sod2 null mutants. *BioGerontology* 10, 637–648.
- Powers, S.K., Sollanek, K.J., Wiggs, M.P., Demirel, H.A., Smuder, A.J., 2014. Exercise-induced improvements in myocardial antioxidant capacity: the antioxidant players and cardioprotection. *Free Radic. Res.* 48, 43–51.
- Puthucherry, Z., Skipworth, J.R., Rawal, J., Loosemore, M., Van Someren, K., Montgomery, H.E., 2011. Genetic influences in sport and physical performance. *Sports Med.* 41, 845–859.
- R, I.D.f., 2016. RStudio, in: Team, R. (Ed.), Boston, MA.
- Rand, D.M., Haney, R.A., Fry, A.J., 2004. Cytonuclear coevolution: the genomics of cooperation. *Trends Ecol. Evol.* 19, 645–653.
- Rera, M., Bahadorani, S., Cho, J., Koehler, C.L., Ulgherait, M., Hur, J.H., Ansari, W.S., Lo Jr., T., Jones, D.L., Walker, D.W., 2011. Modulation of longevity and tissue homeostasis by the *Drosophila* PGC-1 homolog. *Cell Metab.* 14, 623–634.
- Restif, C., Ibanez-Ventoso, C., Vora, M.M., Guo, S., Metaxas, D., Driscoll, M., 2014. CeleST: computer vision software for quantitative analysis of *C. elegans* swim behavior reveals novel features of locomotion. *PLoS Comput. Biol.* 10, e1003702.
- Ryan, M.T., Hoogenraad, N.J., 2007. Mitochondrial-nuclear communications. *Annu. Rev. Biochem.* 76, 701–722.
- Soh, J.W., Hotic, S., Arking, R., 2007. Dietary restriction in *Drosophila* is dependent on mitochondrial efficiency and constrained by pre-existing extended longevity. *Mech. Ageing Dev.* 128, 581–593.
- Sujkowski, A., Saunders, S., Tinkerhess, M., Piazza, N., Jennens, J., Healy, L., Zheng, L., Wessells, R., 2012. dFatp regulates nutrient distribution and long-term physiology in *Drosophila*. *Aging Cell* 11, 921–932.
- Sujkowski, A., Bazzell, B., Carpenter, K., Arking, R., Wessells, R.J., 2015. Endurance exercise and selective breeding for longevity extend *Drosophila* healthspan by overlapping mechanisms. *Aging (Albany NY)* 7, 535–552.
- Teran-Garcia, M., Rankinen, T., Koza, R.A., Rao, D.C., Bouchard, C., 2005. Endurance training-induced changes in insulin sensitivity and gene expression. *Am. J. Physiol. Endocrinol. Metab.* 288, E1168–E1178.
- Thomas, R.J., Kenfield, S.A., Jimenez, A., 2017. Exercise-induced biochemical changes and their potential influence on cancer: a scientific review. *Br. J. Sports Med.* 51.
- Tinkerhess, M.J., Ginzberg, S., Piazza, N., Wessells, R.J., 2012a. Endurance training protocol and longitudinal performance assays for *Drosophila melanogaster*. *J. Vis. Exp.* 61, 3786.
- Tinkerhess, M.J., Healy, L., Morgan, M., Sujkowski, A., Matthys, E., Zheng, L., Wessells, R.J., 2012b. The *Drosophila* PGC-1 $\alpha$  homolog spargel modulates the physiological effects of endurance exercise. *PLoS One* 7, e31633.
- Tranah, G.J., 2011. Mitochondrial-nuclear epistasis: implications for human aging and longevity. *Ageing Res. Rev.* 10, 238–252.
- Venditti, P., Di Stefano, L., Di Meo, S., 2013. Mitochondrial metabolism of reactive oxygen species. *Mitochondrion* 13, 71–82.
- Vigelso, A., Andersen, N.B., Dela, F., 2014. The relationship between skeletal muscle mitochondrial citrate synthase activity and whole body oxygen uptake adaptations in response to exercise training. *Int. J. Physiol. Pathophysiol. Pharmacol.* 6, 84–101.
- Wessells, R.J., Bodmer, R., 2004. Screening assays for heart function mutants in *Drosophila*. *BioTechniques* 37, 58–60, 62, 64 passim.
- Wessells, R.J., Fitzgerald, E., Cypser, J.R., Tatar, M., Bodmer, R., 2004. Insulin regulation of heart function in aging fruit flies. *Nat. Genet.* 36, 1275–1281.
- Xiong, X.Q., Chen, D., Sun, H.J., Ding, L., Wang, J.J., Chen, Q., Li, Y.H., Zhou, Y.B., Han, Y., Zhang, F., Gao, X.Y., Kang, Y.M., Zhu, G.Q., 2015. FNDC5 overexpression and irisin ameliorate glucose/lipid metabolic derangements and enhance lipolysis in obesity. *Biochim. Biophys. Acta* 1852, 1867–1875.
- Yan, Z., Lira, V.A., Greene, N.P., 2012. Exercise training-induced regulation of mitochondrial quality. *Exercise Sport Sci. Rev.* 40, 159–164.
- Zanuso, S., Sacchetti, M., Sundberg, C.J., Orlando, G., Benvenuti, P., Balducci, S., 2017. Exercise in type 2 diabetes: genetic, metabolic and neuromuscular adaptations. A review of the evidence. *Br. J. Sports Med.* <https://doi.org/10.1136/bjsports-2016-096724>.
- Zhang, C.Y., Montooth, K.L., Calvi, B.R., 2017. Incompatibility between mitochondrial and nuclear genomes during oogenesis results in ovarian failure and embryonic lethality. *Development* 144, 2490–2503.
- Zhu, C.T., Ingelmo, P., Rand, D.M., 2014. GxGx for lifespan in *Drosophila*: mitochondrial, nuclear, and dietary interactions that modify longevity. *PLoS Genet.* 10, e1004354.
- Ziegler, D.V., Wiley, C.D., Velarde, M.C., 2015. Mitochondrial effectors of cellular senescence: beyond the free radical theory of aging. *Aging Cell* 14, 1–7.



## **Chapter 4**

*FreeClimber: Automated High Throughput Quantification of Climbing Performance in Drosophila, with Examples from Mitonuclear Genotypes*

Adam N. Spierer, Denise Yoon, Lei Zhu, and David M. Rand

Modified from submission to *Journal of Experimental Biology* (in prep)

## Abstract

Negative geotaxis (climbing) performance is a useful metric for quantifying the health and vigor of *Drosophila* across experimental treatments and conditions. Manual methods to compute climbing performance are slow and tedious, while available computation methods have inflexible hardware or software requirements. We present an alternative with our open-source program `FreeClimber`. This Python-based method performs a very quick background subtraction step to allow for more accurate spot detection on a heterogeneous background. `FreeClimber` quantifies the most linear portion of a velocity curve for each specified vial by performing a local linear regression. Output files report results as either pre-calculated slopes, or as individual spot locations that can be processed further for predictive linking (tracking). We demonstrate `FreeClimber`'s utility in a longitudinal study for endurance exercise performance using six distinct mitochondrial haplotypes paired with a common w<sup>1118</sup> nuclear background.

## Introduction

*Drosophila* are a genetically tractable model system to explore the functional bases of traits at organismal, cellular and molecular levels (Chow and Reiter, 2017). The resources available for manipulation of genetic, cellular, physiological and genomic analyses are extensive (Bellen et al., 2011; Bellen et al., 2010; Lenz et al., 2013; Mackay et al., 2012) providing great opportunities for integrative research spanning the organismal-to-molecular scales.

One of the most common *Drosophila* health metrics is locomotor capacity, easily measured using a negative geotaxis (climbing) assay (Gargano et al., 2005; Jones and Grotewiel, 2011). Here, flies are gently knocked to the bottom of a vial where their movements are captured by image or video as they instinctively climb upward (Ganetzky and Flanagan, 1978; Gargano et al., 2005). Climbing performance is typically reported as some measure of the flies' position vs. time: mean position at a time cutoff (Gargano et al., 2005; Lavoy et al., 2018) or time until a percentage of flies reach a set height (Ma et al., 2014; Podratz et al., 2013; Tsai et al., 2016; Xu et al., 2008).

The climbing assay's popularity is largely due to its accessibility. Experimental setups are easily engineered from common laboratory items, meaning they are relatively inexpensive to implement. Data collection is straightforward requiring simple image capture tools and basic software available on most computers. However, this assay's simplicity is offset by its tedious and time-consuming nature.

Several publications describe protocols for automating the conversion of visual media into data, but these are not always accessible to the general community. Some of these platforms are detectors, while others are trackers. Detectors identify the x,y-coordinates of flies (spots) across frames, which can be evaluated as a function of position vs. time (ex. `RflyDetection` R module (Cao et al., 2017) and an ImageJ-based approach (Podratz et al., 2013)). Trackers are also detectors but incorporate a predictive linking step to connect points between frames based on their proximity and likelihood of being connected (ex. the Hillary Climber tracks single fly vials (Willenbrink et al., 2016), the iFly system tracks multiple flies in a single vial (Kohlhoff et al., 2011), and the DaRT system tracks multiple flies in multiple enclosures (Faville et al., 2015; Taylor and Tuxworth, 2019)). Trackers are challenging to automate because they generally require supervision to discern flies with erratic vertical motions (jumps and falls) or flies that interact laterally with other flies (bump on the same plane or eclipse on separate planes (issue reducing 3D to 2D))(Chenouard et al., 2014). Published methods for detectors and trackers generally require a clean and custom setup, are written in proprietary languages (MATLAB), and/or are only made available locally to the author lab groups and collaborators. Because of these and other factors, no single platform is widely accepted by the *Drosophila*-research community, despite the assay's ubiquity.

We created `FreeClimber` to addresses some of these major issues, correct for common biases in traditional manual approaches, and facilitate the generation of accurate, repeatable, and biologically meaningful data and analyses. This Python 3-based platform can be run interactively, via Graphical User Interface (GUI), and is

capable of automation with high-throughput batch processing, via the modular command line tools. `FreeClimber` utilizes an efficient background subtraction step, so it excels when given videos with high contrast between flies and a clean static background. It also performs respectably with heterogeneous backgrounds with minor movement in a minority of frames. Additionally, our detector implements a local linear regression model for calculating velocity of a group of flies (Olito et al., 2017), which we demonstrate is more biologically meaningful in circumventing violated assumptions associated with traditional, manual analysis. Finally, we demonstrate the utility of our platform for longitudinal *Drosophila* screens analyzing two original data sets of exercise conditioned and unconditioned mitochondrial-nuclear (mito-nuclear) introgression flies. Ultimately, we highlight the usefulness of the `FreeClimber` platform and its ability to quantify subtle differences in phenotype across sample-rich studies, like those frequently conducted in *Drosophila* research.

## Materials and Methods

### *Drosophila* husbandry and generation of lines

Six mitochondrial haplotypes (mtDNAs or mitotypes) were derived from three different *Drosophila* species: *D. melanogaster* (strains: *OregonR* and *Zimbabwe53*), *D. simulans* (subtypes: *sil*, *sill*, and *maull* (which is equivalent to *silll*), and *D. yakuba* (subtypes: *yakuba*) (Montooth et al., 2010; Mossman et al., 2016; Zhu et al., 2014). These mitotypes were each placed on a common, *D. melanogaster* *w*<sup>1118</sup> nuclear background using balancer chromosome crosses and subsequent recurrent male backcrossing using *w*<sup>1118</sup> males (Zhu et al., 2014), with *D. simulans* *maull* and *D. yakuba* lines created by microinjection of cytoplasm donor into an egg (Ma et al., 2014).

Stocks were density controlled for two generations whereby 20 females and 20 males were allowed to lay eggs for three days per brood. Fly cultures were held at 25°C on standard lab food (Mossman et al., 2016) and maintained on a 12h:12h light:dark schedule. Adult males were collected three days post-eclosion using light CO<sub>2</sub> anesthetization and separated into vials of 20 flies. Flies were assayed four days later and transferred to new food every day.

### Video recording set up

While `FreeClimber` does not require a custom set up, we employed one to standardize filming distance, lighting, and timing video capture as we demonstrated the utility of our platform (Figure S1B). This setup uses a `MakerBeam` (Utrecht, Netherlands) frame with a mounted `Raspberry Pi 3 Model B+` connected to an 8

megapixel PiCamera (V2). The camera is held a fixed distance from an LED-light board ([Huion model L4S](#), 10.7 lumens/inch<sup>2</sup>) and custom rig was anchored between the camera and light board. The rig was made of polycarbonate and rubber O-rings to hold six glass vials loaded with 10-25 flies each. It could freely slide vertically along two aluminum rods attached to a polycarbonate base. The rig was dropped from the lowest height to elicit a consistent response (7 cm), which triggered a photosensor to begin recording a video. Five-second videos (.h264) were recorded at 29 frames per second and then analyzed with the `FreeClimber` software after all videos were captured.

### Overview of `FreeClimber` modes

The following steps (Figure 1A) are completed by `FreeClimber`, available at [https://github.com/adamspierer/FreeClimber/tree/dissertation\\_release](https://github.com/adamspierer/FreeClimber/tree/dissertation_release), though the most updated version is available on the master branch:

<https://github.com/adamspierer/FreeClimber/>. The platform can be run in two modes: a Graphical User Interface (GUI) for optimizing detection parameters, and a command line set up for high-throughput batch processing. Both modes run through similar steps, though the GUI outputs optimization plots that the command line tool does not. For the purposes of outlining this method, we will walk through options with the GUI, which can be run with the command (from the main `FreeClimber` folder):

```
pythonw ./scripts/FreeClimber_gui.py --video_file ./example/w1118_m_2_1.h264
```

See File S1 or the link above for a complete tutorial guide on installation and running `FreeClimber`, as well as tips and tricks for increasing data quality.

### Video preprocessing and background subtraction

Videos are read into integer-based n-dimensional arrays (*nd*-array) using the `FFmpeg-python` package (v.4.0.4; <https://github.com/kkroening/ffmpeg-python>). Following user-defined parameters, videos are cropped for the appropriate frame range and positional region of interest (ROI) (Figure 1B), before being converted to gray scale. An output file with the suffix `.ROI.png` is generated to show this region. A matrix representing the static background is calculated from the median pixel intensity of each x,y-coordinate across a user-defined number of frames (default is all frames). This background matrix is subtracted from each individual frame's pixel intensity matrix, resulting in a new *nd*-array corresponding with only regions of movement (flies) in the video (Figure 1C).

### Detector optimization

The background-subtracted frames are passed to a Python-implementation of the Crocker and Weeks particle-tracking algorithm `TrackPy` (v.0.4.2; <http://soft-matter.github.io/trackpy/dev/index.html>)(Crocker and Grier, 1996) for spot detection. Candidate spots are identified by clusters of pixels that meet user-defined parameters for the expected spot diameter (`diameter`), maximum diameter (`maxsize`), and minimum integrated brightness (`minmass`). Each candidate spot receives a roundness (`ecc`; eccentricity), mass and signal score (Figure 1D). Spots must pass minimum mass (`minmass`) and signal threshold values to be considered a `True` spot. The signal threshold can be provided by the user, or `FreeClimber` will calculate an appropriate one using the `SciPy` (v.1.4.1) functions: `peak_prominences` and `find_peaks`. A visualization of these metrics is created in `file_name.spot_check.png`.



### Spot detection

As the program runs, a data frame containing the spatio-temporal data for each spot and its accompanying metrics are saved with the file suffix `.raw.csv`. This file can be used as an input for `TrackPy` to track or predictively link spots (see Step 3: “Link features into particle trajectories”, <http://soft-matter.github.io/trackpy/dev/tutorial/walkthrough.html>).

Spot coordinates are transformed and processed for more accurate estimation of group climbing velocity. The raw data set is filtered for only true spots, described above. Y-coordinates are inverted to account for images being indexed from upper-left to lower-right, instead of lower-left to upper-right (Figure 1E). Spots are auto-assigned to vials by dividing the space between the left-most and right-most spots into the specified number of bins. The data frame containing these points and their vial assignments is saved as `.filtered.csv`.

### Calculating climbing velocity, via local linear regression

The mean y-position for all spots in a vial is calculated for each frame. A sliding window, corresponding with user-specified number of frames it takes for a fast group of flies to climb in the linear portion of a position vs. time curve, is applied to the velocity curve. A linear regression is calculated for each window and the slope of the most linear segment (greatest regression coefficient) is considered that vial’s velocity (Olito et al., 2017) for a given video (Figure 1E). This method is also known as a local linear

regression. In videos where the slope of the regression line is not significantly different from 0 ( $P > 0.05$ ), the slope is set to 0, since this generally indicates flies were present but could not climb.

If conversion factors for pixels-to-cm and frames-to-seconds are supplied and the box is checked to convert the output to cm per second, the program will do so for accurate comparison across research groups and studies.

Files containing regression results (including slopes) for each vial in a video are saved with the `.slopes.csv` suffix. Once `FreeClimber` processes all videos with the specified suffix in a parent directory, it will concatenate the files with the `.slopes.csv` suffix into a master `results.csv` file in the `path_project` folder that can be used for separate statistical analysis.

### *Automated, high-throughput detection of climbing velocity across many videos*

Once the detector is optimized, it can be run from the command line:

```
python ./scripts/FreeClimber_main.py --config_file ./example/example.cfg
```

Using the configuration file created in the GUI, the same settings can be applied over all the videos with the specified `file suffix` nested in the `path_project` path. This mode will only create the following files with suffixes: `.raw.csv`, `.filtered.csv`, and `.slopes.csv`, `.diagnostic.png`.

### Power Tower: the *Drosophila* treadmill

The Power Tower automates the process of eliciting the negative geotaxis (climbing) startle response, effectively acting as a treadmill (Figure S1C) (Sujkowski et al., 2018; Tinkerhess et al., 2012). Up to two trays of 100 vials each could be strapped down to the device. An arm attached to a motor turning at 4 RPM would contact a seesaw-like lever with a pivot on the ground and the other end placed under the Power Tower. The turning arm would depress the lever and cause the mobile portion of the Power Tower to rise. When the arm lost contact with the lever while the Power Tower was still lifted, the vials of flies would drop and flies would begin to climb.

Experimental and control flies on the Power Tower were set up in glass vials with food. Flies allowed to “exercise” were placed in vials with the foam stopper at the top to allow climbing, while their “unexercised” control siblings were placed in vials with the foam stopper 1 cm from the food to limit mobility.

### Longitudinal exercise training program

A longitudinal study over the course of three weeks was conducted with male flies from six mitochondrial haplotypes listed above. Male flies, aged three days post-eclosion, were divided into two groups of 12 vials containing 20 flies under light-CO<sub>2</sub> anesthesia. Flies were conditioned on weekdays for 2 hours the first week, 2.5 hours the second week, and 3 hours the third week, and assayed for climbing performance using the RING assay (Gargano et al., 2005) at the same time each training day before being exercised. Flies were assayed and tested on weekdays and given weekends to recover.

### Endurance exercise fatigue testing

A separate cohort of flies was used to study the mitotypes' ability to resist endurance climbing fatigue. Here, four vials containing 20 flies were set up on the Power Tower (similar to above) and either allowed to exercise (fatigued) or not allowed to exercise (rested). Flies' initial climbing performances were assayed before being placed on the Power Tower for six consecutive hours and then assayed hourly.

### Statistical analysis on longitudinal data

ANOVA of repeated measures was conducted using the `statsmodels` (v.0.10.0) module in Python. The ANOVA was used to quantify significant differences between mitochondrial haplotypes, exercise conditions, and the interaction between the two. This test was conducted using the absolute velocities and the normalized climbing index, which represents the climbing velocity for each vial normalized by the average velocity from the initial time point.

## Results and Discussion

### Local linear regression outperforms a time-based cutoff for climbing velocity

The mean vertical position vs. time curve is generally sigmoidal (Figure 2A-C). There is an occasional lag in the few frames (up to a second) as flies react to the stimulus, and a plateau at the end as flies reach the top of the vial. Taking the mean vertical position at 2-seconds (or any time point) overestimates the cohorts' velocity because it assumes flies increase vertical position linearly. Flies don't necessarily climb in a straight line, and flies can also have a delayed reaction to the stimulus and causes a brief hesitation. This analytical method also assumes flies start at the bottom of the vial, which is not always the case. Some flies jump when startled (which will create biological noise if only a single frame is considered) and begin at a non-zero starting height. Regardless, even for genotypes that all begin at the bottom of the vial, reducing a 3D object down to a 2D image causes issues as depth is translated into height. This means that flies starting at the bottom of the vial in the front have a different starting height than those starting in the back.

One way to address these issues is by calculating climbing velocity directly from the position vs. time curve using a local linear regression. Here, a sliding window is applied to the velocity curve and the slope of the most linear segment (greatest regression coefficient) is selected as the velocity. The sliding window represents the approximate number of frames that "fast" flies climb in the linear portion of the asymptotic or sigmoidal curve. For climbing in a standard narrow glass vial, we estimate a roughly 2-second window was appropriate across strong, moderate, and weak climbers. This

method generates more repeatable and reliable results across vials and is biologically more meaningful than the time-based cutoff. Additionally, this method can handle unpredictable climbing behaviors (jumping or falling) because the average position of flies in each frame means each fly has a fractional contribution to the group's position. By using a regression to find the slope, each frame's mean vertical position is considered in the context of the frames around it.

### *Climbing performance easily quantified for longitudinal studies*

In addition to more accurately estimating the climbing velocity of a group of flies, our method is well adapted for high-throughput screens. FreeClimber can autonomously process videos once detection parameters are optimized. Previous studies demonstrate climbing performance can be affected by genotype (Gargano et al., 2005; Holmbeck et al., 2015; Lavoy et al., 2018), environment (Piazza et al., 2009; Tinkerhess et al., 2012), and genotype x environment effects (Holmbeck et al., 2015; Sujkowski et al., 2018). Accordingly, we chose to test a set of six, phylogenetically diverse (Ballard, 2000; Montooth et al., 2009), mitochondrial introgression flies (mitotypes; Figure 3A). These mitotypes were derived from three different *Drosophila* species: *D. melanogaster* (subtypes: *OregonR* (*OreR*) and *Zimbabwe53* (*Zim*)), *D. simulans* (subtypes: *sil*, *sm21*, and *maull*), and *D. yakuba* (*yak*) and paired with a *D. melanogaster*  $w^{1118}$  nuclear background. Four of these lines (*OreR*;*w1118*, *sil*;*w1118*, *sm21*;*w1118*, and *Zim*;*w1118*) were previously shown to have weak to moderate climbing performance abilities (Sujkowski et al., 2018), while two (*yak* and *maull*) were previously untested.

We conducted a longitudinal experiment where we sought to test whether mitochondrial haplotypes responded differently to an exercise conditioning program. We exercise conditioned 12 cohorts of 20 male flies following a prescribed training protocol (Sujkowski et al., 2018; Tinkerhess et al., 2012), and compared cohorts' daily climbing performance against unexercised controls. Flies experienced age-associated declines in climbing performance (Figure 3B) that was significant by mitotype. While we also observed a significant mitotype x conditioning effect, we failed to identify a significant first-order conditioning effect (Figure S2A, Table S2). These significance terms were unchanged, even after testing the normalized climbing index—which normalizes each cohorts' (unique vial of flies) performance against the average of their initial climbs. While there was no significant exercise conditioning effect, the unconditioned flies generally outperformed their conditioned counterparts. This would suggest exercise training is stressful and not always beneficial for the flies. A previous exercise conditioning study with the  $w^{1118}$  nuclear background suggests it is not sensitive background to exercise conditioning effects (Sujkowski et al., 2018), which our results support.

Under the disrupted coevolution hypothesis (Montooth et al., 2010; Rand et al., 2004), we would expect to see a negative relationship between the divergence between a mito-nuclear pairing and its climbing performance. More distantly related pairings have greater opportunity to accumulate mito-nuclear incompatibilities, which would hinder performance. However, those that were most closely related, *OreR*; $w^{1118}$  and *Zim*,  $w^{1118}$ , were intermediate performers. One divergent line, *sil*; $w^{1118}$ , performed the

worst, supporting the hypothesis, but the two most divergent pairings, *maull;w<sup>1118</sup>* and *yak;w<sup>1118</sup>*, performed the best. A separate study also observed *yak;w<sup>1118</sup>* was longer lived compared to its native mitochondrial-nuclear pairing (Ma and O'Farrell, 2016), providing independent result support against the disrupted coadaptation hypothesis. This finding is surprising, since the *D. melanogaster* and *D. yakuba* sub-species are reproductively incompatible.

Finally, we tested a separate cohort of the same mitotypes' ability to resist fatigue in a six-hour fatigue assay. We followed a similar Power Tower protocol as the longitudinal study, but instead used four cohorts and had the flies on the Power Tower for one six-hour stretch. We measured climbing performance at the start and after each hour. We observed significant mitotype and fatigue effects for both the absolute velocities and normalized climbing indexes, but no two-way mitotype x fatigue interaction (Figure S2B, Table S2). This fatigue resistance test demonstrates that while the Power Tower may be stressful in a multi-day longitudinal study, it still effectively elicits a consistent climbing phenotype that can slowly fatigue flies over a prolonged period. Interestingly, rested *yak;w<sup>1118</sup>* were strong performers, though their fatigued counterparts had the greatest variation between time points of any other mito-nuclear pairing. It is possible that *yak;w<sup>1118</sup>* are strong climbers when undisturbed, but more variable in the climbing performance when stressed.



## Conclusion

FreeClimber is a free and easy-to-use platform for quantifying the climbing velocity for cohorts of flies. It is flexible in the videos it can process so it can be adopted by any lab. It automates the tedious process of detecting and counting flies, and reliably quantifies a biologically relevant climbing velocity. Our results demonstrate the utility of using FreeClimber to quantify climbing performance over a traditional time-based cutoff metric. Finally, we applied our platform to measure the longitudinal climbing performances during an exercise-conditioning program and during a resistance to endurance fatigue assay across six mito-nuclear introgression lines. We demonstrate this proof-of-principle for our detector's ability to identify both strong and subtle differences between genotypes, and the platform's ability to work with longitudinal data sets, like those commonly used in *Drosophila* aging research.

## Literature Cited

**Ballard, J. W. O.** (2000). Comparative genomics of mitochondrial DNA in members of the *Drosophila melanogaster* subgroup. *Journal of Molecular Evolution* **51**, 48-63.

**Bellen, H. J., Levis, R. W., He, Y. C., Carlson, J. W., Evans-Holm, M., Bae, E., Kim, J., Metaxakis, A., Savakis, C., Schulze, K. L. et al.** (2011). The *Drosophila* Gene Disruption Project: Progress Using Transposons With Distinctive Site Specificities. *Genetics* **188**, 731-U341.

**Bellen, H. J., Tong, C. and Tsuda, H.** (2010). TIMELINE 100 years of *Drosophila* research and its impact on vertebrate neuroscience: a history lesson for the future. *Nature Reviews Neuroscience* **11**, 514-+.

**Cao, W. Z., Song, L., Cheng, J. J., Yi, N., Cai, L. Y., Huang, F. D. and Ho, M.** (2017). An Automated Rapid Iterative Negative Geotaxis Assay for Analyzing Adult Climbing Behavior in a *Drosophila* Model of Neurodegeneration. *Jove-Journal of Visualized Experiments*.

**Chenouard, N., Smal, I., De Chaumont, F., Maška, M., Sbalzarini, I. F., Gong, Y., Cardinale, J., Carthel, C., Coraluppi, S. and Winter, M.** (2014). Objective comparison of particle tracking methods. *Nature Methods* **11**, 281.

**Chow, C. Y. and Reiter, L. T.** (2017). Etiology of Human Genetic Disease on the Fly. *Trends in Genetics*.

**Crocker, J. C. and Grier, D. G.** (1996). Methods of digital video microscopy for colloidal studies. *Journal of Colloid and Interface Science* **179**, 298-310.

**Faville, R., Kottler, B., Goodhill, G. J., Shaw, P. J. and van Swinderen, B.** (2015). How deeply does your mutant sleep? Probing arousal to better understand sleep defects in *Drosophila*. *Scientific Reports* **5**.

**Ganetzky, B. and Flanagan, J. R.** (1978). RELATIONSHIP BETWEEN SENESCENCE AND AGE-RELATED-CHANGES IN 2 WILD-TYPE STRAINS OF *DROSOPHILA-MELANOGASTER*. *Experimental Gerontology* **13**, 189-196.

**Gargano, J. W., Martin, I., Bhandari, P. and Grotewiel, M. S.** (2005). Rapid iterative negative geotaxis (RING): a new method for assessing age-related locomotor decline in *Drosophila*. *Experimental Gerontology* **40**, 386-395.

**Holmbeck, M. A., Donner, J. R., Villa-Cuesta, E. and Rand, D. M.** (2015). A *Drosophila* model for mito-nuclear diseases generated by an incompatible interaction between tRNA and tRNA synthetase. *Disease Models & Mechanisms* **8**, 843-854.

**Jones, M. A. and Grotewiel, M.** (2011). *Drosophila* as a model for age-related impairment in locomotor and other behaviors. *Experimental Gerontology* **46**, 320-325.

**Kohlhoff, K. J., Jahn, T. R., Lomas, D. A., Dobson, C. M., Crowther, D. C. and Vendruscolo, M.** (2011). The iFly tracking system for an automated locomotor and behavioural analysis of *Drosophila melanogaster*. *Integrative Biology* **3**, 755-760.

**Lavoy, S., Chittoor-Vinod, V. G., Chow, C. Y. and Martin, I.** (2018). Genetic Modifiers of Neurodegeneration in a *Drosophila* Model of Parkinson's Disease. *Genetics* **209**, 1345-1356.

**Lenz, S., Karsten, P., Schulz, J. B. and Voigt, A.** (2013). *Drosophila* as a screening tool to study human neurodegenerative diseases. *Journal of Neurochemistry* **127**, 453-460.

**Ma, H. S. and O'Farrell, P. H.** (2016). Selfish drive can trump function when animal mitochondrial genomes compete. *Nature Genetics* **48**, 798-+.

**Ma, H. S., Xu, H. and O'Farrell, P. H.** (2014). Transmission of mitochondrial mutations and action of purifying selection in *Drosophila melanogaster*. *Nature Genetics* **46**, 393-+.

**Mackay, T. F. C., Richards, S., Stone, E. A., Barbadilla, A., Ayroles, J. F., Zhu, D. H., Casillas, S., Han, Y., Magwire, M. M., Cridland, J. M. et al.** (2012). The *Drosophila melanogaster* Genetic Reference Panel. *Nature* **482**, 173-178.

**Montooth, K. L., Abt, D. N., Hofmann, J. W. and Rand, D. M.** (2009). Comparative Genomics of *Drosophila* mtDNA: Novel Features of Conservation and Change Across Functional Domains and Lineages. *Journal of Molecular Evolution* **69**, 94-114.

**Montooth, K. L., Meiklejohn, C. D., Abt, D. N. and Rand, D. M.** (2010). Mitochondrial–nuclear epistasis affects fitness within species but does not contribute to fixed incompatibilities between species of *Drosophila*. *Evolution: International Journal of Organic Evolution* **64**, 3364-3379.

**Mossman, J. A., Biancani, L. M., Zhu, C. T. and Rand, D. M.** (2016). Mitonuclear Epistasis for Development Time and Its Modification by Diet in *Drosophila*. *Genetics* **203**, 463-+.

**Olito, C., White, C. R., Marshall, D. J. and Barneche, D. R.** (2017). Estimating monotonic rates from biological data using local linear regression. *Journal of Experimental Biology* **220**, 759-764.

**Piazza, N., Gosangi, B., Devilla, S., Arking, R. and Wessells, R.** (2009). Exercise-Training in Young *Drosophila melanogaster* Reduces Age-Related Decline in Mobility and Cardiac Performance. *Plos One* **4**.

**Podratz, J. L., Staff, N. P., Boesche, J. B., Giorno, N. J., Hainy, M. E., Herring, S. A., Klennert, M. T., Milaster, C., Nowakowski, S. E., Krug, R. G. et al.** (2013). An automated climbing apparatus to measure chemotherapy-induced neurotoxicity in *Drosophila melanogaster*. *Fly* **7**, 187-192.

**Rand, D. M., Haney, R. A. and Fry, A. J.** (2004). Cytonuclear coevolution: the genomics of cooperation. *Trends Ecol Evol* **19**, 645-53.

**Sujkowski, A., Spierer, A. N., Rajagopalan, T., Bazzell, B., Safdar, M., Imsirovic, D., Arking, R., Rand, D. M. and Wessells, R.** (2018). Mito-nuclear interactions modify *Drosophila* exercise performance. *Mitochondrion*.

**Taylor, M. J. and Tuxworth, R. I.** (2019). Continuous tracking of startled *Drosophila* as an alternative to the negative geotaxis climbing assay. *Journal of Neurogenetics* **33**, 190-198.

**Tinkerhess, M. J., Ginzberg, S., Piazza, N. and Wessells, R. J.** (2012). Endurance Training Protocol and Longitudinal Performance Assays for *Drosophila melanogaster*. *Jove-Journal of Visualized Experiments*.

**Tsai, H. Z., Lin, R. K. and Hsieh, T. S.** (2016). *Drosophila* mitochondrial topoisomerase III alpha affects the aging process via maintenance of mitochondrial function and genome integrity. *Journal of Biomedical Science* **23**.

**Willenbrink, A. M., Gronauer, M. K., Toebben, L. F., Kick, D. R., Wells, M. and Zhang, B.** (2016). The Hillary Climber trumps manual testing: an automatic system for studying *Drosophila* climbing. *Journal of Neurogenetics* **30**, 205-211.

**Xu, H., DeLuca, S. Z. and O'farrell, P. H.** (2008). Manipulating the metazoan mitochondrial genome with targeted restriction enzymes. *Science* **321**, 575-577.

**Zhu, C. T., Ingelmo, P. and Rand, D. M.** (2014). GxGxE for Lifespan in *Drosophila*: Mitochondrial, Nuclear, and Dietary Interactions that Modify Longevity. *Plos Genetics* **10**.

**Table S1. Experimental variables available for modification in FreeClimber.** List of variables names and their respective data types and corresponding attribute/role in the FreeClimber pipeline. These variables are generated in a `file_name.cfg` configuration file when running the Graphical User Interface (GUI), or can be modified directly from the provided example file.

Variable name	Data type	Corresponding attribute
x	Integer	Leftmost pixel of Region of Interest (ROI)
y	Integer	Topmost pixel of ROI
w	Integer	Width of ROI
h	Integer	Height of ROI
frame_0	Integer	First frame to view
blank_0	Integer	First frame of range to subtract background
blank_n	Integer	Last frame of range to subtract background
threshold	Integer	Threshold for filtering against points
diameter	Integer	Estimated spot diameter
minmass	Integer	Minimum spot mass
maxsize	Integer	Maximum size of spot diameter to consider
vials	Integer	Number of vials in video
window	Integer	Number of frames for sliding window
pixel_to_cm	Integer	Conversion factor for pixels to centimeters
frame_rate	Integer	Video frame rate
vial_id_vars	Integer	Number of variables in naming convention that are consistent across a time measure (ex. genotype, sex)
naming_convention	String	Experimental conditions corresponding with experimental conditions in the file name.
path_project	String	Path to parent folder containing experimental files
file_suffix	String	Suffix of video being processed
convert_to_cm_sec	Boolean	True if converting output slope to centimeters per second

**Table S2. Mitochondrial haplotype significantly impacted climbing performance.** ANOVA of repeated measured for (A-B) exercise conditioning over an 18-day training period showed a significant first order effect for mitochondrial haplotype in both the (A) absolute velocity and (B) normalized climbing index (velocity for a time point/average velocity of the first time point, different for each unique vial). There was no significant first order effect for exercise training, but there was a significant second order effect for mitochondrial haplotype x exercise conditioning. (C-D) Resistance to endurance fatigue had significant first order effects for both mitochondrial haplotype and flies' resistance to endurance fatigue for both the (C) absolute velocity and (D) normalized climbing index. However, the second order effect was not significant.

Interaction term significance key:  $P \leq 0.05$  (\*);  $P \leq 0.005$  (\*\*);  $P \leq 0.0005$  (\*\*\*)

<b>A</b>				
<b>Exercise conditioning – velocity</b>				
<b>Interaction Terms</b>	<b>F Value</b>	<b>DF</b>	<b>Den DF</b>	<b>Pr &gt; F</b>
Mitochondrial haplotype	59.6481	5	35	0.0000 ***
Exercise conditioning	2.7977	1	7	0.1383
Mitochondrial haplotype x Exercise conditioning	6.5415	5	35	0.0002 ***
<b>B</b>				
<b>Exercise conditioning – normalized climbing index</b>				
<b>Interaction Terms</b>	<b>F Value</b>	<b>DF</b>	<b>Den DF</b>	<b>Pr &gt; F</b>
Mitochondrial haplotype	14.2193	5	35	0.0000 ***
Exercise conditioning	0.0117	1	7	0.9171
Mitochondrial haplotype x Exercise conditioning	7.3355	5	35	0.0001 ***
<b>C</b>				
<b>Resistance to endurance fatigue – velocity</b>				
<b>Interaction Terms</b>	<b>F Value</b>	<b>DF</b>	<b>Den DF</b>	<b>Pr &gt; F</b>
Mitochondrial haplotype	14.9928	4	24	0.0000 ***
Resistance to fatigue	22.7888	1	6	0.0031 **
Mitochondrial haplotype x Resistance to fatigue	1.2479	4	24	0.3176
<b>D</b>				
<b>Resistance to endurance fatigue – normalized climbing index</b>				
<b>Interaction Terms</b>	<b>F Value</b>	<b>DF</b>	<b>Den DF</b>	<b>Pr &gt; F</b>
Mitochondrial haplotype	10.0989	3	18	0.0004 ***
Resistance to fatigue	23.193	1	6	0.003 **
Mitochondrial haplotype x Resistance to fatigue	1.0273	3	18	0.404

Supplemental file 1 is available online:

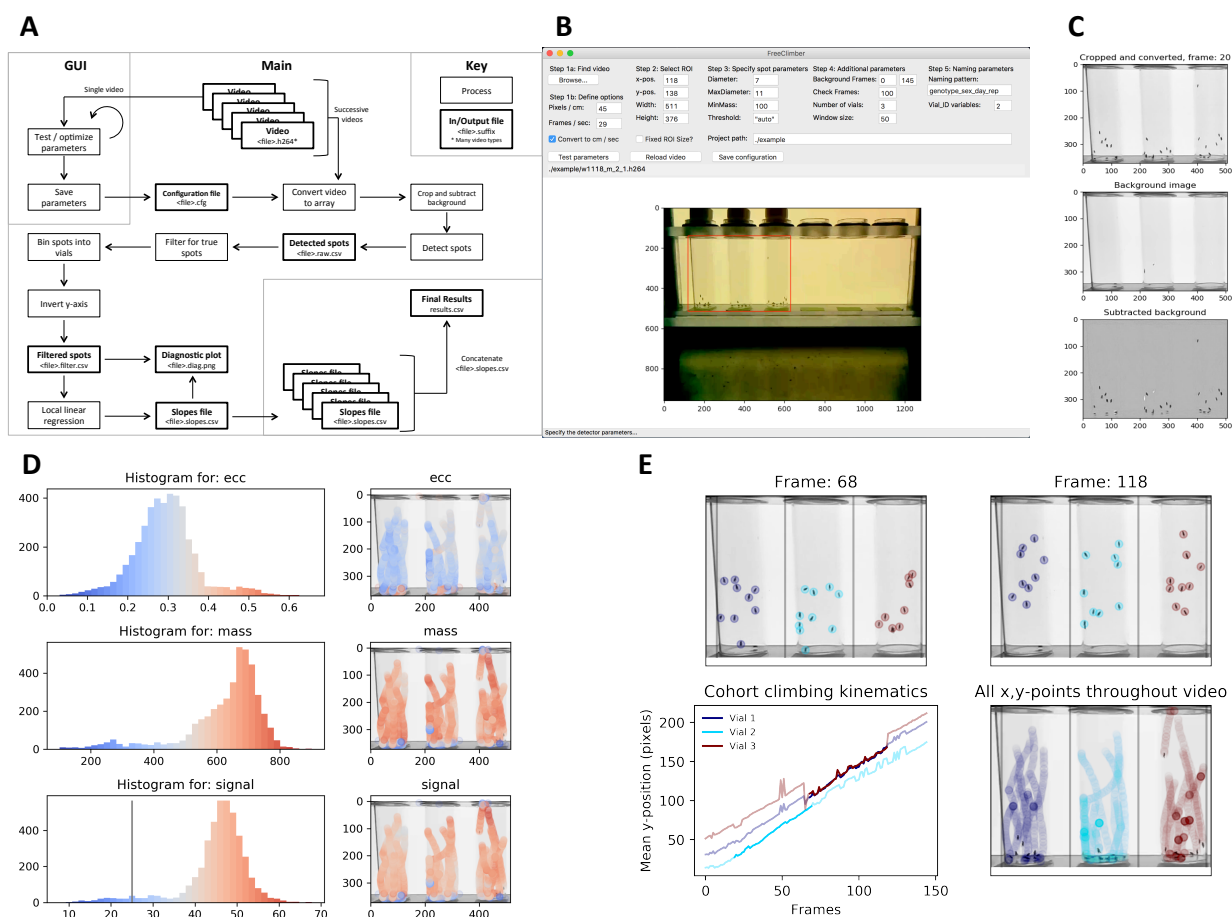
1. <https://doi.org/10.26300/7x8z-5z81>

- NOTE: An GitHub repository for this version of FreeClimber is available online

([https://github.com/adamspierer/FreeClimber/tree/dissertation\\_release](https://github.com/adamspierer/FreeClimber/tree/dissertation_release)),

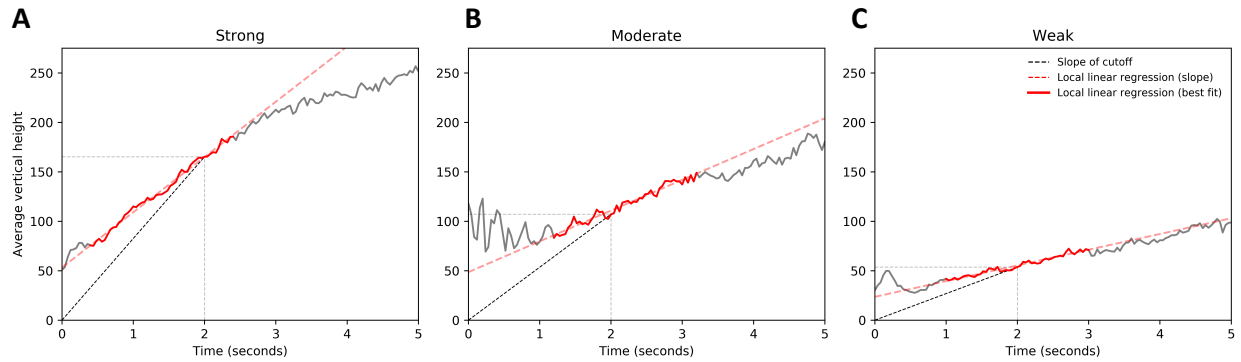
though the most current version of the program is available at:

<https://github.com/adamspierer/FreeClimber>.

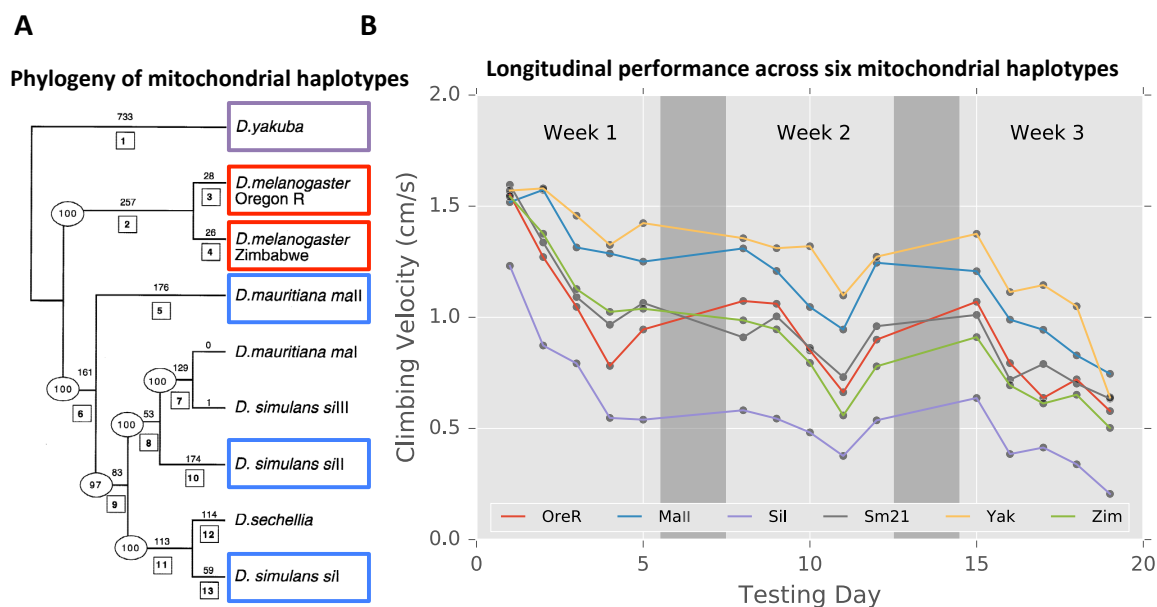


**Figure 1. Overview of FreeClimber platform.** (A) Flow diagram of processes the FreeClimber performs when analyzing a video. The Graphical User Interface (GUI) is designed for parameter optimization (See accompanying Tutorial page for usage), while the command line tool is designed for high throughput processing of many videos with similar detection parameters. (B) Screenshot of GUI with Region of Interest (ROI) drawn on with a red box. (C) Output in `file_name.processed.png` for optimizing ROI and background frame range. The top image is the cropped and grayscaled image used in later scatterplots as a background, the middle image is the background matrix, and the bottom frame is the resulting image generated by subtracting the top and middle frames. FreeClimber detects spots using images like the bottom frame and plots x,y locations of points on images like the top frame. (D) Output in the `file_name.spot_check.png` file corresponding with the distribution and locations for each spot and its respective metric: eccentricity (ecc, roundness), mass, and signal). (E) Output from `file_name.diagnostic.png` showing the x,y-coordinates, color coded by vial, for the first (top-left) and last (top-right) frames of the most linear portion of the local linear regression curve for all points in the video. (Lower-left) The most linear portion (darker shade) of the mean-vertical position vs. frame curve plotted over all frames (lighter shade). (Lower-right) All x,y-coordinates throughout the video are plotted on a single frame.

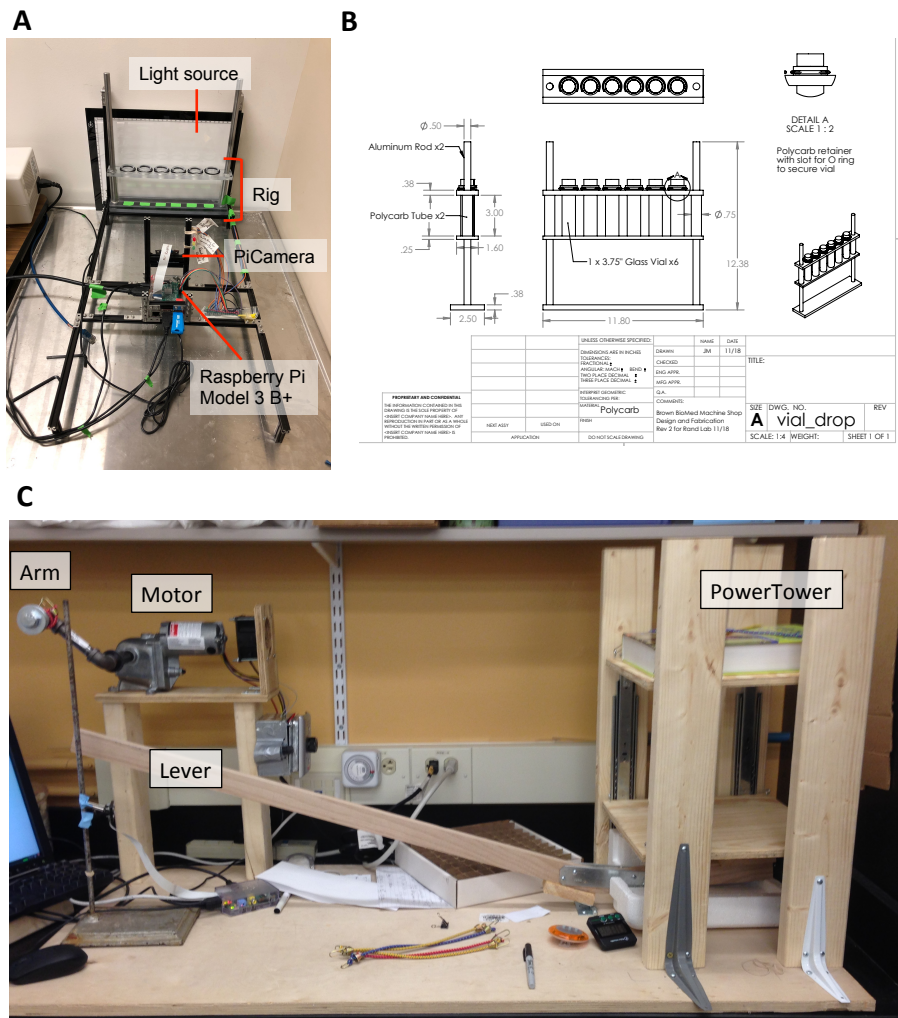




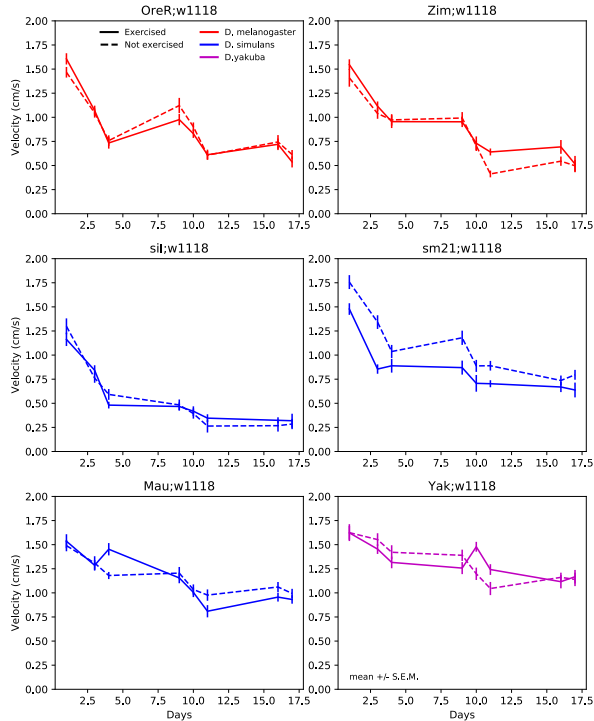
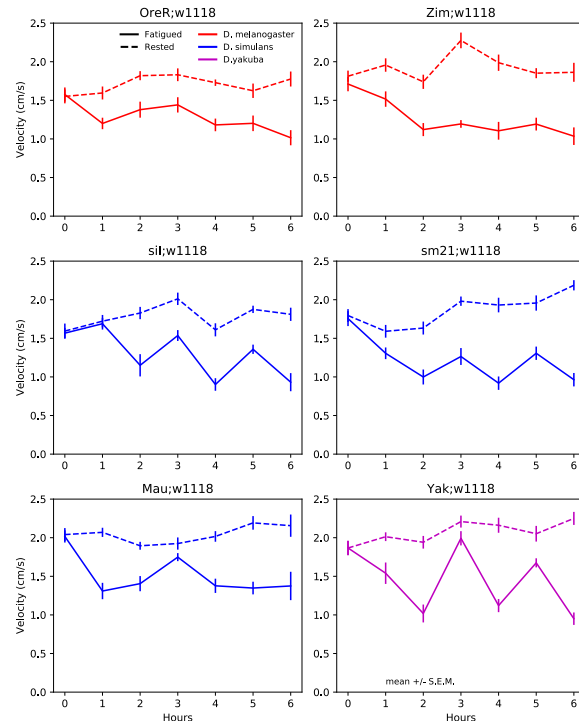
**Figure 2. Method comparison demonstrates a local linear regression is more biologically relevant than quantifying height after 2 seconds of climbing.** Mean vertical-position vs. time (velocity, solid gray line) plots for a cohort of flies measured at (A) 3, (B) 9, and (C) 19 days post-eclosion can be analyzed for climbing velocity two separate ways. The slope of the standard, time-based cutoff at 2 seconds (black dashed line) has a steeper slope than the line of best fit (red dashed line) during the most linear two seconds (50 frames) of a five second (125 frames) climb (red solid line).



**Figure 3. Mitochondrial haplotypes show a differential response to endurance exercise training and resistance to endurance fatigue.** (A) Phylogenetically distinct mitochondrial haplotypes were derived from three clades (*D. melanogaster* in red, *D. simulans* in blue, and *D. yakuba* in purple). Figure modified from (Ballard, 2000). (B) These haplotypes, on a common (*D. melanogaster*  $w^{1118}$ ) nuclear background, were subjected to a three-week endurance exercise training program. Flies were tested on weekdays (light gray) before exercise conditioning on a PowerTower, and allowed to rest on weekends (dark gray). Since there was no significant conditioning effect, conditions were averaged together. Most mitotypes began at roughly the same starting velocity, though *sil*;  $w^{1118}$  started slightly lower, and experienced different rates of age-associated decline in performance. All decreased in their performance overtime, though *yak*;  $w^{1118}$  (yellow) and *mall*;  $w^{1118}$  (blue) were the strongest overall, while *sil*;  $w^{1118}$  was the weakest.



**Figure S1. Experimental set ups for exercise conditioning *Drosophila* and assaying climbing performance.** (A) Exercised flies were assayed for climbing performance using a custom setup to standardize conditions for this manuscript. Here, a MakerBeam frame held a Raspberry Pi Model 3 B+ and PiCamera V2 a fixed distance away from the stage. A light board placed behind the climbing rig backlit flies as they climbed. A light trigger, receiving a signal from the light board or disrupted by a piece of tape on the rig, was constructed from a photoresistor and analog-to-digital converter. When the rig was raised, the system became armed; when the rig was lowered, the system triggered a five second video recording, which eliminated human error in the recording process. The rig (B) was constructed from polycarbonate materials and slid along aluminum rod tracks. Rubber O-rings along the top of each vial slot held vials in place during the assay. (A) The Power Tower is designed to elicit a negative geotaxis startle response in *Drosophila*. Up to two trays of 100 flies are strapped to the Power Tower. An arm connected to a motor turning clockwise at 4 RPM, depresses a lever. The lever pivots around the fulcrum and the other end connects to the bottom platform of the mobile portion of the apparatus. As the motor turns, the vials are lifted. When the arm loses contact with the lever, the vials drop, causing the flies to climb.

**A****Longitudinal Climbing****B****Resistance to endurance fatigue**

**Figure S2. Individual mitotype performance vs. time curves.** Exercised (trained or fatigued, solid line) flies and unexercised flies (Not exercised or rested, dashed line) had different effects across mitochondrial haplotypes (colored by sub-species: *D. melanogaster*, red; *D. simulans*, blue; *D. yakuba*, purple). (A) Longitudinal climbing performance had a significant mitochondrial haplotype effect ( $F = 59.6$ ,  $P < 0.0001$ ) and two-way interaction between exercise training and mitochondrial haplotype ( $F = 6.5$ ,  $P < 0.0005$ ), no significant effect for exercise training ( $F = 2.8$ ,  $P = 0.14$ ). (B) Resistance to endurance fatigue assay, measuring the progressive decline over hours of repeated climbing, had significant mitochondrial ( $F = 15.0$ ,  $P < 0.0001$ ) and exercise effects ( $F = 22.8$ ,  $P < 0.005$ ), but no two-way interaction between the two ( $F = 1.25$ ,  $P = 0.32$ ). Separate sets of flies were used between the two experiments.